UNIVERSITY OF Southampton

University of Southampton Research Repository
ePrints Soton

http://eprints.soton.ac.uk

University of Southampton

Faculty of Natural and Environmental Sciences

School of Chemistry

The Adaption of an Encoded Microparticle Array for Multiplexing Nucleic Acid Hybridisation Assays

e-thesis

Graham Richard Broder

Doctor of Philosophy

December 2011

UNIVERSITY OF SOUTHAMPTON

ABSTRACT

FACULTY OF NATURAL AND ENVIRONMENTAL SCIENCES

SCHOOL OF CHEMISTRY

Doctor of Philosophy

THE ADAPTION OF AN ENCODED MICROPARTICLE ARRAY FOR MULTIPLEXING NUCLEIC ACID HYBRIDISATION ASSAYS

by Graham Richard Broder

Our ever increasing knowledge of genetics is radically changing disciplines in science and medicine. Significantly, the study of gene expression and protein synthesis within both healthy and abnormal cells has advanced understanding of the mechanism of disease at the molecular level. The future treatment of certain diseases may benefit from new classes of nucleic acid based drugs which are currently undergoing development and trialling. Concurrently, assays are being formulated to predict, diagnose and monitor medical conditions. This more detailed patient analysis brings the option of moving away from traditional, textbook treatments and tailoring therapies to the individual, the field of personalised medicine.

Current polynucleotide analysis platforms allow testing for genomic mutations and quantification of gene expression on a massively multiplexed scale with some arrays able to identify more than a million unique target sequences in a single assay. However much development is required to take this analysis technology from laboratory based applications to the bedside. Reductions in assay costs and analysis time are particular concerns. The 4G research group, based at the University of Southampton has developed novel encoded microparticle technology, allowing individual particles to be identified in a mixture. The work herein documents the adaption of this technology for the multiplexed analysis of DNA samples in the form of a suspension/hybridisation assay, a design which may offer advantages over current analysis technologies including reduced assay time and increased array flexibility.

Contents

x

Academic Thesis: Declaration Of Authorship

I, **GRAHAM RICHARD BRODER** declare that this thesis and the work presented in it are my own and has been generated by me as the result of my own original research.

THE ADAPTION OF AN ENCODED MICROPARTICLE ARRAY FOR APPLICATION TO MULTIPLEXING NUCLEIC ACID HYBRIDISATION ASSAYS

 I confirm that:

1. This work was done wholly or mainly while in candidature for a research degree at this University;

2. Where any part of this thesis has previously been submitted for a degree or any other qualification at this University or any other institution, this has been clearly stated;

3. Where I have consulted the published work of others, this is always clearly attributed;

4. Where I have quoted from the work of others, the source is always given. With the exception of such quotations, this thesis is entirely my own work;

5. I have acknowledged all main sources of help;

6. Where the thesis is based on work done by myself jointly with others, I have made clear exactly what was done by others and what I have contributed myself;

7. Either none of this work has been published before submission, or parts of this work have been published as listed below.

Signed: ....

Date: ....

Publications

Multistep synthesis on SU-8: combining microfabrication and solid-phase chemistry on a single material
Cavalli, G., Banu, S., Ranasinghe, R. T., Broder, G. R., Martins, H. F. P., Neylon, C., Morgan, H., Bradley, M., Roach, P. L. *J. Comb. Chem.* **2007**, *9,* 462-472.

Multiplexed analysis using nano-barcodes
Morgan, H., Banu, S., Birtwell, S., Broder, G.R. Galitonov, G., Neylon, D.C., Ranasinghe, R.T., She, J., Zheludev, N., Roach, P.L. *MicroTAS 2007.* **2007**, *11*, 1264-1266.

Diffractive micro bar codes for encoding of biomolecules in multiplexed assays
Broder, G. R., Ranasinghe, R. T., She, J. K., Banu, S., Birtwell, S. W., Cavalli, G., Galitonov, G. S., Holmes, D., Martins, H. F. P., MacDonald, K. F., Neylon, C., Zheludev, N., Roach, P. L., Morgan, H. *Anal. Chem.* **2008**, *80*, 1902-1909.

Multiplex bioassays using a suspension array platform; towards the high throughput screening of drugs targeting cancer stem cells
Broder, G.R., Birtwell, S.W., Hagel, G., Thastrup, O.,Morgan, H., Roach, P.L. *MicroTAS 2010.* **2010**, *14*, 1385-1387.

Kinetics and thermodynamics of biotinylated oligonucleotide probe binding to particle-immobilized avidin and implications for multiplexing applications.
Broder, G. R., Ranasinghe, R. T., Neylon, C., Morgan, H., Roach, P. L. *Anal. Chem.* **2011**, *83*, 2005-2011.

Acknowledgments

I would like to express my gratitude to my supervisor, Dr. Peter Roach whose ideas, assistance, support and encouragement throughout my studies were invaluable.

Thanks also to Prof. Hywel Morgan, Dr. Cameron Neylon and Dr. Eugen Stulz for advice and direction in the project. Special thanks go to Dr. Rohan Ranasinghe, Dr. Gabriel Cavalli and Dr. Joseph She for sharing their experience in helpful discussion and freely giving time and assistance, some of their results, where relevant, has been included in this thesis with appropriate acknowledgment. Further thanks to Drs. Rohan Ranasinghe and Peter Roach for going through the suffering required to proof read early transcripts of this document.

I would also like to thank all the past and present members of the Roach research group and the members of the 4G research group with whom it has been a pleasure working alongside. An honourable mention goes to the Drummond Arms P.H. and its inhabitants for providing a good atmosphere in which to formulate new ideas.

Finally, I would particularly like to thank my parents, my brother and Angela for their continuous support, love and encouragement, they put up with a lot.

Abbreviations

A – adenine/adenosine

AFM – atomic force microscopy/atomic force microscope

APS – adenosine-5'-phosphosulfate

ATP – adenosine-5'-triphosphate

BCA – bicinchoninic acid

b_{max} – maximum binding concentration

bp – (oligonucleotide) base pair

BSA – bovine serum albumin

C – cytosine/cytidine

cDNA – complementary deoxyribonucleic acid

CFTR – cystic fibrosis transmembrane conductance regulator

CPG – controlled pore glass

CPR – chemical phosphorylating reagent

Cy-5 – cyanine-5 fluorophore, ex 650 nm, em 666 nm

δ – chemical shift

D – diffusion coefficient

DCC – *N*,*N'*-Dicyclohexylcarbodiimide

DCM – dichloromethane

ddNTP – dideoxynucleotide triphosphate

DIC – diisopropylcarbodiimide

DIPEA – diisopropylethylamine

DMAP – dimethylaminopyridine

DMF – dimethylformamide

DMSO – dimethylsulfoxide

DMTr – dimethoxytrityl/dimethoxy triphenylmethane

DNA – deoxyribonucleic acid

dNTP – deoxynucleotide 5'-triphosphate

dsDNA – double stranded deoxyribonucleic acid

ε – extinction coefficient

EDC – 1-ethyl-3-(3-dimethylaminopropyl)carbodiimide hydrochloride

EDTA – ethylenediaminetetraacetic acid

EI – electron ionisation

ELISA – enzyme-linked immunosorbant assay

EPFL – école polytechnique fédérale de Lausanne

ESI – electro spray ionisation

EtOAc – ethylacetate

ETT – 5-ethylthio-1H-tetrazole

f – steric factor

F – fluorescence

FACS – fluorescence-activated cell sorter

FDA – Food and Drug Administration

FP – fluorescence polarisation, aka fluorescence anisotropy

G – guanine/guanosine

GMA – glycidyl methacrylate

HEG – hexaethylene glycol

HGP – human genome project

HPLC – high-pressure liquid chromatography

HOBt – 1-hydroxybenzotriazole

HSPyU – *O*-(*N*-succinimidyl)-*N,N,N',N'*-bis-(tetramethylene)uranium hexafluorophosphate

IgG – Immunoglobin G

IP – intellectual property

iTOL – interactive tree of life

Jeffamine® ED-900® – *O,O'-Bis*(2-aminopropyl) polypropylene glycol-*block*-polyethylene glycol-*block*-polypropylene glycol 800

K_d – equilibrium dissociation constant

k_{diff} – diffusion controlled rate constant

k_B – Boltzmann constant (1.38065×10^{-23} Pa m^3 K^{-1})

k_{off} – dissociation rate constant

k_{on} – association rate constant

l – pathlength

LCMS – high-pressure liquid chromatography mass spectrometry

MES – 2-(*N*-morpholino)ethanesulfonic acid

mRNA – messenger ribonucleic acid

MS – mass spectrometry/mass spectrometer

η – viscosity

n – refractive index

NHS – *N*-hydroxysuccinimide

NMR – nuclear magnetic resonance

PBS – phosphate buffered saline

PCR – polymerase chain reaction

PEB – post exposure bake

PEG – polyethylene glycol

PGMEA – polypropylene glycol methylether acetate

pI – isoelectric point/isoelectric pH

PNA – polyamide nucleic acid

PPi – pyrophosphate

QCM – quartz crystal microbalance

R – hydrodynamic radii

READNA – revolutionary approaches and devices for nucleic acid analysis

R_f – retention factor

RNA – ribonucleic acid

RP-HPLC – reverse-phase high-pressure liquid chromatography

rpm – revolutions per minute

rpTLC – reverse phase thin layer chromatography

rRNA – ribosomal ribonucleic acid

s.d. – standard deviation

SDS – sodium dodecyl sulphate

s.e. – standard error

SEM – scanning electron microscopy/scanning electron microscope

SNP – single nucleotide polymorphism

SSPE – sodium chloride, sodium dihydrogenphosphate, EDTA buffer

STR – short tandem repeat

SU-8 – epoxy-based negative photoresist

sulfo-NHS - *N*-hydroxysulfosuccinimide

T – thymine/thymidine

T – temperature

$t_{1/2}$ – half-life

TAQ – *Thermus aquaticus*

TBTU – *O*-(Benzotriazol-1-yl)-*N,N,N',N'*-tetramethyluronium tetrafluoroborate

TEA – triethylamine

TEG – triethylene glycol

THF – tetrahydrofuran

TLC – thin layer chromatography

T_m – melting temperature

Tween-20® - polysorbate 20, a surfactant

UV – ultraviolet

1.0 Introduction

Biological assays encompass methods used to detect and quantify the amount of a particular constituent from a biological sample or to determine the biological or pharmacological potency of drug molecules.

Deoxyribonucleic acid (DNA) contains the genetic information for the majority of known life forms; encoding for and regulating the expression of proteins within the cell. Analysis of a genome can provide a great deal of information ranging from identification and differentiation between individual organisms and between species to the state of their health, evolutionary relationships may be mapped and resistance to disease predicted.

The macro structure of DNA, determined by Watson and Crick in 1953, is that of a highly ordered duplex of polymeric strands, wound in a right-handed double helix (Figure 1). Each strand consists of a phosphate-deoxyribose backbone with nucleobases attached to the sugar; the order of the bases constitutes the genetic information store. The primary objective of DNA assays is to determine the sequence of these bases.

Since the initial publication of the partial human genome in 2001 there has been an ever increasing demand for faster, cheaper and more reliable genetic analysis platforms.[1,2] Without these new technologies the wealth of data divulged from the Human Genome Project (HGP) cannot easily be translated into research and medical advances. To highlight (and attempt to close) the gap between the knowledge of the sequence of bases which encode human life and the implementation of this knowledge a number of initiatives have been set up. These include the four year, European Commission funded REvolutionary Approaches and Devices for Nucleic acid Analysis (READNA) consortium and the altogether more glamorous Archon Genomics X Prize offering $10 million to those who develop a technology capable of sequencing 100 human genomes in 10 days.[3,4]
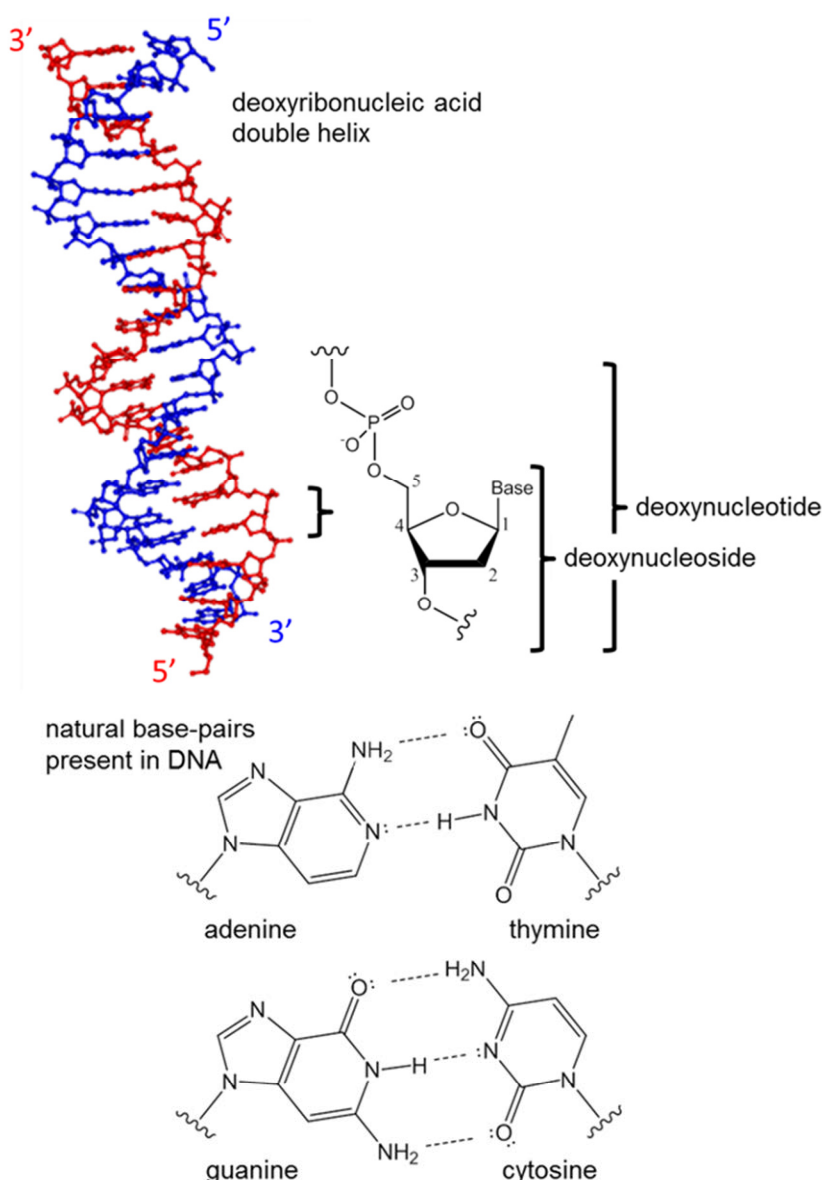
Figure 1. The helical macromolecular structure of double-stranded DNA which consists of a sugar-phosphate backbone linked by phosphodiester bonds. Genetic information is represented by the sequence of the four DNA bases linked to sugar moieties; these bases pair up due to hydrogen bonding interactions which bridge the two strands of the duplex.

An ideal sequencing technology would determine the order of bases in a DNA chain to a high fidelity whilst being economically viable and user friendly. An aim of research in this field is to develop technologies for use at the point of care; small, robust, cheap and disposable devices which can be operated by healthcare professionals (or patients) and which rapidly give results. Product design typically incorporates elements from the physical and life sciences most notably molecular biology, genetics, chemical biology, micro/nano engineering and bioinformatics.

1.1 Benefits of nucleic acid sequencing

The first genome to be fully determined was that of the virus Bacteriophage MS2 in 1976,[5] followed by the first "truly living" organism to be sequenced, the pathogenic bacterium *Haemophilus influenzae* in 1995;[6] since then over 180 organisms have had their genetic sequences read.[7] Sequencing of the human genome was considered essentially complete in 2006, and at present over 95% of the genome has been read by the HGP.[8,9] The bulk of the missing sequence data is for highly repetitive non-encoding regions such as chromosomal centromeres and telomeres and for regions which show variation amongst individuals.[10] As there is variation in the genomes between individuals of the same species, the published sequences can only be considered a framework for the encoding of an organism and for this reason it is accepted that a species has been fully sequenced if $\geq$ 95% of its genome has been determined.

The knowledge of the sequence of bases in a genome is of little use without an understanding of where genes are localised, what proteins they encode and what functions these proteins perform.[11] Work in the field of proteomics is progressing; however the determination of the human proteome is considered a greater undertaking than that achieved by the Human Genome Project.[12] It is estimated that less than 1.5% of the human genome encodes for protein production and these areas are currently the main focus of genomic research (the biological function of most of the remaining 98% is yet to be determined; though some is known to be important for the regulation of transcription and translation processes).[13]

There are a number of benefits that arise from genetic sequencing. Having a template of the human genome, for example, has led to an increased understanding of genetic disease. By comparing DNA from diseased individuals with the (healthy) template (using genome-wide association studies), mutations can be identified which either result in disease or can increase predisposition to disease.[14,15] The identification of common disease causing mutations has resulted in improvements in both diagnosis and prognosis.[16,17] In recent years technological advances have resulted in the reduction of both sequencing time and cost which has lead to commercial screening services being widely available. The deeper understanding of the mechanics of individual diseases is also likely to aid development of improved therapeutics, with

blanket screening of libraries of small (potential drug) molecules being replaced by a more targeted approach.

Studies of evolution are also benefitting from sequencing information. Where organisms have traditionally been classified by observations of their physical characteristics leading to a mostly accurate but not highly detailed understanding of the evolutionary tree, they can now be classified using similarities between genomes, providing a more informed stance as to the evolutionary relationship between species.[18]

The use of genetic testing in forensic science has revolutionised law enforcement, with the sampling of an individual's DNA now standard practice when thought to be on the wrong side of the law. This has aided the judicial process and lead to new convictions, the solving of cold-cases and the quashing of previous convictions where miscarriages of justice have been proven.

1.1.1 Disease diagnosis and prognosis

Genetic analysis can now used for the prediction, screening and diagnosis of many genetic diseases caused by mutations to the healthy genome. Mutations fall into two categories; hereditary and acquired.[19] Prior to the development of a new screen for a particular disease, the location of the affected gene must be identified. To narrow down to a disease causing mutation amongst the 3.2 billion bases in the human genome, samples of DNA from people suffering from the illness are compared with the standard human genome. Historically the entire genome would need to be analysed, for example the mutations responsible for Huntington's disease and cystic fibrosis each took ten years to be identified.[20,21] More recently the localisation of problem base sequences has been aided by the publication of chromosome maps by the HGP.[22,23] These maps document genetic landmarks (specific base sequences) which highlight the loci of genes within the entire genome, assigning them an address along the sequence. Research to identify mutations and omissions from an individual's genome can then be more targeted by looking at the known regions of interest. This research and the demand for testing has fuelled a steady growth in the market for genetic testing. Assays have been developed to screen for more than 2000

different genetic diseases by way of identification of causative mutations (Figure 2).[24]
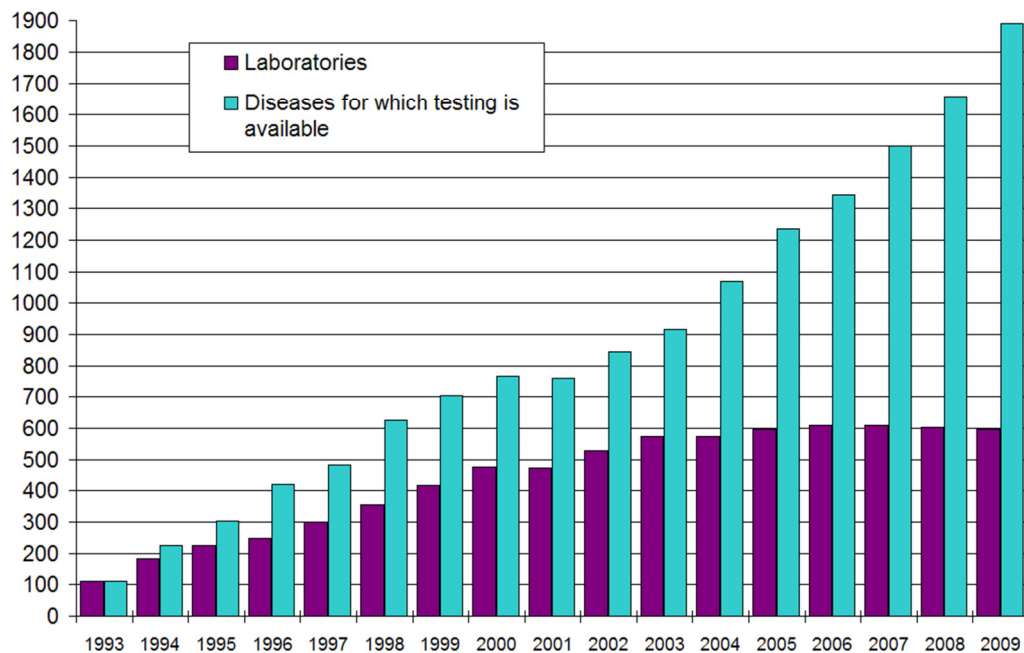
Figure 2. The growth of genetic testing in recent years which is representative of the general trend of growth in the (commercial) genomics sector. Though few new companies have formed since the turn of the millennium, the number of tests for genetic diseases continues to rise with over 2000 tests currently available[24]

The analysis of the genome as a diagnostic tool has significant advantages over proteomic and cytomic assays, diseases may be identified prior to the onset of any symptoms and the exact cause can be determined. Early or pre-symptomatic diagnoses can allow remedial action to be swiftly taken, including therapeutic regimes and lifestyle changes which can lessen the extent of or fully negate later symptoms. Often the presence of a mutation only imparts a predisposition to a genetic disorder and so screening can be used to estimate the risk of a disease developing.[25]

The passing on of hereditary diseases to offspring can also be screened for. Screening is sometimes used in conjunction with *in-vitro* fertilisation when there is a high risk of inherited genetic disease.[26,27] DNA from fertilised zygotes can be screened and only those with healthy sequences subsequently implanted in the womb, avoiding disease inheritance leading to healthy offspring.

Many diseases are symptomatic of multiple mutations; cystic fibrosis for example is caused by combinations from over 1400 mutations of the cystic fibrosis transmembrane conductance regulator (CFTR) gene.[21] Knowing the specific mutations present in the gene alleles gives information as to the likelihood and severity of symptoms, this more detailed diagnosis leaves scope for personalised medicine (theranostics) where a treatment can be tailored to the individual rather than to the average patient. Research into theranostics is at an early stage but is now being used clinically for the treatment of some cancers where markers for virulence and prevalence can be screened informing on the required intensity and duration of prescribed treatment regimes.[28,29]

1.1.2 Gene expression studies

A useful tool for molecular biology is gene expression profiling where messenger ribonucleic acid (mRNA) sequences produced by transcription within the cell nucleus are identified and quantified (or at least assayed relative to a standard).[30] As changes in the quantity of different mRNA sequences correspond to the activation or repression of specific genes, the cellular response to various environmental stimuli can be studied at a genomic level. The expression from thousands of genes can be assayed in parallel with specific genes being turned on or off by different environmental stimuli being identified. Major uses of expression profiling include drug discovery, disease prognosis and cellular research.[31,32] Fundamental studies of the living cell using expression profiling often involve exposing cell cultures to different conditions (physical, chemical or biological) to elicit a response and comparing changes of mRNA levels.[33] This information can be complemented by proteomics and bioinformatics to better understand cell responses aiding research into cell signalling pathways, protein function and identification novel drug targets.[34,35] For example, to aid development of novel cell culture medias, profiling has been used to identify receptors and cell signalling factors expressed during growth.[36] Once these proteins have been identified, the effects of various small molecules and ligands on their corresponding gene expression were tested with the aim of promoting protein production and subsequent maximisation of cellular growth.

Theranostics can be enhanced by combining gene expression profiling with commercial screening arrays currently available for the screening of cancer biopsies.[37] Assaying the expression of various cancer mRNA biomarkers gives an indication as to the virulence of a patient's specific cancer, dictating the treatment prescribed and giving an idea of the probability of remission.[38]

Expression profiling can be used throughout the drug discovery process from the identification of novel drug targets and the screening of potential drug molecules to the assaying of effects drug candidates have on expression across the entire genome and their toxicology to healthy tissue.[39,40]

1.1.3 Species identification and forensics
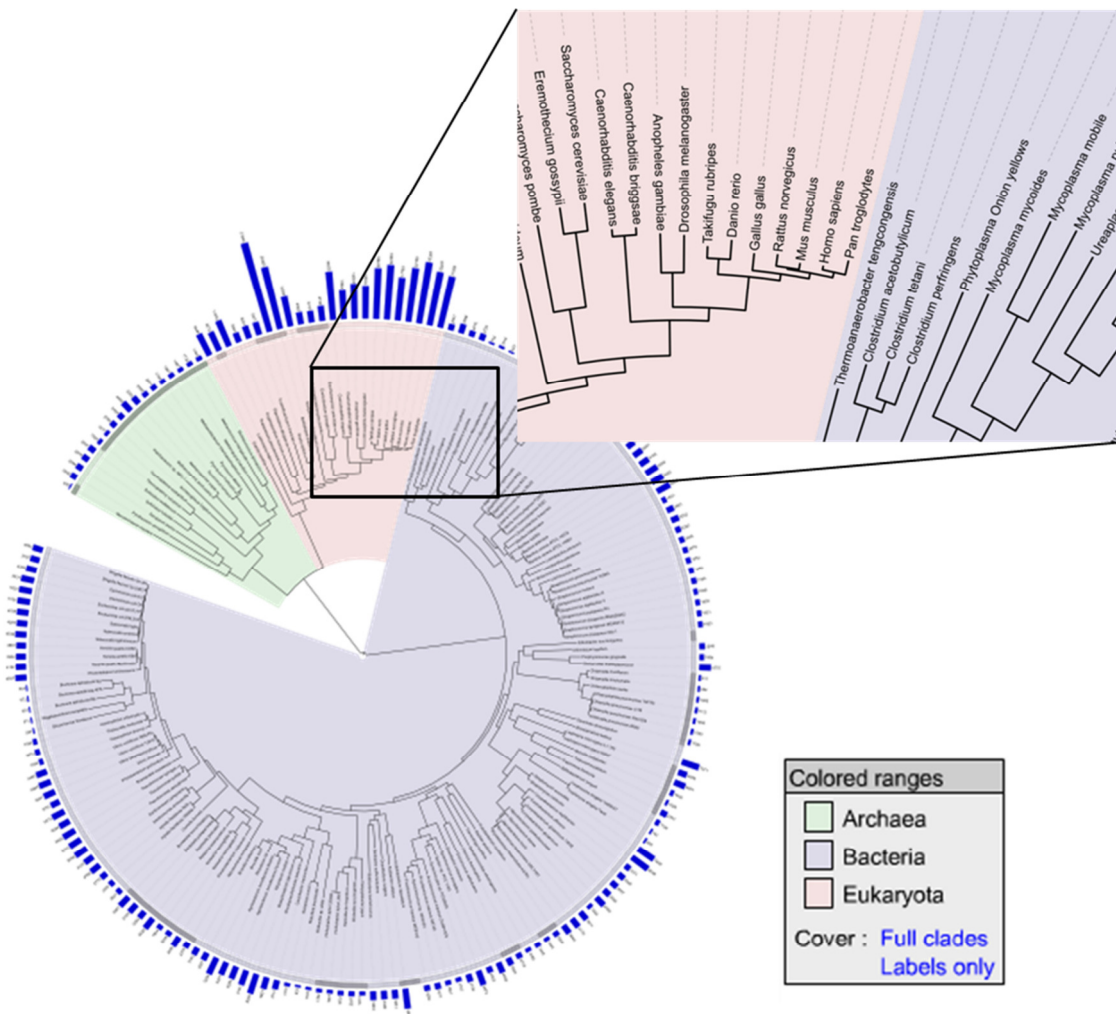
Figure 3. The current map of the phylogenetic tree displaying the genetic relationship between (fully sequenced) organisms. The expanded region shows *H. sapiens* and some of our closest relatives. From the Interactive Tree Of Life (iTOL) project[41]

Due to the high fidelity of certain analytical techniques, changes of a single base can be detected allowing discrimination between different organisms. Phylogenetic arrays have been developed for the identification of species and strains with a particular focus on the differentiation of microbial taxa.[42] A good example of a phylogenetic array is one which targets regions of prokaryotic ribosomal RNA (rRNA) to classify different bacteria. These arrays specifically look at the nucleotide sequence of the 16S rRNA gene as it has both highly conserved and variable regions.[43,44] Analysis of the variable regions provides information used to discriminate closely related species and strains, whereas highly conserved regions

vary between more distantly related taxa.[45] Beyond the classification of life, phylogenetic ecology can be used to track the evolution of pathogens and is useful for the understanding of virulence between different strains of the same disease causing microorganism.[46,47,48] Expanding on this genetic taxonomy by comparing the genomic data of all sequenced organisms it is possible to discern the evolutionary connections between species and online tools have been developed to disseminate this knowledge (Figure 3).

Another use of sequencing technology is in forensic science where DNA profiling is used to identify individuals, establish family relationships and link crime to perpetrator. Identification is based on the assaying of short tandem repeats (STRs) in the genome, these are regions of consecutively repeating bases (1-6 nucleotides long) with the specific number of repetitions varying between individuals. Importantly, these regions are flanked by highly conserved sequences and can therefore be easily localised using complementary DNA (cDNA).[49,50] Most current forensic tests focus on 13 different STR loci, with the lengths of each STR in an individual's genome being analysed, this results in 26 different repeats being measured (two copies of each allele) and gives an (almost) unique DNA "fingerprint".[51] The chances of two randomly chosen individuals sharing the same STR profile has been calculated to be 3×10^{-13} (1 in 3 trillion), however the odds increase for related individuals.[52]

1.1.4 Ethical and legal discussion

The ethical and legal issues surrounding genetic information are constantly evolving as this relatively new field continues to advance, often with moral viewpoints clashing with big business ideology.[53] Solving these dilemmas is primarily a task for policy makers within government and the courts, but it is advantageous for scientists to be aware of moral issues affecting their field.

One area for concern is the right of ownership over sections of, or whole, genomes. Patents have been being awarded for specific gene sequences since the early 1990's both in the U.S. and Europe allowing companies or individuals to control their usage.[54] This appears to contradict historical patenting guidelines where natural materials cannot be covered.[55] Arguments against the patenting of natural sequences

include the thought that it hinders the advancement of genetic research and the development of new bioanalytical technology. Added is the thought that a sequencing company actually holds ownership over part of the human genome. The counterargument in favour of intellectual property (I.P.) claims that the potential for commercial gain drives new research and rewards success in the field. Recently established patents have been successfully challenged in court.[56] As the amount of information increases further problems may arise, for instance presently even short (incomplete) sequences of an individual gene can be protected, when the whole sequence of that gene is determined it too can also be patented and the sequencing of the entire organism's genome can be covered as well. This may lead to the same short base sequence being covered by three different patents; legal wrangling would likely then ensue. It seems inevitable that the way I.P. and genetic information are managed will need a radical overhaul in the not too distant future.

Predictions of a future state of health using an individual's genetic information also warrants discussion. Some genetic mutations cause disease or increase the likelihood of a disease manifesting and genetic screening can provide valuable information for diagnosis, treatment and/or prevention.[33] However regulation has yet to catch up with the commercialisation of genetic testing allowing unsubstantiated claims as providers (in the U.S.) do not yet come under the scrutiny of the Food and Drug Administration (FDA), the situation being similar elsewhere. These tests often give results as a probability of disease manifestation. This may promote a change in lifestyle to counterbalance an increased risk but it may too cause unnecessary worry about a problem which would not necessarily appear. At the very least there is an argument for a greater regulation of service providers and improved education of health professionals and the public.[57]

1.2 Technology overview

DNA sequencing involves the determination of the order of nucleotides in a strand. This can include both the analysis of samples where none of the base order is known as in whole genome sequencing and the more focussed sequencing of regions of interest, for instance an area where the rough sequence is known but is a common loci for mutations.[58] Most sequencing consists of four steps; target amplification,

purification, analysis and identification. Later, this chapter will focus on current methods of analysis.

Often the amount of DNA within a biological sample is insufficient for sequencing and therefore requires amplification; generally two methods are used, molecular cloning or the polymerase chain reaction (PCR).[59,60] The degree of purification required is dependent upon the specificity and robustness of the techniques being used. Generally, purer DNA samples are needed for the sequencing of completely unknown segments (having lengths of 40 – 1000 bases and sequencing utilises enzymatic pathways) than the more targeted sequencing of shorter regions of interest (involving very specific interactions with complementary probes). The purification techniques employed depend upon the amplification methods used, techniques include; precipitation, chromatography, centrifugation and affinity capture.[59]

Once a sample has been analysed, elucidation of the base sequence may require significant computational reconstruction.[61] For example, the sequencing of an organism's entire genome usually requires the whole strand to be cut into smaller, more manageable segments.[62] Once these shorter (overlapping) strands have been sequenced they then have to be reassembled in the correct order; for the human genome this requires the stitching together of 3.2 million shorter sequences, each approximately 1000 bases long, and achieving this reassembly would be extremely difficult without powerful computational methods.[63,64]

There is currently great interest in the advances in sequencing technologies as a result of the publication of the human genome in 2003 and focus has now shifted to the more widespread use of this data. One of the main aims of this development drive are to reduce both the cost and the time required to analyse samples, with secondary aims of minimising sample and equipment size and reducing dependence on infrastructure/manual handling. In essence there is the desire to shift sequencing from large, dedicated laboratories to analytical laboratories, hospitals, GP's surgeries and potentially the home, i.e. the point of care.[65,66]

1.2.1 Sequencing of Medium and long DNA fragments

The most common methods of sequencing make use of a PCR-based synthesis of the complementary strand, the structure of which is then elucidated. Two well established techniques are chain-terminating sequencing and pyrosequencing.

Sequencing by chain termination was pioneered by Frederick Sanger in 1977 and resulted in the first practical (commercial) DNA sequencers.[67] The original method used a mixture of normal deoxynucleotide triphosphates (dNTPs) (some incorporating a radioactive label, ^{32}P which emits beta particles) and modified dideoxynucleotide triphosphates (ddNTPs) (which lack a 3' hydroxyl) during the DNA polymerase-catalysed synthesis of the oligonucleotide complementary to the target sequence (Figure 4). Upon incorporation of ddNTP, synthesis terminates. As the incorporation of either dNTP or ddNTP is statistical, a variety of different oligonucleotide lengths results. By only adding a single ddNTP to each polymerase reaction and separating the product oligonucleotides by length using gel electrophoresis the sequence can be determined.

PCR amplification will be discussed in more detail (Chapter 1.3.1).
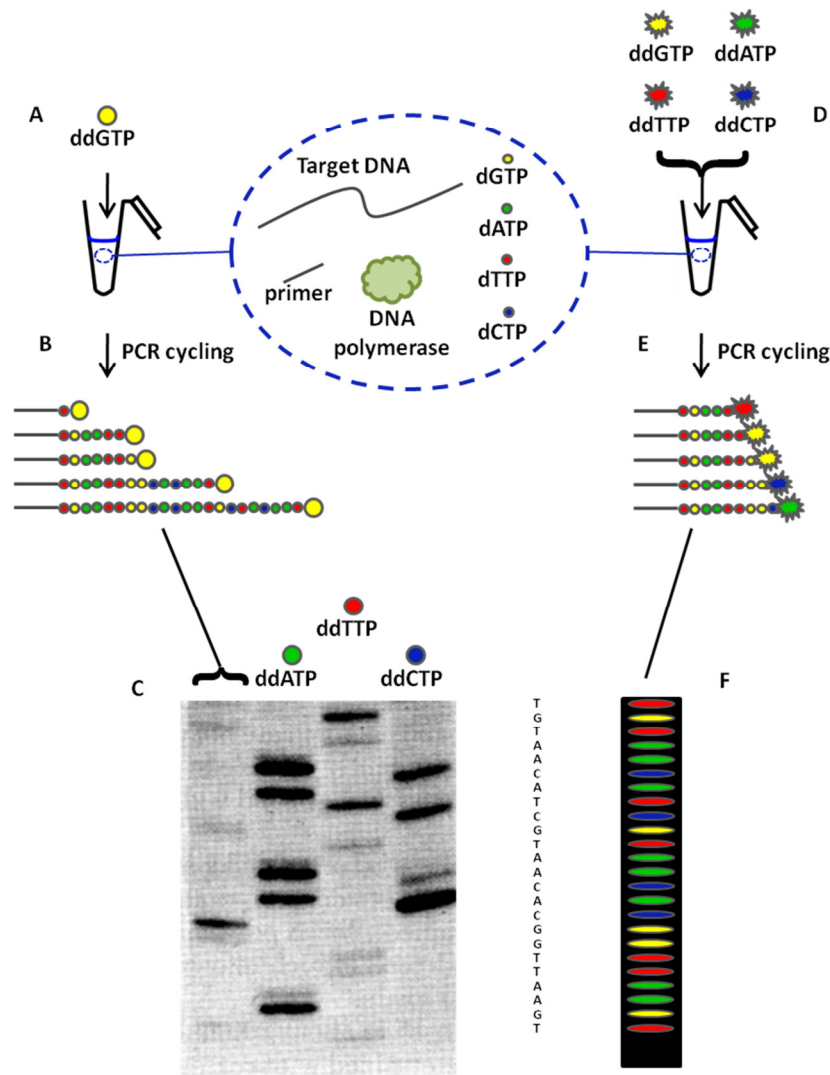
Figure 4. Chain termination (Sanger) sequencing. A. Target DNA is amplified in the presence of a single ddNTP which B. causes termination of polymerisation. C. Gels of the PCR mixtures each containing a single ddNTP can be run sorting the sequences by size and allowing reconstruction of the original base order. D - F. An improved sequencing setup using labelled ddNTPs to facilitate sequencing in a single gel lane. Running gels in multiplex utilising capillary electrophoresis has paved the way for higher throughput sequencing

The method was improved by the use of labelled terminators in what is known as dye-terminator sequencing (Figure 4).[68,69] Using a different fluorophore for each of the four ddNTPs, only a single polymerase reaction is required as the identity of the terminal base in a sequence can be determined by the wavelength of light emitted. A further advancement was the development of capillary electrophoresis which has superseded gel electrophoresis for the size separation of oligonucleotide sequences.[70] Using these 100 μm diameter silica columns for separation results in lower sample consumptions and a decreased read times.[71] These higher throughput techniques paved the way for automation and the development of commercial DNA sequencers

(ABI and Amersham) which allow analysis in parallel (up to 384 capillaries), technology which made the human genome project viable.[72,73] Using the most developed Sanger methods combined with capillary electrophoresis would require approximately 10,000 instrument days and cost £15 million to sequence a human genome (3.2 billion bases).[74]

Pyrosequencing allows real-time analysis of complementary DNA synthesis by monitoring the incorporation of individual nucleotides.[75,76] In the presence of a DNA polymerase and the sample DNA, dNTPs are added sequentially, one at a time, and incorporation is monitored by the indirect quantification of pyrophosphate (PPi) released. Quantification relies on an enzymatic pathway where PPi is initially converted to adenosine triphosphate (ATP) which is subsequently used to drive the oxidation of luciferin, this final step results in the release of photons, the intensity of light emitted being proportional to the amount of deoxynucleotide initially incorporated (Figure 5). Any unincorporated dNTPs and remaining ATP is degraded by the enzyme apyrase. In summary; to a mixture of target DNA sequence, primers, enzymes, adenosine phosphosulfate (APS) and luciferin, a quantity of a single dNTP is added and the reaction monitored for light emission. After pausing to allow time for apyrase to degrade any remaining ATP and nucleotides, the reaction is continued by the addition of the next dNTP. Repeated cycling through of the four deoxynucleotide triphosphates allows the sequence to be read in real-time by detection of light emitted.
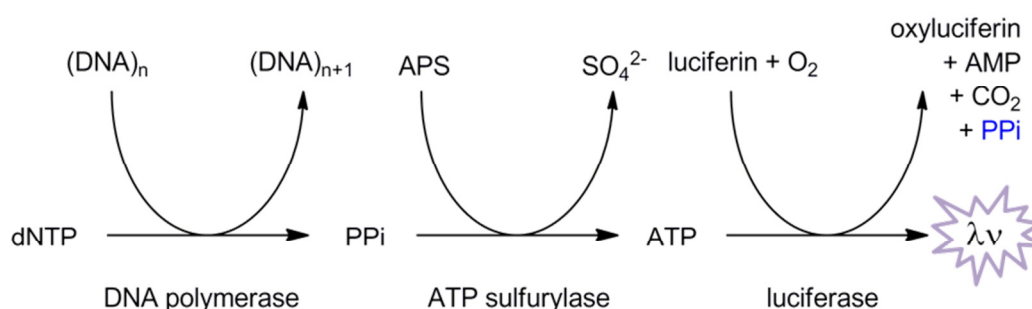
Figure 5. The mechanism of pyrosequencing. The incorporation of a nucleotide into a growing DNA sequence initiates a reaction cascade which results in emission of light. The reaction is self propagating as pyrophosphate is both a reagent and a product (highlighted in blue), therefore after every addition the reaction must be quenched (by the enzyme apyrase). Bases are added sequentially, with continuous monitoring of the intensity of light, a flash indicating incorporation

Pyrosequencing has a number of advantages over Chain-termination techniques including removing the need for labelled primers, modified nucleotides or gel electrophoresis, the monitoring of synthesis is in real-time and is carried out at room temperature and the sequencing is cost effective.[77] The technique does have some limitations, for example it is limited to read lengths of 400-500 bases as nucleotide incorporation is not 100% efficient, leading to an increase in background signal as the reaction progresses.[76] Furthermore the method cannot easily determine the length of regions where the same base is repeated many times (homopolymeric regions), this is because the increase in light intensity becomes (proportionally) less with each additional repeat, this effect becomes prominent after the incorporation of about ten identical adjacent nucleotides.[78] The technology has been commercialised, most notably by 454 Life Sciences (Roche Applied Science) who, by immobilising the target sequence to particles and arraying in microwells, can achieve massively parallel sequencing, claiming 600 million bases read in 10 hours at a cost of ~£10,000.[79,80]

Solexa sequencing (Illumina) differs from pyrosequencing in that the extension of the growing complementary strand (immobilised on a surface) is monitored using fluorescently labelled nucleotides, the surface being imaged after nucleotide incorporation. Following imaging, the fluorescent label and terminal protecting groups are removed allowing the next nucleotide to be incorporated.[81]

The above sequencing methods can be used to elucidate the code of longer DNA chains by breaking the complete sequence down into more manageable chunks. One method is Shotgun sequencing, where target DNA is cut into fragments (often with the use of restriction enzymes), sequenced and then regions of overlap between reads are used to reassemble the original order of bases (Figure 6).[82] Another method is call primer walking, by this method primers are hybridised to a known region of the target DNA and after primer extension the 500 (unknown) bases beyond the 3' primer end are sequenced, now knowing the sequence further along the target DNA, new primers can be designed to hybridise further along the target strand and the process repeated.[83]
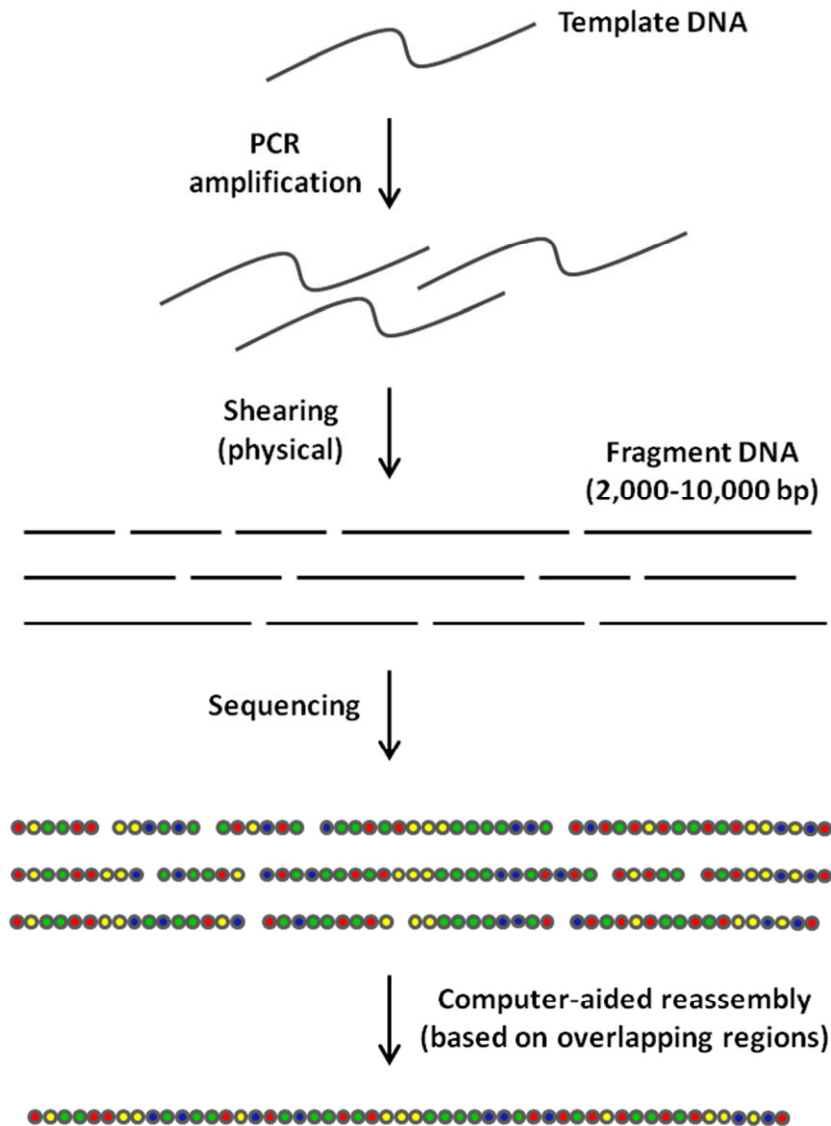
Figure 6. A summary of the shotgun sequencing of long DNA sequences. The target sequence is first amplified and broken into shorter chains with random breaks. Fragments are often inserted into plasmid DNA to be replicated in bacteria before being sequenced. Overlapping regions on the sequence fragments are used to elucidate the original base sequence.

1.2.2 Sequencing of short DNA fragments

Hybridisation assays can be used to detect and decode shorter target DNA sequences upon binding to their complementary strand (which acts as a probe, generally less than 100 bases long).[84,85,86] This methodology requires both a signal generation to indicate when a hybridisation event has occurred and a way of identifying the specific probe which has formed a duplex with complementary target.

With the development of the DNA microarray, it became possible to track the positions of tens of thousands of oligonucleotide probes, and their application to whole genome sequence analysis was investigated.[85] Sequencing of the entire human genome by hybridisation has since been demonstrated to be impractical as probes cannot contain enough of a unique base sequence to permit sequencing.[87] A short oligonucleotide sequence may be repeated within a genome and therefore short probes will not distinguish between them, conversely, as probes increase in length, single base-pair mismatches become less significant (to the overall strength of hybridisation) resulting in difficulty distinguishing between similar target sequences.[88] The design of new arrays has therefore focussed on uses such as expression profiling and single nucleotide polymorphism (SNP) detection.[89,90,91] These are applications where the genome of a species has previously been (at least partially) sequenced and using this information arrays can be designed for the detection of sequences of interest; for expression profiling this relates to the quantification of specific mRNA strands and for SNP detection the discrimination between base variations at a specific site within a genome.

The technological aims are to develop hybridisation arrays to be very high throughput and multiplexed, cheap to produce and give a fast detection response whilst requiring little space, infrastructure or target sample.[92,93]

In summary, the technology is intended for use at the research laboratory/hospital level (at the point of care). Whole genome sequencing using chain termination or pyrosequencing is time consuming, costly and labour and infrastructure intensive. However this sequencing only needs to be carried out on a representative sample of individuals from within a species to generate the basic genome of that species and identify its common positions of variation (polymorphism). On the other hand, actually using this knowledge for most forms of scientific, medical or forensic diagnostics requires sequencing of an individual target (organism) of interest; therefore there is a need for cheap, fast and more portable targeted sequencing technology.

DNA microarrays consist of many oligonucleotide probes immobilised on a planar surface, the location and sequence of each probe being known (Figure 7). As the area functionalised with each probe is very small (less than 250 μm diameter) many

thousands can be fit onto a chip the size of a microscope slide.[94] The probe-functionalised surface is exposed to a sample of target DNA and hybridisation to the specific complementary probe occurs. Binding events are commonly identified by an increase in fluorescence; therefore either target strands carry a fluorophore modification or double-stranded DNA-binding fluorescent intercalators are added.[95,96]
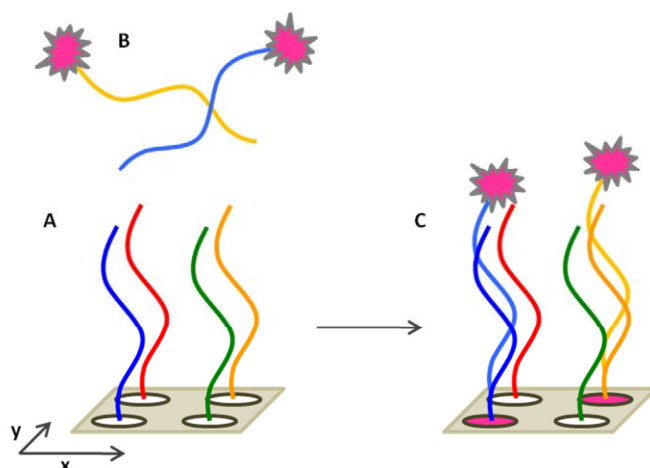
Figure 7. Schematic representation of a DNA hybridisation microarray. A. Short oligonucleotide probes are ordered on a planar surface, probes are identified by their coordinates on an x,y grid. B. Upon exposure to a sample of labelled target DNA complementary sequences hybridise, C, and result in spots of fluorescence on the array surface. Mapping the positions of fluorescent signals to the grid coordinates allows sequence identification

Label-free detection methods are the focus of developmental research, with the double benefit of negating target modification (with fluorophore) during sample preparation and reducing expensive and bulky imaging equipment.[97,98] One area showing promise is the use of nanowires (nanoelectrodes) where a change in potential caused by biomolecule binding can be detected at a surface.[99] For example, nanowires may be fabricated from silicon and functionalised with oligonucleotide probes in a manner similar to that used for microarrays, upon complementary target hybridisation the resistance of the wire is observed to change.[100,101,102] An array of wires, each with a unique probe sequence and an individual electrical connection may perform as a traditional microarray but on a much smaller scale.

Multiplexing arrays where the probes are arranged on a planar surface suffer from some disadvantages including limitations to probe localisation (difficulty in printing probes in well-defined, small areas), an inflexibility of the probe library (where once

an array is fabricated, the probes included may no longer be modified) and slow reaction kinetics (as reagents/target must diffuse onto the surface).[103,104]

An alternative is to immobilise biomolecular probes to the surface of particles to produce a suspension array.[105,106] As the probes are now attached to separate supports they can be moved independently allowing flexibility in the array design after functionalisation. Binding rates are also increased as the particles can be suspended within the sample mixture which results in a decrease in the thickness of the diffusion zone close to the probe-functionalised surface.[107] This results in the binding kinetics being closer to that observed for solution-phase interactions, and this effect should be more pronounced when the concentration of target is low and the diffusion zone around a probe-functionalised surface would be likely to show target depletion.[108,109,110]

The theory behind multiplexed sequence analysis using suspension arrays is akin to microarray technology, but modified so that instead of spots on a chip, the fluorescence of individual particles increases upon complementary target hybridisation (Figure 8). The requirement is to know to which particles each different probe is attached to and this can be achieved by designing particles to be easily differentiated. There are a number of different encoding methodologies including spectral (incorporation of varying fluorophore levels to give a particle-unique emission spectrum), physical (particles of differing shape), graphical (patterning of the particle surface) and holographic (where light is diffracted by the particle) allowing particles to be uniquely tagged.[111,112]. The ability to control the probe-particle pairs by flow cytometry can be an additional benefit to suspension arrays (over microarrays) as particles can be analysed in a continuous flow. Other examples also exist where particles have been fabricated and functionalised in a stream, which gives options for the continuous monitoring of biological samples.[113]
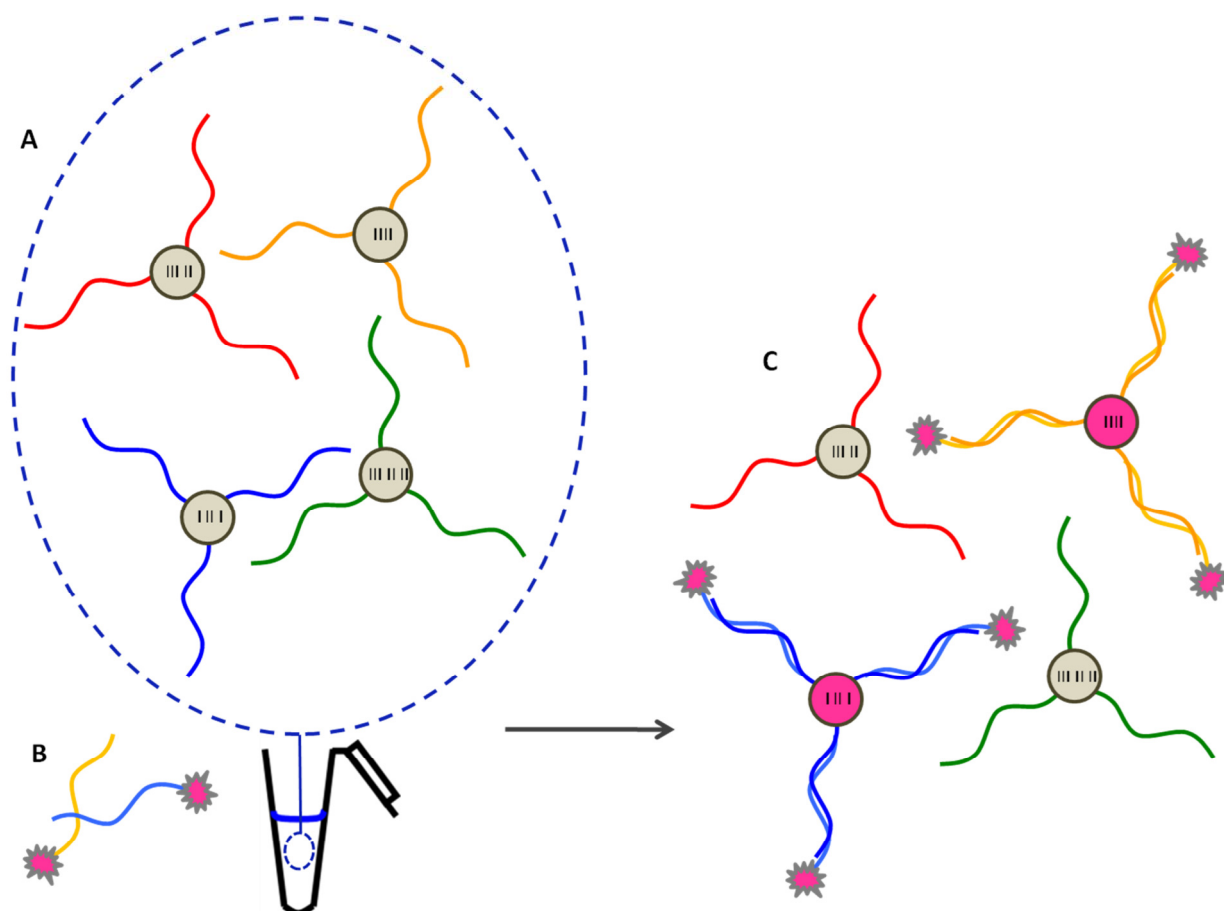
Figure 8. Schematic representation of a DNA hybridisation suspension array. A. Short oligonucleotide probes are immobilised on a particle surfaces, probes are identified by the encoding on each unique probe-particle conjugate. B. As with DNA microarrays, upon exposure to a sample of labelled target DNA complementary sequences hybridise which results in, C. particles with increased fluorescence. Decoding the particles displaying fluorescent signals allows sequence identification

In recent years suspension array technology has been commercialised, most notably by Luminex Corporation (U.S.) which use microparticles encoded by the impregnation of precise quantities of two fluorescent dyes, the ratio of the dyes being unique within each particle.[114] This technology has an encoding capacity of 100 (the number of different codes available) and arrays have recently been developed to identify and genotype subtypes of the flu virus (H1N1).[115]

The current drawbacks to the more widespread use of suspension arrays over microarrays appear to be the high cost of fabricating encoded particles in sufficient quantities, the requirement for great robustness of encoding and fidelity of decoding, and the difficulty in functionalising different particles with unique probes whilst tracking the immobilisation, some of these issues are discussed in more detail below.[116]

1.3 Target and probe preparation for DNA hybridisation suspension arrays

As previously noted, before the DNA in a biological sample can be analysed using a hybridisation array, the amount of target must usually be amplified. As these arrays are often designed to investigate specific genomic regions and detect the presence of known mutations this amplification may be focussed on replicating just the regions of interest. Furthermore, the target or the probe usually requires modification (labelling) so that any binding events may be detected.

1.3.1 The polymerase chain reaction

PCR is a routinely used laboratory technique for the exponential amplification of a region of interest on within a DNA sample exploiting naturally occurring cellular DNA and RNA repair and replication enzymes.[117] This makes it ideal for genetic testing such as SNP genotyping or disease diagnosis where although the exact base sequence in the variable (mutation) region is unknown and of interest, the sequence of bases in adjacent (non-variable) regions is known.[118,119,120] PCR is summarised in Figure 9. Briefly; a mixture of sample DNA, two primers complementary to sequences flanking the region of interest, all four dNTPs and a heat stable (e.g. Taq) DNA polymerase is placed in a thermal cycler.[60] The temperature is raised to 95 °C to denature the DNA duplex then cooled to 55 °C allowing annealing of the primers to the ss.DNA. Extension (polymerisation) is performed at 72 °C resulting in two ds.DNA sequences, with the rate of chain extension being greater than 60 nucleotides per second.[121] By cycling the temperature the three steps may be repeated until the desired concentration of the target sequence has been reached or dNTP has been depleted. As the concentration of the target sequence increases exponentially over 1 million copies can be made by temperature cycling less than 20 times (in approximately 1 hour).
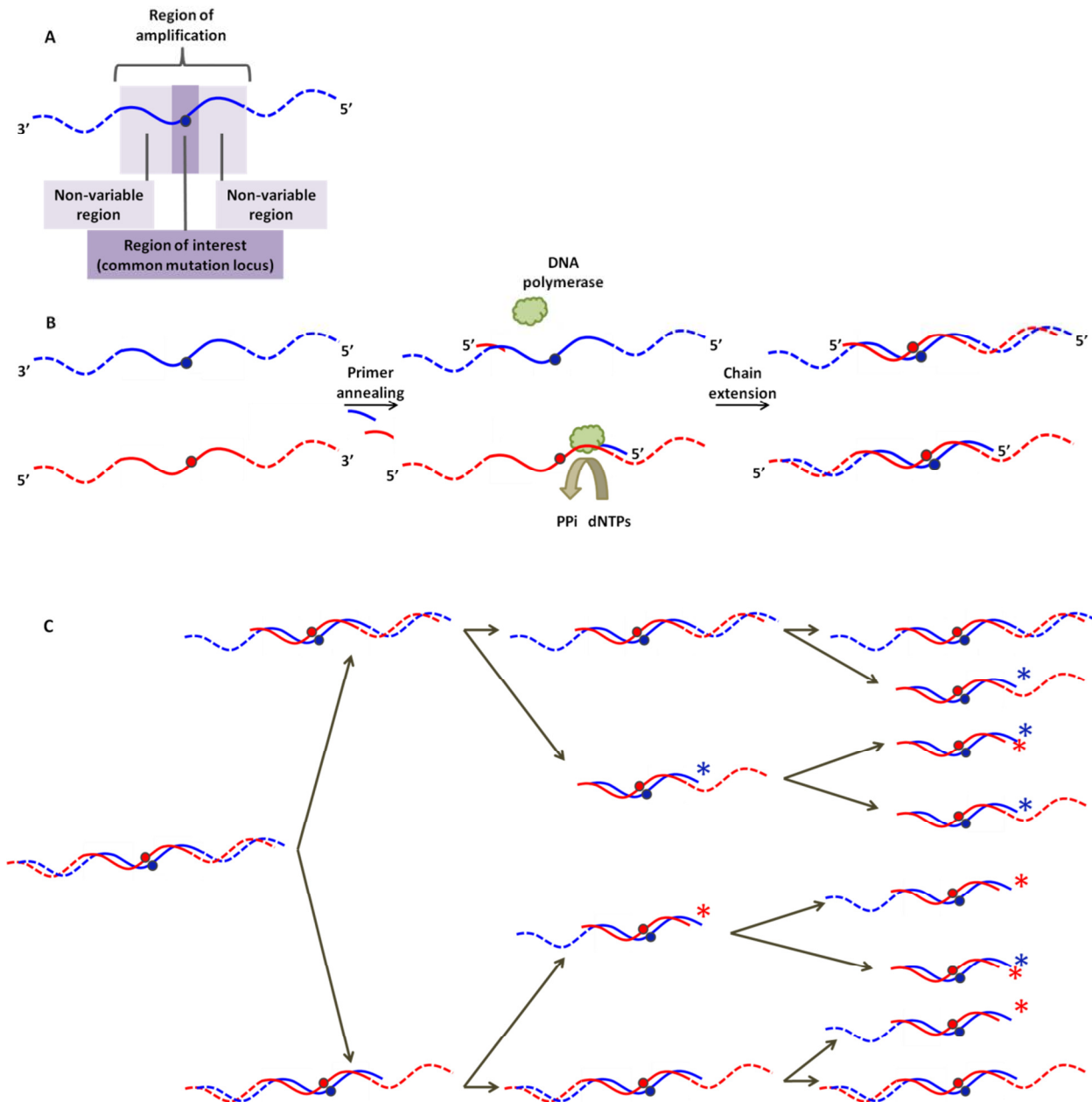
Figure 9. A graphical summary of PCR; A. PCR is used to amplify a region of interest on the sample DNA, primers can be designed to be complementary to regions flanking this variable region. **B.** Primer annealing is followed by chain extension with incorporation of dNTPs, extension is catalysed by thermally stable DNA polymerases such as Taq Polymerase. **C.** Products of the first three thermal cycles, each arrow represents a denaturing, annealing, extension cycle. Compare the linear increase in the concentration of the unwanted long chain sequence with the exponential increase in the desired short chain product (as denoted by *)

1.3.2 Fluorescence labelling

Most hybridisation assays use a fluorescence increase as an indicator of complementary target capture. Conjugates between amplified target DNA and a fluorophore may be prepared pre, midst or post PCR.

Fluorescently labelled PCR primers can be used in the amplification process which would result in product sequence with a label at (or near) the 5' terminus. [68,122] Primers thus used are often expensive and primer annealing can be adversely affected. Enzymatic methods include the use of fluorescently modified dNTPs during the chain extension which are incorporated into the sequence. [123,124] The efficiency of modified dNTP incorporation is dependent upon recognition by the DNA polymerase, for this enzymes displaying high fidelity are not always the best to use.

Modified primers and dNTPs which include specific chemical functionalities can be exploited for labelling after PCR amplification, for example click chemistry has received interest due to the high yielding and specific nature of the reaction between two groups not normally found in biomolecules. [125] Post amplification labelling by enzymatic means can also be used, one example of this being the exchange of the 3' terminal nucleotide for a fluorescent nucleotide in a reaction catalyzed by a sub-fragment of DNA polymerase (Klenow fragment). [126,127,128]

For some hybridisation arrays it is not necessary to pre-label target sequences as an optical signal can be generated upon hybridisation to the immobilised complementary probe. One example of this is primer extension where the 5' overlap of a hybridised target sequence is utilised as a template for the 3' extension of the tethered probe sequence. [129,130] Using a reverse transcriptase and labelled nucleotides, a fluorophore is incorporated onto the probe DNA only if the probe is hybridised. A disadvantage to this strategy is the difficulty in discriminating duplexes containing a single base mismatch from the complementary pairing, especially if the mismatch is distanced from the probe's 3' end. [131] One method to overcome this is to use a nucleotide degrading enzyme (e.g. apyrase) to compete with the reverse transcriptase. This works because extension on a complementary duplex is fast compared with on a mismatching duplex, therefore less labelled nucleotide is incorporated into the mismatching duplex in the limited time available before all free nucleotide is enzymatically degraded. Mismatching signal is thus reduced compared with that expected from complementary hybridisation.

Another technique for target detection requiring no prior modification of target is the use of intercalators which become more fluorescent upon incorporation into double

stranded DNA (dsDNA). These can be tethered to the probe sequence to be kept in close proximity of any formed duplex.[132,133] Molecular beacons can also be used to detect non-labelled targets, these are oligonucleotide probes which are modified with both a fluorophore and a quencher are opposing ends, when not hybridised to a specific target sequence partial self-complementarities result in a hairpin looped structure bringing these two modifications into close proximity (Figure 10).[134] However, hybridisation to the complementary target is favoured, upon forming the duplex with target the probe becomes linear and a signal is observed. Molecular beacons have been immobilised to solid supports for use in hybridisation arrays.[135]
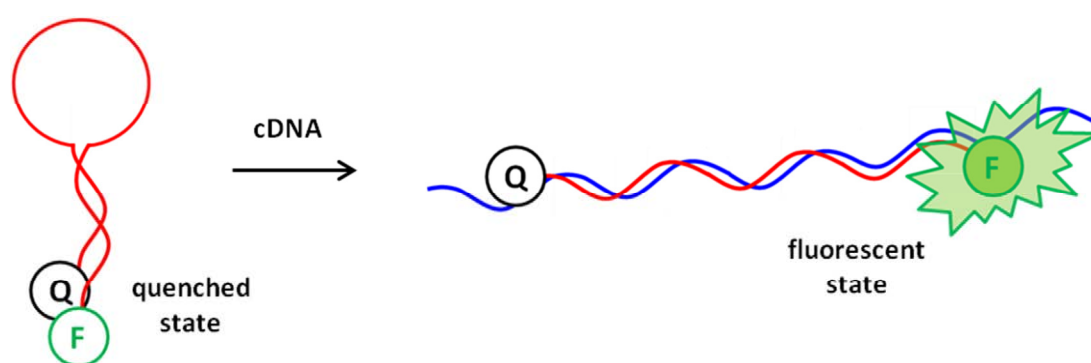
Figure 10. Molecular beacons are oligonucleotide probes complementary to a region of interest on a target sequence. The terminal bases (at both 3' and 5' ends) are self complementary and are modified with fluorophore and quencher pairs. In the absence of cDNA the beacon has a hairpin loop conformation resulting in fluorophore quenching, however hybridisation to cDNA is energetically favoured, when this occurs the fluorophore is distanced from quencher and becomes active.

The choice of labelling method used in hybridisation suspension arrays is situation dependant, multiple parameters need to be taken into account and so there is not one universal technique which works best. Often the materials (supports) used, the specific target sequences and the assay scale rule out the use of certain methods, whilst issues of time, cost and expertise as ever need to be taken into account.

1.3.3 DNA synthesis

The contemporary method for oligonucleotide synthesis is on the solid phase using phosphoramidite nucleosides.[136,137,138] This is a step-wise synthesis, adding one base at a time to a sequence growing from (and immobilised at) the 3' end. As the reaction to incorporate these building blocks is not 100% efficient the length of

sequence is limited to about 200 bases, however in most hybridisation arrays probe lengths of only 10 – 30 bases are required so this is not a problem.[139,140]

The oligonucleotide synthetic cycle involves three steps, repeated for the incorporation of each additional nucleotide and ends with a final step to release the complete sequence from the support (Scheme 1).

Step 1: Coupling. Synthesis exploits the reactivity of the 5' hydroxyl group of a support-bound nucleotide towards the P^{III} centre of phosphoramidite reagents (**1**), forming a phosphite linkage. All hydroxyl groups other than those on the resin-bound terminal nucleotide are protected hindering side reactions and uncontrolled polymerisation.

Step 2: Oxidation. The phosphite centre (**2**), being chemically unstable, is required to be oxidised to a more stable phosphate (P^V) (**3**).

Step 3: Deprotection. The acid labile dimethoxytrityl (DMTr) protecting group (**25**) of the new 5' hydroxyl, which prevents multiple nucleotide couplings in each synthetic cycle, is removed.

These three steps are cycled, adding an extra nucleotide to the growing chain each time.

Step 4: Deprotection and Cleavage. Once the oligonucleotide (**4**) is complete all protecting groups on the phosphate centre and the bases are removed and the sequence (**5**) is released from the support under basic conditions.

Significantly for array development the costs and labour required to synthesise oligonucleotides is kept low by automation, with the first automated DNA synthesisers being produced by Applied Biosystems, Inc in 1983.[137,138]

Due to the wide range of phosphoramidite reagents available DNA, RNA and unnatural polynucleic acids can all be synthesised, furthermore chemical functionality can also be incorporated at any point in the sequence. The use of unnatural polynucleic acids is of particular interest in the design of hybridisation arrays as they often impart beneficial characteristics. For example phosphorothioate linkages are formed by the replacement of the oxidation step with sulfurisation; these

are structurally similar to the natural phosphodiester backbone (with P-OH replaced by P-SH) but are resistant to hydrolysis by nucleases.[141]
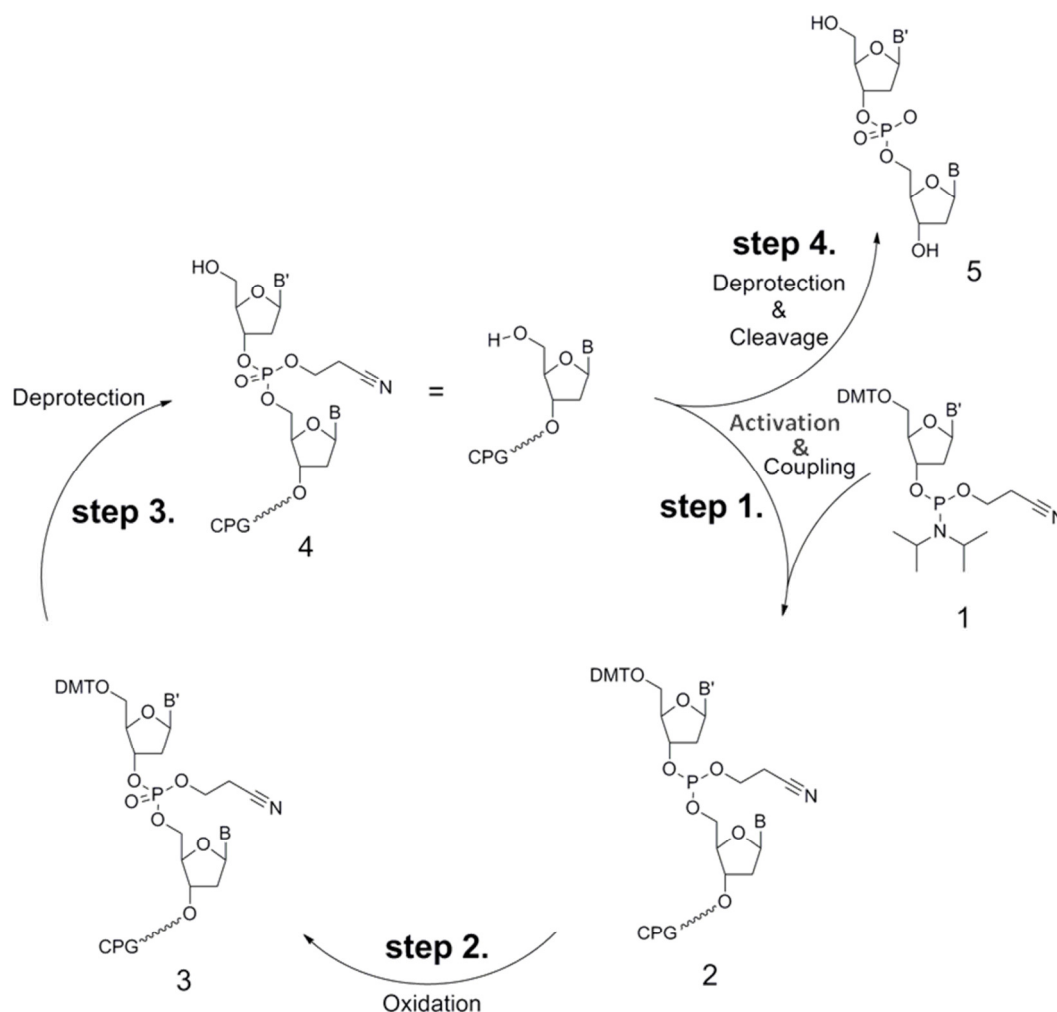
Scheme 1. Solid phase oligonucleotide synthesis. Sequences can be synthesised by the sequential coupling of phosphoramidite nucleotides (1), followed by oxidation of the resulting phosphite linkage (2) to phosphate (3) and an acid deprotection of the terminal hydroxyl group of the growing tethered oligonucleotide (4). Once the oligonucleotides are fully formed, a basic deprotection and cleavage step separates the sequence (5) from the controlled pore glass (CPG) support. By using a non-labile linkage between the first nucleotide and the solid support, cleavage would not occur in the final step, allowing the immobilised oligonucleotides to act as immobilised probes useful for the design of hybridisation arrays

Polyamide nucleic acid (PNA) is another unnatural DNA probe which uses an amide (rather than phosphodiester) backbone and therefore can be produced using peptide synthesis techniques.[142] As with phosphorothioate backbones, PNA show resistance towards degradation by DNA nucleases.[143] Furthermore, as the backbone is uncharged electrostatic repulsion is reduced in the PNA/DNA duplex compared with a DNA/DNA duplex of identical base sequence making hybridisation more

thermodynamically favoured leading to an increase in the melting temperature (T_m).[144] This removal of charge density has also been shown to increase the rate of duplex formation to immobilised PNA probes (compared with the equivalent immobilised DNA probe) as the target is not electrostatically repulsed when in close proximity to the surface.[144]

1.3.4 Large probe libraries

Solid phase synthesis can be adapted to produce large libraries of nucleic acid (and other types of oligomeric) probes using relatively few coupling cycles. Standard synthesis uses the glass support, CPG, packed into columns amenable to automated systems. In a technique known as split and mix synthesis differently functionalised supports are mixed together after each coupling cycle and then split between separate vessels for the coupling of the next nucleotide.[145,146] In the case of oligonucleotide synthesis four reaction vessels would be used (Figure 11), one for the coupling of each base. After the first coupling cycle (coupling one nucleotide to the CPG in each vessel) the supports are mixed then split evenly between the vessels. As a result, each separate pot has examples of all four different nucleotide-functionalised supports and after a second round of (four) coupling reactions, 16 unique probe-particle pairs will have been synthesised. Upon mixing, splitting and a third round of coupling, 64 different probes would have been produced. This linear synthesis leads to an exponential growth in the number of different oligonucleotide sequences, with 4^n unique probes produced where n is the number of coupling cycles completed.

In the case of DNA suspension arrays, split and mix probe synthesis can be used to make many different probe-particle pairs. Tracking particles by reading their encoding allows the location (i.e. reaction vessel) of each individual particle during each coupling cycle to be monitored, the oligonucleotide sequence of the probes and their encoded particle tethers can therefore be recorded.[147,148] In this way, thousands of different oligonucleotide probes can be made very quickly, but crucially both the base sequences and their locations are known.
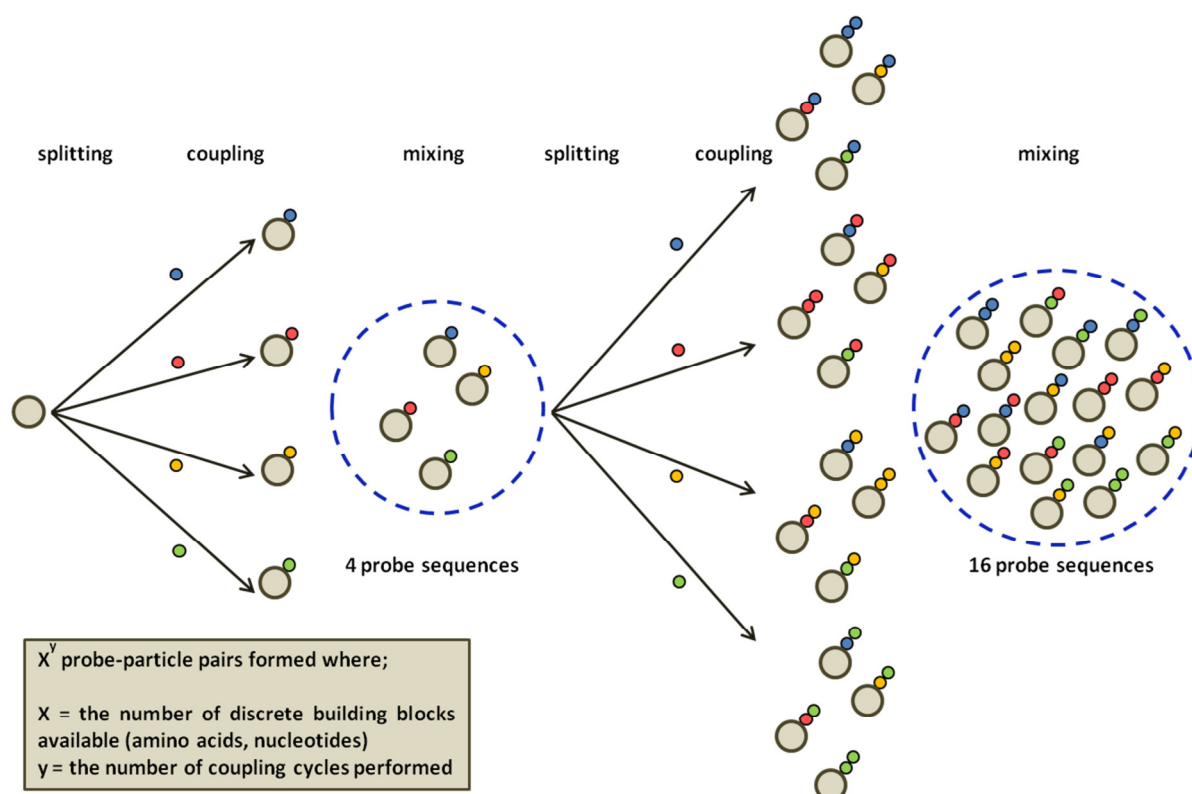
Figure 11. Split and mix synthesis can be used to synthesise large numbers of different particle-bound oligonucleotide or peptide probes, with each particle surface consisting of multiple copies of a single sequence. The above example represents oligonucleotide synthesis. The number of probe-particle pairs increases exponentially with repeated coupling cycles

1.4 Probe immobilisation

A well designed multiplex DNA hybridisation array affording real-time sample analysis requires many short probe sequences to be immobilised in known locations, whether they be to a planar surface in a grid-like pattern or to the surface of particles which have been encoded. This immobilisation has to be sufficiently stable to limit probe movement throughout the timescale of the assay as any probe mixing would render the array unreadable.[149] The choice of immobilisation technique used to attach probes therefore predominantly depends upon the robustness of the linkage formed. Other considerations when developing new array technology include the spacing, density and orientation of oligonucleotide sequences in order to maximise hybridisation, the minimisation of DNA and other biomolecule nonspecific binding and (with the aim of being a commercial success) ease of manufacture and cost.[105] The relative merits and disadvantages of commonly encountered immobilisation methods are discussed below.

1.4.1 Adsorption

Adsorption relies on electrostatic, hydrogen bonding or Van der Waals forces between two functionalities. Often in the case of oligonucleotide probe immobilisation a positively charged surface would be required to interact with the negatively charged phosphate backbone of the probes. An example of the immobilisation of DNA to surfaces via electrostatic interactions is in the use of cationic microparticles as a drug delivery system. In this system DNA is adsorbed onto the particle surface and is slowly released over time (75% unbinding over the course of 14 days).[150] Another example is in hybridisation sensors where DNA has been adsorbed to the sensor tip of a quartz crystal microbalance (QCM).[151] Note that neither of these examples risk contact between different oligonucleotide sequences.

Attachment by adsorption has multiple disadvantages which preclude its widespread use in suspension and microarray technology. Firstly, immobilisation is not permanent and once probes start migrating across or between surfaces the array would sooner or later become useless.[150,152] Any working array would not allow for much variation of pH range, ionic strength, temperature or probe length as alteration of these parameters could disrupt absorption.[153,154] Secondly, as probes are held to the surface via electrostatic attraction via backbone phosphate groups, the oligonucleotide is relatively flat on the surface.[155] This orientation is less than ideal for hybridisation as the probe would be less accessible to cDNA in the bulk sample, the formation of the rigid duplex would be less favoured (energetically) too as any change in probe orientation must weaken interaction with the surface.[156] A final drawback of using this type of probe immobilisation is that a positively charged surface (by nature of the design) is indiscriminate of the negatively charged species it attracts, therefore significant nonspecific binding of target DNA and acidic proteins would be expected. In summary, adsorption is not an ideal method for probe attachment with ease of manufacture being its only major advantage over other methods; as probe and surface simply require mixing followed by washing steps assays can be set up without special knowledge. Adsorption is often used in arrays where probes are physically separated so mixing cannot occur, a common example being in enzyme-linked immunosorbant assays (ELISAs) performed in a 96-well plate format.[157]

1.4.2 Affinity capture

The specific non-covalent interactions between proteins and their relevant ligands can be utilised for the immobilisation of biomolecular probes to surfaces. Generally surfaces are functionalised with a binding protein whilst the probes are modified with the corresponding binding ligand, following mixing of the two species, the probe becomes immobilised on the surface via a relatively strong protein-ligand interaction.[158] The suitability of a protein-ligand pair for use in affinity capture mostly depends on the binding equilibrium dissociation constant (K_d) and rate constants (k_{on}, k_{off}) which give measures of the strength and speed of binding, the stability of the protein and the orientation upon immobilisation (where the binding site must be accessible to the ligand). Examples of affinity binding systems include using Penta-His antibody or Ni^{2+} nitrilotriacetic acid (Ni-NTA) to bind His-tagged probes,[159,160] protein A to bind antibodies[161] and avidin or streptavidin to bind biotin.[162,163]

The (strept)avidin biotin system is often used in the design of biological assays due to having the strongest ligand binding known, other attributes contributing to its widespread use include being highly stable withstanding a wide pH range, denaturants and high temperatures (up to 100 °C when ligand is bound).[164,165,166] As both proteins are tetrameric in structure, each binds four biotin ligands, this is useful as upon immobilisation on a surface binding sites may be sterically hindered but having multiple binding sites increases the chances of some sites being accessible. The orientation of immobilised proteins can sometimes be manipulated to optimise ligand accessibility, for instance by attaching through a specific amino acid residue on the opposing face to the binding site. ELISAs often make use of the (strept)avidin-biotin system both for the immobilisation of probes and as a signalling molecule.[167,168] A good example of the system being used in a biosensor is in the immobilisation of DNA probes to avidin-functionalised quartz crystal microbalances, used to study DNA hybridisation.[169]

Affinity immobilisation is used in commercial assay protocols as it can be very user friendly and flexible; surfaces can be pre-functionalised with the capture protein and different probe sets can be purchased linked to binding ligands. All the modifications requiring operator-training and hazardous chemicals are therefore handled by the

manufacturer, leaving the end user with the simple task of mixing ligand-probes with the functionalised surfaces in an aqueous buffer.[114]

Despite its incorporation in commercial bioassays, this type of probe immobilisation is far from ideal for use in biological sensing. This is partly due to frequently observed increases in non-specific binding, resulting in high background readings, false positives and a shortening of the array's life-expectancy. Non-specific binding occurs because of the charged nature of the capture-protein, avidin for example has a pI of 10 and a net positive charge under physiological conditions, thus avidin-functionalised surfaces have a tendency to attract negatively charged molecules. This unwanted attribute can be reduced by using engineered proteins, like NeutrAvidin and avidin-DN in which parts of the structure not essential for correct protein folding and functionality are modified to alter the overall charge and hydrophilicity.[170] Another limitation to affinity capture is the non-permanent nature of the linkage formed, most assays utilising affinity immobilisation will remain intact and usable for a few weeks, the reported half-life of the avidin-biotin complex is 200 days making it potentially usable for long term assay setups, but this is an exceptionally strong capture system.
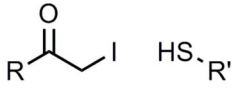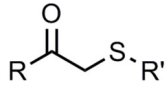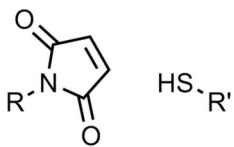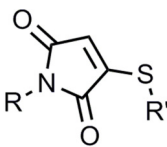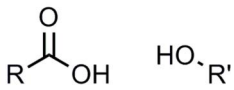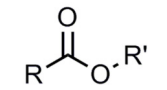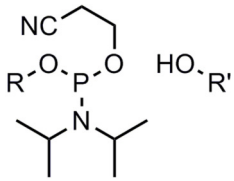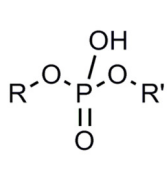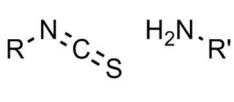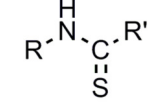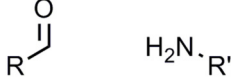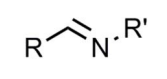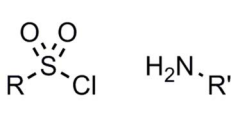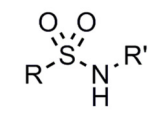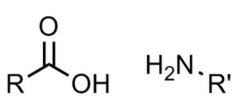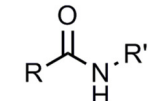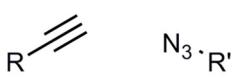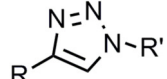
1.4.3 Covalent bonding

For many array designs a more stable probe immobilisation is required, whether for long-term storage, long-term data collection or to increase sensitivity and fidelity.[154] Immobilisation via a covalent bond is desirable, forming a permanent linkage between biosensor surface and probe moiety.[171] Chemical modification of the surface also allows a finer control of some surface properties; this can be advantageous as important design considerations including probe spacing, probe loading levels, charge, hydrophilicity and non-specific binding may be manipulated.

Due to the scope of chemical modification available probes can be covalently immobilised on most materials desirable for use in biosensing, including glass, metal and polymeric surfaces.[172,173,174,175] A summary of some of the more widely used covalent linkages is given below (Table 1).

Table 1. Some common covalent chemistries for the conjugation of modified (oligonucleotide) probes to functionalised surfaces

Linkage	Example reagents	Resultant crosslinking	Notes
thioether			Reagents unstable.[176]
succinimidyl thioether			Useful for site-specific coupling,[177,178] linkage susceptible to hydrolysis.[179,180]
ester			Susceptible to hydrolysis.[181]
phosphate			Used in oligonucleotide synthesis.[136,137,138]
thiourea			Linkage unstable.[182]
imine			Often reduced to amine, linkage not inert.[174,175]
sulfonamide			Sulfonyl chloride reagent unstable,[183] linkage formed very stable.[184]
amide			Stable linkage, used in peptide synthesis.[174,175]
1,2,3-triazole			Stable linkage, few side reactions.[185,186]

Covalent coupling can be used to maximise specific binding to immobilised probes by controlling probe distribution and orientation, the former by the use of blocking reagents to space out reactive groups on a surface to the desired loading density and the latter by selection of the correct coupling chemistry to react with the desired chemical group on the probe. Intelligent selection of spacer and blocking groups can also impart beneficial properties to an array (in addition to their use in optimising probe loading density). An example of this would be the use of polyethylene glycol (PEG) groups to increase the hydrophilicity of hydrophobic surfaces, as it has been

shown that non-specific binding of organic (and biologically derived) matter decreases with increased hydrophilicity.[187,188] PEG groups can be immobilised with a range of terminal functionalities making them ideal for use as linkers baring reactive groups.

Covalent immobilisation of probe molecules is more involved than either adsorption or affinity capture as it can require the use of hazardous chemicals, fume-hoods and experienced technicians. Due to the permanent nature of covalent immobilisation it is ideal for preparing arrays well in advance of use, with suitable storage times in the range of months to years.[189,190] Covalent probe coupling is therefore routinely used in most commercial array formats where multiplexing kits are sold with probes pre-arrayed.

1.4.4 On-particle probe synthesis

The immobilisation methods summarised so far have been examples of 'top-down' approaches where probes have been attached as a fully formed unit. An alternative to this is the 'bottom-up' synthesis of probes directly on the surface. Oligonucleotide and peptide synthesis is well established and is usually performed on the solid-phase with the final step in any synthesis being deprotection and cleavage from the support resin (Scheme 1), thus it is often possible to grow probes on a surface by modifying the established synthesis protocols and omitting the final resin cleavage step.[138,191] Synthesis cycles generally require anhydrous conditions and the expertise of trained technicians but often they are automated to greatly reduce overall reaction times.

Aptamer synthesis can be adapted to very quickly form an array of particle-bound probes with an extremely high (multiplexing) capacity by using split and mix chemistry (Figure 11).[145,146] With the development of particle encoding and reading technologies it is conceivable that split and mix synthesis could be tracked for each individual particle, the location of all resulting probes would then be identifiable, however to date no examples of this have been published.

1.5 An overview of the 4G project

The 4G project was so named as its main aim was to develop technology capable of sequencing the entire human genome within a day; at the time of the project's conception the human genome was overestimated to be 4 billion, or 4G bases long (the "3.2G" project, though more accurate, did not warrant a name change).

This ambitious aim was to be accomplished by developing novel microparticle encoding technologies and by realising the potentials of combinatorial chemistry for the tracked split and mix synthesis of large libraries of short oligonucleotide probes. Assay reading was to make use of a custom microfluidic fluorescence detector/particle decoder/particle sorter setup, reading "on the fly". Although the original goal was ultimately to prove unachievable, advances were made, particularly within the fields of bioinformatics, microparticle encoding and microparticle functionalisation.

Funding came in the form of a five year research grant from the EPSRC Basic Technology Program. This multidisciplinary project was initially a collaboration between two mostly autonomous groups based at the University of Southampton (M. Bradley) and the University of Cambridge (T. Bland), later the Southampton group split with the original principal investigator moving to the University of Edinburgh (to be replaced in Southampton by H. Morgan). The Cambridge group had a particular focus on magnetic encoding technologies, whilst work at Southampton explored optical and holographic encoding, assay development and analysis. The following chapter summarises advances made by others in the 4G project at the University of Southampton to which the results in this thesis are complementary.

1.5.1 Bioinformatics

The modelling of short duplex hybridisation and melting within the bioinformatics group has lead to improved predictive models of probe and target interactions.[192] These in turn can be used to design oligonucleotide probe-sets where all complementary probes exhibit a similar duplex T_m, this allows the conditions under

which multiplex assays are performed to be optimised to best distinguish between fully complementary sequences and those mismatch.[193]
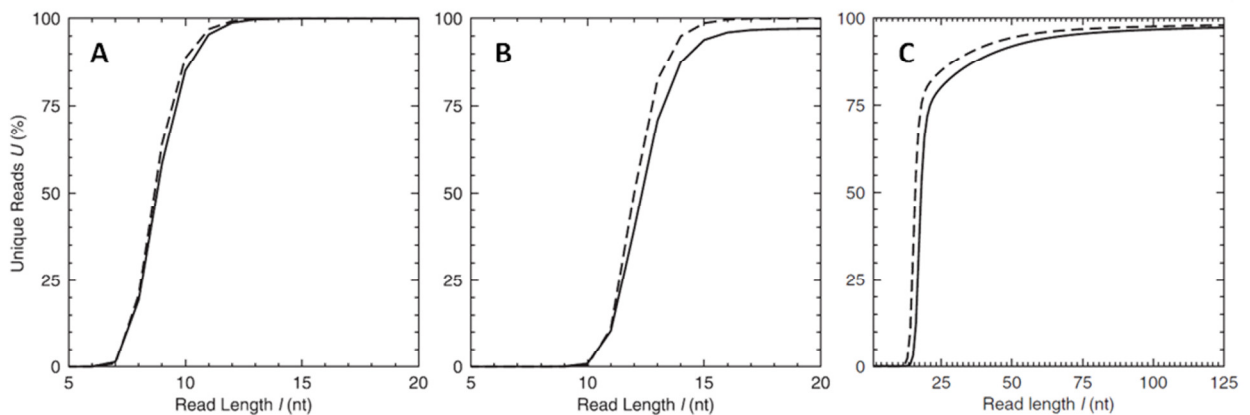
Figure 12. The amount of an organism's genome which can be ascertained by short read (hybridisation) sequencing using oligonucleotide probes of differing lengths (read lengths), A. λ-phage, B. *E. coli*, C. human. Incomplete sequencing is the result of repeated sequences of genome which cannot be detected using short probes. Dotted lines simulate the sequencing of a random genome of comparable length to the organisms' selected[87]

Fundamental to the original project goal was the determination of the probe length required for an accurate sequencing of the human genome.[87] By creating models incorporating total sequence length, sequence repeats and the length of probe used (read length), the total amount of an organisms genome that could be sequenced was determined. For organisms coded by very short genomes, for example the viral λ-phage (GenBank accession no. NC_001416 size: 48 kb) almost complete sequencing could be achieved by analyzing the hybridization of probes just 13 bases long (13-mer) (Figure 12). However for larger genomes, subsequence repeats result in a requirement for longer probes, for example sequencing 97% of the *Escherichia coli* (GenBank accession no. NC_000913 size: 4.6 Mb) genome needs probes 18 bases long. A further complication in the genomes from more complex organisms (like *E. coli*) are the presence of larger repeat sequences, including genes or intergenic repeat units and to distinguish between these very long oligonucleotide probes are required.[194] Therefore it was concluded that it is only practical to obtain a partial genome of organisms more complex than viruses by short probe hybridisation assays. These problems are greatly multiplied for the human genome where the reading of 97% of the sequence would require probes 80 bases long (4^{80} unique

probes!). The poor sensitivity of a hybridisation array using probes this long means it could not be used to differentiate between complementary sequences and those incorporating a single base mismatch, a level of accuracy which requires probes to be less than 30 nucleotides in length.[88]

Therefore the original project aim to sequence an entire human genome in a day using a hybridisation array was determined to be practically impossible due to the incompatibility of the technology to the task. However it had been shown that the assay principal could be used for the sequencing of very small (viral) genomes which would be of use, for example, for monitoring and identifying cold and flu viruses subtypes.[115] The array could also be used for the detection of specific known sequences, for example, for forensic uses and testing for pre-mapped genetic diseases.

1.5.2 Microfabrication of polymer particles

Microparticles were fabricated by crosslinking monomeric SU-8 (**6**), an epoxy-based negative photo resist which can be used to fabricate structures with a high aspect ratio (Figure 13). SU-8 was considered ideal due to its already widespread use for fabrication of well defined, high aspect ratio microstructures, necessary for the particles' coding features.[195] The particles were fabricated on silicon wafers in batches of 160,000 using the general methodology described (Figure 13).[196] For the purposes of encoding it was important to control polymerisation by selectively blocking UV transmission as only areas of the monomer exposed to light crosslink, the shape of particles can therefore be controlled by placing a mask between monomer and light source (photolithography). An additional advantage to SU-8 which our research exploited is the residual surface epoxide which remains from incomplete cross-linking. This could be used in subsequent steps as a handle for functionalisation.

It should be noted that throughout the project the particles suffered from a lack of consistency after fabrication. Particles exhibited a range of surface epoxide loading densities, changing solvent swelling properties and a varying of the structural

definition regarding encoding features. A number of factors contributed to this variation including the method of production (batch processing, months between each batch, fresh and not so fresh reagents), a number of different researchers tasked with fabrication and changes to the fabrication facilities used (particles were firstly made on-site in the Mountbatten Building which was destroyed by fire, production was then shifted to the École Polytechnique Fédérale de Lausanne (EPFL), Lausanne before returning to temporary cleanrooms constructed at Southampton). On the whole, these causes were unavoidable, but the problem of inconsistency affected all areas of the project.
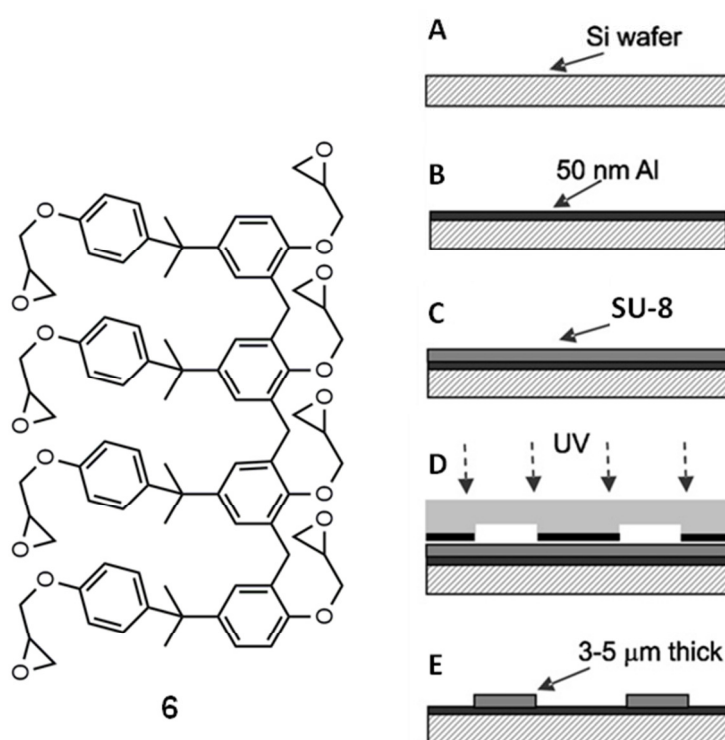
Figure 13. Structure of monomeric SU-8 (6) from which microparticles are fabricated. Particle fabrication uses silicon as a substrate, A, onto which a sacrificial layer of aluminium is deposited, B. A solution of SU-8 monomer, photoacid initiator and solvent is spin coated to a thickness of 5 μm and heated to drive off solvent (soft bake), C. After cooling, the monomeric mixture is selectively exposed to UV radiation through a mask and heated in a post exposure bake (PEB), D, where areas exposed cross-link. Uncrosslinked SU-8 is then removed in a developer solution leaving particles mounted on the Al/Si substrate, E. When required, particles are released from the substrate using a solution of 2% ammonium hydroxide to etch the aluminium sacrificial layer[196]

1.5.3 Encoding technologies

Developing novel encoding technology was a principle aim of the project with the team based in Southampton focussing on diffractive encoding methods.[111] By fabricating the particles to be tiny, one dimensional diffraction gratings the angle of any intersecting parallel light gets bent, the magnitude of this diffraction is controlled by the distance between individual features on the particle which are a product of the photolithographic fabrication process (Figure 14).[197] Different particles are distinguished by the degree to which incident light is diffracted, accomplished by intersecting the particle with a laser beam.
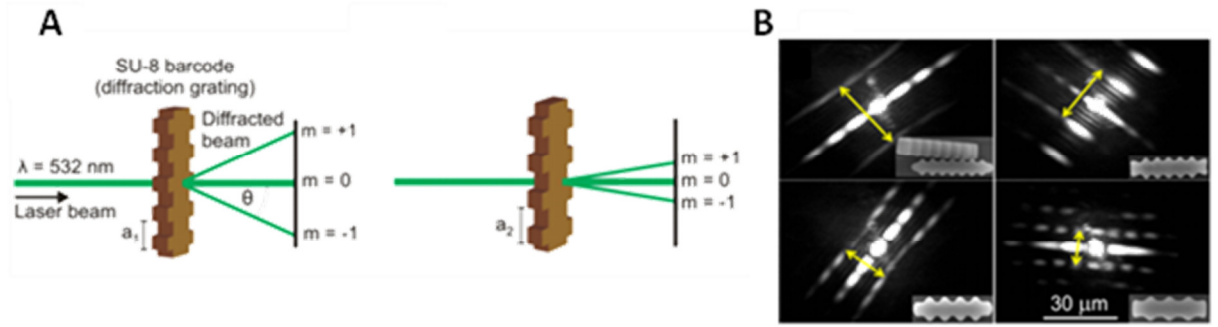
Figure 14. A. Principles of simple, 1 dimensional diffraction gratings (encoded microparticles) showing how the angle of diffraction decreases as the size of grating features increases. **B.** SEM images of 4 different SU-8 microparticle diffraction gratings and their corresponding diffraction patterns as projected onto a screen. The code is determined by measuring the distance between 1st order diffraction lines as indicated by the yellow arrows. The scale bar refers to the SEM particle images[197]
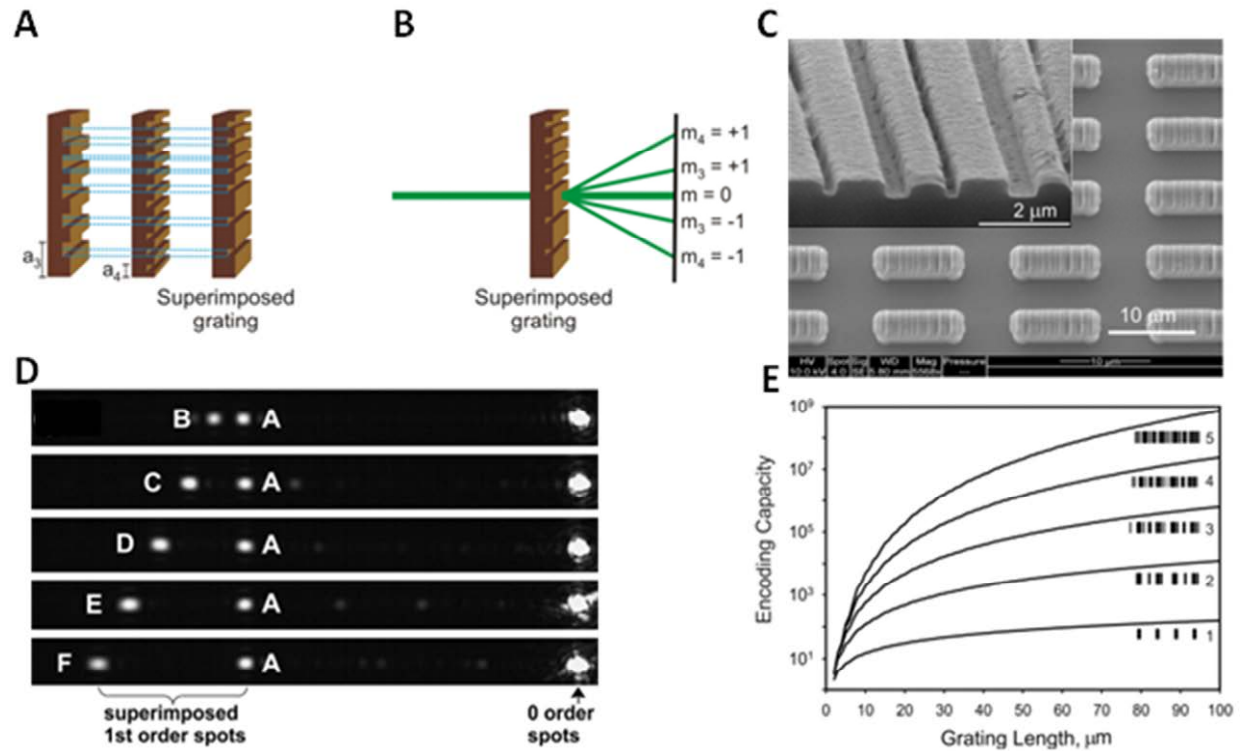
Figure 15. A. In order to increase the system's encoding capacity (the number of unique diffraction gratings), two or more gratings may be superimposed, **B.** the diffraction resulting from parallel light intersecting these two superimposed gratings exhibits two angles of 1st order diffraction. **C.** Superimposed diffraction gratings produced by nanoimprinting into SU-8 blocks, this technique results in better feature definition than photolithography. **D.** Diffraction patterns from five different superimposed diffraction gratings. **E.** The encoding capacity as a function of grating length and degree of superimposition, more than 1 million unique codes can be fabricated using five times superimposed, 30 µm gratings[198]

It was observed that encoding capacity could be increased by overlaying multiple diffraction gratings to form individual superimposed gratings, this resulted in a more complex diffraction pattern and would allow millions of unique microparticles to be produced (Figure 15).[198] An extremely high encoding capacity procedure was also developed using holographic encoding to produce two dimensional diffraction gratings (Figure 16).[199]
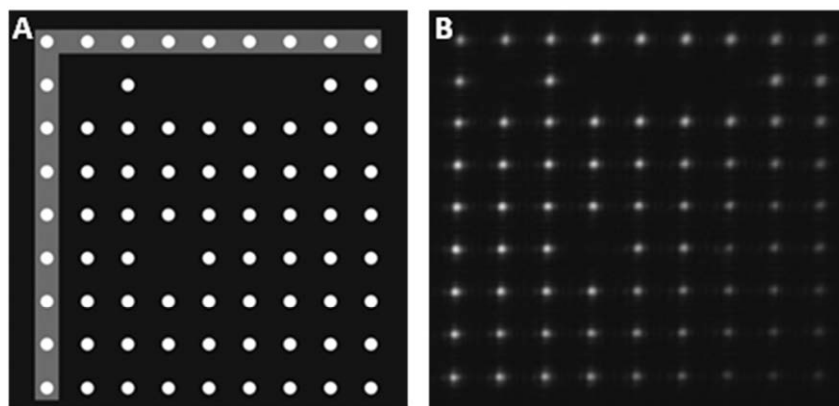
Figure 16. A. Theoretical diffraction pattern produced from a two dimensional diffraction grating, the output being binary. Highlighted along the top and down one side are alignment features. B. A real diffraction pattern as projected onto a screen from a 2D SU-8 diffraction grating. The encoding capacity of this particular example is 2^{64} unique codes[199]

1.5.4 Biological assays

With the realisation that human genome sequencing using short read oligonucleotide hybridisation was practically impossible, assay development was shifted towards more realistic targets.[87,88] The detection of short lengths of specific genomic sequence for disease diagnostics and genotyping was one target, this required particle functionalisation with oligonucleotide probes and a similar hybridisation assay format proposed for sequencing. Another target application was for use in multiplexed immunoassays, for the detection of human antibodies and cytokines as signallers of disease.[200,201] The development of these two array formats proceeded in parallel, with development of oligonucleotide arrays being the main focus of the work described herein.

1.5.5 Analysis technologies

To monitor and quantify bioassay results a range of analysis technologies were required. From the outset particles were analysed using a fluorescence activated cell sorter (FACS) and by fluorescence microscopy.[202,203,204] The FACS worked by forming solution micro-droplets from a "cell" (or in our case a microparticle) suspension, the droplet fluorescence would then be measured at a number of wavelengths. Most droplets are empty and give no signal, however droplets containing a single particle result in a change in fluorescence. The FACS was able to measure the fluorescence of large sample sizes very quickly (~500 particles min^{-1}) and at multiple wavelengths in parallel. Limitations to FACS use included large standards deviations in the data output meaning the measurement of small sample sizes was prone to large errors and the inability to distinguish between differently encoded particles. The FACS was therefore generally used for assay development and optimisation where multiplexing capabilities were not required.

Fluorescence imaging of particles using microscopy could only be achieved at a much lower throughput but yielded detailed information as to the uniformity of surface functionalisation, lower standard deviations for intensity measurements and enabled differently encoded particles to be distinguished.
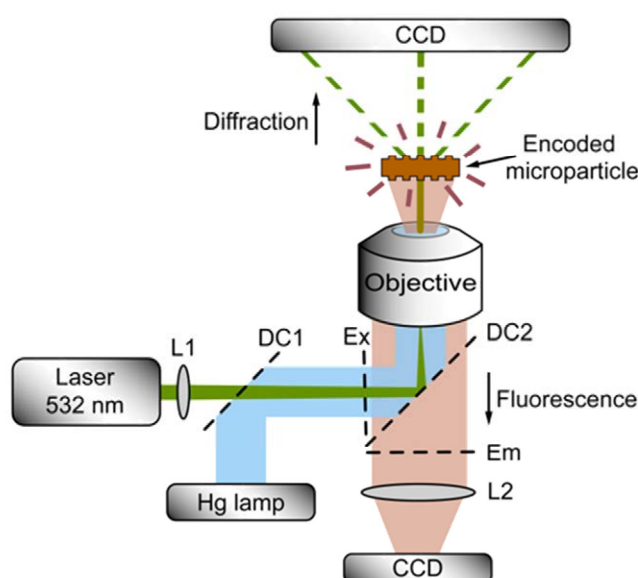
Figure 17. A schematic of the integrated particle fluorescence/code reading device which allowed almost concurrent measurements of fluorescence intensity (reflectance mode) and diffraction pattern (transmission mode) for individual encoded microparticles

As the project advanced a dedicated integrated particle fluorescence and code reading device was constructed (Figure 17). Particles arrayed on a microscope slide could be aligned with an excitation source (mercury lamp) and the reflected light (fluorescence) imaged. Then by changing the light source to a green laser the diffraction pattern of transmitted light imaged. The fluorescent signal and the encoding could thus be ascertained for individual particles, useful for the analysis of multiplexed bioassays.

2.0 Hybridisation suspension arrays utilising affinity immobilisation of oligonucleotide probes

When developing encoded microparticle-based multiplexed suspension arrays one key consideration is the type of linkage used to attach probe to particle, this must be stable, easy to construct and have little influence on the probe binding kinetics. For this project, an affinity-based probe immobilisation method was developed utilising the exceptionally strong binding between the hen egg white protein avidin and its ligand vitamin H, also called biotin.[205,206] From reported dissociation data the avidin-biotin complex has a half-life ($t_{1/2}$) of over 200 days, which would allow different probe particle sets to be stored together for months without significant loss of probe from the surface.[162]

We chose a tetrameric form of avidin (designated avidin DN) which is isolated by affinity chromatography from hen egg white, it is claimed that this form of avidin exhibited very low nonspecific binding to nucleic acids.[207] We investigated both affinity and covalent protein immobilisation methods and thoroughly characterised the strength of ligand binding to these functionalised particles. Avidin DN particles were also used for the singleplexed and multiplexed identification of oligonucleotides using encoded microparticles.

2.1 The protein functionalisation of SU-8 particles

SU-8 microparticles were functionalised with avidin DN using three different methodologies. Two methods resulted in the covalent immobilisation of protein to carboxyl functionalised particle by use of carbodiimide coupling reagents; either with coupling reagents *in situ* (Type I) (**10**) or by the pre-activation of the acid moiety using *N*-Hydroxysuccinimide (NHS) (Type II) (**11**) (Scheme 2). The third method first involved the functionalisation of the particle surface with biotin followed by immobilisation of avidin DN by affinity capture (Type III) (**13**). These immobilisations of avidin followed a divergent synthetic route where the native epoxide surface of the SU-8 particles (**7**) first underwent a nucleophilic ring opening with the *bis*-amine Jeffamine® ED-900® (**14**) yielding amine functionalised supports

(**8**) (amine was quantified by reaction with ninhydrin, surface loading density was found to be $5.3 \pm 0.9 \times 10^{-9}$ mol cm^{-2}). Next, depending upon the desired protein immobilisation strategy the amino surface was acylated using either succinic anhydride or biotin, resulting in carboxy (**9**) and biotin (**12**) functionalised surfaces respectively. Avidin DN was covalently coupled to the succinated particles using the coupling reagent *N*-Ethyl-*N'*-(3-dimethylaminopropyl)carbodiimide hydrochloride (EDC) to activate the immobilised carboxylic acid moieties to nucleophilic attack by protein lysine residues. This coupling was performed both in a single step with EDC *in situ* (SU-8 Avidin DN Type I (**10**)) and in two steps where the acid was first reacted with EDC and NHS to form the activated but stable NHS ester, thus allowing for excess coupling reagents to be washed from the particles before the subsequent addition of protein (SU-8 avidin DN Type II (**11**)). Avidin DN was immobilised by affinity capture to biotin modified particles simply by the incubation of the particles with the protein (SU-8 avidin DN Type III (**13**)).
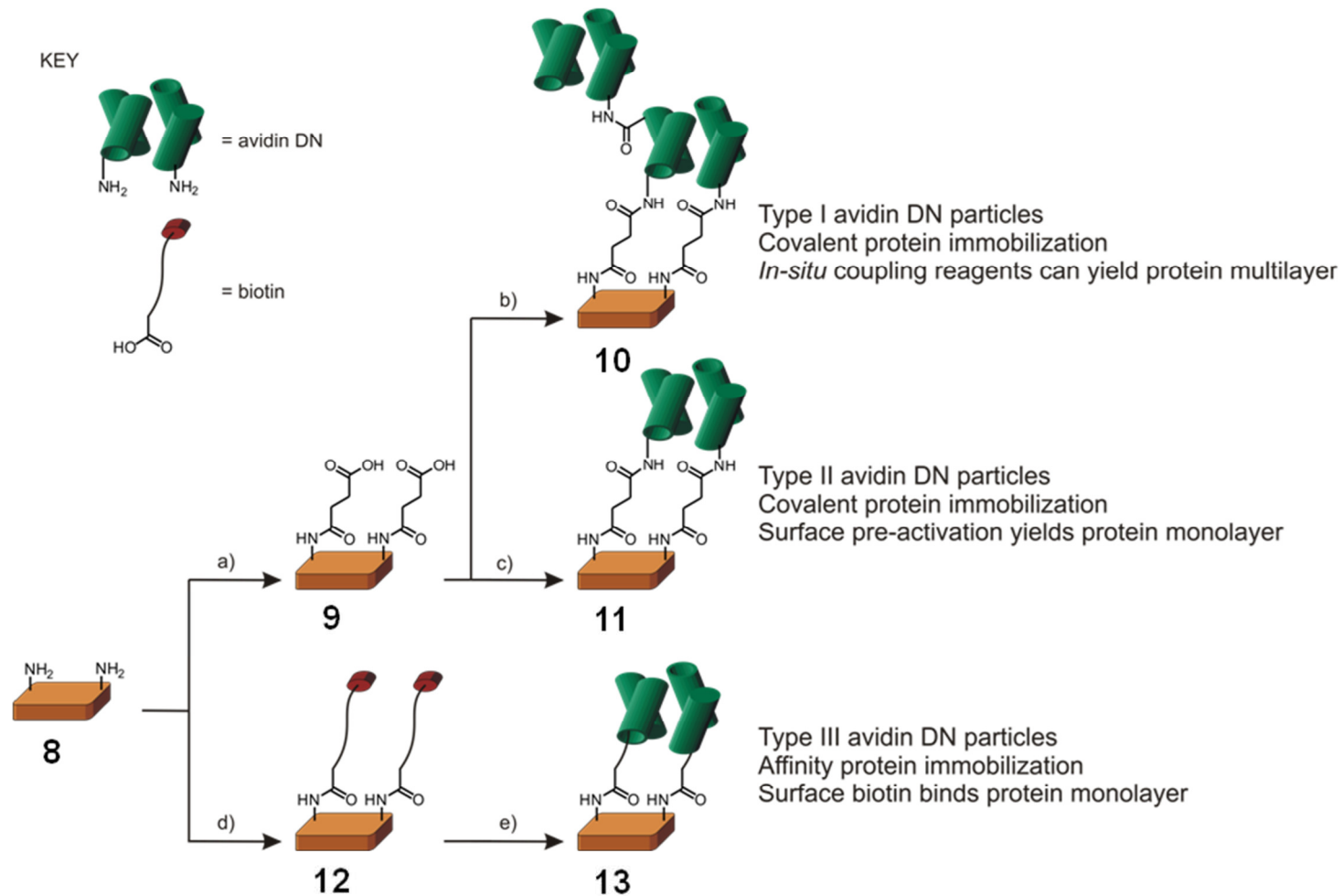
Scheme 2. Three different routes to avidin-functionalised particles starting from amine functionalised particles (8). a) succinic anhydride, DMAP, DIPEA, DMF, b) avidin DN, EDC.HCl, imidazole buffer pH 7.0, c) i) EDC.HCl, sulfo-NHS, MES buffer pH 5.0, followed by avidin DN, PBS pH 7.4 d) biotin, DIC, DIPEA, DMF, DMSO, e) avidin DN, SSPE buffer pH 7.0

Immobilised protein was quantified using the bicinchoninic acid (BCA) assay (a colourimetric assay determining the reduction of Cu^{II} to Cu^{I} ions in the presence of peptide bonds) where all three immobilisation routes resulted in higher loading densities of avidin than predicted (i.e. formed surface multilayers).[208,209] The crystal structure of the avidin tetramer indicates dimensions of $5.6 \times 5 \times 4$ nm.[210] Assuming avidin is close packed on the surface, each protein tetramer covers a minimum area of 2×10^{-13} cm^2 (5×4 nm). The BCA assays performed on the avidin immobilised particles found an average protein tetramer loading density of 3.5×10^{-11} mol cm^{-2}, which equated to a monolayer of close packed avidin tetramers measuring 4.2 cm^2, therefore the particles had approximately four times more protein than would be expected if a monolayer were forming. After prolonged suspension (48 h) of the particles in wash buffer (SSPE (5×), 0.02% Tween-20®) buffer, with occasional replacement of buffer, BCA assay protein quantification was repeated and loadings were found to have decreased for all three particle types, with protein quantities now equivalent to monolayers (Table 2). Extended suspension in buffer (4 weeks) resulted in no further reduction in protein loading suggesting the linkage of avidin DN to SU-8 particles was strong. Subsequent immobilisations of protein to microparticles were followed by a thorough wash step to remove all nonspecifically bound protein.

The stability of protein immobilisation was further investigated by the attachment of a fluorescently labelled avidin DN by all three methodologies. Extended washing of the particles over the course of 4 weeks resulted in no loss of fluorescence intensity. Furthermore, the agitation of these labelled protein particles with both native epoxy SU-8 particles and (unlabelled) avidin DN particles showed no changes to the fluorescence signal of any particle type. These results reinforced the belief that the linkage between particle and protein was stable for all three immobilisation types and furthermore, the surface-bound avidin tetramer was stable with no breakdown into monomer subunits being observed.

Table 2. A summary of Avidin DN functionalised SU-8 particles with protein immobilised by three routes, showing protein loading densities and the maximum binding density (b_{max}) of the biotinylated and fluorescently labelled oligonucleotide FP1

Avidin immobilisation method	Avidin tetramer loading (mol cm^{-2}) ($\times 10^{-12}$)	Avidin layers	FP1 b_{max} (mol cm^{-2}) ($\times 10^{-12}$) (SSPE ($5\times$) buffer pH 7.0, 0.02% tween-20$^{®}$)		Avidin sites showing biotin affinity (%)
			specific	non-specific	
I (EDC *in situ*) (**10**)	11.58 ± 4.36	1.39 ± 0.53	0.61 ± 0.02	0.95 ± 0.05	1.33 ± 0.33
II (NHS ester) (**11**)	6.69 ± 1.02	0.81 ± 0.12	1.73 ± 0.06	1.29 ± 0.06	6.48 ± 0.68
III (affinity capture) (**12**)	8.26 ± 2.25	0.99 ± 0.28	0.75 ± 0.02	0.36 ± 0.07	2.28 ± 0.43

Though final protein loading was found to equate roughly to a monolayer by all three immobilisation strategies, Type I particles (with coupling reagent *in situ*) were found to have the highest avidin loading density. This may indicate a limited degree of protein to protein intermolecular coupling with cross linking occurring between the lysine residues found on the surface of one tetramer and aspartate or glutamate residues on a different tetramer.

2.2 Proof of principle DNA hybridisation assays

Type I avidin DN SU-8 particles (**10**) were used to test the principles of the DNA hybridisation assay. Two biotinylated oligonucleotide probes, **PA** and **PB**, were incubated separately with samples of Type I particles, after 20 minutes the particles were washed to remove any excess probe which had not immobilised specifically. The two samples of probe particles were each split 3 ways allowing for hybridisations at 55 °C to three labelled target sequences, **TA, TB** & **T2** (Scheme 3), samples of particles were washed and then analysed by flow cytometry (FACS) and fluorescence microscopy. The three targets represented complementary, partially mismatching and completely mismatching sequences, the intensity of particle fluoresce acted as a measure of hybridisation.

Both complementary targets were found to have hybridised to the relevant probe particles as indicated by the high fluorescence signal of 7300 a.u. (FACS, gain = 500 V), whereas particles exposed to the completely mismatching sequence showed no fluorescence increase compared with blank SU-8 particles, 1000 a.u.. Though these results were expected, they validated the principles of the particle-based hybridisation assay, showing the successful hybridisation of complementary sequences and the discrimination from completely mismatching sequences. This result also showed that the target DNA exhibits very little nonspecific interaction with the immobilised probe particles.

Interestingly, the two partially mismatching sequence pairs differed in behaviour with a duplex forming between **PA** and **TB**, 6500 a.u. whilst no hybridisation was detected for the oligonucleotides **PB** and **TA**, 1000 a.u.. The high thermal stability of the partially mismatching **PA/TB** duplex can be explained by the relatively strong non Watson-Crick base pairs formed; studies on the hybridisation between short DNA sequences containing single base mismatches have consistently found G·T and G·A mismatches to be the most stable, and three of these such interactions are likely in any **PA/TB** duplex formed.[211,212,213] Concerning the lack of hybridisation between the partially mismatched **PB** and **TA** sequences at 55 °C, the same studies also found A·C to be one of the most destabilising mismatches, with T·A and T·T interactions only displaying mediocre stability. So the **PA/TB** duplex would be expected to have a greater thermal stability compared with the **PB/TA** duplex. It should be noted that the stabilities of non Watson-Crick base pairs are dependent upon multiple factors including the flanking bases (nearest neighbour) in the sequence, the order of mismatch stabilities is therefore variable and dependent on the specific environment within each duplex.[214] These particles were also visualised using microscopy, white light and fluorescence images of the complementary and partially mismatching immobilised-probe particles after mixing with the labelled target, **TA**, are shown (Figure 18).
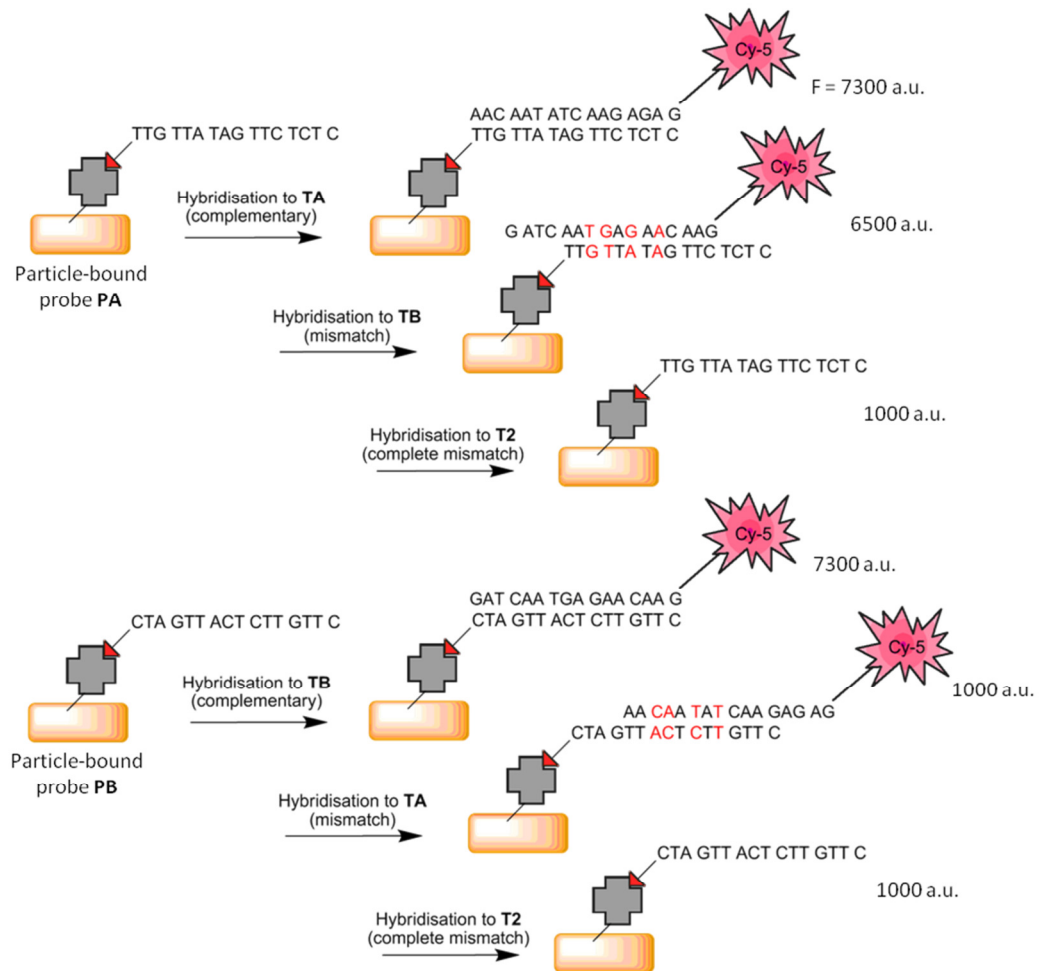
Scheme 3. A diagram of the DNA hybridisation array proof of principle showing the hybridisation of different fluorescently labelled target oligonucleotides to immobilised-oligonucleotide probe SU-8 particles
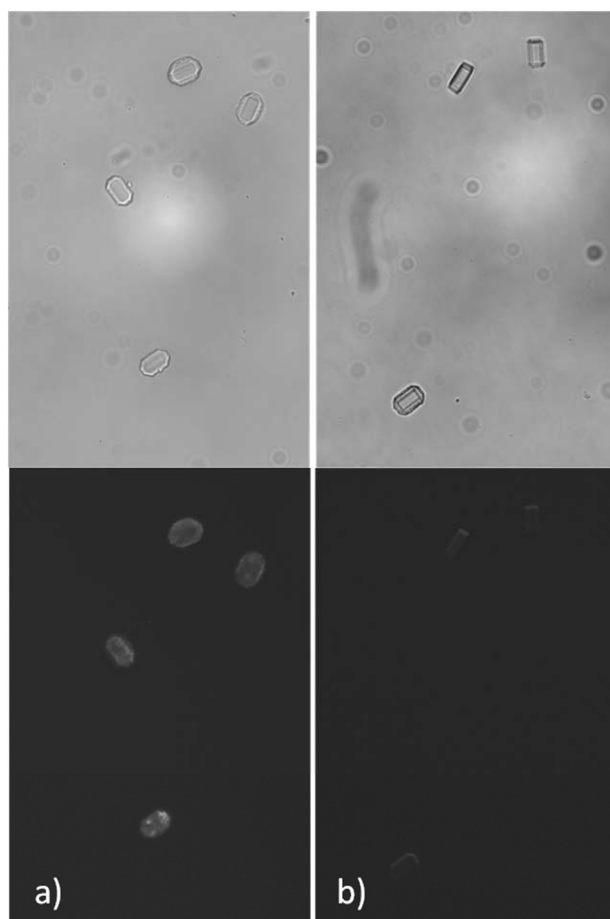
Figure 18. White light (top) and fluorescence microscopy images of labelled oligonucleotide target, TA, exposure to a) complementary immobilised-probe, PA, particles and b) 4 base mismatching immobilised-probe, PB, particles

2.3 Probing the nature of the biotinylated-probe/avidin-particle interaction

The binding of biotinylated probes to avidin functionalised particles was studied using the biotinylated and fluorescently labelled oligonucleotide, **FP1**. This 16 base long (16-mer) probe was labelled with cyanine-5 (Cy-5 (**14**)) fluorophore at the 5' end and biotin at the 3', **FP1** was used as a standard throughout the studies detailed in this chapter. Fluorescence intensity on the particles was measured using flow cytometry and by fluorescence microscopy. The intensity of particle fluorescence is proportional to the concentration of **FP1** bound; using this observation the loading density of affinity captured **FP1** could be measured. It should be noted that at higher concentrations in aqueous solution cyanine dyes have been shown to dimerise which leads to fluorescence quenching, therefore a very high density surface layer might also self-quench.[215]

FP1 was captured on avidin coated particles by agitation in SSPE (5×) buffer with 0.02 % Tween®-20 ([**FP1**] ≤ 100 nM) followed by thorough washing in buffer. The observed increase in particle fluorescence (microscopy) indicated **FP1** had bound to all three particle types. Type II avidin particles were found to have approximately twice the probe loading compared with the other two particle types, which both exhibited similar loading levels.

Titrating **FP1** against Type I avidin particles (**10**) enabled the conversion of measured fluorescence intensity to a calculated immobilised probe density and gave information on both the proportion of bound to free probes at any given probe concentration (K_d) and the maximum probe binding (b_{max}) (Figure 19).
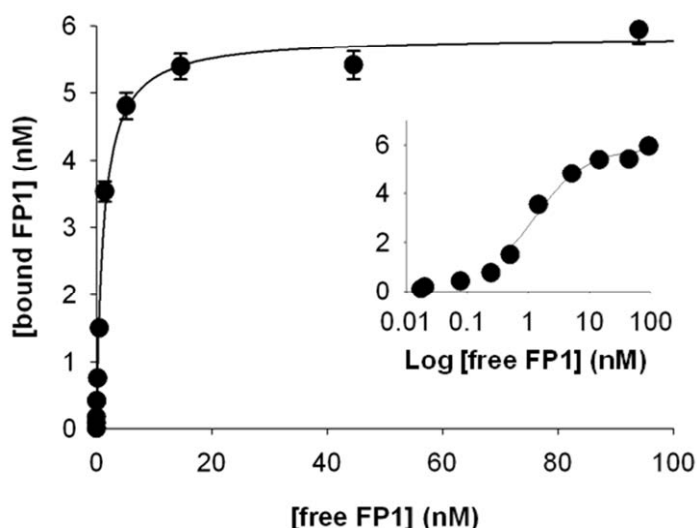
Figure 19. The titration of the labelled biotinylated oligonucleotide FP1 against Type I avidin SU-8 particles (1 mg mL^{-1}, 5.64 cm^2 mL^{-1}), inset: log plot

The **FP1** loading density upon saturation (b_{max}) was extrapolated as $1.03 \pm 0.02 \times 10^{-12}$ mol cm^{-2}. The K_d was found to be $1.2 \pm 0.1 \times 10^{-9}$ M, a figure much greater than the reported value of binding between unmodified (wild-type) avidin and biotin (0.57×10^{-15} M).[162] A number of theories were proposed to explain the binding being more than 6 orders of magnitude weaker than the wild-type system. Firstly the avidin DN and biotin are extensively modified; the protein being covalently tethered to a support and the ligand (244 Da) being conjugated with a labelled oligonucleotide (~3 kDa). Secondly, avidin DN is one specific, affinity-isolated form of the protein;

reported avidin studies have mostly worked with wild-type avidin containing a mixture of all forms of the protein, not all forms may display identical affinity for biotin.[216] Thirdly, immobilisation to solid supports often leads to a reduction in the rate of any reactions/binding events due to poor bulk mixing at the surface and this may affect the position of the binding equilibrium.[217] Finally, the value obtained for the equilibrium dissociation constant may represent the mean binding of a rather complex system, that is to say there may be more than one type of binding event, with each type displaying different affinities. In an attempt to better understand the binding between **FP1** and the SU-8 immobilised avidin DN, and to determine the suitability of affinity probe-capture for use in multiplexed DNA assays, a number of fundamental kinetic and thermodynamic studies of biotinylated oligonucleotide probe binding to avidin DN were required. Initially the extent of nonspecific **FP1** binding to immobilised avidin particles was determined.

2.3.1 The nonspecific binding of biotinylated oligonucleotides

When avidin particles already saturated with **FP1** were exposed to a concentrated biotin solution (1.25 mM), a drop in particle fluorescence over time was observed as the biotinylated **FP1** dissociated from the immobilised avidin tetramer to be replaced by the excess of unlabelled biotin (Figure 20). However, rather unexpectedly this displacement appeared biphasic in nature with both a fast and a slow probe release. There are literature examples of biphasic avidin-biotin dissociation, however these involve the fast release of the fourth biotin from a saturated avidin tetramer followed by the slower release of the other three bound ligands.[218,219] This model did not fit our system where it was improbable that all four binding sites on the surface-immobilised protein would be accessible to biotinylated species.
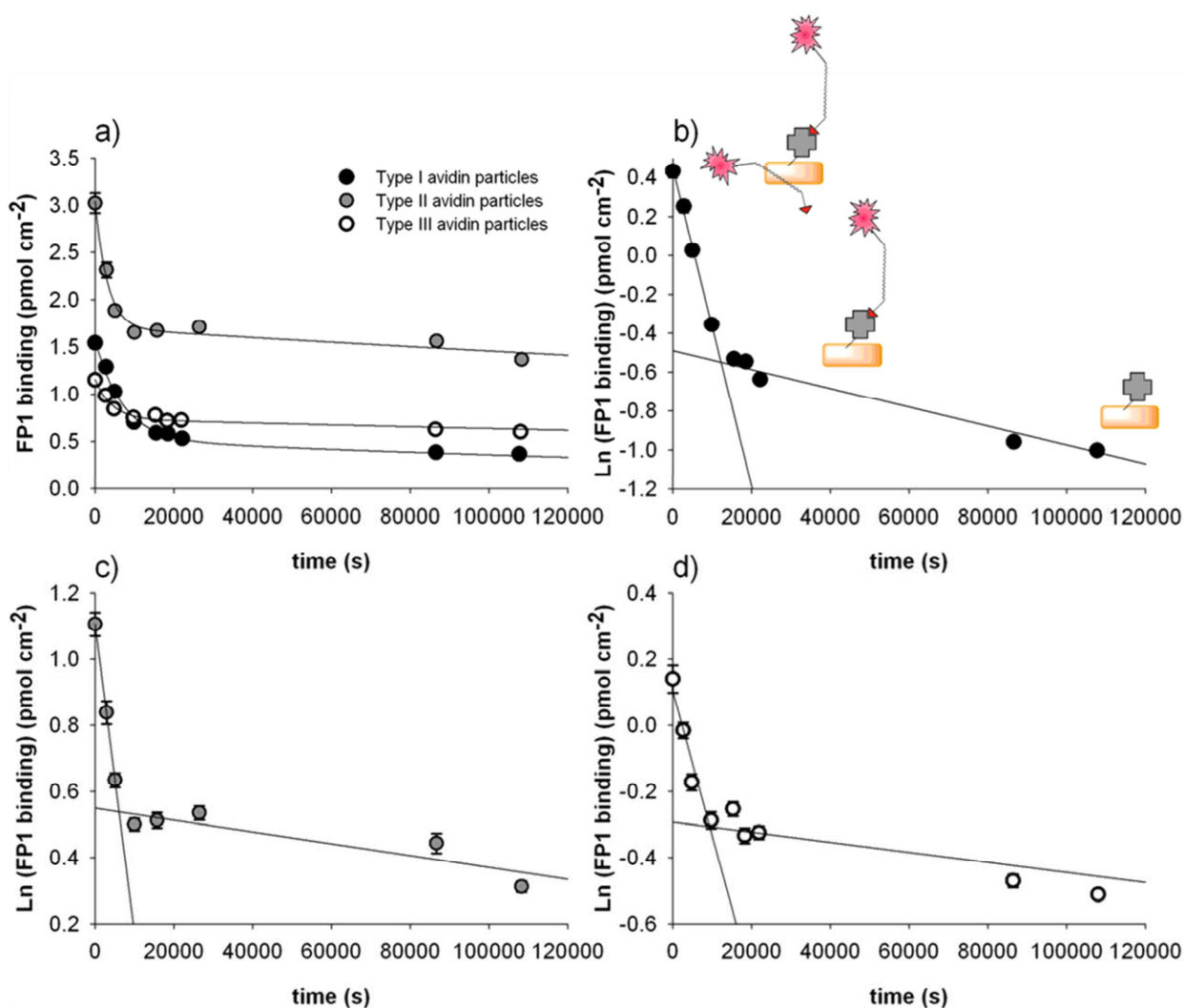
Figure 20. a) FP1 dissociation from avidin DN SU-8 particles in an excess of unlabelled biotin exhibiting biphasic dissociation, b) – d) integrated log plots for the three different protein immobilisation methods are displayed. Particle images are included to illustrate the conjectured degree and type of biotin binding at three points in the dissociation timecourse

An alternative explanation for the fast initial phase of probe dissociation was considered which was dependant on the electrostatic interaction between oligonucleotide probes and avidin. At neutral pH the phosphate backbone of the probe is largely deprotonated and thus negatively charged whilst avidin, with an isoelectric point (IP) of 10, has a net positive charge.[162] For our studies, avidin DN had been selected due to the reported low nonspecific DNA binding, however this would prove not to be the case as further investigation would determine significant levels of nonspecific **FP1** binding.[216]

This nonspecific binding of **FP1** was observed by a simple saturation experiment; a sample of Type I immobilised avidin DN particles was incubated in a solution of un-labelled biotin (1 μM) in order to saturate all of the (specific) biotin binding sites. After the washing of excess biotin, these particles were suspended in solution with **FP1** (10 nM). The fluorescence from biotin pre-saturated particles was compared with that for avidin particles which had not previously been exposed to biotin but which too had been suspended with **FP1**. Relative binding was quantified using fluorescence microscopy (Figure 21). Both samples were highly fluorescent, with the pre biotin-saturated particles (Figure 21b) showing a fluorescence intensity just 40% lower than the unblocked particles (Figure 21a). This experiment demonstrated that a high proportion (60%) of the fluorescence signal from **FP1** bound avidin particles (Type I) was due to the nonspecific binding of **FP1** rather than the specific interaction between the ligand and the protein active site.
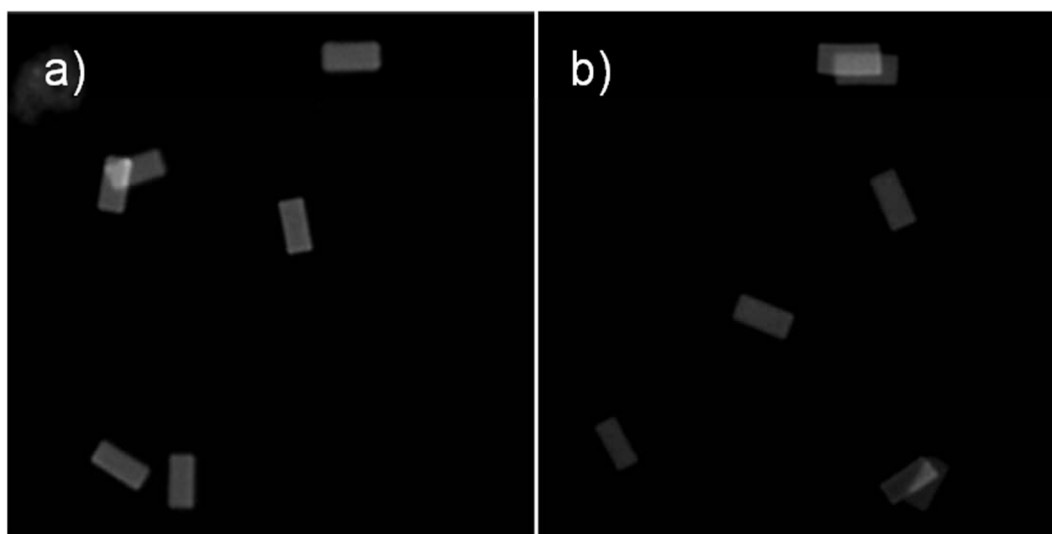
Figure 21. FP1 binding in SSPE (5×) buffer with 0.02% Tween-20® to a) Type I avidin SU-8 particles and b) biotin saturated Type I avidin SU-8 particles showing no significant difference in fluorescence intensity indicating high levels of nonspecific FP1 binding

2.3.2 Blocking of biotinylated oligonucleotide nonspecific binding

Minimising the observed nonspecific interaction was important for the accurate measurement of specific binding between biotinylated probes and immobilised

avidin DN, and to ensure the stability of immobilised oligonucleotide probes for later use in multiplexed DNA assays.

The effects of different surfactants and blocking agents on the nonspecific binding of **FP1** were investigated; once again the fluorescence of pre biotin-saturated avidin particles (representing nonspecific binding) was compared with that for unblocked particles (representing the total specific + nonspecific binding). No reduction in the level of nonspecific binding was achieved by incubation with either BSA (1%), sodium phosphate (100 nM) or the unlabelled 22-mer oligonucleotide (**O2**). However surfactants were shown to have an effect on the unwanted nonspecific binding. Earlier studies had been carried out in aqueous buffer containing 0.02% (v/v) Tween-20$^®$ to aid particle aggregation (pellet formation) upon centrifugation, as in the absence of any surfactant particles would interact (stick) with the inner wall of the Eppendorf$^®$ tube. By increasing the Tween-20$^®$ concentration to 1% the non-specific binding of **FP1** was found to be reduced to near the lower (fluorescence) detection limit, and thus this problem was negated. (Figure 22).
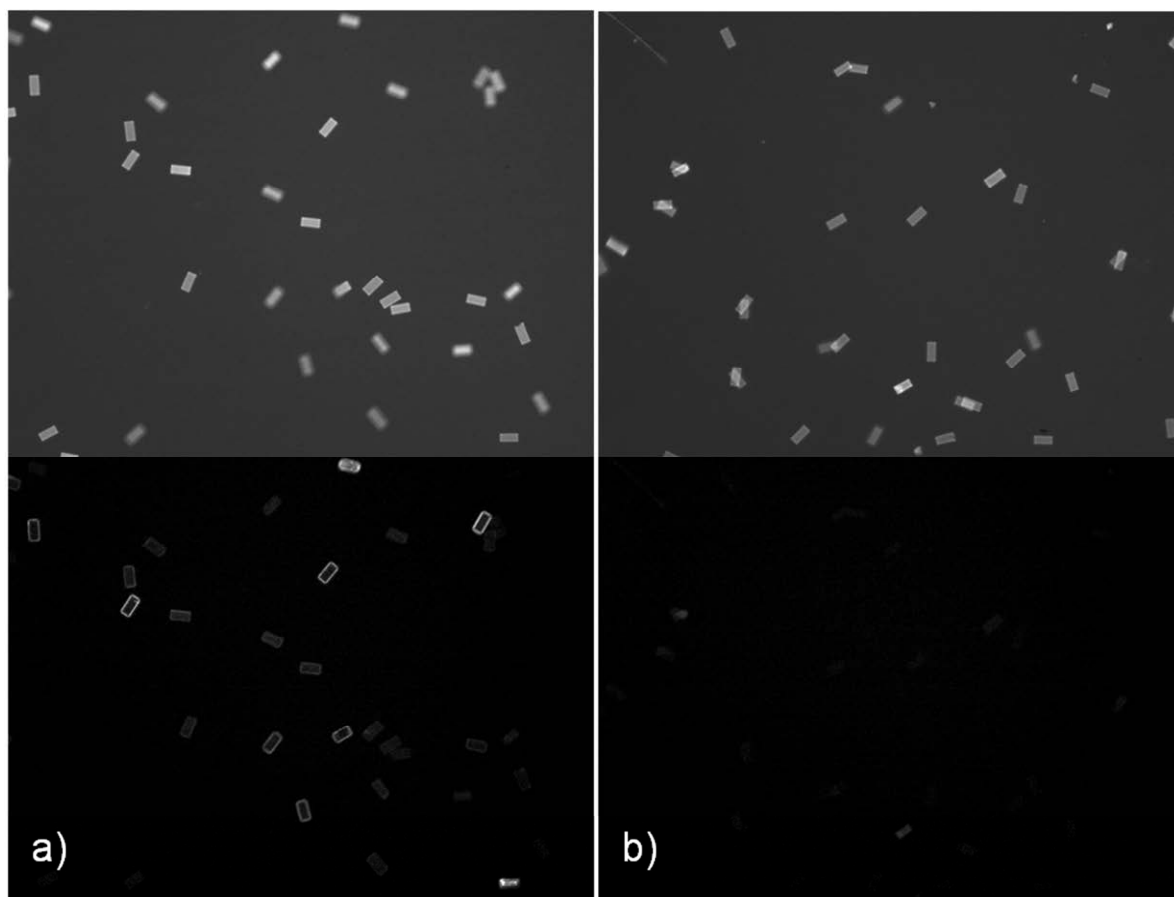
Figure 22. SU-8 autofluorescence (top) and Cy-5 fluorescence images of FP1 binding in SSPE (5×) buffer with 1.0% Tween-20® to a) Type I avidin SU-8 particles and b) biotin saturated Type I avidin SU-8 particles

The effects of varying the concentration of surfactant on both nonspecific and specific binding were then studied further. Measurements were taken of the fluorescence of pre biotin-saturated and unsaturated Type II avidin particles after exposure to **FP1** in buffer solutions containing increasing concentrations of Tween-20® (0 to 2.0% v/v) (Figure 23a). Fluorescence of the saturated particles (nonspecific binding) was consistently lower than the unsaturated samples (total binding) at each Tween-20® concentration. Fluorescence intensity was also observed to decrease with increasing surfactant. The difference in fluorescence intensity between the two particle types represented specific binding, therefore subtracting the fluorescence of the saturated from the unsaturated particles allowed the plotting of relative levels of specific and nonspecific binding at each concentration (Figure 23b). As can be seen, nonspecific binding decreased exponentially with increasing Tween-20® whereas specific binding decreased linearly. The ratio of specific to nonspecific binding is

greatest between 0.6 and 1.2% (v/v) Tween-20® with nonspecific binding being negligible above 1%.
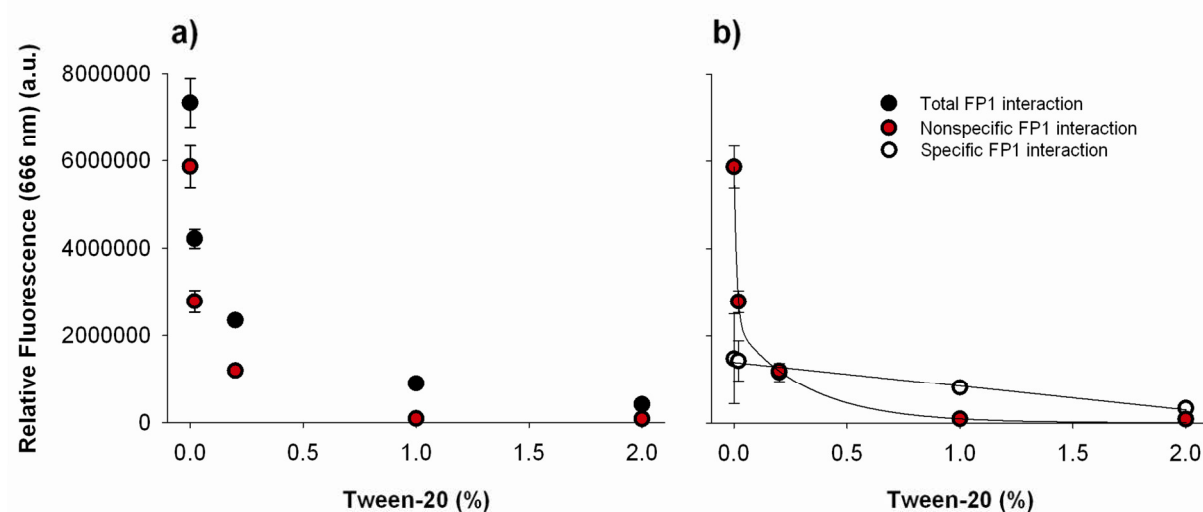
Figure 23. a) The measured total binding and nonspecific binding of FP1 to Type II avidin SU-8 in SSPE (5×) buffer with increasing concentrations of Tween-20® and b) the calculated specific binding of FP1 compared with nonspecific binding

As Tween-20® had been shown to also affect the specific binding of **FP1**, a sample of **FP1** saturated Type II avidin particles in SSPE (5×) buffer with 1% Tween-20® (v/v) was observed over a period of 4 days (Figure 24). Some variation in fluorescence intensity was observed due to the small sample size (N = 20-30 particles per measurement), however, the overall mean fluorescence intensity showed little change. This result implied that increased surfactant did not denature the immobilised protein (if the protein were being damaged one would expect to observe a decrease in fluorescence intensity, i.e. **FP1** binding, over time) and that the previously observed decrease in fluorescence upon increasing surfactant concentration was likely due to the binding sites being directly blocked by Tween-20® molecules (Figure 25).
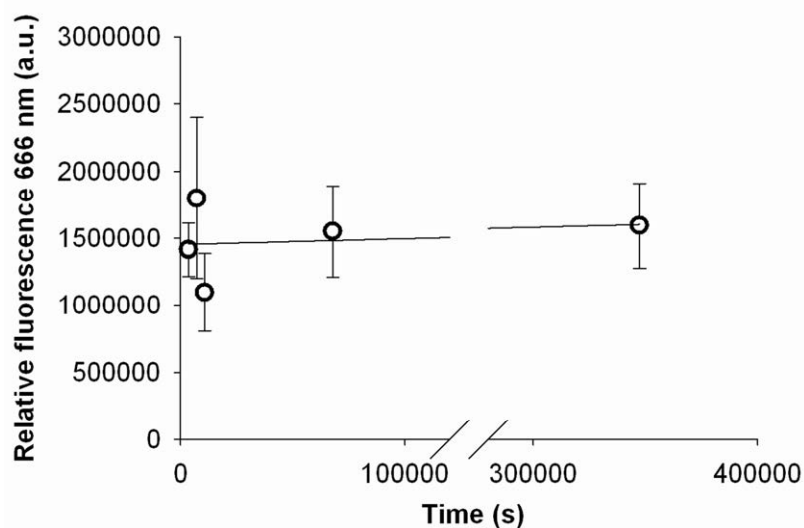
Figure 24. Time course fluorescence measurements of a sample of FP1 saturated Type II avidin SU-8 particles in SSPE (5×) buffer with 1.0% (v/v) Tween-20®
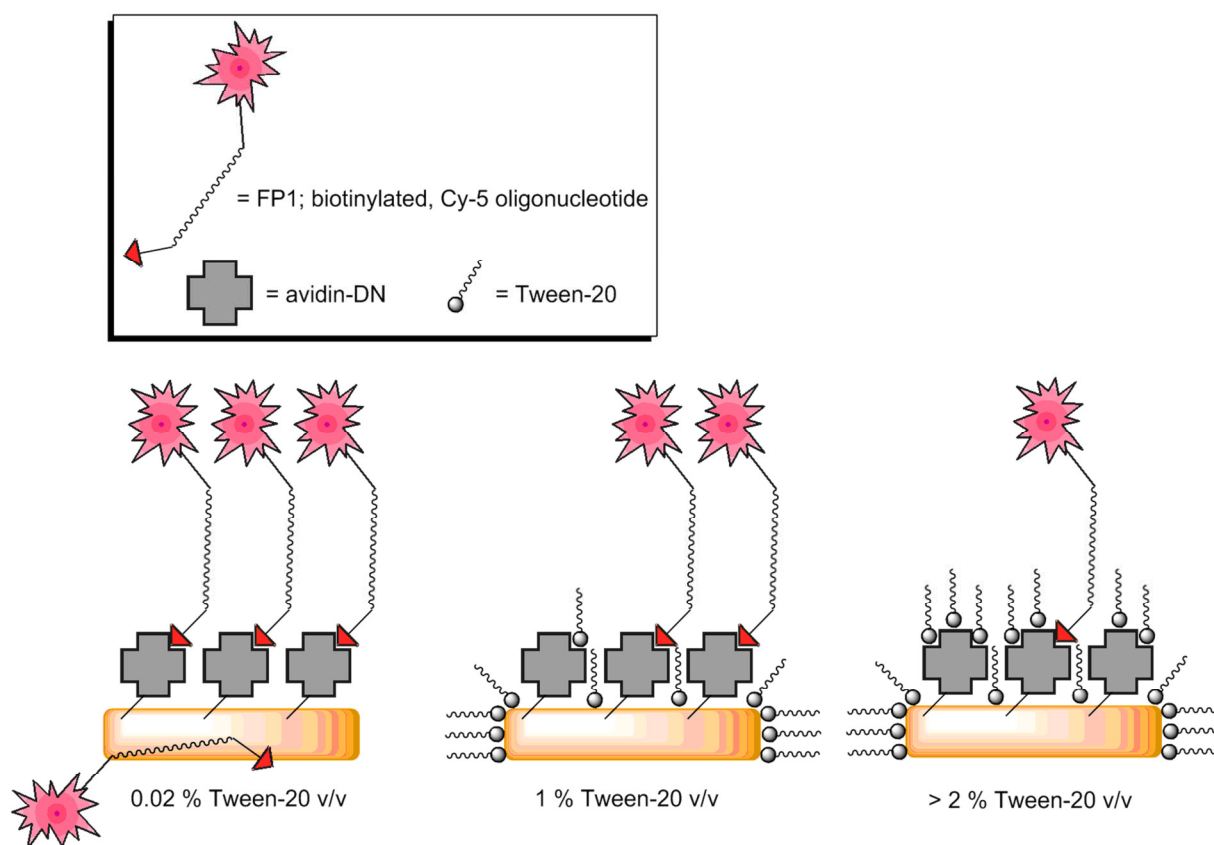
Figure 25. A representation of the effects of increasing Tween-20® **surfactant, blocking of both nonspecific and specific FP1 binding to avidin DN SU-8 particles**

The ionic surfactant Sodium dodecyl sulfate (SDS) was also shown to affect the binding of **FP1** to avidin immobilised particles, with 0.2% SDS reducing both specific and nonspecific binding by a similar amount to 2.0% Tween-20®. However as SDS is commonly used as a protein denaturant and Tween-20® had been shown to have no detrimental effect on the activity of immobilised avidin (Figure 24), all future studies of immobilised avidin particles used buffers containing 1% (v/v) Tween-20®.

Later studies of the kinetics of particle-immobilised complex dissociation under the new Tween-20® conditions found the system to follow 1st order exponential decay, showing no biphasic dissociation, with these results being discussed in detailed later in the chapter. Further analysis of the biphasic dissociation results (Figure 20) yielded information about the total amounts of specific and nonspecific **FP1** binding to each particle type and gave some kinetic data (Table 2). Type I avidin DN particles were found to have the highest **FP1** nonspecific binding under low Tween-20® conditions (61% of the total **FP1** binding) compared with Type II and Type III particles (43% and 32% respectively). The cause of this increased nonspecific binding was unknown, however the distribution of protein on the surface may have had an effect.[220] Affinity captured avidin (Type III) is likely to form the most ordered surface, as binding to covalently immobilised biotin causes all avidin tetramers to adopt the same configuration, forming a close packed, flat monolayer. This ordered surface may help to minimise nonspecific binding by providing a lower surface area and reducing cavities within which molecules could become trapped. On the other hand, avidin immobilised with the EDC coupling reagent *in situ* (Type I) is likely to have some degree of protein-protein crosslinking (as evidenced by greater-than-monolayer quantities of immobilised protein (Table 2), forming a disordered protein layer with higher surface area, congenial to greater levels of nonspecific binding. Further evidence for a disordered surface on Type I particles may come from the kinetics of nonspecific binding dissociation (Figure 20, natural log plots), these particles exhibit the lowest rate of dissociation of nonspecificly bound FP1 (k_{off} = $1.39 \pm 0.22 \times 10^{-4}$ s^{-1}) compared with avidin immobilised by the Type II or Type III routes (k_{off} = $3.20 \pm 0.66 \times 10^{-4}$ s^{-1} and $2.36 \pm 0.44 \times 10^{-4}$ s^{-1} respectively). Though the rate constant is not greatly lower, the smaller value may be indicative of

a reduced rate of **FP1** diffusion from the particle due to the surface being disordered and having more cavities.

The dissociation constant of **FP1** specifically bound to immobilised avidin under low Tween-20® conditions (0.02% v/v) was also calculated from the data for each particle type (Figure 20). Again particles with avidin immobilised using EDC *in situ* (Type I) showed a difference compared to the avidin immobilised via other routes (k_{off} = 4.84 ± 0.21 × 10^{-6} s^{-1} compared with 1.79 ± 0.52 × 10^{-6} s^{-1} for the NHS activated (Type II) and 1.52 ± 0.25 × 10^{-6} s^{-1} for the affinity captured (Type III) avidin DN particles). Though this data came from preliminary studies, it indicated a weakened complex was formed between immobilised avidin DN and FP1 compared with the complex between free avidin and biotin. Half-lives ranged between 1.7 and 5.3 days. This had implications for the use of this system in particle based multiplex assays where different oligonucleotide probe particles are required to be kept mixed together for long periods of time, requiring probe immobilisation to be robust. The kinetics of specific probe binding and dissociation would therefore be studied in more detail.

2.4 Biotinylated-probe/avidin DN solution-phase binding

$$[avidin\ DN] + [\textbf{FP1}] \underset{k_{off}}{\overset{k_{on}}{\rightleftharpoons}} [avidin\ DN - \textbf{FP1}]$$
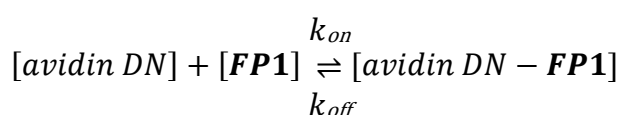
Equation 1.

The thermodynamic and kinetic parameters controlling the binding between **FP1** and untethered avidin DN were studied (Equation 1). The determination of this data was important as it provided values to which ligand binding to immobilised avidin DN could be directly compared. Discrepancies between the binding kinetics and the position of the binding equilibrium compared with the well studied avidin biotin system could also be made. Having this data for **FP1** binding to immobilised protein

and untethered protein would provide information as to the effects of both the protein immobilisation and the protein and ligand modifications on the binding equilibria.

Fluorescence polarisation (FP) (aka fluorescence anisotropy) was used to measure the kinetic rate constants (k_{on} and k_{off}) and the equilibrium dissociation constant (K_d) of the protein-ligand complex in solution. Briefly; free **FP1** being a (relatively) small molecule (3 kDa) has a high rotational diffusion (tumbles fast in space), therefore any polarised light absorbed by the fluorophore is re-emitted at both a longer wavelength and with reduced polarisation (due to the movement of the fluorophore between absorption and emission). Counter to this, avidin-complexed **FP1** is a much larger species (71 - 80 kDa) with a much lower rate of rotational diffusion therefore emitted light is released retaining a greater degree of polarisation. By exposing solutions of protein and **FP1** to polarised light at the Cy-5 excitation wavelength (648 nm) and measuring the FP of emitted light (666 nm), we get a measure of the proportion of ligand which is complexed, where a higher FP value would indicate a larger percentage of the total amount of ligand being bound.

2.4.1 Measuring the fluorescence polarisation of FP1 binding to Avidin

To measure the binding between **FP1** and avidin DN complex in solution, avidin DN was titrated against **FP1** (12.5 nM), with the FP of the mixtures being measured after a position of equilibrium had established. A problem was apparent; when FP was plotted against increasing protein the expected ligand binding curve of a rise to a maximum was not obtained. Instead polarisation initially dropped as more avidin was added until reaching a minimum at a point where the ratio of protein tetramer to ligand was slightly greater than 1:4 i.e. when the total binding sites equalled the total amount of biotinylated probe. Increasing the amount of protein further resulted in an increase in the measured FP, leading to a maximum (Figure 26). Further investigation revealed that fluorescence intensity followed a similar trend (Figure 26, insert). The cause of this apparent reduction in fluorescence was likely to be quenching of the Cy-5 fluorophores as cyanine dyes are known to from dimeric complexes when in high concentrations in aqueous environments and this leads to a

decrease in fluorescence intensity (quenching).[215] **FP1** free in solution is fluorescent, but when complexed with avidin, the close proximity to adjacent **FP1** ligands in a saturated tetramer must result in a high (local) concentration of Cy-5. This could lead to Cy-5 dimer formation between adjacent ligands which would lead to fluorescence quenching. This would explain the observation that fluorescence was at a minimum when **FP1** and avidin DN were in a 4:1 ratio and most avidin tetramers were fully saturated with ligand. As the quantity of available binding sites exceeds the amount of labelled biotin, binding occurs but the protein tetramers are no longer saturated resulting in less quenching and an increase in fluorescence intensity. This alone should not affect our polarisation measurements as FP compares the intensity of parallel to perpendicular light and both these light channels are affected equally by any dimming of fluorescence, however, the plate reader does not read both channels equally as the two cameras used have different gain values. Therefore any change in fluorescence intensity could affect parallel and perpendicular polarised light readings to different extents which would then alter the FP readout.
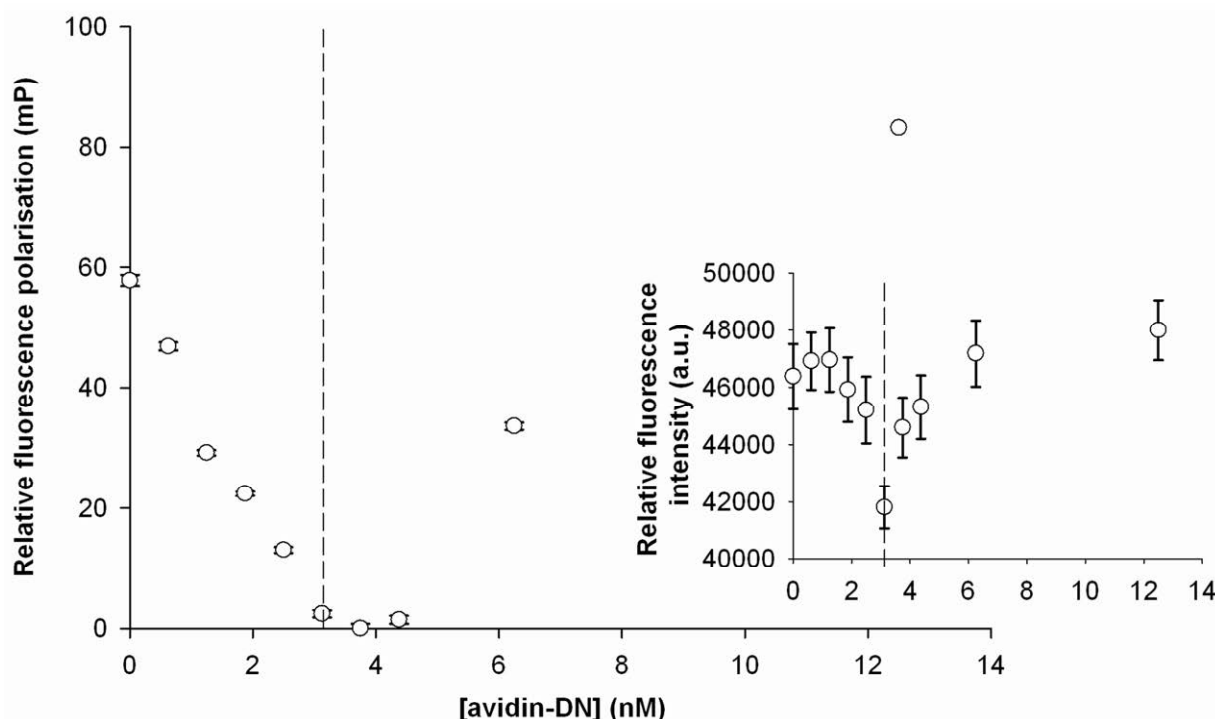
Figure 26. The fluorescence polarisation and the fluorescence intensity (insert) of the titration of avidin DN with FP1 (12.5 nM) in solution, a 4:1 ratio of FP1 to protein tetramer is indicated by the dashed line

This problematic fluorescence quenching was minimised by the dilution of **FP1** with a solution of (unlabelled) biotin to result in an **FP1** to biotin ratio of 10:87. This lowered multiple **FP1** bindings to the same protein tetramer whilst maintaining a sufficient amount of the labelled biotin as to be detectable by the plate reader under the low concentrations required by the experimental design. When a repeat of the protein to ligand titration was carried out using this diluted **FP1** solution FP was seen to increase in the presence of more avidin DN, fluorescence intensity was not affected by the addition of avidin.

The lower detection limit of the plate reader was measured, accurate FP could be made of solutions with Cy-5 concentrations as low as 1 nM. Using the **FP1**/biotin mixture to prevent quenching effects meant that the FP of ligand solutions could only be measured down to 10 nM (~1 nM **FP1**). This hindered the direct measurement of the equilibrium dissociation constant, K_d for the untethered avidin DN-**FP1** complex as discussed later (**2.5.4**) but did allow the kinetic rate constants, k_{on} and k_{off} to be determined.

2.4.2 Biotinylated-probe/avidin solution-phase association kinetics

$$\frac{\delta[avidin\ DN-\boldsymbol{FP1}]}{\delta t} = k_{on}[avidin\ DN][\boldsymbol{FP1}]$$

Equation 2.

The solution phase association kinetics of the avidin DN **FP1** system was studied (Equation 2). To obtain k_{on}, the rate of binding between the two species was monitored by measuring increasing FP with time. A 10:87 FP1 to biotin ligand mixture (10 nM) was added to an equivalent amount of avidin DN binding sites (2.5 nM tetramer) and the increasing polarisation as binding occurred was monitored. Binding was complete within ten minutes. The rate of binding could not be lowered to allow for a longer window of data collection as any further dilution of the ligand mixture would reduced the concentration of the fluorescent species to below the

instrumentation detection limit. FP was converted into a measure of complex concentration to give a binding time course (Figure 27).
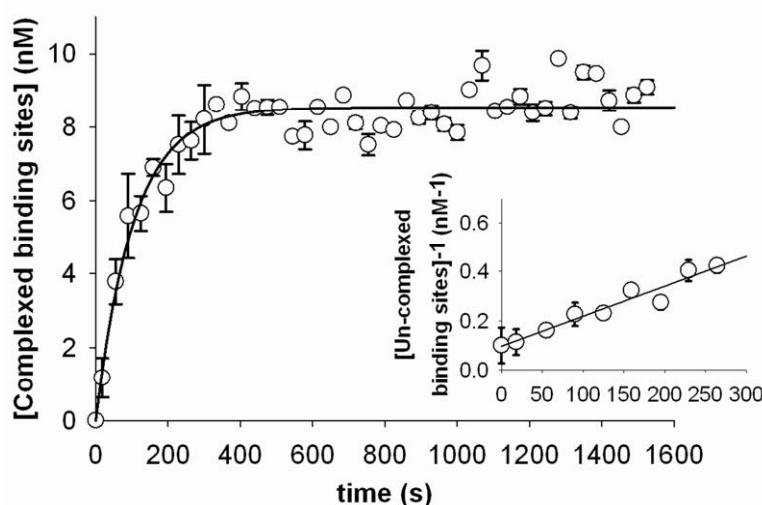
Figure 27. A timecourse measurement of the rate of association of FP1 and biotin ligands (10 nM) to avidin DN (2.5 nM) in solution. Inset: integrated data

The solution phase association rate constant was determined from the experimental data; $k_{on} = 1.22 \pm 0.11 \times 10^6$ M^{-1} s^{-1}, slower than that exhibited by the wild-type avidin biotin complex (70×10^6 M^{-1} s^{-1}).[162] To determine whether the binding kinetics of the system were diffusion limited, and only slow compared with the wild-type due to the increase in the size of the biotin ligand used, the collision frequency between avidin DN and **FP1** was estimated using the Smoluchowski equation (Equation 3), where N_A is Avogadro's constant (mol^{-1}), $R_{\alpha\beta}$ the sum of the (hydrodynamic) radii of avidin DN and the biotin probe (m) and $D_{\alpha\beta}$ the sum of their diffusion coefficients (m^2 s^{-1}).[221]

$$k_{diff} = 4\pi R_{\alpha\beta} D_{\alpha\beta} N_A \, 10^3$$

Equation 3.

This gives the theoretical maximum association rate constant, the diffusion controlled rate constant (k_{diff}) for the reaction between two freely mobile substrates (α and β), dependant on the collision between the two binding species. If the kinetics

of the system studied are diffusion limited then we would expect k_{on} to be a similar value to k_{diff}, if diffusion were not the limiting factor then $k_{on} \ll k_{diff}$.

The hydrodynamic radii (R) and the diffusion coefficients (D) are related by the Stokes-Einstein-Sutherland equation (Equation 4).

$$D = \frac{k_B T}{6\pi\eta R}$$

Equation 4.

Where k_B is the Boltzmann constant (1.38065×10^{-23} Pa m^3 K^{-1}) T is temperature (293.15 K) and viscosity of the medium is represented by η (1.098×10^{-3} Pa s).

Diffusion coefficients and hydrodynamic radii for the avidin DN and the biotinylated and labelled oligonucleotide FP1 in the present study can be approximated and calculated from similar values in the literature.

Avidin has dimensions 5.6 × 5 × 4 nm and an experimentally determined hydrodynamic radius of 3.27×10^{-9} m.[210,222] D is calculated as 5.98×10^{-11} m^2 s^{-1} (Equation 4).[223] The avidin DN we have studied has a similar structure to the wild-type avidin so it is reasonable to assume it has a similar rate of diffusion.

The diffusion coefficient of an oligonucleotide (**T1**), which has a similar to structure to **FP1**, has been determined by others using fluorescence cross correlation spectroscopy as being 8.4×10^{-11} m^2 s^{-1}.[224] This 13-mer sequence was labelled at the 5' terminus with Alexafluor 488 and the size and shape is comparable to our biotinylated and Cy-5 labelled oligonucleotide. The hydrodynamic radii of **T1** was calculated as 2.33×10^{-9} m (Equation 4). **FP1** is slightly larger than **T1** and therefore was expected to have a slightly larger hydrodynamic radius and thus a slightly lower diffusion coefficient, however the differences would be negligible due to the small increase in mass and the well ordered DNA structure. Thus it was assumed that the values calculated for **T1** were reasonable estimates for the values of **FP1**.

With estimates of the physical properties of avidin DN and **FP1** we could calculate the expected diffusion controlled rate constants for protein ligand binding in solution

(Equation 3). This value is not exact due to the equation being built for simple molecular reactions employing collision theory, it therefore does not taking into account that only a small proportion of the avidin surface is made up of the active site.[225] Thus the value for k_{diff} is the maximum possible rate. The diffusion controlled association rate constant for solution phase binding between avidin DN and **FP1** was calculated as $k_{diff} = 6.09 \times 10^9$ M^{-1} s^{-1}.

Comparing the calculated k_{diff} and determined k_{on}, 6.09×10^9 M^{-1} s^{-1} and $1.22 \pm 0.11 \times 10^6$ M^{-1} s^{-1} respectively, the measured k_{on} is significantly lower. This would imply that the rate of ligand association was limited by a factor other than diffusion, however the difference in values may also be explained by the system's low steric factor (f) (where only a small fraction of the surfaces of avidin and biotin are involved in binding, resulting in the probability of complex formation from any one collision being much less than 1).[226] The steric factor can be described as the ratio between the observed and diffusion limited rate constants and for the solution phase binding discussed herein is calculated as f = 0.0002.

2.4.3 Biotinylated-probe/avidin solution-phase dissociation kinetics

$$\frac{\delta \, [\textbf{FP1}]}{\delta t} = k_{off}[avidin \, DN - \textbf{FP1}]$$

Equation 5.

The dissociation of the complex between avidin DN and **FP1** in solution was monitored once again using FP (Equation 5). As with previous solution binding studies, a mixture of unlabelled biotin and **FP1** was used to limit the number of fluorescently labelled ligands in order to reduce the incidence of multiple fluorophores bound to each protein tetramer to minimise the occurrence of fluorescence quenching. Firstly avidin binding sites were saturated using an equimolar amount of the ligand mixture of **FP1** and biotin, resulting in a solution exhibiting a high FP due to the predominately complexed state of **FP1**. This was followed by the addition of a large excess of biotin. As **FP1** dissociated from the

active sites on the tetramer, the vacant binding site was filled by biotin which prevented any **FP1** rebinding. This dissociation was evident by the decreasing FP over time. FP measurements were converted into a concentration of the protein-ligand complex which could be plotted as a dissociation time course (Figure 28).
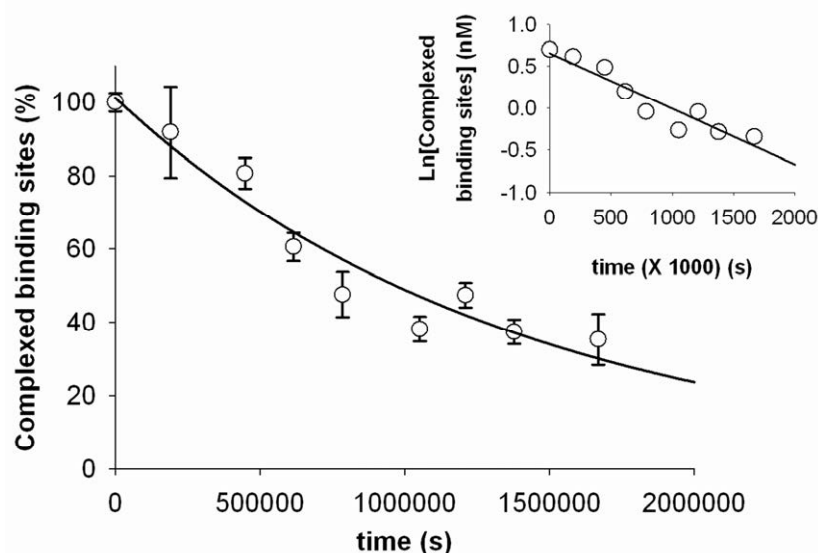
Figure 28. A timecourse measurement of the rate of FP1 dissociation from Avidin DN in solution. Inset: integrated data

FP1 dissociation from avidin DN in solution gave a kinetic value, $k_{off} = 7.28 \pm 0.61 \times 10^{-7}$ s^{-1}. This value is more than an order of magnitude larger than that reported for the wild-type system ($k_{off} = 0.4 \times 10^{-7}$ s^{-1}) and has implications for the immobilisation of probes by affinity with the intended use in assay systems due to the complex having a t$_{\frac{1}{2}}$ of only eleven days. Though there are no literature values for the dissociation of biotinylated oligonucleotides from avidin some studies have made modifications to the structure of biotin to identify the chemical groups which interact with the protein active site and stabilise the complex.

One study found the imidazolidone ring and to a lesser extent the thiophane ring of biotin as having the strongest interactions with the active-site of avidin and therefore essential for tight binding, modification of the terminal carboxylic acid was shown to have a much lesser detrimental effect on complex stability.[227] The labelled biotin used in our studies retained this double ring system. However, other studies have indicated that the terminal carboxylic group does interact directly with the protein active site. Crystal structures of the complex indicate the two carboxylate oxygens

form five hydrogen bonds, two to the polyamide backbone ($R_2N–H$) of alanine (Ala-39) and threonine (Thr-40) and three to the side chain groups (R–OH) of threonine (Thr-38) and serines (Ser-73 and -75) (Figure 29).[228] Studies quantifying the effects of the alteration of the carboxylic acid moiety of desthiobiotin have also been published.[165] Here it was found that modification of the acid to the corresponding methyl ester resulted in an eight-fold increase in the rate of complex dissociation.
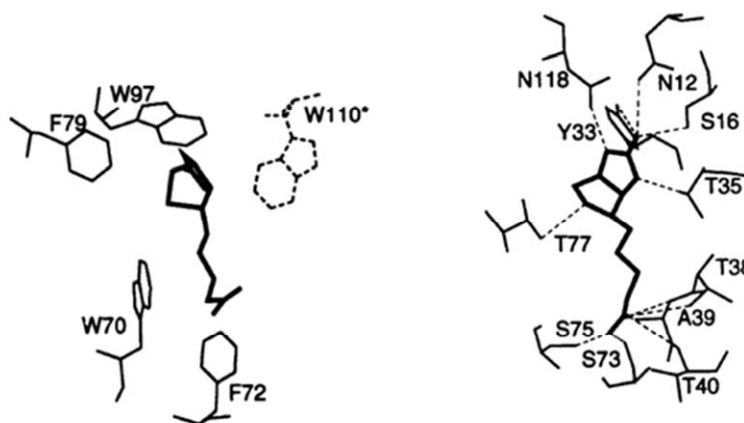
Figure 29. The crystal structure of the filled active site of avidin showing the favourable interactions between biotin and hydrophobic residues (left) and hydrophilic residues[228]

The biotin moiety of **FP1** is conjugated to the oligonucleotide via an amide linkage, which replaces the terminal carboxylic acid. As the above literature reports suggest, a number of minor favourable interactions are lost between modified biotin and the active site of avidin, therefore the measured increase in the rate of **FP1** dissociation from avidin DN compared with the unmodified biotin complex with avidin (wild-type) could be explained.

2.4.4 Biotinylated-probe/avidin DN solution-phase equilibrium thermodynamics

Due to the lower detection limits of the plate reader, the most dilute **FP1** biotin ligand mixture which could be studied was 10 nM, this was too concentrated for an accurate measurement of the equilibrium dissociation constant (K_d) of avidin DN binding to be made. At nanomolar concentrations the protein and ligand are essentially 100% complexed, resulting in no equilibrium to actually measure. A

value for the K_d can though be calculated from the experimentally determined association and dissociation rate constants (k_{on} and k_{off}) (Equation 6). The calculated value ($K_d = 6.0 \times 10^{-13}$ M) was 1000 times greater than that reported for wild type avidin biotin binding ($K_d = 5.7 \times 10^{-16}$ M) indicating much weaker binding. This resulted from both the decrease in the association rate constant due to the increased size of the biotin species, and from the increase in the dissociation rate constant due to the loss of hydrogen bonding sites on the biotin resulting from its conjugation to oligonucleotide.

$$K_d = \frac{[avidin\ DN][\boldsymbol{FP1}]}{[avidin\ DN - \boldsymbol{FP1}]} = \frac{k_{off}}{k_{on}}$$

Equation 6.

The measured kinetic and the calculated thermodynamic parameters of **FP1** binding to avidin DN in solution are summarised (Table 3).

Table 3. A summary of experimentally determined and calculated kinetic and thermodynamic parameters of avidin biotin binding in solution and of avidin DN FP1 binding both in solution and immobilised on SU-8. †measurements were made in SSPE (5 ×) buffer with 1% v/v Tween-20® to eliminate nonspecific FP1 binding

Complex	k_{on} (M^{-1} s^{-1}) ($\times 10^6$)	k_{off} (s^{-1}) ($\times 10^{-6}$)	$t_{1/2}$ (days)	k_{off}/k_{on} (M) ($\times 10^{-12}$)	K_d (M) ($\times 10^{-12}$)	specific b_{max} (mol cm^{-2}) ($\times 10^{-12}$)[a]
avidin biotin sol [162]	70	0.04	200	0.00057	-	-
avidin DN **FP1** sol†	1.22 ± 0.11	0.73 ± 0.06	11.0	0.598	-	-
Type I avidin SU-8 **FP1**†	0.54 ± 0.04	4.15 ± 0.29	1.9	7.726	10.03 ± 1.72	0.44 ± 0.02
Type II avidin SU-8 **FP1**†	0.52 ± 0.03	1.57 ± 0.16	5.1	3.041	4.49 ± 0.85	1.38 ± 0.05
Type III avidin SU-8 **FP1**†	0.52 ± 0.06	1.52 ± 0.08	5.3	2.910	4.05 ± 0.46	0.58 ± 0.01

2.5 Biotinylated-probe/avidin DN solid-phase binding

The binding rates and interaction strength between biotin and particle-immobilised avidin were measured. This data could be compared with the previous measurements made on the untethered avidin DN and would show how detrimental to activity immobilisation of the protein was. Samples of particles were analysed using fluorescence microscopy to give a measure of the amount of **FP1** bound to the support surface. Due to the relatively low proportion of working/accessible biotin binding sites, fluorescence quenching because of Cy-5 dimer formation had not previously been observed on the particles, therefore dilution of the **FP1** ligand in a solution containing biotin (as in the studies of untethered avidin DN) was no longer necessary.

2.5.1 Fluorescence microscopy imaging of the supports and fluorophore stability

When exposed to light of the correct wavelength, a fluorophore will absorb photons and enter an excited (high energy) state, some energy is lost (as heat) in vibrational relaxations whilst the remaining energy is released as a photon to return the fluorophore to the low energy ground state (Figure 30).[229] The photon released is of lower energy to the one absorbed (thus at a longer wavelength) due to the prior energy loss through vibrational relaxation. This fluorescence cycle is very rapid; Cy-5 will emit a photon within 1 ns of absorption.[230] Being in the high energy state can lead to side reactions which damage the fluorophore, this is referred to as photobleaching.[231] Excited state oxygen (singlet oxygen, $^1O_2$) produced on the photillumination of aqueous media has also been found to degrade ground state cyanine dye; reaction occurs at the polymethine chain which links the two aromatic ring systems and results in the loss of extended conjugation.[232,233]
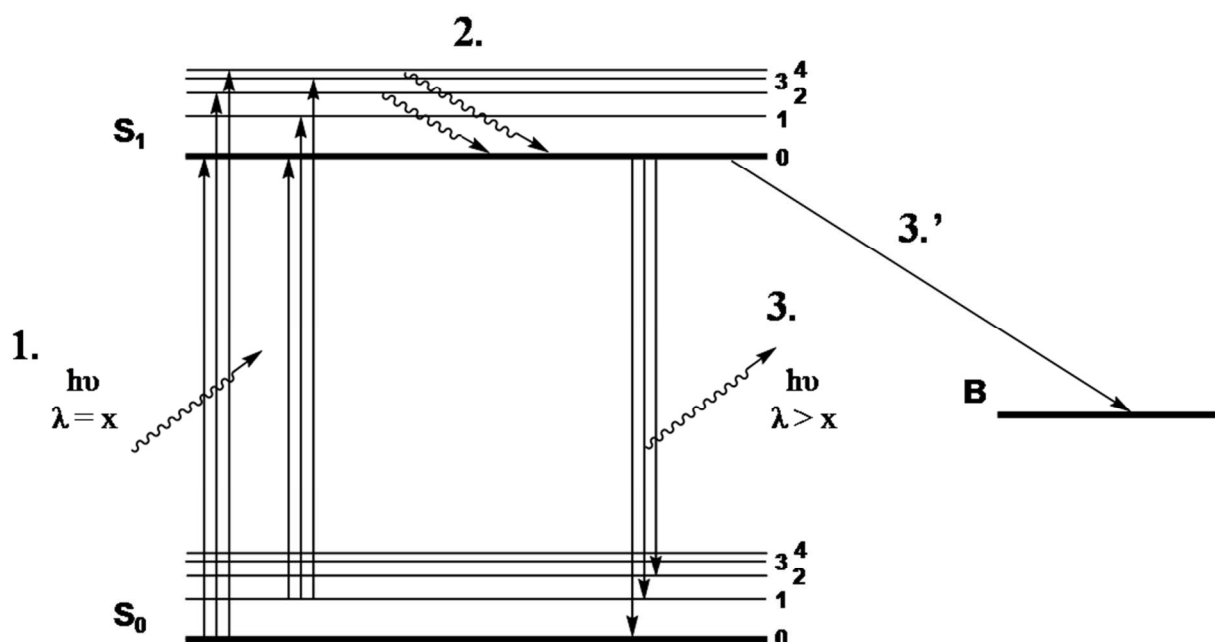
Figure 30. Jablonski diagram detailing the energy state of a fluorophore during photoillumination. Initially the fluorophore in is a ground electronic state (S_0). A photon of specific energy is absorbed (1.) and the fluorophore moves to an electronically excited state (S_1). Vibrational relaxation reduces the molecule to the lowest energy level of the excited state (2.), with this energy being lost to the environment as heat. The molecule loses energy as a photon emission (fluorescence) and drops back to the ground electronic state (3.). As some energy had previously been lost due to vibrational relaxation (2.) the photon released is of lower energy than the photon originally absorbed, the released photon is therefore of a higher wavelength, this change in wavelength is referred to as the Stoke's shift. An alternative pathway (3.') can result from the molecule being in a high energy state where a photoreaction occurs, changing the structure of the fluorophore (B), this is an example of photobleaching

When the fluorescence intensities of the particles used in this work are measured by microscopy, they are exposed to excitation wavelength light for a number of seconds; therefore it was important to know the stability of the Cy-5 molecule under our experimental conditions to make sure photobleaching had little effect on experimental results. The effects of photo illumination on Immunoglobin G (IgG) immobilised particles was studied, we used IgG particles as the binding of the corresponding Cy-5 labelled anti IgG resulted in much greater fluorescence intensity than the particles used for DNA hybridisations (this was due to there being multiple fluorophores per protein compared with only a single fluorophore conjugated to each oligonucleotide).

Three particles with bound Cy-5 labelled anti IgG were continuously exposed to excitation light whilst the fluorescence emitted was monitored (Figure 31, a). As expected the intensity of fluorescence decreased with continued excitation, as the cyanine molecules degraded. Importantly, this degradation took place over the

course of minutes, a few seconds exposure does not have a marked effect on the emission intensity. Interestingly, over the initial 100 seconds of excitation, the fluorescence intensity actually increased with time. It is unknown why this should be the case, one explanation proposed that having multiple Cy-5 groups coupled to each antibody (i.e. in close proximity) resulted in a degree of fluorescence quenching then, upon continuous illumination, fluorophores start to degrade. If one fluorophore is degraded any adjacent fluorophores may no longer be quenched which leads to the observed initial increase in the fluorescent signal.
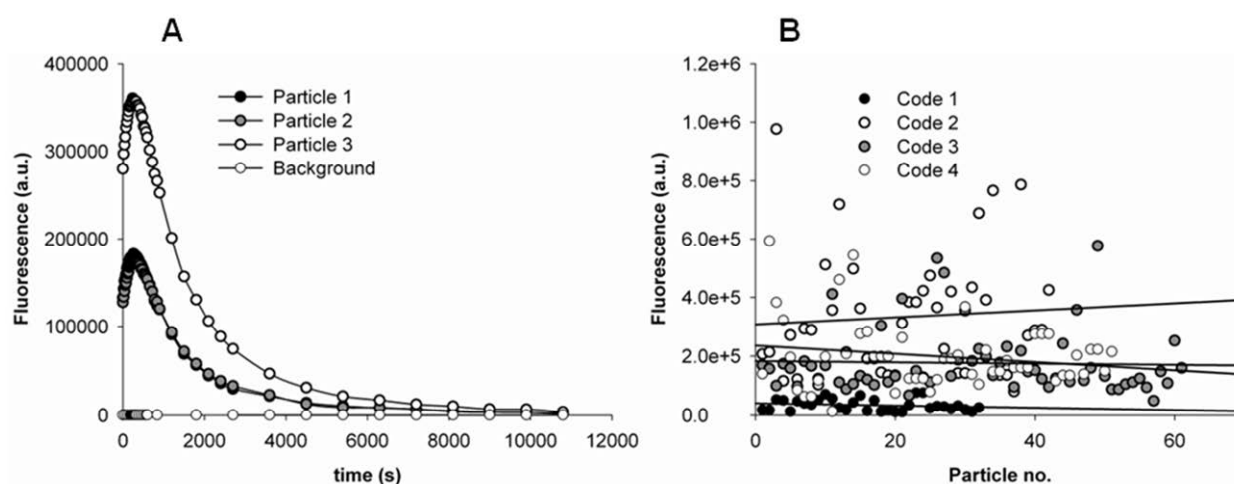
Figure 31. A) The fluorescence intensity of three Cy-5 functionalised particles under continuous excitation, displaying fluorescence quenching. B) Fluorescence intensities of the particles in four different encoded populations taken from an immunoassay multiplex, throughout sample analysis mean fluorescence intensity (as indicated by fitted curves) shows little change indicating fluorescence quenching has little effect on assay reading

To confirm that the fluorescence of a population of particles changed little during analysis by microscopy a sample of the fluorescent antibody particles was mounted on a slide and the intensity of emitted light measured for 60 particles (Figure 31, b). Though there was variation in the signal between individual particles, the mean signal did not vary as more particles were measured and the cumulative exposure to excitation light increased. This showed that though photobleaching did take place, the relatively long timescale over which it occurred meant that it did not affect on data collection, therefore the minimal effects of photobleaching on the experimental results can be suitably ignored.

2.5.2 Biotinylated-probe/avidin DN solid-phase association kinetics

The association kinetics of **FP1** binding to avidin DN immobilised on SU-8 particles were studied. The binding of **FP1** in each of these particle assays is presented in terms of concentration for clear comparison with the untethered avidin DN studies. A particle suspension of 1 mg mL^{-1} was used in all experiments, 1 mg of contains approximately 8.06×10^5 particles with a total surface area of 5.642 cm^2. Complexed **FP1** loading density was measured in mol cm^{-2}.

Avidin DN particles were suspended in SSPE (5 ×) buffer under the high Tween-20$^{\circledR}$ conditions (1% v/v) in order to block any nonspecific DNA binding. **FP1** was added to these particle suspensions which were gently agitated. At intervals, samples were removed and any uncomplexed active sites quenched by the addition of an excess of biotin. The average particle fluorescence intensity was measured for each sample (N ~ 30 particles per sample); this could then be converted to a measurement of the surface loading density of protein-ligand complex and an overall concentration (Figure 32).
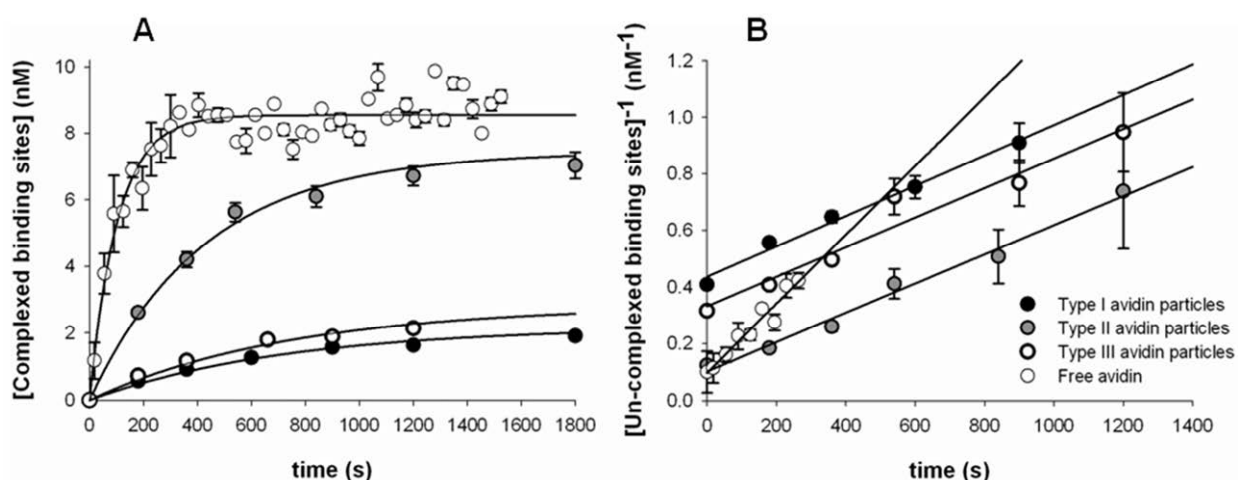
Figure 32. A) Specific FP1 association to avidin DN functionalised particles showing a slower binding rate than that to non-immobilised protein (data included for comparison), different immobilisation methods were found to not affect the rate of association. B) Integrated data

The association rate constants for the specific binding of **FP1** to avidin DN particles did not differ greatly between the different protein immobilisation routes; all three particle types gave a similar value, $k_{on} \approx 5.3 \times 10^5$ M^{-1} s^{-1} (Table 3).

The measured association rate constants were compared with the theoretical maximum rate constant as determined by collision theory. This diffusion controlled rate constant (k_{diff}) for the reaction between one freely mobile substrate (β) and one immobilised substrate (α) is described by a modified version of the Smoluchowski equation (Equation 7).[234,235]

$$k_{diff} = 2\pi R_{\alpha\beta} D_\beta N_A 10^3$$

Equation 7.

Calculating the theoretical k_{diff} for ligand binding to a surface immobilised receptor using R and D values of avidin DN and **FP1** results in $k_{diff} = 1.78 \times 10^9$ M^{-1} s^{-1}. Comparing this with the experimentally determined value of 5.3×10^5 M^{-1} s^{-1}, once again as found previously for solution-phase binding, the measured rate is much slower possibly due to the system's low steric factor (f).

Comparing the two theoretical maximum association rates (solution and immobilised) as calculated (Equations 3 & 7), solution-phase binding is predicted to be 3.4 times faster. From the experimental results, solution-phase binding was determined to be 2.3 times faster. The similarity between these two pairs of values indicates that the measured decrease in the rate of association upon avidin immobilisation is wholly due to the limiting of the ligand's vectors of approach (to the binding site, due to the particle surface), rather than any effects on the specific protein-ligand interaction itself. This also implies that in fact the binding is diffusion limited and backs up the previous calculation for f being 0.0002 (Chapter 2.4.2).

The association rate constants obtained from this study of immobilised avidin DN can be compared with related systems reported by others. Two studies differ to the system studied herein in that they measured the binding of mobile avidin to a biotinylated surface, the two groups also obtained very different values for the association rate constant, $k_{on} = 1.2 \times 10^5$ M^{-1} s^{-1} and 1.9×10^8 M^{-1} s^{-1}.[235,236] A single reported value can be found for the association between a biotinylated protein and avidin immobilised by adsorption on a surface, $k_{on} = 2.21 \times 10^5$ M^{-1} s^{-1}.[237] A value

similar to the system reported here, with a slightly lower rate, as expected for a larger biotin species which would have a reduced rate of diffusion.

2.5.3 Biotinylated-probe/avidin DN solid-phase dissociation kinetics

The dissociation rate constant for specific **FP1** uncomplexing from avidin DN particles was determined by monitoring the loss of fluorescence over time of **FP1** saturated avidin particles exposed to an excess of unlabelled biotin. As **FP1** dissociates it is quickly replaced by biotin, thus preventing **FP1** reattachment. Nonspecific binding was minimised by using SSPE (5×) buffer with 1% Tween-20®. A 1st order exponential complex dissociation was observed (Figure 33). Complexed avidin DN immobilised by the three routes was found in all cases to have a faster rate of dissociation compared with that previously measured for the untethered avidin DN (Table 3). The most unstable complex being between **FP1** and Type I avidin DN particles (EDC *in situ*) (**10**), whilst the other two particle types showed similar rates of dissociation. The **FP1** dissociation from Type I particles was six times faster than the solution based system and the resulting complex half-life was reduced to less than two days.
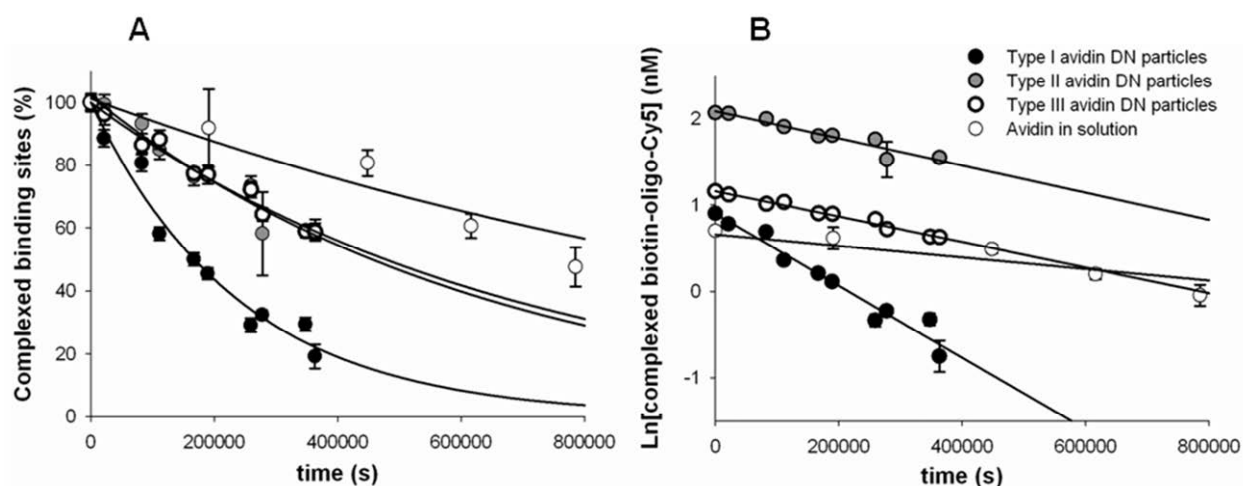
Figure 33. A) Specific FP1 dissociation from avidin DN functionalised particles. Immobilisation resulted in a decrease in complex stability compared with the non-immobilised complex (data included for comparison), with Type I immobilisation forming the weakest complex. B) Integrated data

Upon biotin binding, conformational changes occur within the avidin structure which work to 'lock' the ligand within the protein structure, contributing to the normally very high stability of the complex. Some studies have shown evidence of cooperative binding, where the binding of a second and third biotin is stronger than the first (the forth biotin is held relatively weakly in comparison), though the immobilised avidin tetramers studied are unlikely to bind more than one **FP1** molecule each and so will not benefit from cooperative binding.[228,238,239] Crystal structures of the avidin-biotin complex also indicate a structural rearrangement which blocks the entrance/exit to the binding pocket upon complex formation. It is postulated that the covalent immobilisation and close-packing of avidin may restrict any conformational rearrangements which contribute to the high complex stability; this could explain the observed reduction in the complex stability for all three immobilised systems compared with the untethered system. Type I avidin DN particles are likely to have some degree of cross-linking between protein molecules which are absent in the other two particle types, this could further constrict any rearrangements beneficial to the complex stability and explain the greater rate of dissociation determined for these particles.

Two related studies have been reported, these both measured avidin dissociation from a biotinylated surface and published two widely different rate constants. The values reported were $k_{off} = 3.3 \times 10^{-7}$ s^{-1} (t$_{\frac{1}{2}}$ = 24 days) and $k_{off} = 3.8 \times 10^{-4}$ s^{-1} (t$_{\frac{1}{2}}$ = 0.5 hours).[235,236] The rate constants determined by the studies herein lie between these prior reported values. To the best of our knowledge, no experimental determination of a dissociation rate constant for an immobilised avidin and free biotin system has been reported.

2.5.4 Biotinylated-probe/avidin DN solid-phase equilibrium thermodynamics

By titrating **FP1** against immobilised avidin the equilibrium dissociation constant (K_d) can be experimentally determined and the specific **FP1** binding (b$_{max}$) quantified. A direct measurement of the K_d could also be compared with the value calculated from the kinetic data previously obtained (Equation 6). Suspensions of avidin particles (SSPE (5 ×) buffer with 1% v/v Tween-20®) were exposed to varying concentrations of **FP1** and allowed to reach a binding equilibrium before

quantification of particle fluorescence and conversion into a measure of complex concentration (Figure 34). K_d and b_{max} values are given, the equilibrium dissociation constants were found to closely match the equivalent value as calculated from the rate constants (Table 3). This confirmed the weakened binding of the immobilised complex compared with both the untethered avidin DN/**FP1** and the wild type avidin/biotin complexes. As expected, total specific **FP1** binding (b_{max}) was 20-30% lower than found under low Tween-20® conditions (0.02%) (Figure 23).
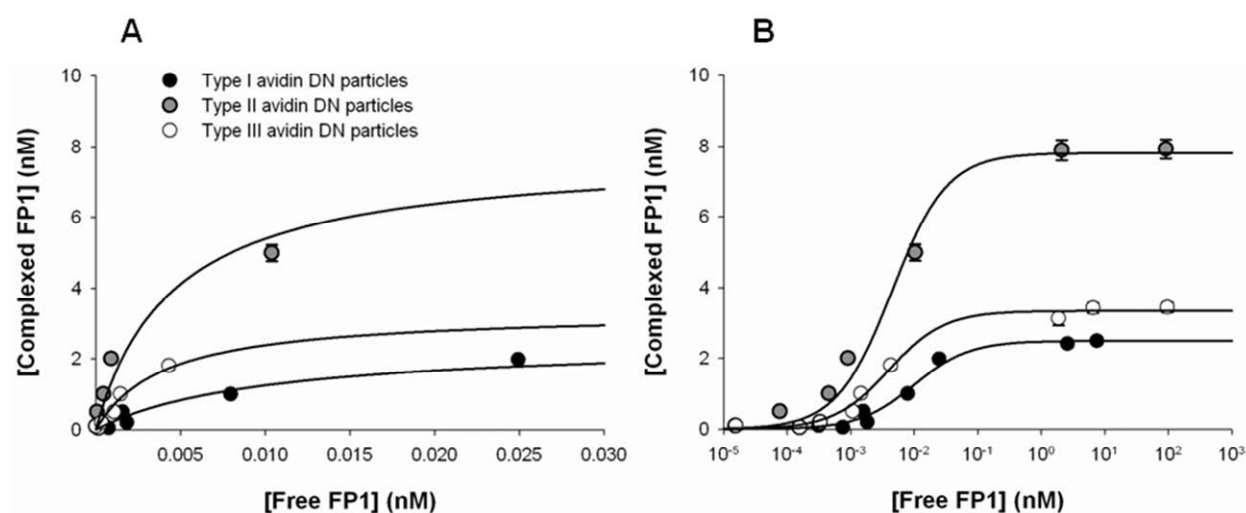
Figure 34. FP1/particle-immobilised avidin DN titrations displayed as A) linear and B) log plots. Equilibrium dissociation constants obtained closely matched predicted values as calculated from the experimentally determined kinetic data

2.6 Analysis of the supports by flow cytometry

Results from when the fluorescence of SU-8 particles has been analysed using the fluorescence activated cell sorter (FACS) have shown very broad fluorescence populations. Identically treated particles often give intensity readings over a two order of magnitude range, whilst particles from the same sample, when analysed by fluorescence microscopy, display a very low intensity variation. This observation of particles by microscopy would suggest that the broad range of fluorescence observed by FACS analysis was due to error induced by the instrumentation or the analysis method rather than a real fluorescence variation.

To confirm the cell sorter as the source of this fluorescence error the FACS machine was used to sort populations of particles which were then re-analysed in the same

machine. The idea being that particles collected within only a narrow range of fluorescence intensities from a population with a broad fluorescence range should show the same narrow fluorescence range when re-analysed by the cell sorter. If the sorted particles were to show a similar range of fluorescence intensities to the mother sample then the broad range of intensities would likely be an artefact of analysis by FACS.

A mixture of particles exhibiting two distinct fluorescence populations between 30 and 9000 a.u. was analysed, particles from between 200 – 800 (P2 in red) and 1000 – 4000 a.u. (P1 in blue) were sorted and retained whilst all particles outside of these ranges were discarded (P3 in grey) (Figure 35). When these sorted particles were re-analysed each sample only contained only a single fluorescence population which indicated that the original two populations had been successfully separated. Each population had a much greater range of fluorescence intensities compared with the stringent gating used to initially sort the particles; analysis of particles collected between 200 and 800 a.u. showed fluorescence between 30 and 4000 a.u., likewise the particles collected between 1000 and 4000 a.u. now exhibited fluorescence between 200 and 9000 a.u.
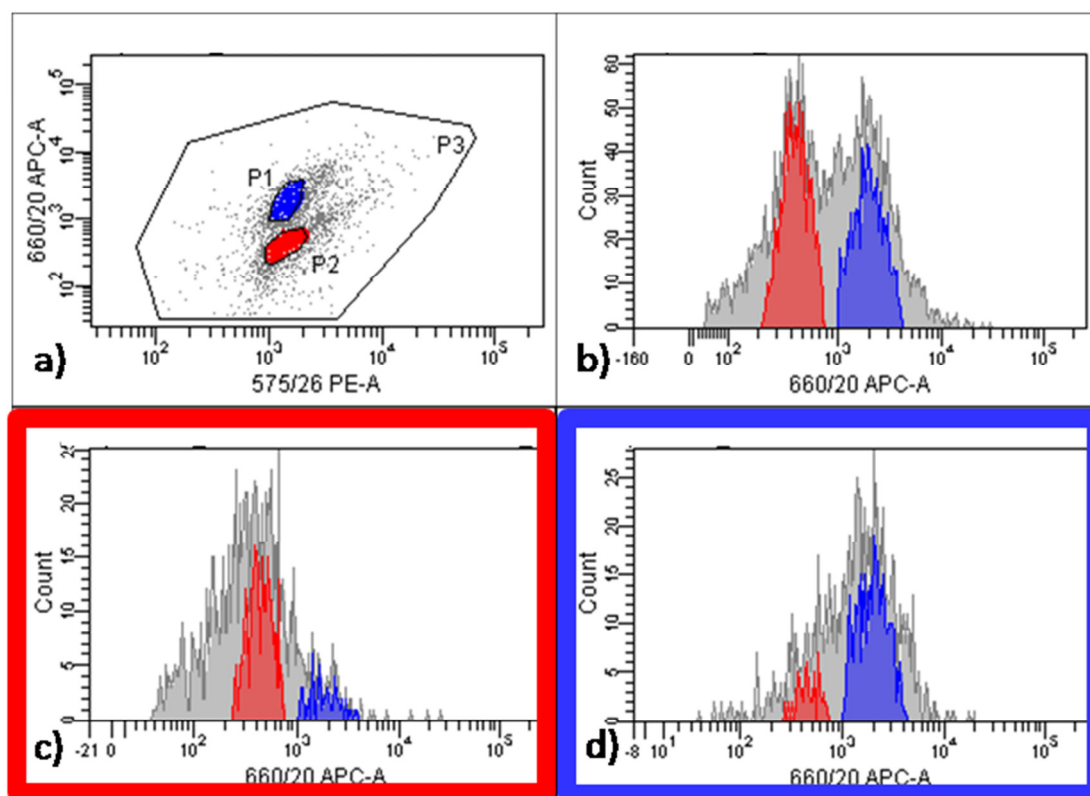
Figure 35. Two representations of FACS data for a sample of SU-8 particles containing two differently fluorescing populations a) dot plot showing fluorescence of individual particles at 575 nm and 660 nm wavelengths and b) histogram showing the same results as a count of hits at varying fluorescence intensities in the 660 nm wavelength. Populations were gated based on their fluorescence intensity at 660 nm (the higher fluorescence population was designated P1 and coloured blue, the population with lower fluorescence was designated P2 and coloured red). P1 and P2 were sorted and the rest of the particles (P3) discarded. The sorted samples were re-analysed with c) showing a single low fluorescence population and d) a single high fluorescence population. Populations displayed a broad range of fluorescence intensities even after stringent sorting

This error in the measurement of fluorescence of SU-8 particles could be due to the (random) orientation of the particle in relation to the detector. As the particles are cuboids different faces will emit different total fluorescence intensities and so the angle at which measurements are taken may affect the value obtained. In order to test this theory the orientation of SU-8 particles during cell sorter analysis would need to be controlled so that the same surface could be measured every time. This modification is beyond the scope of this project but perhaps could be achieved using hydrodynamic focusing or by electrode deflection.[240,241,242,243] Measuring GMA beads, which are spherical, did result in narrow fluorescence ranges of 0.2 orders of magnitude.

During the course of this work the FACS was often used to analyse samples of particles even though this would result in a large standard deviation (s.d.) between individual particles. However this data was valid due to the very large numbers of particles analysed for each sample allowing errors to be quoted as standard errors (s.e.), (s.d./√(number of readings). The large standard deviation would cause problems with the analysis of multiplexed assays where it could make two or more particle populations with differing fluorescence intensities indiscernible (as the different normal distributions overlap. One of the aims of the 4G project was to develop a working particle sorting device in order to automate the multiplex analysis of biological samples, it was thus considered desirable to continue using the FACS for analysis of DNA multiplex assays in the developmental stage as these results would be more akin to the end system. However, it became apparent that the in-house designed cell sorter would not become a reality, leaving less emphasis on FACS analysis. Both the cell sorter and microscopy are used as analytical tools throughout the research contained herein with microscopy (with a much lower inherent error) becoming the analytical method of choice towards the latter stages of the work.

2.7 Optimisation of hybridisation conditions

The degree of hybridisation between two complementary DNA strands is affected by environmental conditions; most notably temperature, salinity, pH and the concentrations of the two strands.[244,245] Though DNA duplex formation has been studied extensively, the complexity of the many environmental variables and the uniqueness of each DNA sequence make predictions of the optimal conditions for hybridisation of specific sequences difficult. Calculations for the melting temperature (T_m) of duplexes have been developed.[246] Predictions become further complicated by the inclusion of overhanging sections of DNA and in the presence of mismatching base pairs. Further to this, hybridisation to immobilised probe DNA has been less thoroughly studied and is likely to be affected by the immobilisation strategy and the support used. For these reasons a number of experiments were designed to investigate hybridisation to DNA probes immobilised on SU-8 particles

by affinity capture, with the purpose of optimising conditions for particle based multiplex assays.

2.7.1 Assays at elevated temperature

The effect of increasing the temperature on particle-bound probe hybridisation was investigated. Increasing the temperature would reduce the amount of hybridisation as duplexes become less stable. The single base mismatching target, forming a less stable duplex with the probe sequence, would be expected to melt at a lower temperature than the complementary target, therefore discrimination between complementary and single base mismatching targets may be achieved by hybridisation at elevated temperature. Immobilised probe-particles (**PC** and **PD**), in separate vessels, were exposed to either labelled target, **TC** (11 nM) which was complementary or to **PC** which represented a single, mid sequence guanine:guanine (G:G) mismatch to **PD**. The T_m of the complementary duplex was calculated to be 48 °C therefore these singleplex hybridisation suspensions in SSPE (5 ×) buffer, were heated to 60 °C then gently agitated at either 47, 49 or 51 °C overnight.[246] The particle suspensions were washed with hybridisation buffer and the fluorescence intensity of the complementary and mismatching particles was compared using the FACS (Figure 36, no urea wash). Results indicated that complementary hybridisation had occurred at 47 and 49 °C, but was reduced at 51 °C. The single G:G mismatch hybridisation followed a similar pattern but the total amount of hybridisation (fluorescence intensity) was lower than with the complementary at the lower temperatures. Focusing on the lower temperature hybridisations we get a complementary to mismatch signal ratio (c:m) of 12:10 and 15:10 (47 and 49 °C respectively), the particles can therefore discriminate between different target sequences (when not in multiplex).
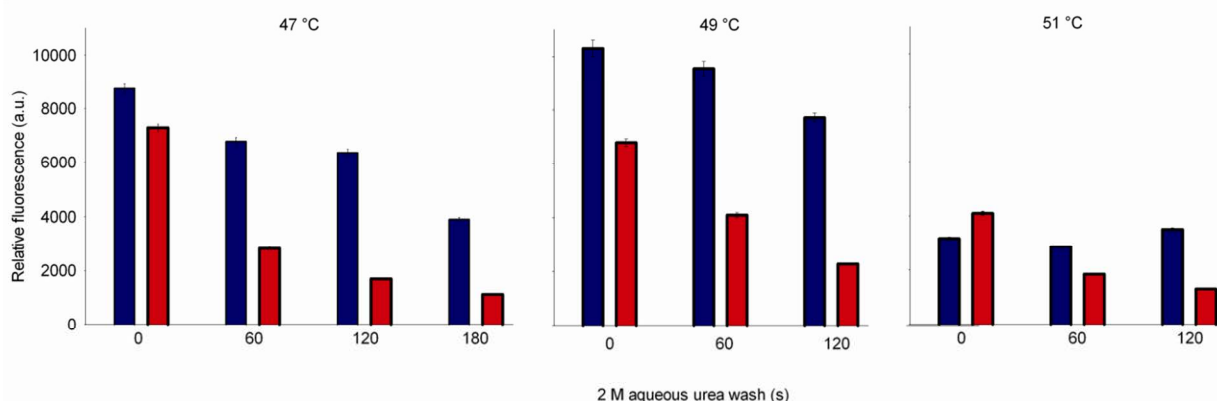
Figure 36. The effects of hybridisation temperature and subsequent suspension in aqueous 2 M urea on target, TC, hybridisation to complementary probe, PC, particles (blue) and single G:G mismatch probe, PD, particles (red)

A c:m ratio of 15:10, however, is not very large, if the two particle types were mixed and analysed using the FACS, only one broad population of particles would be observed (due to the inherently high instrumentation error). If particles could be sorted based upon their encoding then the particles could be used to discriminate between the two target sequences in multiplex, however the technology at this point only allowed discrimination by fluorescence intensity.

This result would suggest that discrimination by varying the temperature of hybridisation alone would not be sufficient. Fine temperature control was difficult with the experimental setup, which required placing an agitator (to keep particles well suspended) within an oven. Temperature was noted to vary by $\pm$ 2 °C and once the samples (within eppendorf® tubes) were removed they started to quickly cool before washing. Further to these problems, the difference in T_m of a mismatching duplex compared with the complementary may be smaller for immobilised DNA than in solution. When probes are immobilised on a support, the localised concentration of ssDNA is very high, this can have the effect of increasing the T_m of any probe target duplex formed. This effect is not very prominent when most of the immobilised probe is hybridised, as in the case of complementary sequences. However, when more of the probes are single stranded the balance of equilibrium for any target in the close vicinity could be shifted to a hybridised state and lead to an increase in the mismatching duplex T_m and a broadening of the associated melting curve (Figure 37).[247,248]
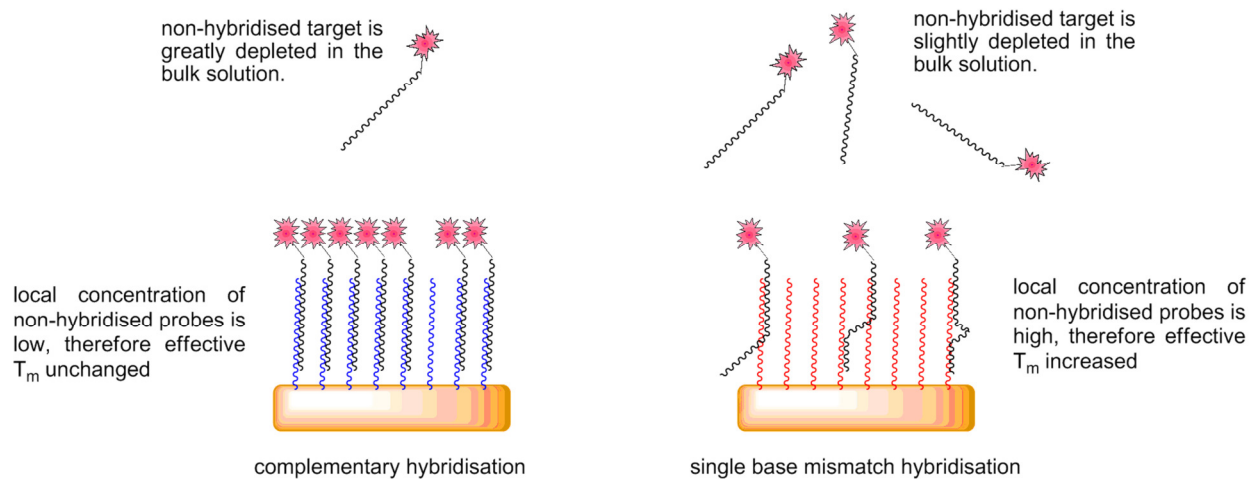
Figure 37. The effects to T_m of the high localised concentration of probe DNA in immobilised probe systems

A further complication with the use of temperature to obtain differentiation would be when large multiplex assays were developed (e.g. 100 different immobilised probe particles discriminating between target solutions), each immobilised probe would exhibit a different complementary duplex T_m, as each assay could only be done at a single temperature the conditions would never be optimal for all the complementary sequence pairs. Therefore, attempts were made to increase the difference in hybridisation between a complementary and a mismatching target sequence without the use of temperature control.

2.7.2 Hybridised probe washing

Washing in aqueous solutions of 2 M urea was found to improve complementary and mismatching sequence discrimination. Washing in 2 M urea resulted in a decrease in the amount duplex for both types of hybridisation, but the effect was more pronounced for the mismatching sequences. Prolonged exposure to urea eventually resulted in complete loss of duplex from both duplex types, implying that discrimination was a kinetic process where the rate constant for the melting of a mismatching duplex was greater than for the complementary duplex. For hybridisations carried out at 47 °C, the initial c:m is 12:10, after 1 minute exposure to 2 M urea the ratio has increased to 24:10 and with a second minutes exposure it is further increased to 38:10, subsequent exposure reduced the ratio (after 3 minutes

c:m = 35:10) as by now little mismatch duplex remained. An overlaid FACS image of the complementary (grey) and mismatched (red) particles after 2 minutes of 2 M urea washing shows the differentiation between the two populations (note; the fluorescence of particles in these two populations were measured independently, i.e. singleplexed) (Figure 38).
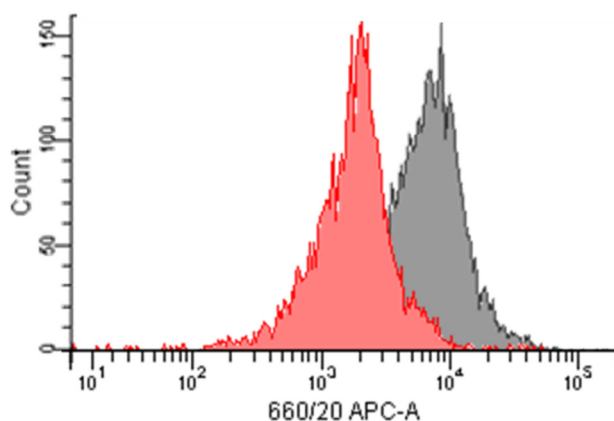
Figure 38. Overlaid FACS histograms of target, TC hybridisation to complementary probe, PC particles (grey) and single G:G mismatch probe, PD particles (red) after 2 minutes exposure to 2 M aqueous urea

2.8 Multiplex DNA assays using encoded-microparticle based affinity-captured probes

2.8.1 Initial multiplex optimisation

The hybridisation of a target oligonucleotide, **TC** to an immobilised complementary sequence, **PC** and a completely mismatching sequence, **PE** were studied. Hybridisations were performed as singleplexes at room temperature, discrimination between the two targets was achieved using a 2 minute wash in 2 M aqueous urea. The two particle suspensions were analysed using the cell sorter (FACS) to measure the fluorescence intensity of individual particles (Figure 39, a – d). Probe particles which were complementary to the target sequence showed a high fluorescence intensity (25000 ± 1600 a.u., N = 890) compared with the non-complementary probe particles (540 ± 28 a.u., N =747). Overlaying fluorescence histograms (Figure 39, e) indicated that differentiation between the two populations would not be possible in a multiplex due to overlapping of the broad intensity range over which each population extended. If the two populations were mixed, one very broad peak would result from

histographic display. By instead displaying the fluorescence data as a dot-plot (Figure 39, f), where each particle was represented by a single point plotted against fluorescence in two channels, 660 nm (Cy-5 emission) and 575 nm (SU-8 autofluorescence), gave a much clearer differentiation between the differently fluorescing particle populations.
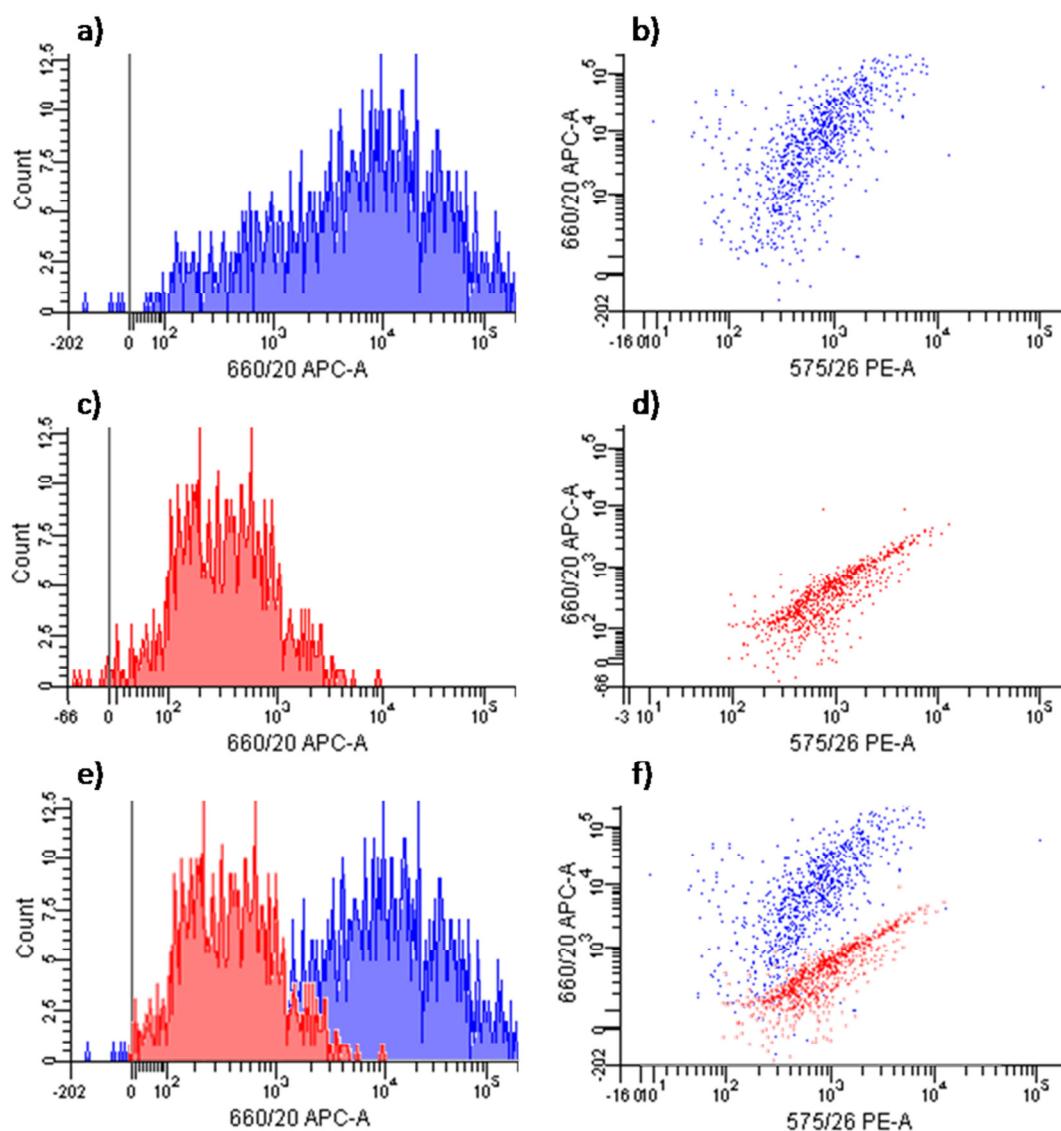
Figure 39. FACS data in the form of fluorescence histograms (left) and fluorescence dot-plots for labelled target, TC hybridisation to immobilised complementary, PC (a and b) and completely mismatching, PE (c and d) probes. Hybridisations were not in multiplex. Overlaid images are shown (e and f) showing more obvious population differentiation using the dot-plot representation

The same probe particles were used to differentiate between target sequences in multiplex. This time **TC** was added to a sample containing both immobilised complementary probe **PC** particles and completely mismatching probe **PE** particles

in suspension. Conditions of this multiplex hybridisation were identical to the previous singleplexed experiments Once again a 2 minute wash in 2 M urea solution was used to discriminate between complementary and mismatching duplexes, however when the sample was analysed, discrimination was very poor (Figure 40) and two populations could barely be discerned.
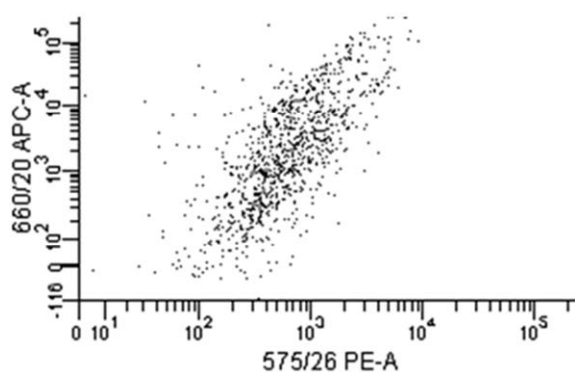
Figure 40. FACS dot-plot of a multiplex hybridisation assay showing attempted labelled target TC discrimination using particle immobilised complementary, PC and mismatching, PE probes in a mixed suspension. The assay had been left for 16 hours to reach equilibrium

Next, separate samples of immobilised probes, **PC** and **PE** which had each been pre-hybridised with the labelled target, **TE** and washed, were combined. The fluorescence intensity of these particles, now in a mixed suspension, were analysed using the FACS (Figure 41). A merging of the two particle populations was found to take place. Initially, two distinct fluorescence populations were easily distinguished, with one at a higher fluorescence intensity (660 nm), representing probe particles which were complementary to the target DNA. When the mixed suspension was re-analysed 16 hours later, only one fluorescence population could be distinguished. The ability of probe-particle mixtures to discriminate between complementary and mismatching DNA appears to diminish with time.

This represented a problem when carrying out hybridisation assays in multiplex. It was likely the result of biotinylated probe oligonucleotide dissociating from the avidin particles to which it had originally been attached and reassociating elsewhere. As has been determined, biotinylated oligonucleotide binding to immobilised avidin DN is much weaker than the binding between unmodified biotin and avidin in solution (Table 3). The half-life of the affinity binding in the immobilised system

was found to be a few days, however, probe dissociation appears to have a marked effect on the analysis of multiplex hybridisation assays within 16 hours.
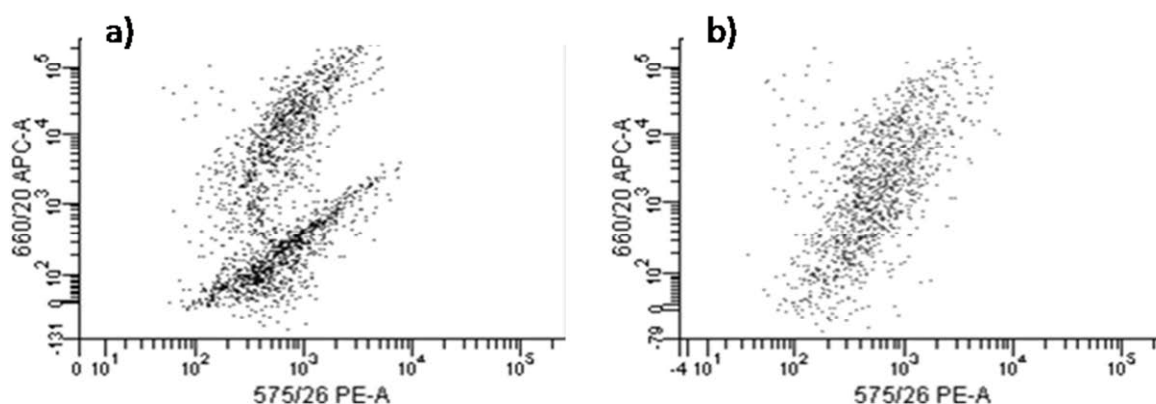
Figure 41. FACS data showing the homogenisation of immobilised probe particles. Labelled target, TC was pre-hybridised to immobilised complementary, PC and completely mismatching, PE probe particles in separate vessels. a) Initially after the two particle samples were mixed, two fluorescent populations were easily discernable, b) within 16 hours probe dissociation resulted in a homogenisation of the different particles' surfaces resulting in a single fluorescence population

2.8.2 Homogenisation of heterogeneous probe-particle mixtures

Further investigation of probe dissociation from the avidin DN particles was made. To a sample of Type II avidin DN particles was bound the labelled and biotinylated oligonucleotide **FP1**. These fluorescent particles were next mixed with a sample of Type II particles to which the unlabelled biotinylated oligonucleotide, **PC** had been bound. The fluorescence of particles in the mixed suspension was monitored (Figure 42). The two populations were initially fluorescently distinct, however an obvious merger of the two fluorescence intensity populations was observed within three hours, by 19 hours two separate populations could no longer be differentiated.
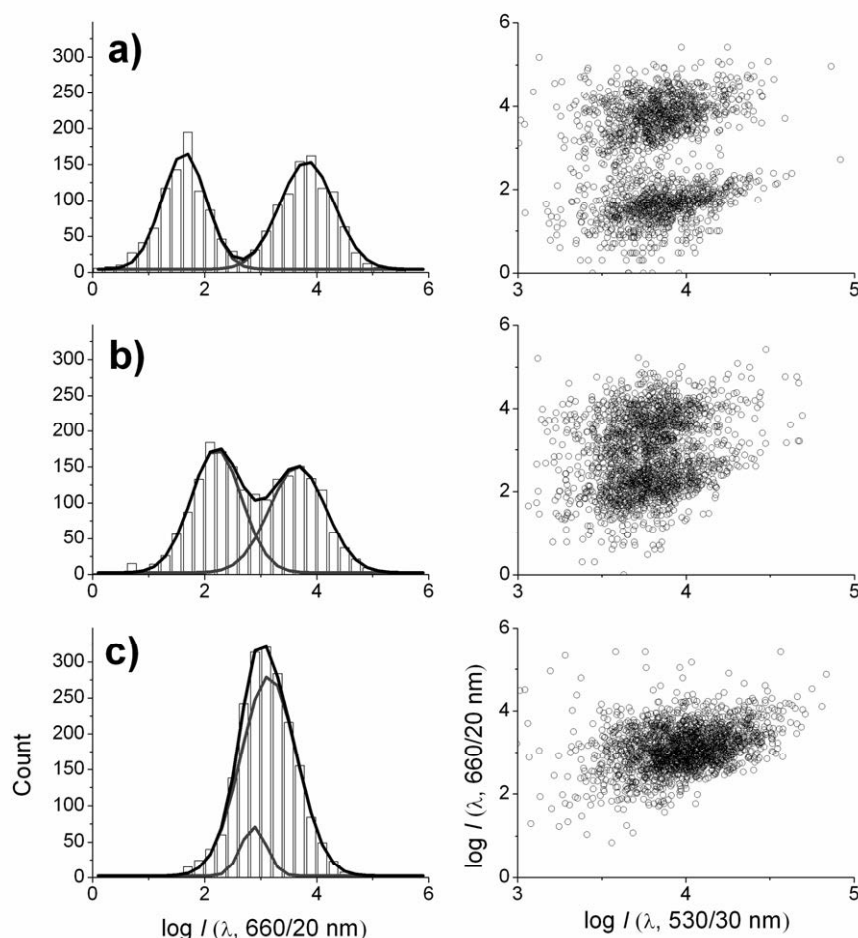
Figure 42. a mixture containing both particles with a fluorescent probe (FP1) and particles with an unlabelled probe (PC) bound. Measurements were taken at t = 0, 143 and 1114 minutes (a), b) and c) respectively) and show the merging of the two populations as the biotinylated probes dissociate and reassociate between particle-immobilised avidin tetramers. This results in each particle eventually having a similar surface containing a mixture of all probe sequences

This instability of probe binding presents a problem for hybridisation assays in multiplex. Most obviously, multiplex hybridisations have to be performed and analysed quickly to achieve the best differentiation between complementary and mismatching sequences. This may not allow time for the system to reach equilibrium which would lead to a reduction in the total fluorescence intensity as hybridisation has not reached a maximum. The problem also means that different probe-particles may not be stored together; biotinylated probes may be immobilised in advance, however these particles need to be separated from any other particles with different probes bound.

2.8.3 An encoded microparticle based multiplex hybridisation assay to discriminate between complementary and completely mismatching DNA sequences

Despite the problems identified with the use of the biotin avidin system for microparticle immobilisation of DNA probes, a number of multiplex assays were successfully performed. These demonstrations of multiplexing were useful for developing different particle handling techniques. Statistical tests were used to help determine the parameters of a working particle-based multiplex assay.

The multiplex discrimination of complementary and mismatching target sequences was attempted using probe oligonucleotides affinity bound to encoded microparticles. Biotinylated oligonucleotide probes were immobilised to particles with differing diffractive encoding (**PE** immobilised to particle type 2 and **PC** to particle type 3). After washing, samples of each probe particle conjugate were combined and exposed to a solution containing the labelled target oligonucleotide, **TC** (350 nM). Assays were allowed to equilibrate in suspension for just 40 minutes (to minimise loss of probe) this was followed with a wash in hybridisation buffer (SSPE (5 ×), further, more stringent urea washing was not found to be necessary to achieve sequence differentiation. Particles were imaged by fluorescence microscopy, where the two particle types displayed different fluorescence intensities (Figure 43). The assay mixture was then analysed using the fluorescence activated cell sorter (FACS) where two clear fluorescence populations were once again visible (Figure 44). These two populations were gated (FACS) and sorted into separate vessels based upon their fluorescence intensity. Finally, these high and low fluorescence samples containing sorted particles were assessed by microscopy where the particles were decoded both visually (by the operator) and by using the in-house designed integrated particle fluorescence and code reading device (Figure 45) (which at this developmental stage could not be used to quantify fluorescence, hence the requirement for pre-sorting of the different particle-fluorescence populations using the FACS). The device combined imaging of the diffraction of light by individual particles and software to measure the angle of diffraction (the encoding) which was unique for each particle type.

This analysis method incorporating sorting by fluorescence intensity followed by particle decoding was repeated for probe particle mixtures exposed to the second complementary target sequence (**TE**).

Figure 43. White light (left), SU-8 autofluorescence and Cy-5 fluorescence images of the multiplex analysis of a sample containing (TC) using immobilised probe DNA. The complementary probe (PC) was bound to type 3 particles (5 ridges visible) whilst the completely mismatching probe (PE) was bound to type 2 particles (4 ridges visible). Note only type 3 particles (complementary) exhibit Cy-5 fluorescence

Figure 44. FACS analysis of the complementary and completely mismatching DNA discrimination multiplex assay showing two clear fluorescence populations. The two populations were gated (the population with greater Cy-5 fluorescence emission, in blue, represented a high degree of hybridisation) and sorted according to fluorescence intensity

A summary of the analysis of these samples is shown (Table 4). Sorting by fluorescence resulted in 100% accuracy. For the multiplex with the target sequence (**TC**), 100% (50/50) of the particles in the higher fluorescence population were identified (visually) as being particle type 3 representing complementary hybridisation. Likewise 100% (51/51) of the particles in the population with lower fluorescence were identified as being type 2, those with the mismatching probe

bound. Using the code reader to measure the angle of light diffraction correctly identified 98% (49/50) of the particles in the high fluorescence population with one particle being misread as having a different encoding which corresponded to a particle type not present in the assay. Similarly 96% (49/51) of the particles in the population with lower fluorescence were correctly identified as type 2, a single particle was incorrectly read having type 3 encoding and another particle as being unidentifiable by the software due to structural damage. Analysis of the multiplex assay exposed to target oligonucleotide (**TE**) was equally robust. Once again all of the particles of the higher fluorescence population were visually identified as being those with the complementary probe bound whilst all the particles at the lower fluorescence had the mismatching probe. The software identified the particles correctly in 94% of these reads.
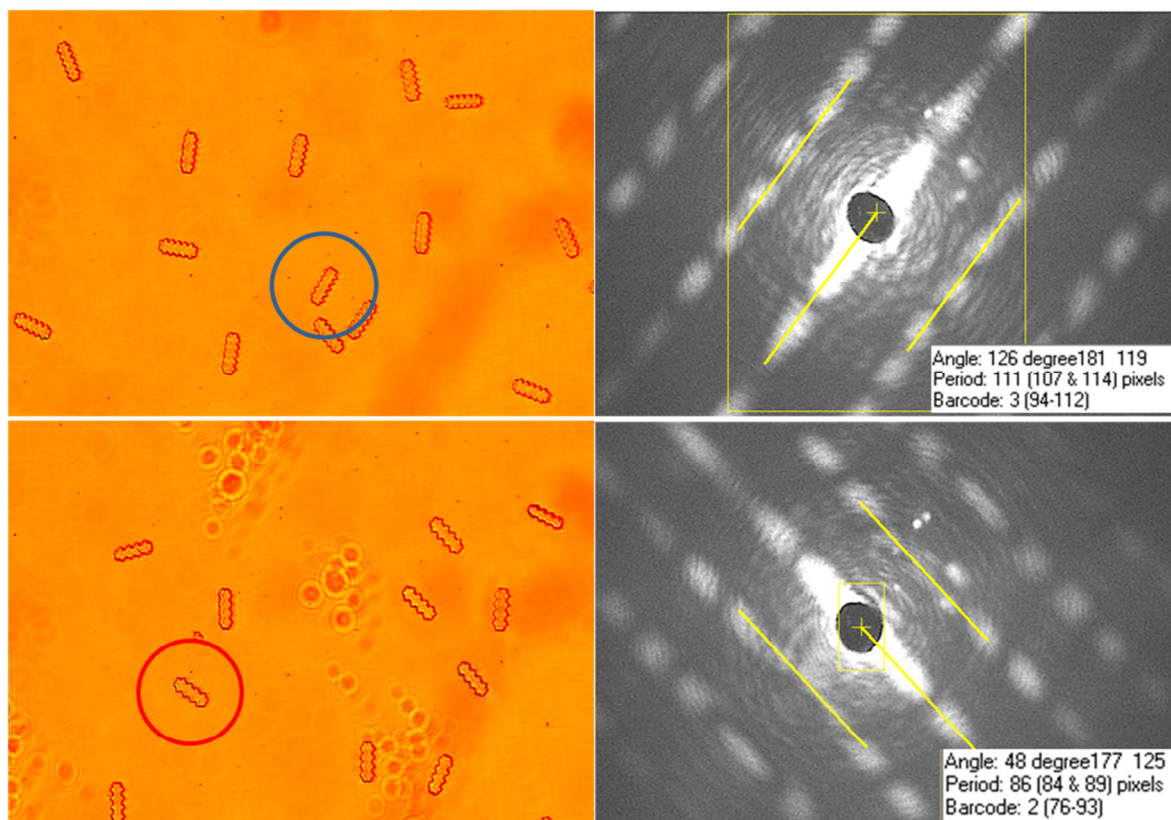
Figure 45. Images of FACS sorted populations of fluorescent particles from the complementary and completely mismatching DNA discrimination multiplex assay. Particles from the higher fluorescence population (top) represented complementary hybridisation and were found to be exclusively of type 3 encoding, an image of the corresponding diffraction of light by the encircled particle (the encoding) is also shown. Likewise, particles from the population with lower fluorescence (bottom) were identified as being exclusively of type 2 encoding

Table 4. A summary of the fluorescence measurement and particle identification of differently fluorescing particle populations in the complementary and completely mismatching DNA discrimination multiplex assay. This is the analysis of particle samples after having been sorted (FACS) into two populations based upon fluorescence intensity

Labelled target DNA	Mean particle fluorescence (a.u.)	Number of particles identified (visually/diffractively) for each encoding type				
		1	2	3	4	unidentifiable
(**TC**)	5090 ± 61	0/0	0/0	50/49	0/1	0/0
(**TC**)	651 ± 6	51/49	0/0	0/1	0/0	0/1
(**TE**)	2865 ± 49	52/49	0/1	0/0	0/0	0/2
(**TE**)	634 ± 6	0/0	0/0	52/49	0/1	0/2

This experiment demonstrated the multiplex discrimination between complementary and completely mismatching oligonucleotide sequences using encoded particles. Analysis was semi-automated and had a 96 % correct read percentage, which, with further optimisation of the read software could be improved. Furthermore, complementary and mismatching sequences were discriminated with a 100 % success rate, with all the particles observed in the higher fluorescence populations being visually identified as representing complementary hybridisation. This result suggested that the major problems in previous experiments, most notably the nonspecific binding of target DNA and the dissociation of probe molecules from the particle surface could be circumvented by the use of Tween$^{®}$-20 surfactant and by the decrease in the total time over which different particle types were mixed.

2.8.4 An encoded microparticle based multiplex hybridisation assay to discriminate between complementary DNA and sequences containing a single base mismatch

The multiplex hybridisation assay was used to differentiate between oligonucleotides differing by a single base. Biotinylated probes were bound to avidin DN functionalised encoded particles, with probe (**PC**) attached to particle type 3 (5 ridges) and probe (**PD**) to particle type 2 (4 ridges). Both types of probe-immobilised encoded particles were combined and the mixed suspension was exposed to the labelled target oligonucleotide (**TC**) (350 nM) for 40 minutes. This target sequence was complementary to the probe (**PC**) immobilised on particle type 3 and

represented a single, mid-sequence G:G mismatch to the probe (**PD**) on particle type 2. After washing in the hybridisation buffer (SSPE (5 ×)) the particles were washed for 2 minutes in a 2 M aqueous urea solution to aid in the differentiation between complementary and mismatching hybridisation. Particles were analysed as previously where the particle mixture was first imaged by fluorescence microscopy (Figure 46), followed by FACS analysis (Figure 47) and sorting into two populations based on fluorescence intensity, the particles in these populations were then decoded both visually and using the automated setup, results of which are presented (Table 5).
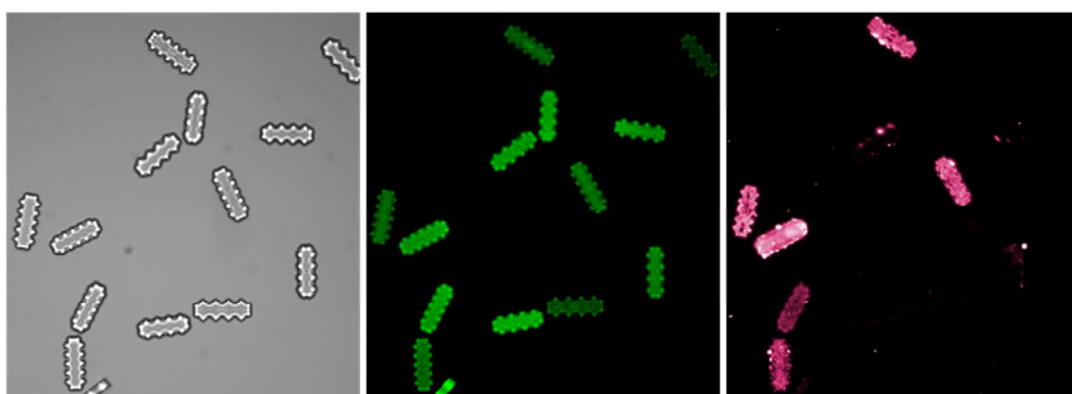
Figure 46. White light (left), SU-8 autofluorescence and Cy-5 fluorescence images of the multiplex analysis of a sample containing (TC) using immobilised probe DNA. The complementary probe (PC) was bound to type 3 particles (5 ridges visible) whilst the single base (G:G) mismatching probe (PD) was bound to type 2 particles (4 ridges visible). Note only type 3 particles (complementary) exhibit Cy-5 fluorescence
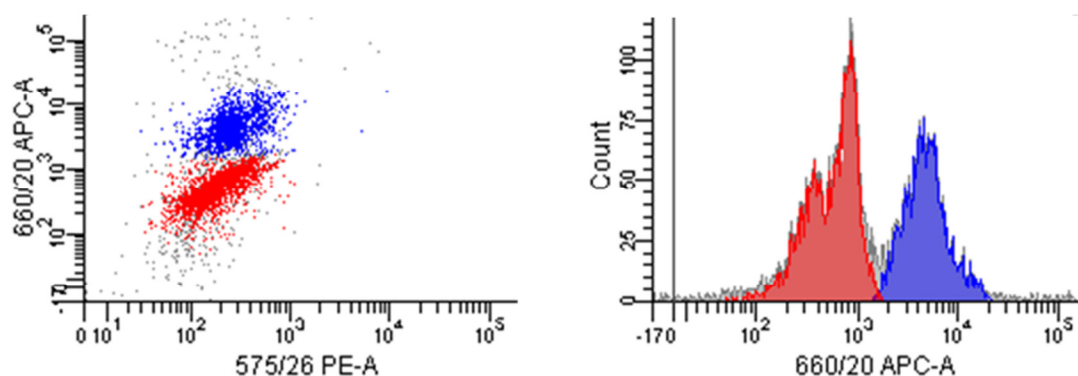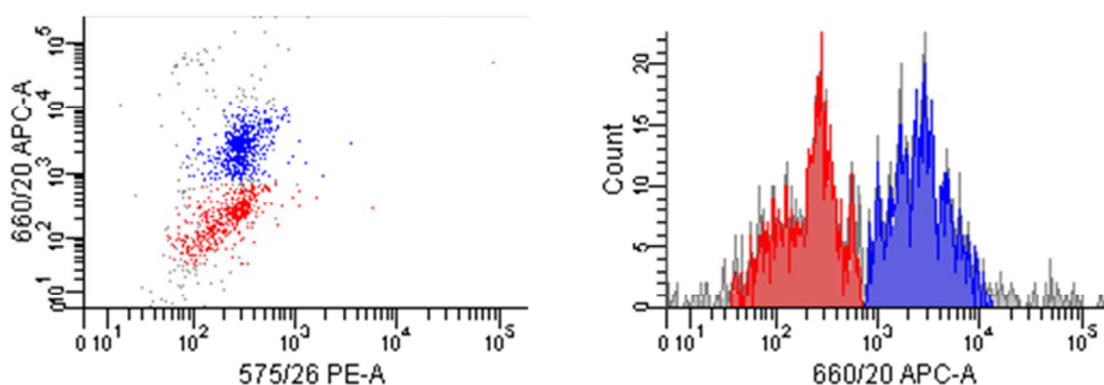

Figure 47. FACS analysis of the complementary and single base mismatching DNA discrimination multiplex assay showing two clear fluorescence populations. The two populations were gated (the population with greater Cy-5 fluorescence emission, in blue, represented a high degree of hybridisation) and sorted according to fluorescence intensity

Table 5. A summary of the fluorescence measurement and particle identification of sorted fluorescence populations from the complementary and single base mismatching DNA discrimination multiplex assay, target sequence (TC) was complementary to probe (PC) immobilised on type 3 encoded particles

Mean fluorescence intensity (a.u.)	Particle identified (visually/diffractively)				
	1	2	3	4	unidentifiable
3054 ± 80	2/3	0/0	48/42	0/5	0/0
237 ± 6	48/44	0/0	2/5	0/0	0/1

The analysis of the sorted fluorescence populations indicated that 96% of the particles found in the highly fluorescent population were of type 3, encoding for the complementary sequence, whilst 4% of the particles identified were of type 2. The reverse was found for the population with lower fluorescence, with 96% of the particles having type 2 encoding. The encoded microparticle based multiplex hybridisation assay had been shown to successfully discriminate between a complementary and a mismatching sequence differing by a single base.

2.9 Conclusions

The kinetic and thermodynamic properties of the binding between a labelled and biotinylated oligonucleotide and avidin DN immobilised on polymer microparticles via different attachment chemistries have been thoroughly investigated. Rates of association were found to be diffusion limited, as they are for the free avidin biotin system. However the rate was significantly reduced compared with the wild-type. One reason for this was because the rate of biotin diffusion was significantly lowered by conjugation to an oligonucleotide probe which made the ligand a much larger species. Another reason was the steric hindrance which came from being immobilised to a large surface, blocking the approach of biotin from one side and reducing the chances of a collision. Rates of dissociation were increased compared with the non-immobilised avidin system, which in turn displayed rates increased compared with those reported for the wild-type avidin biotin complex. These results indicated that both the modification of the carboxylic acid moiety of biotin and the immobilisation of avidin DN have significant effects on complex stability, leading to our system having a complex $t_{1/2}$ of only five days. This increased dissociation rate

has implications for the use of avidin affinity as the immobilisation method in multiplexed assays when probes are sharing the same solution. This weakened complex was a very obvious problem as when different probes were immobilised on different particles and mixed in the same solution, probe swapping occurred resulting in the originally differently functionalised particles being indiscernible within a day.

Our kinetic results were similar to the incomplete and imprecise data for immobilised avidin which has previously been reported. When comparing with more comprehensive studies using immobilised biotin, we obtained a similar equilibrium dissociation constant but differing rate constants, with values between those of the two sets of reported data.

Comparisons were made between the three different protein immobilisation methods investigated. Stable protein mono-layers were formed in each case, however having the coupling reagent (EDC) *in-situ* resulted in both the highest levels of non-specific biotinylated-probe binding and the lowest levels of avidin activity, furthermore, complex stability was reduced with a $t_{1/2}$ of less than two days. The NHS pre-activation and affinity capture methods lead to identical rate constants and similar degrees of non-specific binding, however the covalent attachment resulted in a significantly greater avidin activity, binding the most biotinylated probe.

Despite the transient probe immobilisation, these encoded microparticles were used for a number of hybridisation assays, both in singleplexed sample analysis for methodology development and in multiplexed analysis as a technology demonstrator. Multiplexes were made possible by only allowing probe-functionalised particles to be mixed for short lengths of time, complex dissociation was therefore minimal and probe migration between different particles not observed.

Affinity capture was clearly not a good long-term strategy for probe immobilisation in the design of our multiplexed suspension array, a more permanent tether was required.

3.0 Particle-immobilisation of oligonucleotide probes by amide coupling

The immobilisation of oligonucleotide probes via affinity binding had been found to be inappropriate for use in our particle based multiplexed DNA assays due to the increased rate of biotinylated DNA probe dissociation from the particle's avidin-functionalised surface (2.9.2). Transient probe immobilisation lead to particles which initially each had a single probe sequence bound, having a surface populated by all the different probes in a multiplex. Encoded particle multiplex assays make use of oligonucleotide probes immobilised on particles, these particles can be identified by a unique code and therefore each probe sequence can be localised. The link between the code and the probe needs to be stable to have a high degree of confidence in the identity of the probe once the code has been read.

Covalent probe attachment has a number of benefits, most importantly for our assay systems a permanent bond would be formed eliminating problems of probe loss or swapping. In addition, it would be possible to develop a more flexible assay system as the linkage would be more stable to extremes of temperature and pH than any affinity binding. Furthermore, solid phase chemistry techniques are well established and permit an array of attachment chemistries, this allows the surface functionality to be modified giving a handle for the control of various physical and chemical properties.

The covalent attachment of oligonucleotide probes to epoxy SU-8 microparticles was investigated. The aim of this work was to develop stable covalent attachment chemistries which gave control of the density of probe molecules and the overall charge properties on the surface, allowing the optimisation of complementary target DNA hybridisation and the minimisation of nonspecific DNA binding to be achieved in tandem.

3.1 SU-8 microparticles

SU-8 particles (**7**) are fabricated by the acid catalysed polymerisation of epoxy SU-8 monomer (**6**). Polymerisation is initiated by the activation of the photoacid under UV

illumination and propagated by heat. Microstructures including the encoded microparticles used in this work can be patterned using a mask to selectively block exposure during illumination (Figure 13). After polymerisation, any excess SU-8 monomer is leaving particles with an epoxy surface functionality derived from the uncrosslinked sites along and at the termini of polymer chains (Figure 48). Epoxide functionality gives a handle for the chemical modification of SU-8.

7
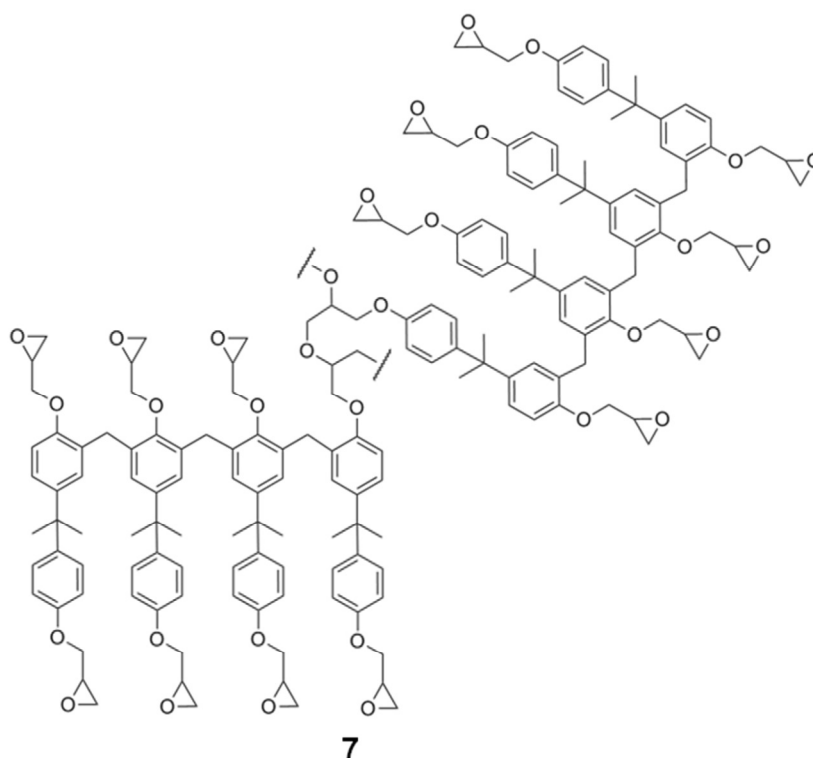
Figure 48. Two subunits of an SU-8 polymer chain. Two epoxide groups have been polymerised to form ether bridges within the bulk polymer, any uncrosslinked epoxide groups are retained and are available for chemical modification

During the studies of the covalent attachment of avidin to the particle surface, polymerised epoxy SU-8 was modified with bis-amines and succinylating reagents to afford an amine or an acid surface functionality (Scheme 2). Stable protein attachment was attained by using carbodiimide coupling reagents with carboxylate SU-8 particles, resulting in attachment via an amide bond. These results indicated that polymerised SU-8 was amenable to standard coupling chemistry protocols and potentially solid phase synthesis.[191]

3.1.1 The distribution of functional groups on the surface of SU-8 particles

Covalently coupling avidin (Type II) previously resulted in a monolayer of protein as calculated from the quantity of protein attached and as observed from the uniform surface fluorescence obtained when labelled biotin species were bound (Table 2). However, a difference in the coverage between different sides of the particles was sometimes observed when studying protein particles complexed with labelled biotin. Here the two largest faces (top and bottom during fabrication) would often have a much lower fluorescence intensity compared with the four side faces, indicating a lower protein coverage on these faces. An example of this can be seen on avidin functionalised particles to which the labelled probe, **FP1**, was specifically bound (Figure 22a). This indicated that not all sides of the SU-8 particles had an equal density of epoxide groups.

Further investigation of the distribution of available functionality used the direct coupling of carboxylate Cy-5 (**14**) to amine modified SU-8 microparticles (**8**) in order to map the functional group distribution. Coupling was successfully achieved under both organic and aqueous conditions (HOBt/TBTU in DMF and EDC in water), with both methods resulting in particles (**15**) with similar fluorescence intensities (Scheme 4).
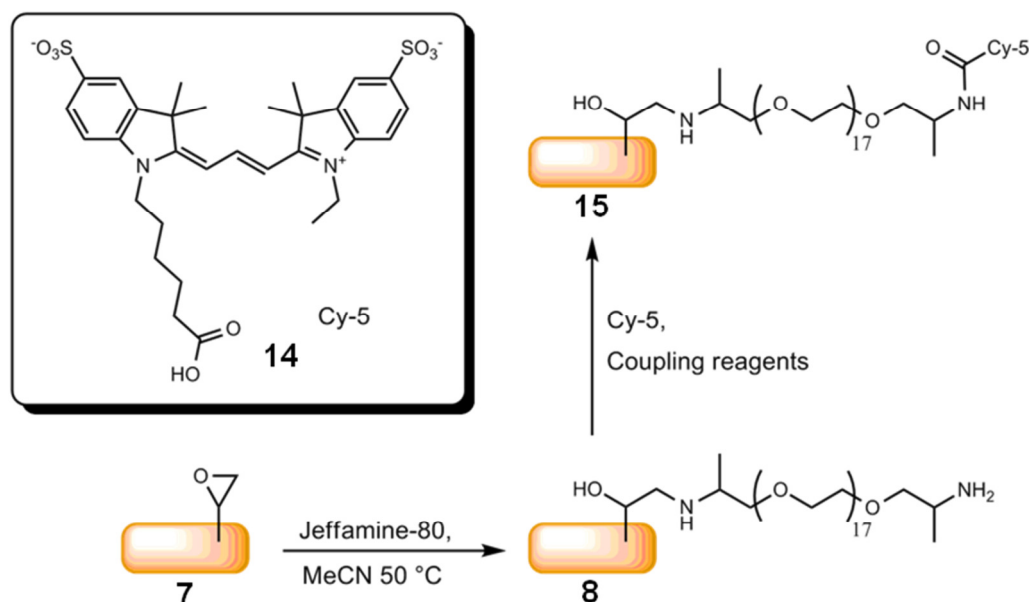
Scheme 4. The reaction of a bis-amine (Jeffamine® ED-900®) with epoxy SU-8 particles and the subsequent amide coupling of Cy-5. Coupling was successful under both organic and aqueous conditions. Coupling reagents consisted of either HOBt, TBTU, DIPEA, DMF (organic) or EDC, imidazole buffer pH 7.0 (aqueous)

Imaging under the fluorescence microscope, when particles were observed perpendicular to the largest face a low fluorescence signal of 6 a.u. was recorded (Figure 49, a, b & d), whereas when observed perpendicular to the smaller faces an intense signal of 83 a.u. was detected (Figure 49, a, c & e). From a side-on viewpoint looking at the smaller faces (Figure 49, c & e), the distribution of fluorescence was more obvious where the observed face showed uniform signal (83 a.u.) increasing in intensity when approaching the edges connecting with the two other small faces (139 a.u.). This increase in intensity was not observed along the long edges which connected with the largest of the particle's faces. To rule out internal reflection as an explanation for this uneven fluorescence signal distribution under aqueous conditions, particles were observed suspended in glycerol as the refractive index (n) of glycerol is 1.47 (similar to that of the glass slide and cover slip) whereas for water n is 1.33. The fluorescence distribution was unchanged in glycerol, indicating the distribution of fluorescence was the result of an uneven distribution of Cy-5 fluorophore on the particle surface. From this result it was inferred that the four smaller faces of the SU-8 particles had a much greater loading density of epoxide available for functionalisation than the two largest faces.
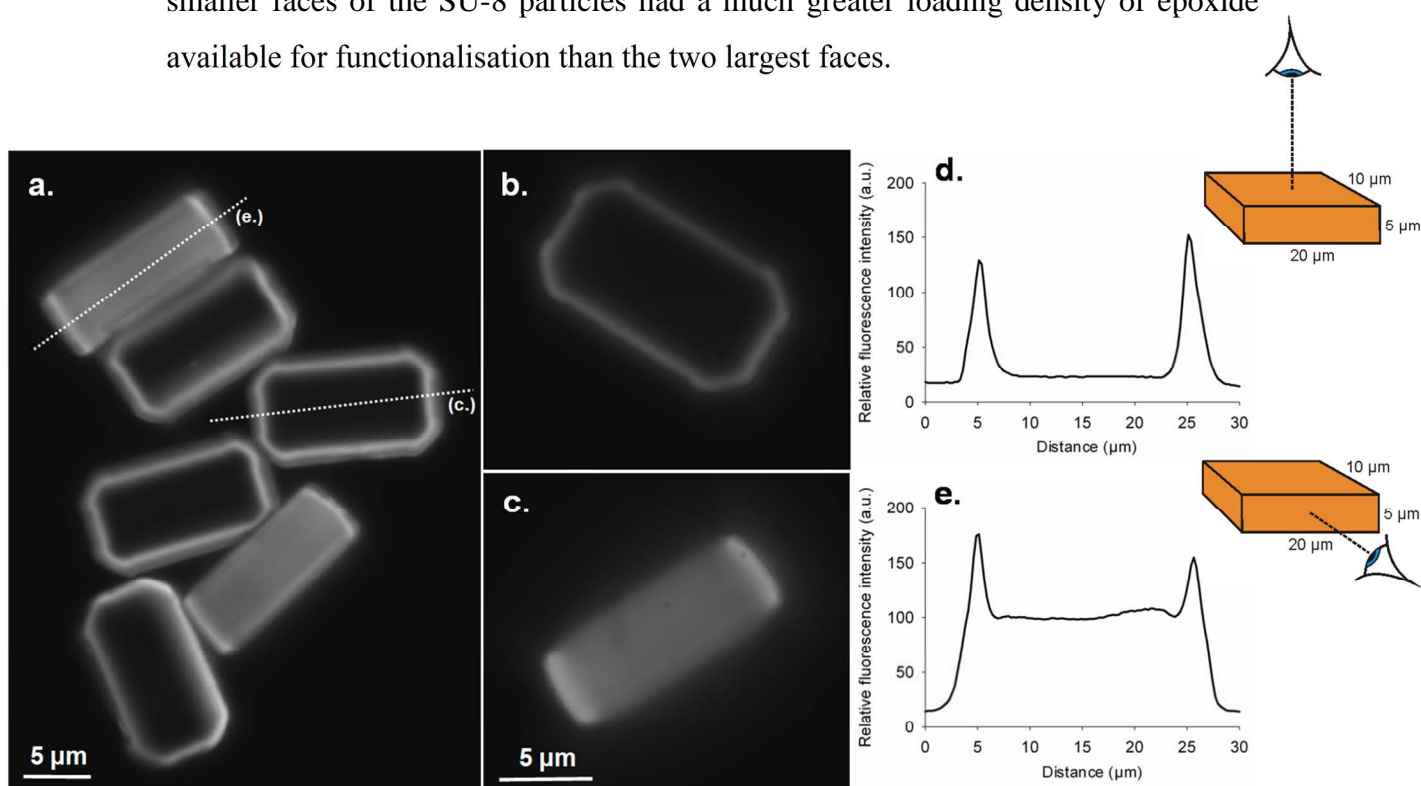
Figure 49. a) A fluorescence microscopy image of Cy-5 coupled SU-8 particles (15) with images highlighting b) a view perpendicular to the particle's largest face and c) perpendicular to a smaller face. Fluorescence intensity cross sections across d) the largest face and e) a smaller face

It was unclear how the differences between surfaces of the same particle had been introduced. This was a batch phenomenon where some particle production runs would result in the uneven distribution of accessible epoxide whereas others would result in a uniform coverage with all six sides having similar loading. There was continuity within a production run where all the particles from the same batch would exhibit an identical distribution. Batches of particles were produced by apparently identical microfabrication protocols.

As some batches did result in a high (and uniform) epoxide loading density on all six particle faces, there did not seem to be a fundamental problem with the fabrication process itself. The occasional variation problem was likely to be due to changes in baking and UV illumination times, as these were more variable (being controlled by an operator). Having longer illumination and/or baking steps and higher temperatures results in a greater degree of cross-linking between monomer units which would lead to a reduction in the amount of residual epoxy functionality remaining.[249] The fabrication could be improved by the use of automated illumination and heating steps to achieve a greater consistency between particle batches. Another cause of variation comes from the evaporation of solvent from the commercial SU-8 monomer preparation used. The same bottle of monomer/photo-acid/solvent would be used for multiple batches of particles; however once a bottle was opened, solvent evaporation would occur which would result in a higher concentration of monomer and lead to a greater degree of cross linking.[251] Automated exposure steps and the use of fresh SU-8 monomer preparation would have improved the reliability of particle fabrication, resulting in less epoxide loading density variation between different particle batches and more reproducible results.

The surfaces of the particles were imaged under very high magnification using SEM which revealed structural differences between the top/bottom faces and the side faces (Figure 50).[250] The two large faces were revealed to be very smooth, whereas the smaller faces were far rougher with distinct pits and bumps (features with diameters of approximately 100 nm). This showed that the different environments the particle faces were exposed to during fabrication had an effect on the physical properties of those faces in addition to the chemical properties previously discussed. SEM and AFM images of the surface of polymerised SU-8 layers have been published, comparing the structures of these layers after having undergone different degrees of

cross linking.[251] In the published work, the amount of cross linking was lowered by reducing the concentration of SU-8 monomer in the solvent during UV exposure. The SEM images published were in good agreement with the surfaces observed on our particles (Figure 50); where under high monomer concentration/high cross linking conditions a smooth, featureless surface was achieved, whereas polymerisation at lower concentrations/reduced cross linking resulted in a rough surface with 10 – 20 nm features.

During the fabrication of our particles it seems likely that the concentration of SU-8 monomer was higher near the surface than in the bulk liquid due to solvent evaporation. This may result in a higher degree of cross linking on the large top face than on the on the small side faces which were immersed in the solvent/monomer bulk. The bottom face (the other large face) is unlikely to be affected by solvent evaporation, however nor is it in contact with liquid monomer SU-8, therefore under high cross linking conditions (long illumination and/or long heating cycles) polymerisation could still go to completion again leaving little residual epoxide.
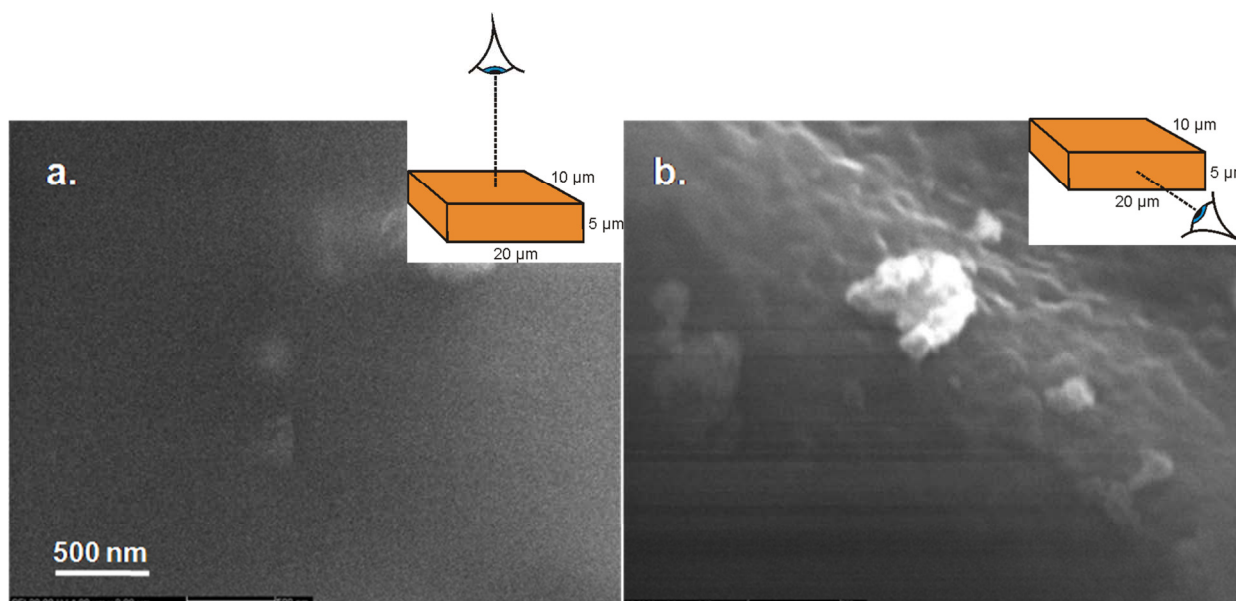
Figure 50. Scanning electron microscopy (SEM) images of SU-8 particles focused on a), a large face and b), a smaller (side) face

It is possible to (re)generate surface functionality of polymerised SU-8 under harsh conditions, possibly by acid treatments (discussed later) and by oxygen plasma treatments.[252] These treatments are not ideal for the chemistries studied herein as a

mixture of different functional groups are formed, for example, exposure to oxygen plasma oxidises the cross-linked SU-8 to form a mixed surface of ether, alcohol, aldehyde and carboxylic acid groups. Chemical oxidation could be used to convert these alcohol and aldehyde moieties to carboxylic acids (e.g. using Jones reagent, Cr^{VI}), however plasma etching also damages (etches) the polymer surface.

As epoxide distribution varied between different batches of particles; those with no top/bottom face functionality were used for initial testing of various immobilisation chemistries whereas particles with more uniform distribution were used for assessing the probe loading levels, quantifying non specific binding and in actual multiplex assays.

3.2 Probe immobilisation using amide chemistry

Amide coupling between amine and carboxylic acid modified substituents is a commonly used method for covalent linking.[253,254] There are many examples of oligonucleotide probes being immobilised in this way, often utilising the reaction between an amino oligonucleotide and a support with acid functionality.[255,256,257] The technique is widely used due to the ease of both oligonucleotide and surface modifications, the large range of available coupling reagents, the robustness of the reaction and the option of coupling under either organic or aqueous conditions.

As a proof of principal, oligonucleotide probes were immobilised to SU-8 particles with a carboxy surface using carbodiimide-mediated amide coupling. Probes were purchased with a terminal amine modification and were coupled to acid particles which had previously been activated using EDC and sulfo-NHS to give a reactive NHS-ester surface (Scheme 5). One sample of carboxyl particles incorporated a 58 atom Jeffamine® ED-900® (**8**) spacer, whilst another did not (**17**). Successful probe immobilisation was observed by the immobilisation of Cy-5 labelled amino oligonucleotide (**FP2**), whereupon the surface of the particles became blue and was highly fluorescent (60,000 a.u.).
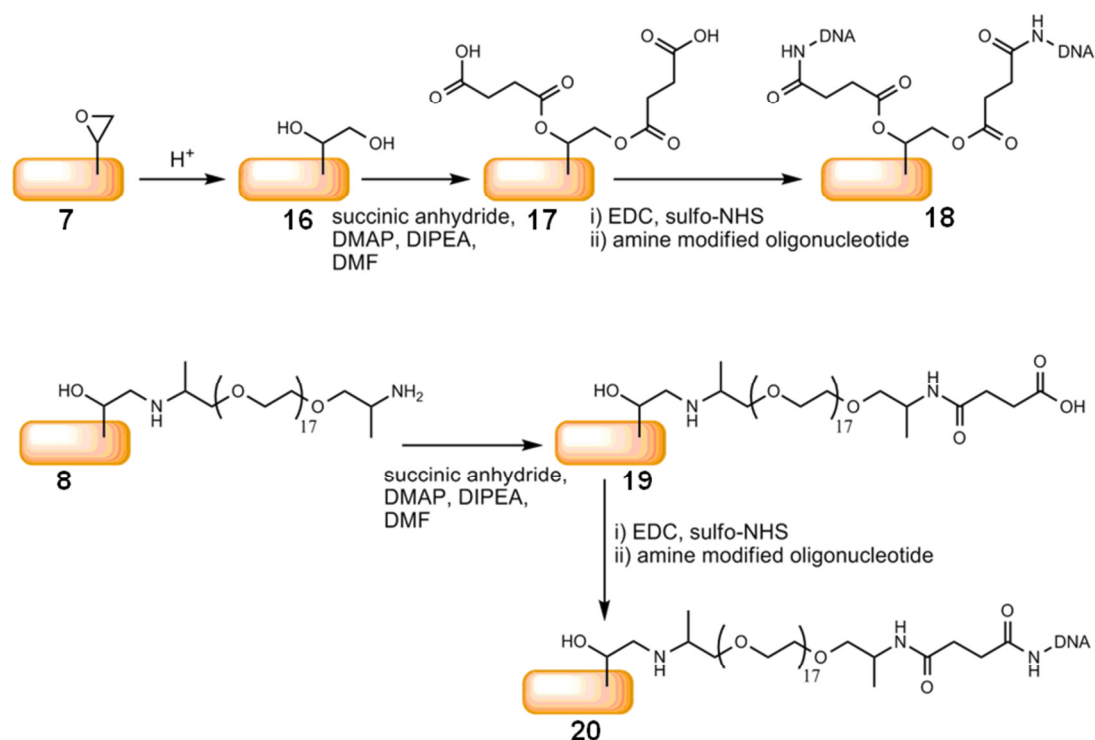
Scheme 5. The amide coupling of amino modified oligonucleotide probes to SU-8 particles without and with a 58 atom Jeffamine® ED-900® spacer group

Using particles with the amide coupled probe, **P2**, test hybridisations were carried out at room temperature using complementary, **T2**, and completely mismatching, **T3**, labelled target sequences. Complementary hybridisation occurred and gave a greater fluorescent signal compared with the non-complementary (10,000 compared with 2000) demonstrating that our SU-8 particles can be used for oligonucleotide identification after probes have been immobilised by amide coupling. Though this experiment was a successful proof of principal, a number of problems were highlighted which would need addressing. Firstly, though the non-specific binding of labelled target sequences to probe particles was very low (as evident by the low signal from particles used for the non-complementary hybridisation assay), the non-specific binging of target to carboxylic acid particles was high. This was unexpected as both the target sequence and the particle surface have the same net charge. Furthermore, exposing carboxy particles to **FP1** (without any carbodiimide reagents) resulted in a high fluorescence intensity showing that the amine modified probe sequences also exhibit high levels of non-specific binding, likely due to electrostatic interactions between amine and acid moieties. This non-specific probe to surface

interaction was found to be a lot more stable than the target to surface interaction, and could not be reduced by repeated washing steps.

The second problem identified was the low hybridisation efficiency of the particles, where probe particles exposed to the labelled complementary target were much less fluorescent (10,000 a.u.) than particles with labelled probe directly coupled (60,000 a.u.). A number of factors could affect the number of immobilised probes which are able to form complementary duplexes including probes being in a poor orientation making hybridisation unfavourable and the surface probe density being too high resulting in steric hindrance.[258]

3.3 Calculation of the optimal surface density of oligonucleotide probes

The DNA duplex has a much larger cross sectional diameter than monomeric sequences. If oligonucleotide probes are immobilised upon a support to the maximum surface coverage, complete hybridisation to the complementary sequence is (thermodynamically) disfavoured due to steric constraints. An increase in the amount of duplex formed can be achieved by sacrificing a proportion of the immobilised probes to give room for hybridisation to occur.

The geometric cross sectional diameter of a DNA duplex is 2 nm, however this does not take into account the charge of the molecules, the effective diameter has been calculated and measured as 2.7 nm (in 1 M $Na^+_{(aq)}$).[259,260] We can calculate the maximum number of 2.7 nm diameter circles which can fit within 1 cm^2 by using hexagonal close packing models developed by Carl Friedrich Gauss (1777-1855) and László Fejes Tóth (1915-1995), which equates to 1.58×10^{13} circles per square cm.[261] Therefore the maximum possible surface density of DNA duplexes on a flat surface is 1.58×10^{13} cm^{-2}.

Experimental determination of the density of immobilised DNA monolayers has been published. Most studies quote values between 0.9 and 1.2×10^{13} units cm^{-2} (1 M Na^+ or K^+) for single strand immobilisation, whilst immobilising duplex DNA results in a less dense surface coverage of 0.3×10^{13} units cm^{-2}.[248,262,263] The achieved loading densities for single stranded DNA are very close to the theoretical maximum for hybridised DNA and they have been found to result in incomplete

hybridisation, with hybridisation efficiency reduced to 10 – 30%.[248,262,263] Reducing the probe density leads to greater duplex formation, tending towards 100% of immobilised probes forming duplexes. In the three studies discussed, all probes were hybridised to the complementary target sequence once the surface density was below 0.56, 0.4 and 0.2×10^{13} units cm^{-2}.[248,262,263]

Under the assumption that the surface of our particles is flat, the loading density of amine is 5 nmol cm^{-2} or 3×10^{15} molecules cm^{-2}. The succinylation of amines goes to completion (resulting in a negative Kaiser test) and so we had a much greater surface density of reactive functional groups than should be necessary to achieve an efficiently hybridising probe monolayer. Therefore it was thought unsurprising that hybridisation on our particles was inefficient as the loading density of probe on the surface was likely too high. To achieve the same densities which literature studies found to give 100% hybridisation we only need to functionalise approximately 0.1% of the surface carboxylic acids with oligonucleotide probes.

Reducing the density of probes bound may solve the problem of probe overcrowding. The problem of non-specific target binding to SU-8 particles might be addressable using the 99.9% surplus of functional groups. Thus the requirements for the design of future particles included the need for control of both probe loading densities and of blocking groups designed to minimise non-specific binding.

3.4 Phosphoramidite coupling chemistry

In order to control surface functionality and properties, a versatile linker technology was required which would allow different chemistries to be incorporated and which was amenable to DNA chemistry. Phosphoramidite chemistry was seen as the logical choice as it is used for the solid phase synthesis of oligonucleotides and a wide variety of different functionalities could be incorporated using the same basic coupling reaction. This would allow the surface to be simultaneously modified with two different functional groups by coupling two different phosphoramidite reagents at the same time. Furthermore, each phosphoramidite coupling would incorporate a phosphodiester linkage, it was expected that this phosphate, with negative charge under neutral conditions, would reduce the non-specific binding of DNA.
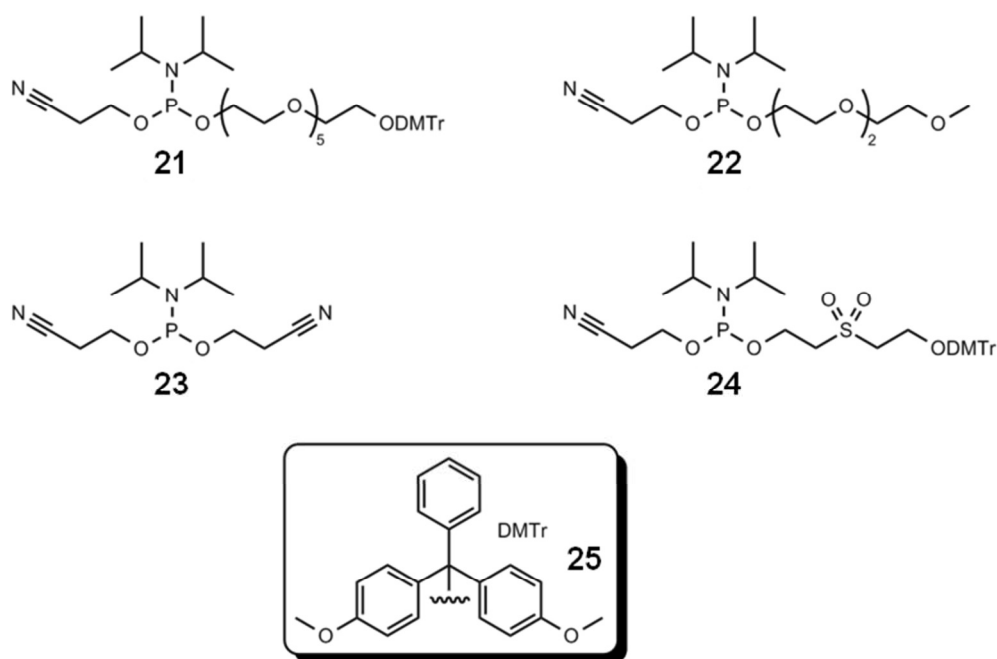
Figure 51. Phosphoramidites used to functionalise SU-8 particles for the immobilisation of oligonucleotide probes by amide coupling

3.4.1 The amide coupling of oligonucleotide probes to SU-8 particles modified with a hexaethylene glycol phosphoramidite

Before attempts were made to control the loading density and physical properties of the surface of particles by using combinations of different phosphoramidite reagents, the surface was functionalised with a single phosphoramidite. The dimethoxytrityl (DMTr) protected hexaethylene glycol (HEG) phosphoramidite (**21**) was used to achieve HEG functionalised particles (**26**) (Scheme 6). The reaction between diol functionalised SU-8 particles (**16**) and the HEG phosphoramidite (**21**), could be monitored quantitatively by the spectroscopic analysis of the deprotection supernatant. The DMTr protecting group (**25**) is labile under acidic conditions therefore deprotection with perchloric acid results in a HEG modified surface and the release of DMTr cations (DMTr$^+$) into solution. These cations show a strong absorbance at 503 nm, which can be quantified and used to determine the surface loading density of HEG. This was found to be $8.86 \pm 3.5 \times 10^{-9}$ mol cm^{-2}, a similar density as that found for Jeffamine$^®$ ED-900$^®$ functionalised SU-8 (**8**) ($5.3 \pm 0.9 \times 10^{-9}$ mol cm^{-2}). HEG functionalised particles could then be further modified using

117

succinic anhydride to achieve a carboxylate surface (**27**) to which amine modified oligonucleotides could be amide coupled (**28**).
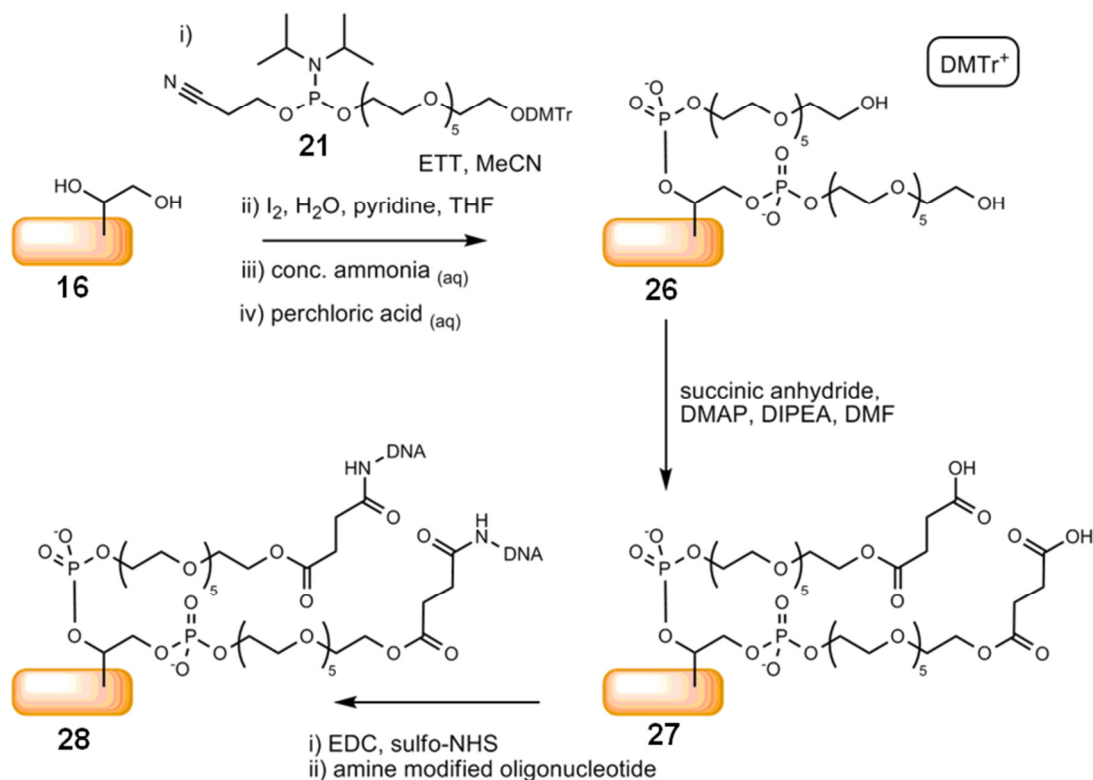
Scheme 6. The amide coupling of oligonucleotide probes to SU-8 particles modified with HEG phosphoramidite (21)

The coupling of fluorescently labelled oligonucleotide probes was investigated under a range of conditions (Figure 52). The results indicated that the coupling of and/or non-specific binding of amine modified probes to HEG functionalised SU-8 particles (**26**) was minimal as indicated by the low fluorescence signal (~5000 a.u.) whereas the coupling between probes and a carboxylate surface (**27**) had been achieved (54,000 a.u.). However, the exposure of carboxylate functionalised particles to amine modified oligonucleotide without the coupling mediators EDC and sulfo-NHS also resulted in a high fluorescence signal (36,000 a.u.) indicating significant non-covalent binding. The exposure of the carboxylate particles to a labelled target oligonucleotide (without any amine modification) showed non-specific binding to be low (3500 a.u.) in this system. This suggested that the high levels of non-covalent binding observed were the result of charge interactions between the surface coupled carboxylate (negative at pH 7) and the probe coupled amine (positive). Extensive

washing (48 hours) in SSPE (5×) buffer did result in a reduction in the fluorescence intensity of all the samples (excluding the blank), with the loss of non-covalently immobilised probe being greater than that for probe coupled in the presence of EDC and sulfo-NHS. These washing studies indicated that approximately 50% of the total immobilised probe was actually covalently coupled to the particles when EDC and sulfo-NHS coupling mediators were used, the other 50% being an electrostatic interaction.
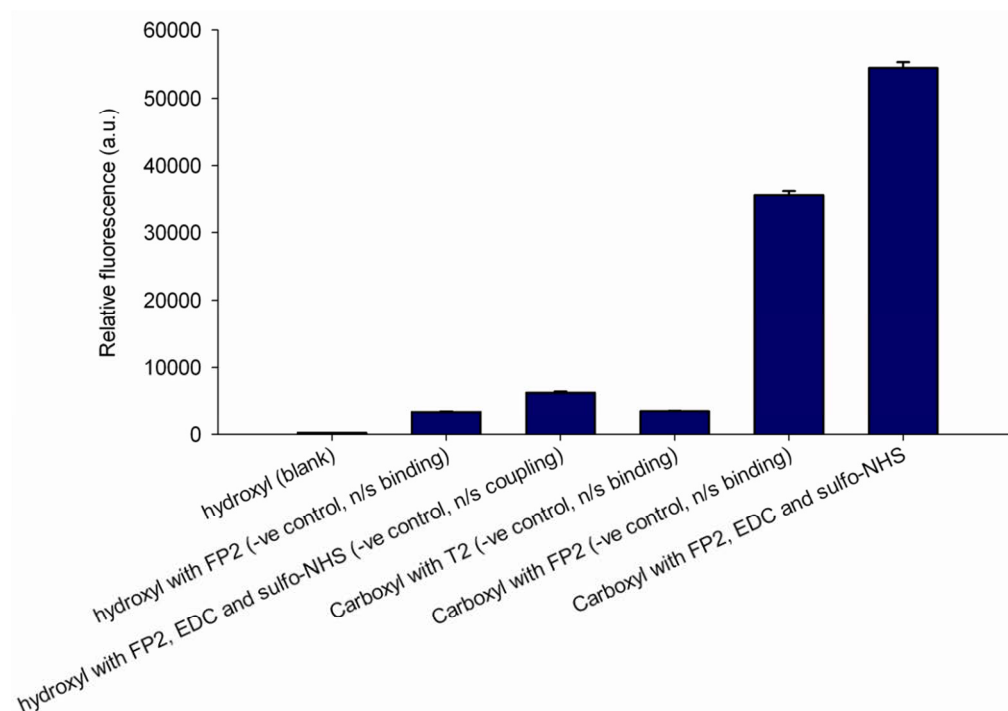
Figure 52. The amide coupling of amino functionalised oligonucleotide probes to carboxyl SU-8 particles. FP2 is a fluorescently labelled oligonucleotide with a 3' amine modification, T2 is a similarly labelled oligonucleotide lacking the amine modification. Negative controls showed coupling to be selective towards carboxyl (rather than hydroxyl) surfaces and that the non-specific binding of oligonucleotides was relatively minimal except in the case of amine modified sequences, this indicated a strong electrostatic interaction between the modified 3' end of the oligonucleotide and the surface which would be oppositely charged at neutral pH

An unlabelled but amine modified oligonucleotide, **P1**, was covalently immobilised on the surface of carboxylate SU-8 particles (**27**), these particles were then used to assess the discrimination between labelled target oligonucleotides with differing sequences (Figure 53).
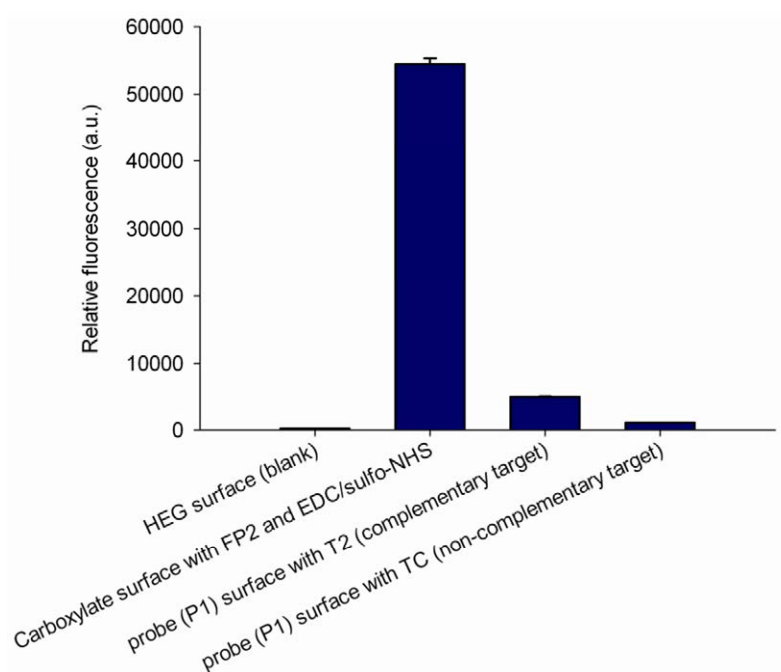
Figure 53. Hybridisations to oligonucleotide probes which had been immobilised by amide coupling to carboxylate SU-8 particles (27), shown are the fluorescence signals of blank particles, a positive control of the coupling of a labelled probe, exposure to a labelled complementary target oligonucleotide and exposure to a labelled non-complementary target

The studies showed the immobilised probes could discriminate between complementary and non-complementary target sequences, giving a fluorescence ratio of 6:1 after no optimisation of the hybridisation conditions. However the hybridisation efficiency was still observed to be poor, with only 9% of the probe sequences able to form the complementary duplex.

As discussed previously, this poor hybridisation efficiency may have been the result of steric hindrance where the surface concentration of probes was too high impeding duplex formation (Chapter 3.3). This problem would be investigated in later studies with attempts to control the loading density of probe using mixtures of different phosphoramidites.

3.4.2 Stability and recycling of probe-functionalised SU-8 particles

The stability of the amide linkage of oligonucleotide probe functionalised SU-8 particles (**28**) was investigated under different environmental conditions. The fluorescently labelled probe, **FP2**, was coupled to the particles and a sample of these particles was heated to 70 °C for 20 minutes, whilst a second sample was suspended in 2 M urea solution for 2 minutes. These particle samples were then washed using SSPE (5×) buffer and then imaged by fluorescence microscopy. Heat treatment was found to result in only a small reduction of the fluorescent signal (5% drop compared with signal prior to heating). Suspension in urea resulted in a slightly greater loss (10%). These reductions in the fluorescent signal may have been a result of damage to the cyanine fluorophore rather than any loss of probes from the surface, however, for under the conditions examined, probe loss or damage was certainly minimal.[264]

To assess the re-usability of probe functionalised particles (**28**), a sample was subjected to successive hybridisation and denaturation cycles with the fluorescent signal being measured at each stage (Figure 54). Two complementary hybridisation cycles were performed where probe functionalised particles were exposed to the labelled complementary sequence and the fluorescence measured, followed by heating to 70 °C for 20 minutes to denature any duplex formed. The same sample of particles was then exposed to the non-complementary sequence, followed by a further heat denaturation. The particles were then hybridised a fourth time, once again to the complementary target. The results showed the probe functionalised particles to be stable to at least two hybridisation and heating cycles, suggesting that the same particles could be used for more than one hybridisation assay, reducing operating costs and materials used. It could also allow the perpetual monitoring of an environment, a type of continuous monitoring. This particle recycling was not possible when using the less robust affinity immobilisation, only covalent coupling results in a sufficiently stable linkage.
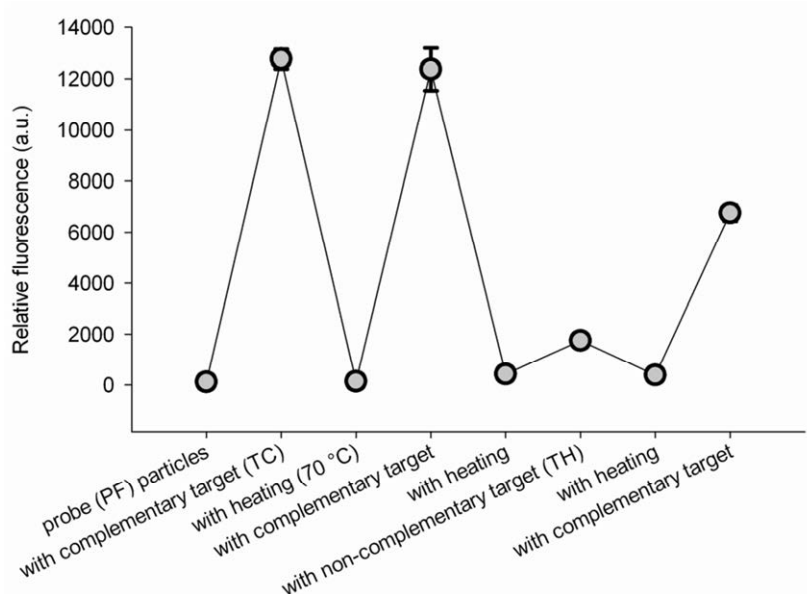
Figure 54. Multiple hybridisation and duplex denaturation cycles on probe functionalised SU-8 particles (28). Probe, PF, was immobilised via amide bond formation to carboxylate functionalised SU-8 (27). The particles were then exposed sequentially to complementary, TC, and non-complementary, TH, target oligonucleotides sequentially, interspersed with heating steps. The results found the probe functionalised SU-8 particles to be stable to multiple assay repeats (at least three repeats) allowing the possible reuse of individual particles

3.4.3 Control of functional group loading density using a methoxy triethylene glycol blocker group

To improve the hybridisation efficiency of immobilised oligonucleotide probes we desired control of the loading density of the reactive HEG moiety, working under the premise that reducing the density of HEG groups would lead to a less crowded probe surface making duplex formation more favourable. The synthetic route to HEG coated SU-8 particles (**26**) was modified to include a methoxy triethylene glycol (TEG) phosphoramidite (**22**) to space out the HEG functionalisation. The resulting surface was expected to consist of a mixture of reactive HEG and blocking methoxyTEG moieties in the same proportion to that used in the reaction (Scheme 7).
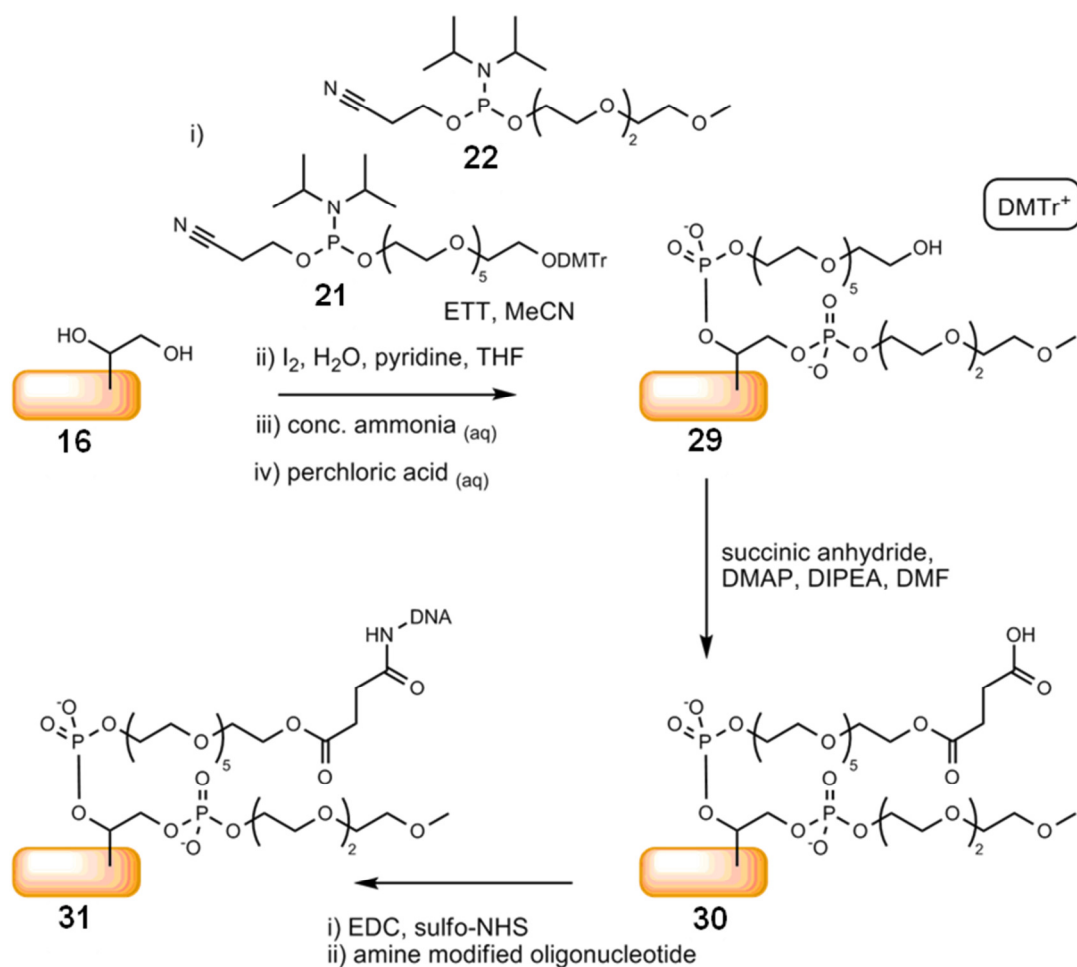
Scheme 7. The amide coupling of oligonucleotide probes to SU-8 particles modified with a mixture of methoxyTEG phosphoramidite (22) and HEG phosphoramidite (21). The resultant probe loading is dependent upon the initial phosphoramidite ratios used

By reaction with varying ratios of HEG (**21**) and methoxyTEG (**22**) phosphoramidites the loading density of surface hydroxyl was controllable. Quantification of trityl ion (DMTr$^+$) in the deprotection supernatant revealed that loading densities of 0.07, 0.19, 0.97 and 9.7 nmol cm^{-2} were obtained.

However, after the reactive HEG moiety had been converted to carboxylate (**30**), the amide coupling of an amine-modified and fluorescently labelled oligonucleotide giving (**30**) showed no dependence on the different particle loading densities (Figure 55). Coupling of an unlabelled amine probe allowed hybridisation studies, these too showed no change between particles with differing hydroxyl loading densities with hybridisation efficiency remaining poor (~20%).
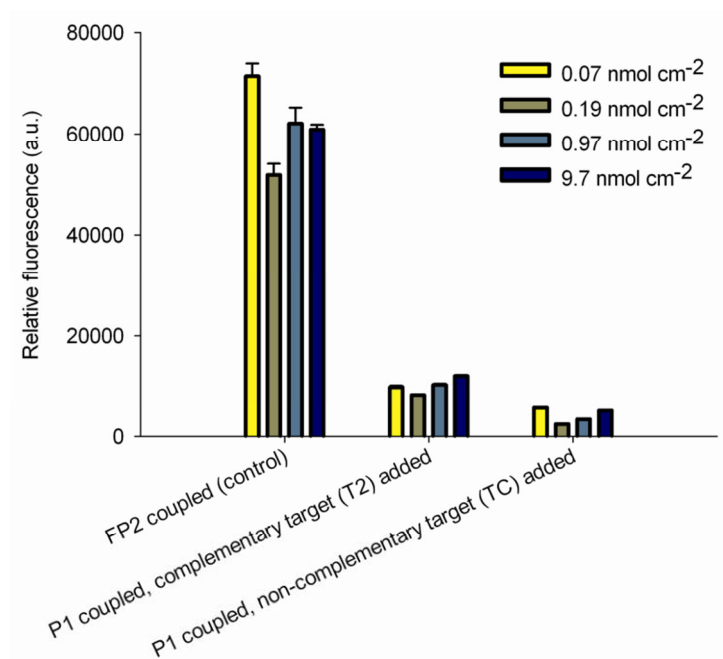
Figure 55. The amide coupling of fluorescently labelled and un-labelled probes to carboxylate SU-8 particles (29) of differing HEG loading densities, the fluorescence of un-labelled probe particles (30) when exposed to labelled complementary and mismatching sequences is shown. The reduction of HEG loading density (from 9.7 to 0.07 nmol cm^{-2}) had no effect on either the final loading density of FP1 or the hybridisation efficiency

This result suggested that although control of the loading density of HEG on the particle surface had been achieved, this did not translate into control of the loading density of oligonucleotide probes subsequently immobilised. The immobilisation of amine modified probes via amide coupling resulted in a similar loading density for all samples. This loading density was likely similar to HEG functionalised SU-8 particles (**26**) (with no methoxyTEG blocking groups) discussed previously, as the fluorescence intensities upon **FP2** coupling and hybridisation efficiencies were similar (comparing Figure 53 with Figure 55) in both particle types.

Subsequent studies would reveal a fundamental flaw to this coupling strategy which explained the apparent loss of loading control, these will be discussed towards the end of the chapter (**3.5**).

3.4.4 Altering surface functionality to reduce nonspecific oligonucleotide binding

The hybridisation of a labelled target oligonucleotide to probe functionalised SU-8 particles (**31**) (with control of HEG loading density) was studied. Different probe sequences had been coupled to the particles, which were then exposed (separately) to the target sequence, **TC**. The immobilised probes represented a complementary sequence, **PF**, two non-complementary sequences, **PH** and **PI**, and one sequence representing a single, mid-sequence, base-pair mismatch, **PG** (a G:G mismatch) (Figure 56). Discrimination between the complementary and the two non-complementary pairings was achieved under mild washing protocols (a 2 minute aqueous wash), whilst discrimination between the complementary and the single base mismatch pairings required a more stringent washing protocol (aqueous wash followed by suspension in 2 M urea solution for 2 minutes). The ratio of the fluorescence of particles exposed to the complementary and the single base mismatching targets was 6:1 after stringent washing.
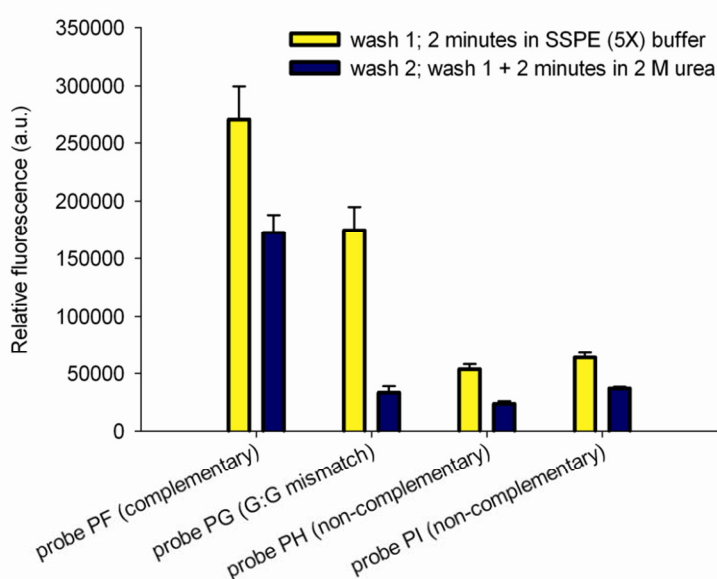
Figure 56. The exposure of SU-8 particles (31) functionalised with different probes to a labelled oligonucleotide target, TC. The loading density of HEG was measured as 0.01 nmol cm^{-2}, with methoxy TEG as a blocking group. The immobilised probes represented the complementary, a single G:G mismatch and two completely non-complementary sequences for the target oligonucleotide. Urea washing resulted in discrimination between the complementary and the single base mismatching sequence pairs (6:1 fluorescence ratio).

To maximise the difference in signal between probes exposed to the corresponding complementary sequences and any mismatching target, non-specific binding has to

be negligible. The non-specific binding of labelled DNA to differently functionalised SU-8 surfaces were investigated (Figure 57).[265] Binding was measured to SU-8 functionalised with diol (-OH), HEG (-OH), methoxy (-OMe) and phosphate (-OPO$_3^{-2}$) surfaces. Target DNA showed moderate to high levels of binding to diol, HEG and methoxy SU-8 whereas the phosphate surface significantly reduced non-specific binding. This study showed the methoxyTEG phosphoramidite to be a poor choice for a blocking group, as non-specific DNA binding was high. Much better would be the use of phosphate as a blocking moiety to improve discrimination between complementary and mismatching target sequences.
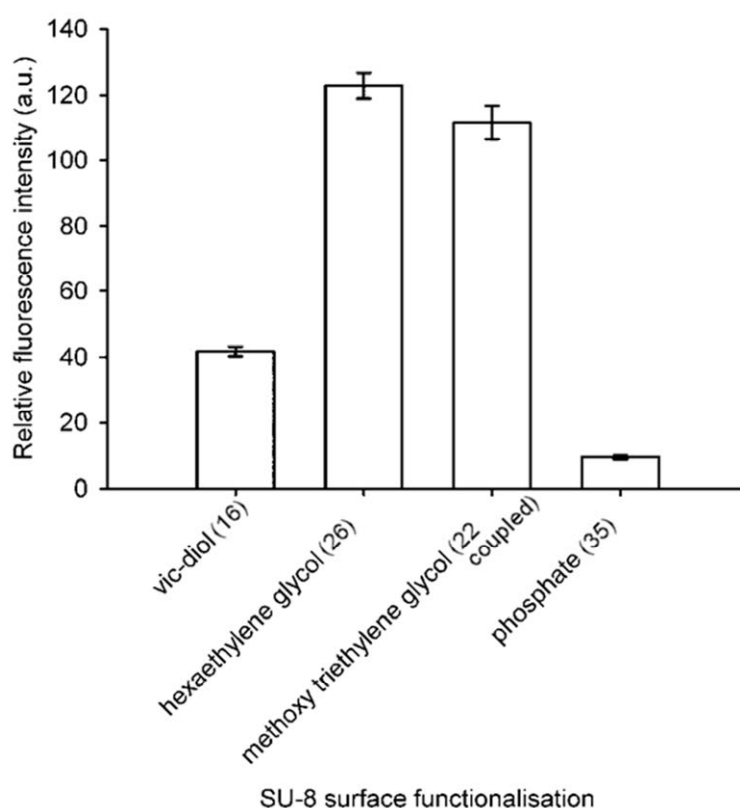
Figure 57. A study of non-specific binding of an antibody and an oligonucleotide to various SU-8 surface functionalities

3.4.5 Control of functional group loading density using a phosphate blocking group

A biscyanoethyl phosphoramidite (**23**) was used to install a phosphate blocking moiety on the SU-8 particle surface. Attempts were made to achieve a mixed HEG and phosphate surface using similar methods to those used previously for a mixed methoxyTEG/HEG surface (Scheme 7). However, control of the HEG loading

density could never be achieved, with all samples having a similar (and high) HEG loading. This was different to the previous problems encountered, where control of HEG loading had been achieved but had not then resulted in control of probe loading. NMR analysis of the biscyanoethyl phosphoramidite (**23**) showed it to have degraded to the oxidised phosphoramidate.
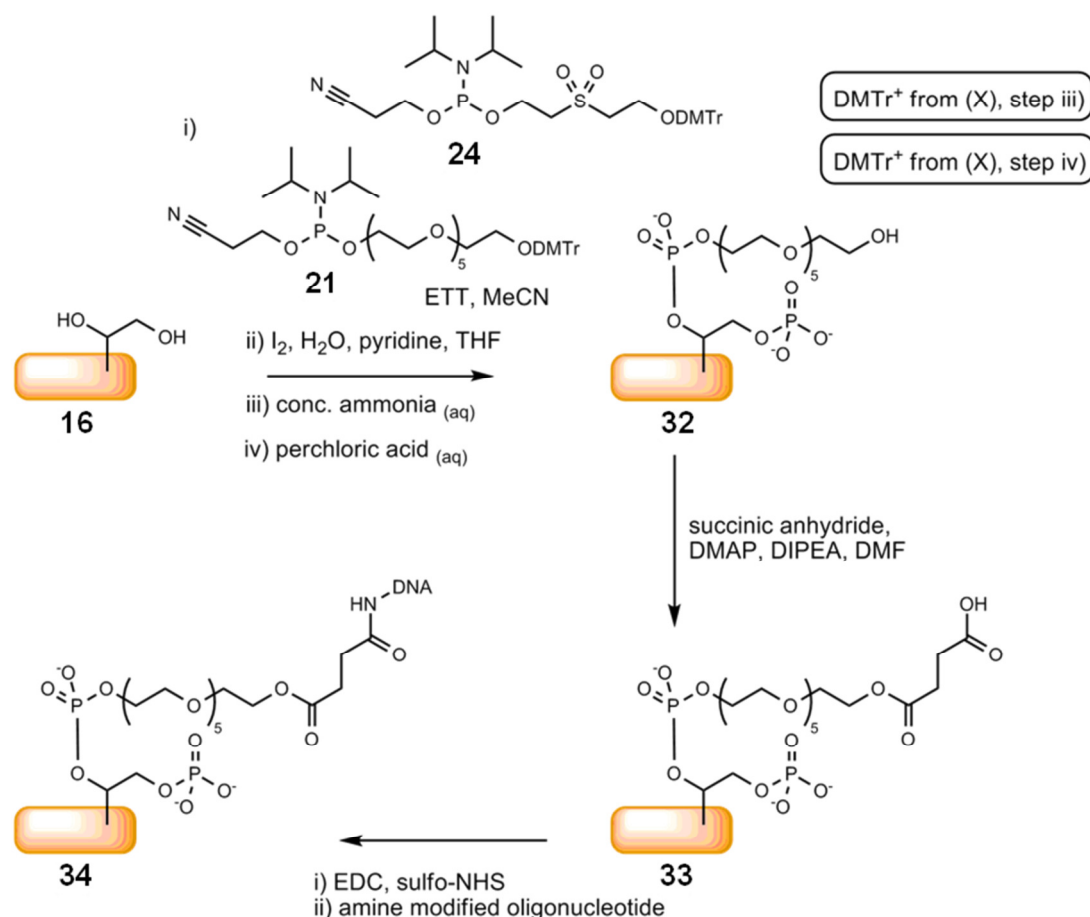
Scheme 8. The amide coupling of oligonucleotide probes to SU-8 particles modified with a mixture of CPR phosphoramidite (**24**) and HEG phosphoramidite (**21**)

A different phosphoramidite was used to act as a blocking moiety on the particle surface and still result in a predominantly phosphate functionality to reduce non-specific target binding. The synthetic route to probe functionalised SU-8 particles using chemical phosphorylating reagent (CPR) phosphoramidite (**24**) as the blocking group was modified from that used previously to obtain varying HEG and methoxyTEG surface densities (Scheme 8). Control of the HEG loading density was achieved when using CPR phosphoramidite (**24**) as a phosphate blocking group (Figure 58).
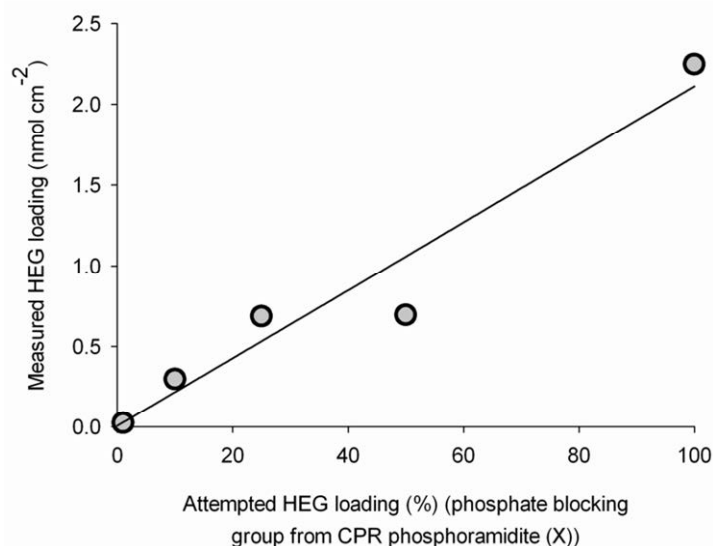
Figure 58. Control of the loading density of HEG functionalised SU-8 particles (32) using CPR phosphoramidite (24) to impart a phosphate blocking group

Though varying CPR (**24**) to HEG (**21**) phosphoramidite ratios during particle functionalisation did result in control of the HEG loading density, this once again did not translate into control over the density of immobilised probes. Particles functionalised with varying HEG loading densities were reacted with succinic anhydride to form a carboxylate surface (**33**) to which the amine modified and Cy-5 labelled oligonucleotide, **FP2**, could be coupled using carbodiimide chemistry. Though these particles (**34**) previously had defined loading densities as measured by trityl ion quantification, all particles now fluoresced with a similar intensity regardless of the expected probe loading density. Negative control particles which had an entirely phosphate surface (no reactive HEG groups) also fluoresced after the attempted amide coupling of labelled probe (Figure 59, a.), implying flaws in the use of phosphate blocking groups with an amide coupling strategy.

3.5 The incompatibility of phosphate-functionalised SU-8 with an amide immobilisation strategy

The nonspecific binding of both amino modified and unmodified, labelled DNA to phosphate functionalised SU-8 (**35**) was investigated. Amino modified and labelled oligonucleotide showed significant binding when mixed with phosphate functionalised particles whereas labelled oligonucleotide lacking a terminal amine

modification showed very little nonspecific binding (Figure 59, b. and d.). The amino modified and labelled oligonucleotide probe has a net negative charge at neutral pH, but is zwitterionic due to the terminal amine, thus there is likely an electrostatic attraction between the positive amine and the negative phosphate surface which could help to immobilised the probe. This interaction may result in a degree of order at the surface, with probes being immobilised via the terminal amine and thus available for hybridisation. This result showed the phosphate group used to control loading levels and reduce nonspecific DNA binding is incompatible with the coupling of amine modified probes as the charge interactions lead to nonspecific binding to the phosphate surface. This problem might have been mitigated by changing the pH of the wash buffer to change the net charges of the surface or probe; however in the light of more serious problems being identified, the effect of the pH environment was never tested.

A labelled oligonucleotide without a terminal amine moiety, **TC**, was shown to couple to phosphate particles when EDC and sulfo-NHS coupling mediators were present (Figure 59, c.). The resulting fluorescence was equal to the coupling of amino modified probes and showed that the phosphate group reacted with DNA indiscriminately, coupling sequences with or without terminal amine modifications (**36**). The fluorescence was thought to arise as a result of coupling between the phosphate and nucleophilic, exocyclic amines in the oligonucleotide to form a phosphoramidate linkage (Scheme 9). Controlling the loading density using phosphate blocking groups was thus not compatible with the immobilisation of DNA via amide coupling chemistry as the probe couples to both the blocking phosphate groups as well as any carboxylate groups, resulting in all particles having an approximately equal probe loading density regardless of the initial phosphate to acid ratio. In fact, oligonucleotide probes have been reported to be immobilised via the phosphate backbone, coupling to amine-modified sensor surfaces.[266] Any probes immobilised with attachment through the aromatic base amines would be arranged flat on the particle surface and likely not in an ideal configuration for hybridisation. It is perceivable that amine-modified probes could also be attached both through the terminal amine and the mid-sequence base amines. The poor probe orientation which would likely result would impede duplex formation, helping to explain the poor

hybridisation efficiency of our immobilised probes, where only approximately 15% of probes form a duplex with their labelled complementary target.
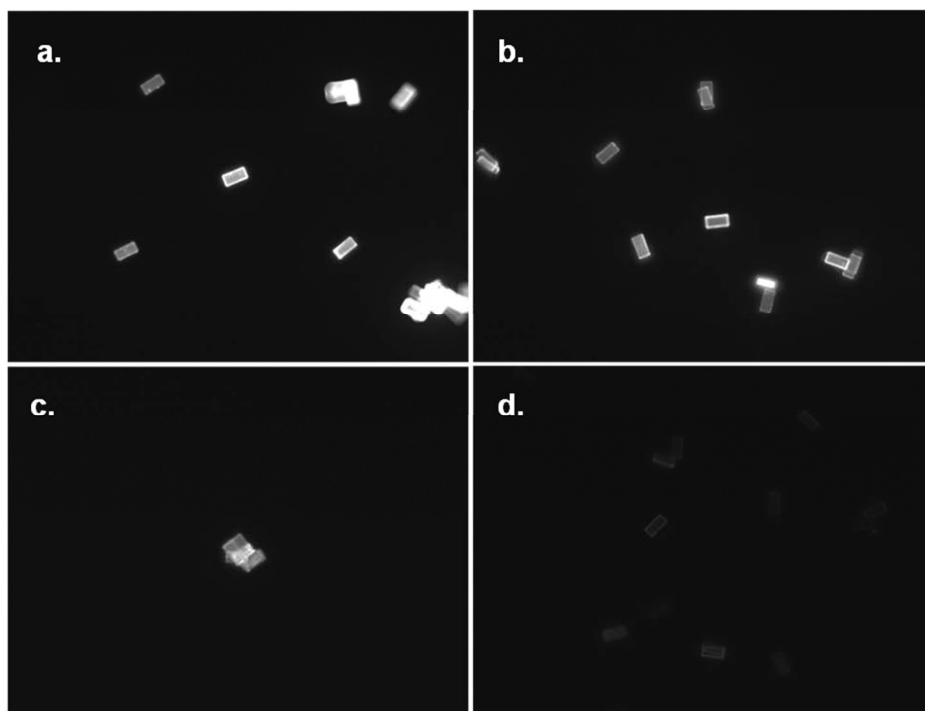
Figure 59. Phosphate SU-8 with a.) aminoDNA, EDC and NHS (measuring specific probe coupling), b.) aminoDNA (electrostatic interaction, c.) DNA, EDC, NHS (coupling via DNA base amines) and d.) DNA (non-specific binding)
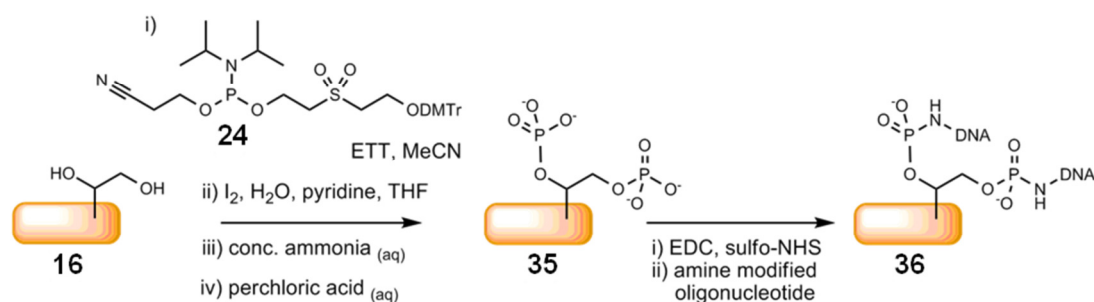
Scheme 9. The likely formation of a phosphoramidate bond between phosphate SU-8 particles and an amine modified oligonucleotide

3.6 Conclusions

Phosphoramidite coupling had been found to be a versatile method for the surface modification of SU-8 microparticles, allowing for a choice of various blocking and reactive functionalities, control of loading density and the inclusion of spacer groups. Oligonucleotide probes modified with a terminal amine had been covalently coupled

to carboxyl functionalised particles and these particles were shown to discriminate between complementary and mismatching target sequences with minimal washing steps required. Discrimination of hybridisation between complementary sequences and those mismatching by a single base pair required a more stringent urea wash, the linkage immobilising DNA probe to the particle surface was demonstrated to be stable under washing and denaturing conditions. As the probe immobilisation was strong, probe functionalised particles were shown to be recyclable allowing future uses in continuous monitoring.

Control of the loading density of surface functionality did not, however, translate into control of oligonucleotide probe density. This was because the phosphate blocking group had been found to be incompatible with amide coupling. This meant that either different blocking groups or a change of probe coupling chemistry were required to effect control over non-specific binding <u>and</u> hybridisation efficiency. The phosphate blocker had proven to significantly reduce non-specific oligonucleotide binding, was easy to couple and the loading of which could be easily monitored, therefore the decision was taken to focus on changing the probe immobilisation chemistries used.

3. Amide probe immobilisation

4.0 Hybridisation suspension arrays with probe immobilisation via the Cu[I] catalysed Huisgen 1,3-dipolar alkyne-azide cycloaddition reaction

Huisgen 1,3-dipolar cycloaddition reactions fuse alkyne and azide functionalities to form 5-membered hetrocycles (triazole).[185] Interest in this reaction was sparked by Sharpless, who highlighted it as an important component of his 'click chemistry' philosophy, detailing the facile synthesis of diverse libraries of compounds exhibiting biological activity from simple reagents using a limited number of very efficient reactions.[267] The discovery of the catalysis by copper (I) of the triazole forming reaction between alkyne and azide, allowing 1,3-dipolar cycloadditions to be performed at room temperature, opened up further uses for the reaction.[268,186] These reactions were found to be highly chemoselective, only occurring between alkyne and azide, and regioselective, predominantly forming 1,4 (rather than 1,5) disubstituted triazoles (**45**) from substituted reagents. Since it works equally well under either organic or aqueous conditions and on solid supports the reaction has found uses beyond synthesis and is commonly used as a linking reaction. Two separate molecules may be linked in a controlled manner if one contains an accessible alkyne (**38**) and the other an azide (**41**). Though copper salts have been found to degrade oligonucleotides, tris-triazole ligands have been developed which serve to both stabilise the Cu(I) ion under aqueous conditions and reduce degradation.[269,270] As both alkynyl and azido moieties are rarely found in nature the reaction is often utilized to link two biomolecules in a well defined manner after having artificially incorporated the reactive groups.[271] A proposed reaction scheme, incorporating the stabilising tris-triazole ligand is shown (Scheme 10).[274]

Though the term click chemistry as defined by Sharpless, encompasses a variety of important reactions, for the purposes of clarity and conciseness in this work, click chemistry and the click reaction refer specifically to the Cu(I) catalysed Huisgen 1,3-dipolar cycloaddition.
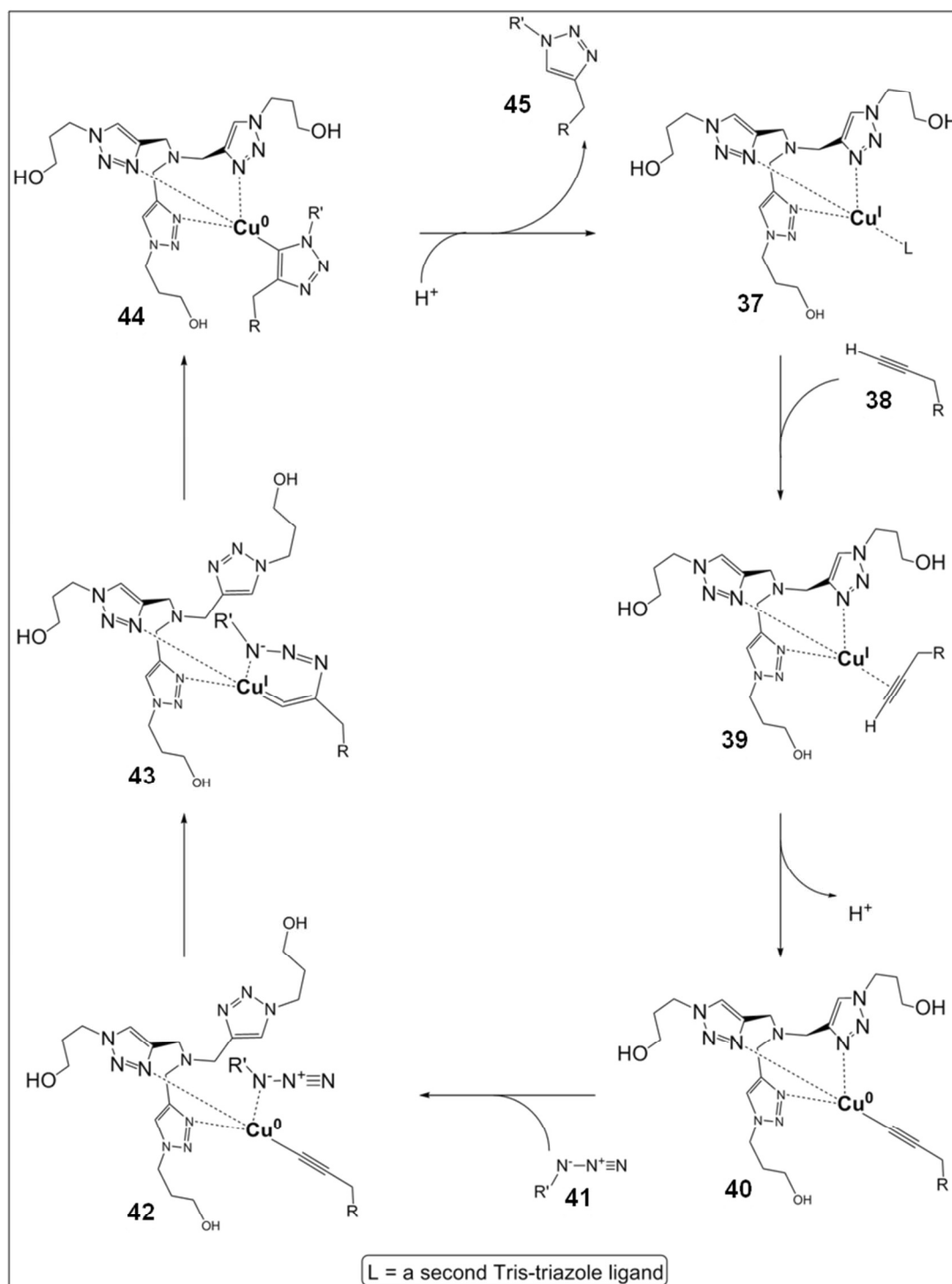
Scheme 10. A proposed mechanism for the copper catalysed Huisgen 1,3-dipolar cycloaddition between alkynes and azides, with the Cu(I) stabilising tris-triazole ligand present

4.1 Optimisation of the click reaction on the solid phase

Due to the chemoselectivity and regioselectivity of the Cu(I) mediated 1,3-dipolar cycloaddition, the reaction was used to immobilise oligonucleotide probes to the SU-

8 particle supports. By functionalising SU-8 particle surface with alkyne and terminally modifying oligonucleotide probes with an azido moiety, probes were expected to attach to the surface 'end-on' and form a highly ordered monolayer with probes in an ideal orientation for efficient hybridisation. This strategy was expected to be compatible with the phosphate blocking group which had previously been shown to reduce the nonspecific binding between DNA and SU-8, this would be in contrast to the amide coupling previously attempted (Chapter **3.0**) which displayed poor chemoselectivity with reaction occurring between amine and both acid and phosphate groups. One aim was for the improved selectivity to be utilised to control probe loading density, giving further scope for optimisation.

In order to functionalise amine-terminated oligonucleotide sequences a 6-azido hexanoic acid NHS-ester (azide modifier) was synthesised, this could be coupled to amino-DNA with the final sequence having a terminal azide.[272] The azide modifier was also used to functionalise Cy-5 fluorophore, giving (**47**) for use as a standard and positive control. Cy-5 was considered a good control for DNA immobilisations due to both its use as a label in target sequences and its net negative charge under neutral aqueous conditions. The Cu(I) stabilising tris-triazole ligand (**48**) was also synthesised in high yield. Some phosphoramidites for the functionalisation of particles with phosphate and alkyne were commercially available.

4.1.1 Optimisation of the click reaction using GMA beads
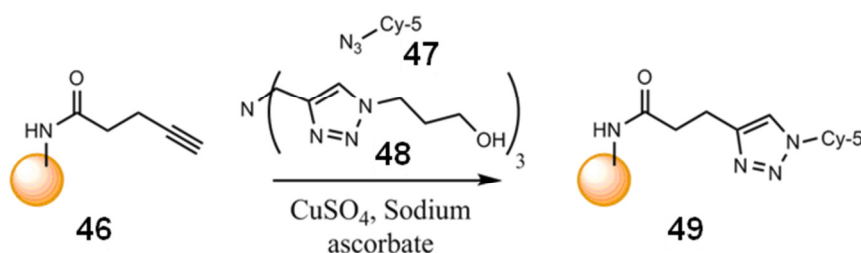
Scheme 11. The click coupling of azido Cy-5 to alkyne modified glycidyl methacrylate (GMA) beads

Early studies set out to optimise the click reaction on the solid support with initial optimisation being carried out on GMA beads as a large quantity was available. Amino GMA beads (amine loading at ~1 nmol cm^{-2}) were functionalised with

pentynoic acid to afford an alkynyl surface (**46**). Azido Cy-5 (**47**) was coupled to the alkynyl particles using click chemistry (Scheme 11). Early results indicated little coupling was taking place, but by increasing the reagent concentrations {azide (100 μM), Cu (2 mM)} coupling was complete within four hours. The immobilisation of Cy-5 was evident by the blue staining of the previously white GMA particles (negative control particles, being a combination of all the reagents with the exception of the Cu(I) catalyst, remained white (Figure 60). Fluorescence however was extremely low. Measurements of the fluorescence of amino GMA particles using the FACS (gain set at 500 V) gave a value of ~100 a.u. whilst after Cy-5 coupling this rose only slightly to ~560 a.u.. Washing with dilute $NaOH_{(aq)}$ was expected to remove any unreacted azido Cy-5 which was non-specifically bound and decrease the intensity of fluorescence, however upon washing an increase in bead fluorescence was instead observed (~900 a.u. after 10 minutes wash). The intense blue colour of the beads and the low initial fluorescence which increased with washing suggested that coupling had been successful and had actually resulted in a very high density of fluorophore at the surface leading to the formation of cyanine dimers and subsequent fluorescence quenching.[215, 273] This result demonstrated that the click reaction could be used to functionalise supports similar to SU-8 and had established an initial protocol to use for click coupling.
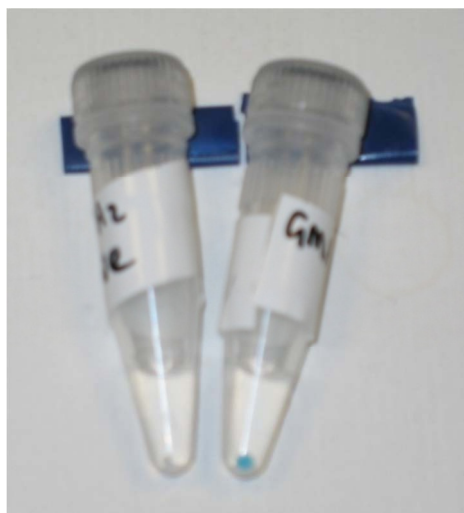
Figure 60. Results of the Huisgen 1,3-dipolar cycloaddition between azide-modified Cy-5 and alkyne functionalised GMA. Pelleted beads are shown, with the right-hand tube containing all reagents and the left-hand tube acting as a negative control containing all reagents minus the required copper catalyst

4.1.2 Optimisation of the click reaction on SU-8 microparticles
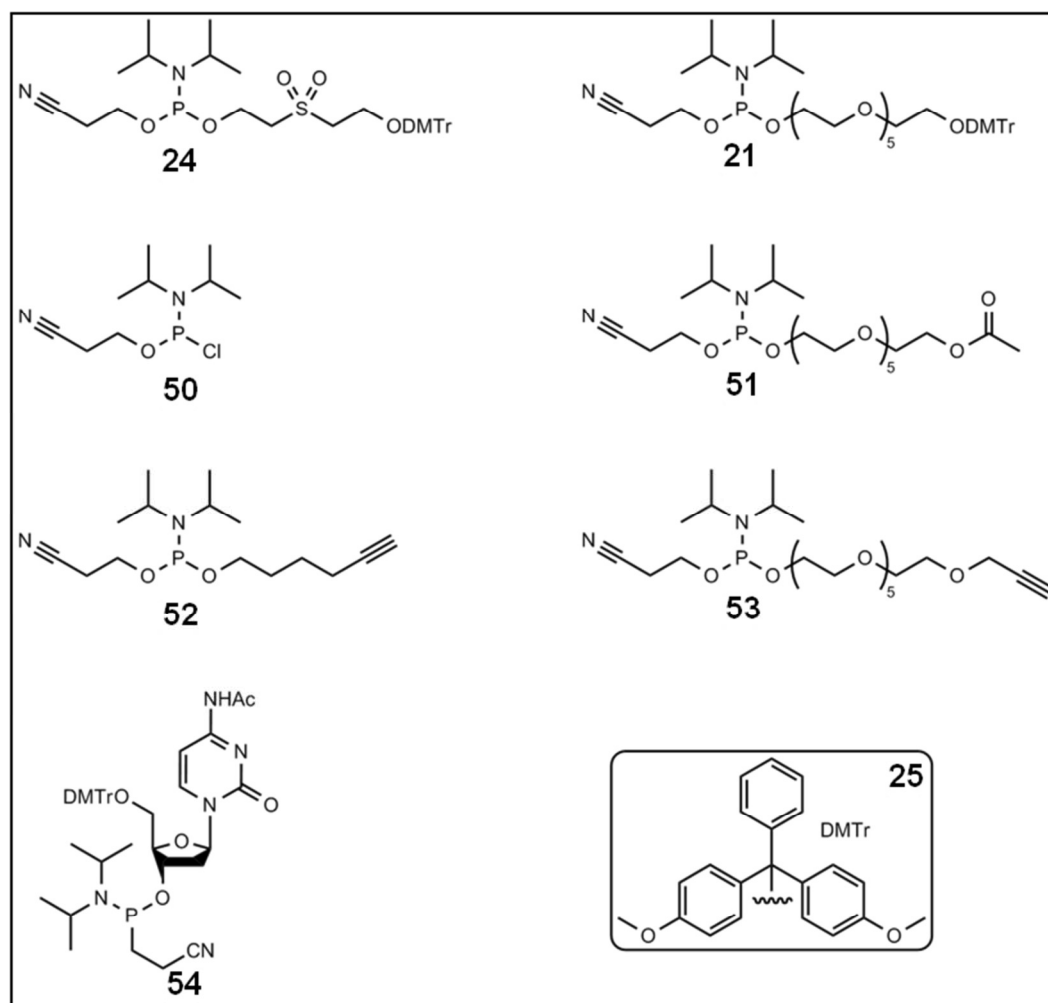
Figure 61. The structures of phosphoramidites used for SU-8 functionalisation

Following optimisation on GMA, the click coupling was attempted on SU-8 particles. Diol particles (**16**) were modified using mixtures of CPR blocking phosphoramidite (**24**) (phosphate) and reactive alkynyl phosphoramidite (**52**) to yield particles (**55**) with a range of loading levels, measured by trityl ion analysis (Figure 62). Azido Cy-5 (**47**) was then click coupled using the same conditions which had previously resulted in coupling to GMA beads. SU-8 particles did not change colour but did show an increase in fluorescence, the intensity of which appeared inversely proportional to the loading of surface phosphate (and therefore can be assumed to be directly proportional to the surface loading of alkyne), indicating successful and selective click coupling (Figure 63). Fluorescence intensity was not very high {~18,000 a.u. (FACS gain set at 500 V), at 7.5 nmol cm^{-2} alkyne loading}, this and

the lack of a colour change suggested the click coupling reaction had not gone to completion.
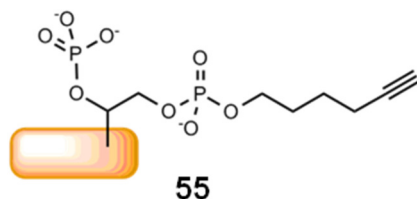
Figure 62. SU-8 particles functionalised with alkyne (52) and phosphate (24) phosphoramidites, no spacer incorporation
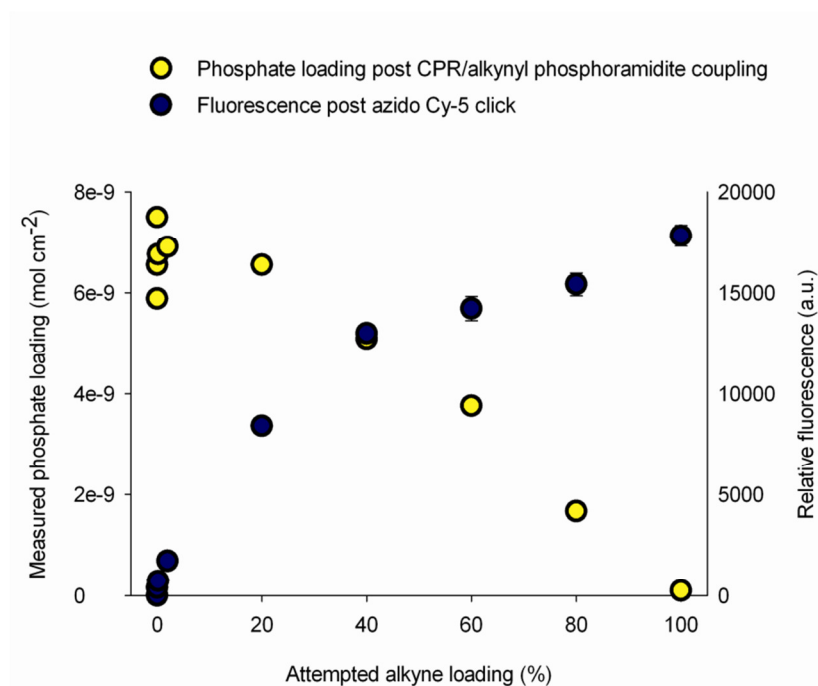
Figure 63. Control of surface alkyne loading density using a mixture of alkynyl (52) and blocking phosphoramidites (24), subsequent click coupling of azido Cy-5 confirmed that loading control had been maintained
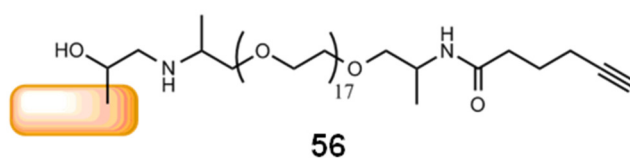
Figure 64; SU-8 particles functionalised with alkyne incorporating the 64-atom Jeffamine® ED-900® (14) spacer

SU-8 particles with an amino surface (Jeffamine® ED-900®) (**8**) are chemically more similar to GMA beads to which click reactions had proven to be high yielding, therefore these particles were alkyne-functionalised using pentynoic acid (with product particles (**56**) testing negative for amine by ninhydrin quantification) (Figure 64). Click chemistry was again used to link azido Cy-5 (**47**), this time particles were stained intensely blue and were found to fluoresce brightly. The fluorescence of these particles incorporating a 64-atom spacer could not be directly compared with those modified previously (using the 9-atom phosphoramidite spacer) due to fluorescing above the FACS's detection limit when measured under the previously used settings (F > 260,000 a.u. with gain set at 500 V). Changing the cell sorter instrumentation settings by lowering the gain to 300 V allowed precise measurement of particle fluorescence. Intensity was initially 42,000 a.u., upon thorough aqueous NaOH washing fluorescence dropped to 32,000 a.u. implying most of the signal was from covalently immobilised fluorophore. Though the reaction worked well on alkyne modified particles incorporating a 64-atom Jeffamine® ED-900® spacer (**14**), these particles could not be a substitute for phosphoramidite modified particles due to both having no control over probe loading densities and the amine surface displaying relatively high DNA non-specific binding.

4.1.3 Combining spacer groups and loading control for high yielding click reactions

Figure 65. SU-8 particles functionalised with alkynyl (52) and phosphate (24) phosphoramidites incorporating the 29-atom HEG phosphoramidite (21) as a spacer

Phosphoramidite chemistry was adapted to incorporate spacers between the alkyne and the surface which would allow the probe loading density to be controlled. Particles were first functionalised with HEG phosphoramidite which was followed by a second round of phosphoramidite coupling, this time using a mixture of CPR (**24**) and alkynyl (**52**) phosphoramidites. This yielded particles (**57**) which once again had a mixed surface of reactive alkynyl and blocking phosphate groups but now all functionality was distanced from the surface by a 29-atom HEG spacer (Figure 65). One sample of the HEG particles was functionalised using equal measures of the CPR and alkynyl phosphoramidites, whilst a second (control) sample of particles was wholly functionalised with CPR phosphoramidite. The two particle types were found to have phosphate loading densities of 4.8 and 8.3 nmol cm^{-2}. Click coupling of azido Cy-5 to the 50% alkyne-functionalised particles was instantly recognisable by being stained blue, whereas particles containing no alkyne remained uncoloured.
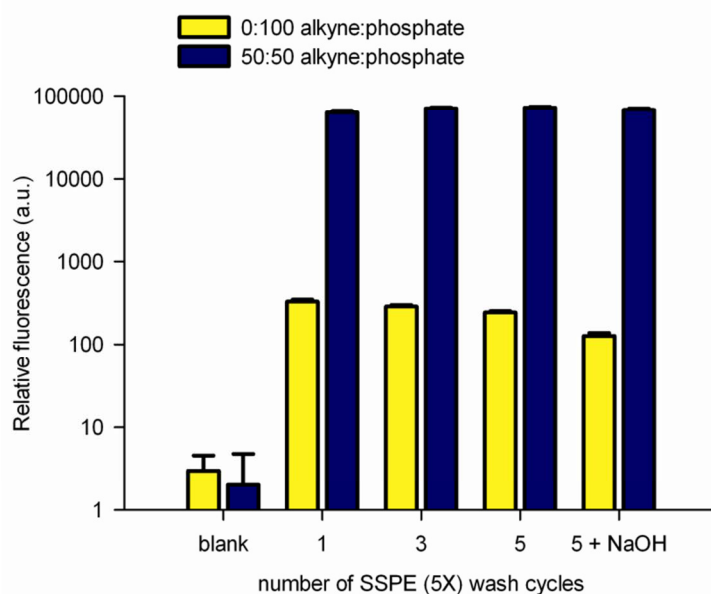
Figure 66. The fluorescence intensities of two particle surfaces (100% phosphate {–ve control} and 50:50 alkyne:phosphate) after the attempted click coupling of azidoCy-5. Fluorescence of the alkyne surface is 2 orders of magnitude more intense than to the blocked surface and is more stable to aqueous wash steps, indicating successful coupling

Similar to when click coupling fluorophore to alkyne SU-8 incorporating a Jeffamine® ED-900® spacer (**56**), the fluorescence when having coupled to 50% alkyne HEG-particles (**57**) was too intense for quantitative analysis using the FACS set to previous gain settings. Gain was reduced to 300 V and fluorescence was

measured as 62,400 a.u. compared with just 330 a.u. for the blocked phosphate particles (Figure 66). Further washing using SSPE(5×) buffer with 0.02% Tween-20® added and the subsequent suspension for 10 minutes in 1 M NaOH$_{(aq)}$ had no effect on the fluorescence of 50% particles whilst the level of non-specific binding to the blocked particles reduced resulting in the lower fluorescence intensity of 120 a.u. (giving a signal to noise ratio of 540:1).

In summary, these results showed the aqueous click protocol to link an azide modified species to an alkyne functionalised surface to be efficient, experimentally simple and compatible with phosphate functionality. Loading control of alkyne had been maintained through the reaction and non-specific binding of the azido Cy-5 was found to be very low.

The experiments did highlight the importance of a spacer group to distance the alkyne moiety from the particle surface. Coupling had been found to be poor to alkyne particles (**55**) where the reactive moiety was less than 9 atoms from the polymer surface. However adding a spacer (29-atom HEG phosphoramidite (**21**) or 64-atom Jeffamine® ED-900® (**14**)), led to efficient click coupling. This prominent spacer effect was likely the result of reduced steric hindrance during the reaction. Though the exact structure of the intermediate complex formed between the copper catalyst, tris-triazole ligand, immobilised alkyne and azido Cy-5 has not been characterised, it is certain to be rather large.[274,275] Expanding on literature speculation, one possible structure for this intermediate complex (**42**) is proposed (Figure 67), a large complex indeed when R represents a 1000 μm^3 particle and R' an azido-fluorophore with a molecular weight exceeding 700 Da. Further to the steric factors discussed, poor reaction may also be accounted for by the effects of the diffusion layer, where reactions on surfaces are limited by mass transfer rather than bulk mixing effects, this is a result of the liquid in close contact with the surface (interphasic boundary) being shielded from bulk mixing forces.[276,277] The longer the spacer group, the closer the alkyne moiety is to the bulk liquid and any azide present, resulting in a faster rate of reaction.
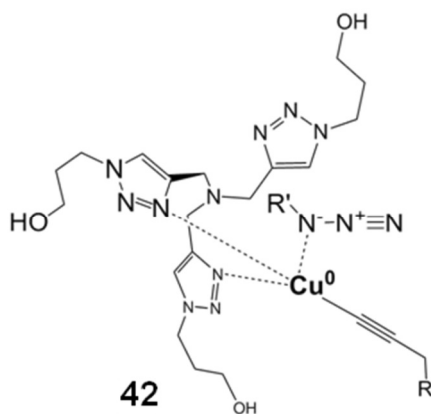
Figure 67. A proposed intermediate/transition state complex formed during copper catalysed Huisgen 1,3-dipolar cycloaddition

4.2 Control of loading density through sequential phosphoramidite couplings

With the necessity of spacer groups having been established, attention was turned towards the positioning of the phosphate group. This group was included to limit the nonspecific binding of DNA to the particle surface and to space-out surface immobilised probe. The result of including phosphate should therefore lead to both a reduction in background signal (noise) and an increase in the efficiency of specific hybridisation in subsequent DNA assays.

Previous iterations of particle functionalisation had added loading control during the final phosphoramidite coupling and resulted in good regulation of alkyne and phosphate loading densities. However by this sequence of coupling both reactive and blocking groups were tethered on the end of HEG spacers. The close proximity of the phosphate to any click-coupled oligonucleotide probes was a cause for concern as it was feared that the high density of negative charge may interfere with the specific hybridisation of any complementary DNA targets.

The next design of alkynyl particle placed the phosphate much closer to the particle surface and thus distanced it from any probe coupling (and therefore any hybridisation events), control of loading density was now achieved in the initial phosphoramidite coupling rather than during the final coupling.

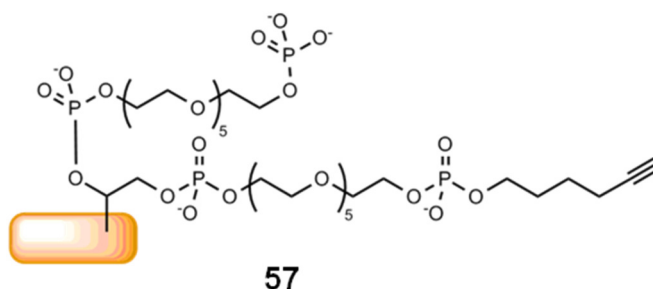4.2.1 Spacing the reactive alkyne further from the blocking phosphate functionality

58
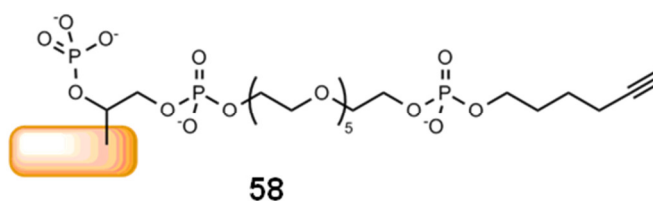
Figure 68. SU-8 particles functionalised with alkynyl (52) and phosphate (24) phosphoramidites incorporating the 29-atom HEG phosphoramidite (21) spacer and employing loading control early in the synthetic route

Particles were functionalised to compare yield of the click reaction and control of loading density when phosphate was either on the end of a 29-atom spacer (**57**) (Figure 65) or when close to the surface (**58**) (Figure 68). Differing alkyne to phosphate ratios were coupled for both spacer arrangements yielding particles with 100% and 10% alkyne surfaces or surfaces fully blocked with phosphate (as a negative control). After azido Cy-5 had been coupled and the particles washed thoroughly, samples were analysed using fluorescence microscopy (Figure 69).
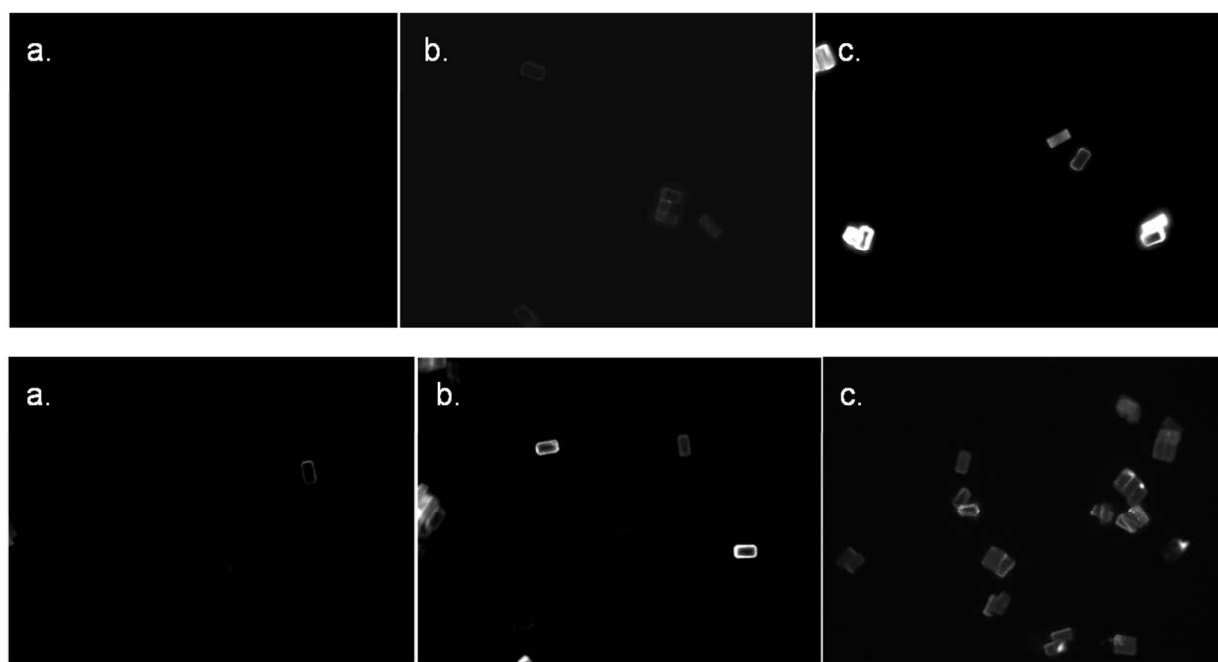
Figure 69. Fluorescence microscopy images of functionalised SU-8 particles after the click coupling of azido Cy-5. Particles in images on the top row incorporated a HEG spacer for both phosphate and alkyne moieties and control of alkyne loading density was afforded by the final phosphoramidite coupling step (coupling to (57)). Particles in images on the bottom row incorporated a HEG spacer only for the alkyne moiety with phosphate closer to the surface, here control of alkyne loading density was afforded by the initial phosphoramidite coupling step (coupling to (58)). Attempted phosphate : alkyne ratios are a) 10:0, b) 9:1 and c) 0:10

Little difference was observed in the yields of the click reaction with respect to the spacer layout, this was indicated by the similar fluorescence intensity of azido Cy-5 coupling to both types of fully alkyne functionalised particles (Figure 69,c) and this indicated that the close proximity of spacer-coupled phosphate to the alkyne did not interfere with the click reaction. A difference was observed between the two spacer designs with regard to the control of loading density. As for previous couplings, good loading control had been achieved when differing ratios of the two phosphoramidites were coupled together in the final step (Figure 69, top row), however when loading control was attempted in the initial couplings it was not carried through by later functionalisation steps (Figure 69, bottom). Coinciding with this disappearance of loading control, measurements of trityl ion after deprotection did correlate with the various phosphate and alkyne ratios indicating loading control had been achieved.

In summary, attempts to control functional group loading density during the initial coupling of phosphoramidite mixtures had proved successful (as measured by trityl ion analysis), however with subsequent rounds of phosphoramidite coupling this control was lost. It was proposed that a regeneration of surface hydroxyl had occurred at some point during functionalisation, negating the prior blocking.

4.2.2 Acidic degradation of SU-8

Coinciding with the discovery of the poor retention of loading control, degradation of polymerised SU-8 was noted upon prolonged immersion in acidic media.[272] The effect of acid on the surface of particles was further investigated using a range of acidic solutions and immersion times. Minor particle damage and surface etching (roughening) was observed under acidic conditions compared with suspension in water (Figure 58). If polymer cross-linking were unstable to acid, new hydroxyl groups could be formed which would be available for the coupling of phosphoramidite.

During the trityl deprotection step of HEG phosphoramidite coupling to particles the polymer is exposed to perchloric acid, at which point control of hydroxyl loading could be lost (Scheme 12). This is not observed for either the deprotection of the

phosphate phosphoramidite (**24**) as this is achieved under basic conditions or when loading control is effected by the final phosphoramidite coupling step as the alkynyl phosphoramidite (**52**) for the same reason. Literature reports corroborate our results, with cross-linked SU-8 etching rates of up to 10 μm min^{-1} under more extreme conditions (98 % H$_2$SO$_4$).[278]
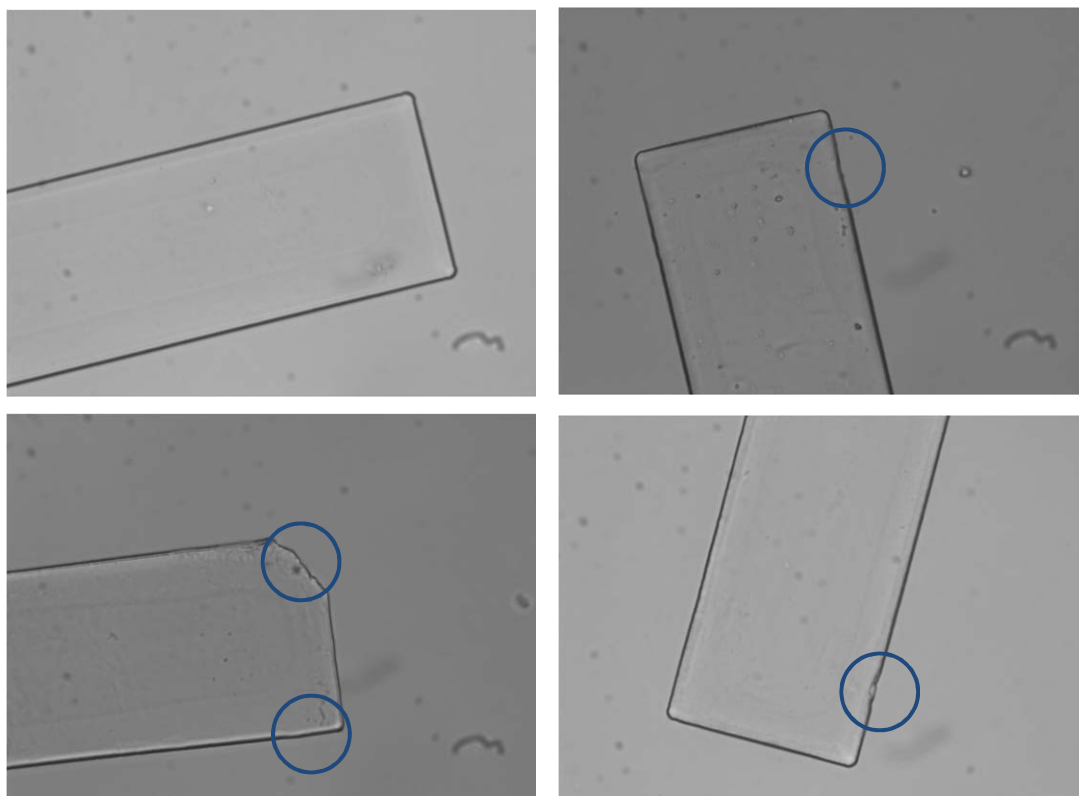
Figure 70. Evidence of SU-8 etching after 36 h under various acidic conditions, clockwise from top left; water (control), 2% dichloroacetic acid in toluene, 60 % perchloric acid in methanol and 5 % trichloroacetic acid in toluene. Damage is indicated
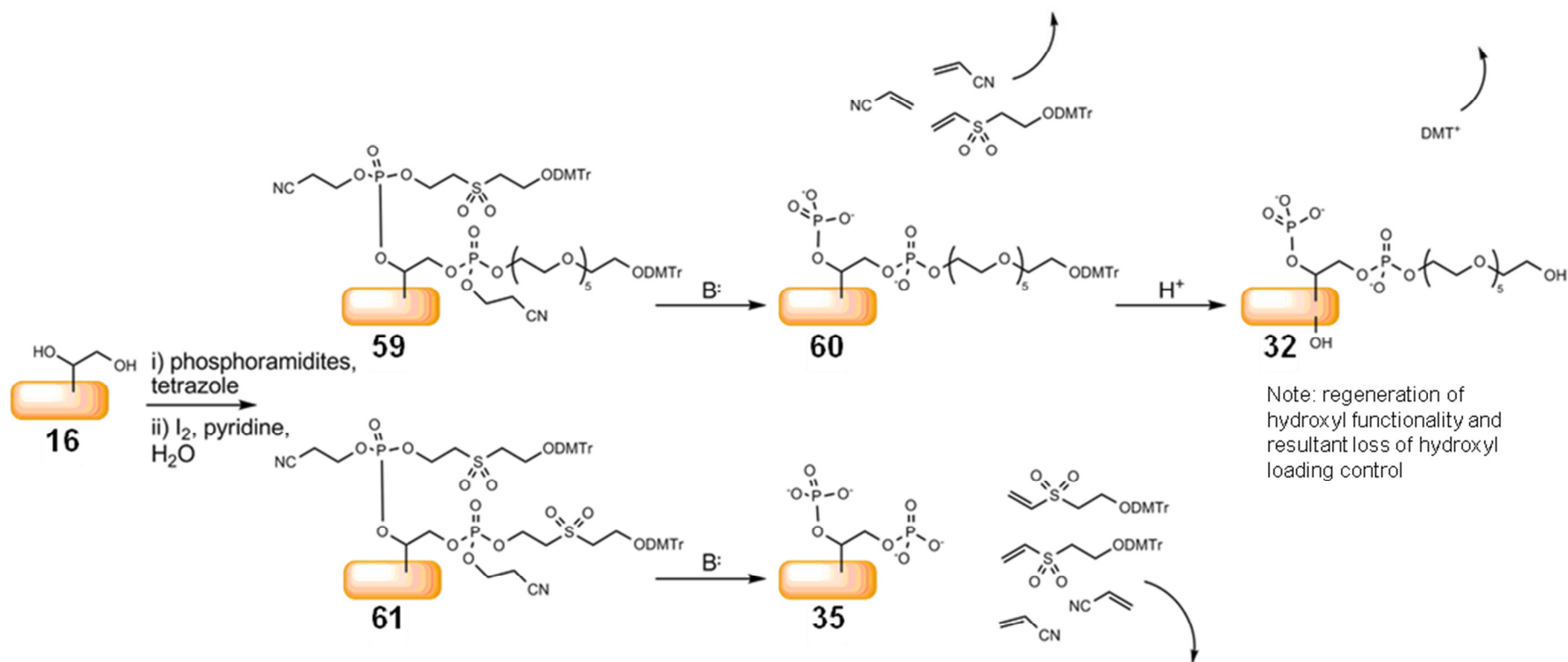
Scheme 12. Phosphoramidite coupling highlighting issues with retaining loading control during trityl deprotection using perchloric acid. The use of acid has been observed to etch cross linked SU-8 possibly leading to the regeneration of surface hydroxyl. Note this had not been previously observed as niether CPR (24) nor alkynyl (52) phosphoramidites require deprotection under acidic conditions

4.2.3 Synthesis and use of a hexaethylene glycol spacer phosphoramidite with a base labile protecting group

Knowing that particle hydroxy loading is unaffected under the basic conditions used for cyanoethyl deprotections, the acetyl-protected HEG phosphoramidite (**51**) was synthesised from mono-acetyl HEG and 2-Cyanoethoxy-N,N-diisopropylaminochlorophosphine (chlorophosphitylating reagent) (**50**). Coupling of this phosphoramidite could not be directly quantified therefore surface loading densities could only be inferred by measuring trityl ion concentrations resulting from deprotection of any phosphate blocking groups coupled. When analysing mixed CPR (**24**) and acetyl-HEG (**51**) phosphoramidite coupled particles a low phosphate coverage (by trityl analysis) would imply a high HEG coverage and vice versa.

The acetyl protected HEG phosphoramidite was used in conjunction with CPR phosphoramidite to obtain particles with varying hydroxyl loading; control of which it was hoped would be carried through subsequent coupling steps (Figure 71).
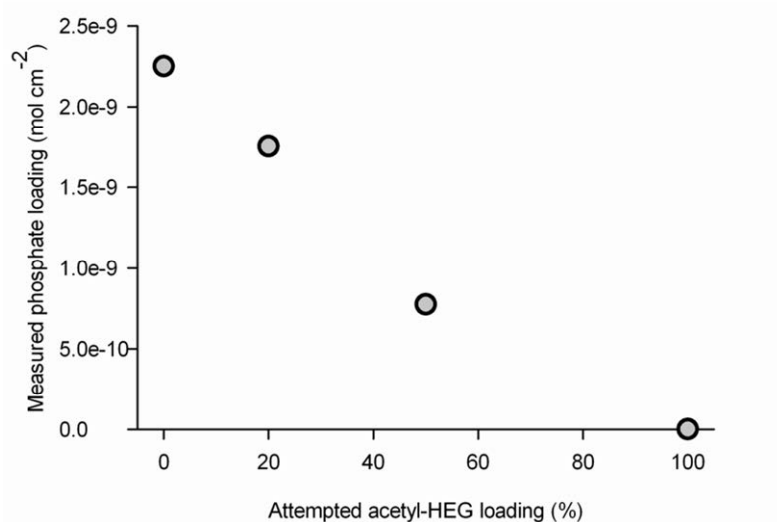
Figure 71. The trityl analysis of SU-8 particles coupled with varying ratios of CPR (24) and acetyl-protected HEG (51) phosphoramidites. Measured trityl was found to be in a near linear relationship with the amount of the blocking phosphoramidite added, indicating both phosphoramidites react with a similar rate to surface hydroxyl. From the above data it was assumed that particles functionalised with a 100% acetyl-HEG surface would have a similar loading density to that measured for the phosphate surface (2.25 × nmol cm^{-2})
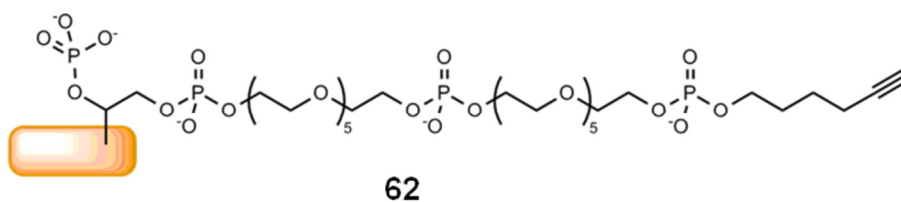
Figure 72. SU-8 particle functionalised with alkynyl (52) and CPR (24) phosphoramidites including two sequential couplings of the acetyl-protected HEG phosphoramidite (51) resulting in the incorporation of a 49-atom spacer

Subsequent phosphoramidite couplings to these base-deprotected HEG-functionalised particles were attempted, hoping to retain loading control whilst aiming for an alkyne functionalised surface. To one sample of particles at each HEG loading density alkynyl phosphoramidite (**52**) was coupled (Figure 68), whilst to another sample a second acetyl protected HEG phosphoramidite (**51**) was coupled first before the eventual alkynyl addition (Figure 72). Alkyne groups would then be held on the ends of 29-atom (**58**) or 49-atom (**62**) spacers respectively. Upon click coupling of the azido Cy-5 standard (**47**) particle fluorescence were measured (Figure 73, e) showing intensity to be proportional to the surface loading of reactive functional group (Figure 71). This matched the relationship expected if loading control had been retained throughout the multiple phosphoramidite coupling and deprotection steps.

Though loading control had been retained under basic deprotection conditions, total fluorescence intensities were lower than for previous click couplings of the azido Cy-5 standard. Comparing particles incorporating the 29-atom spacer (**58**), those with a purely alkyne surface (Figure 73, d) before fluorophore coupling exhibited less than three times the fluorescence intensity of those with a purely phosphate surface (Figure 73, a), for clarity this result should be contrasted with similarly functionalised particles (Figure 69) which showed alkyne particles to fluoresce much more intensely than phosphate particles. This low fluorescence was indicative of a low yielding functionalisation route which could have been caused by either poor coupling efficiencies of the second and third phosphoramidite, poor efficiency of the acetyl-deprotection steps or poor coupling efficiency of the azido Cy-5 standard. The low fluorescence was unlikely to be caused by variation between SU-8 particle batches as the initial coupling of phosphoramidite had been monitored and loading

densities were found to be only slightly lower than normal (approximately 2.5 nmol cm^{-2}) (Figure 71). The final fluorescence intensity of particles incorporating two acetyl-protected HEG phosphoramidite couplings (49-atom spacer) (**62**) was even lower than those having undergone only a single HEG inclusion, if phosphoramidite couplings were high yielding these two particle types would be expected to exhibit a similar intensity. This observation therefore suggested that low fluorescence was an effect of poor yielding phosphoramidite couplings.
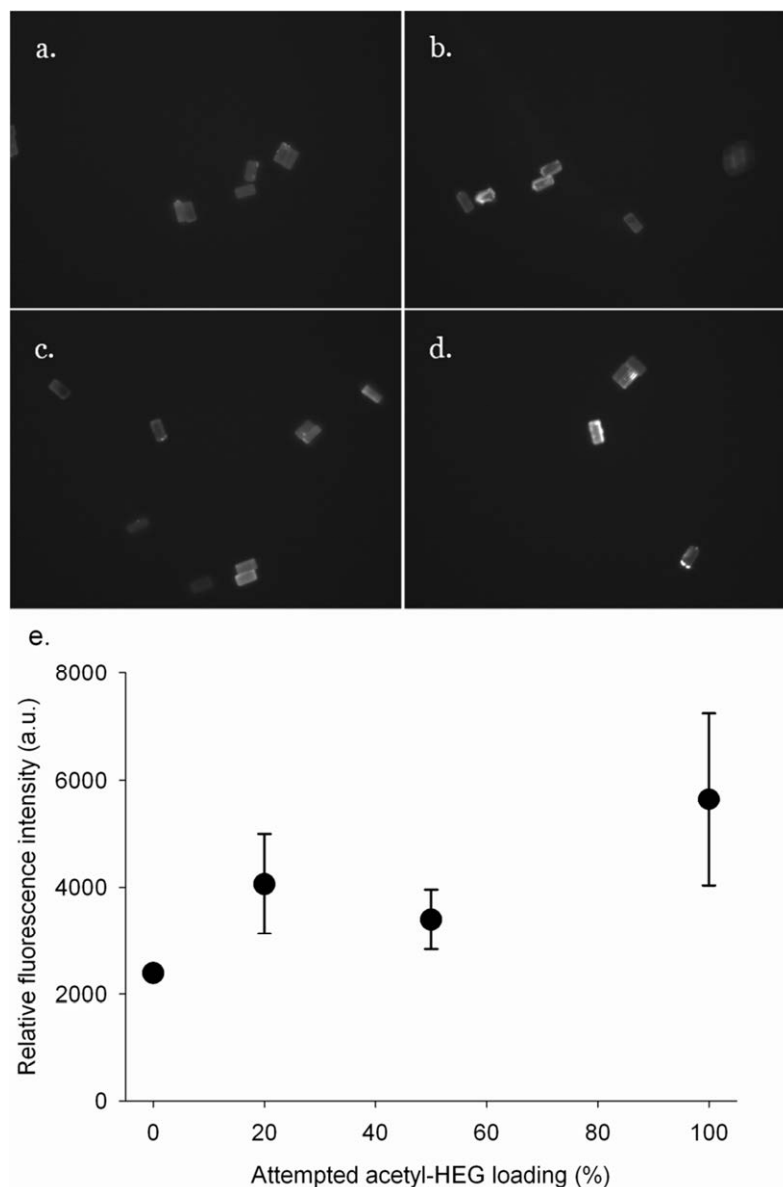
Figure 73. Fluorescence microscopy images of SU-8 particles initially functionalised with varying mixtures of CPR (24) and acetyl-protected HEG (51) phosphoramidites followed by base deprotection, alkyne phosphoramidite (52) coupling and azido Cy-5 (47) click coupling. Initial attempted acetyl-HEG loadings were a) 0, b) 20, c) 50 and d) 100 %. Mean fluorescence intensities were compared and were found to correlate to attempted acetyl-HEG (and subsequent alkyne) loading, however total fluorescence intensities were low indicating poor fluorophore loading levels

To investigate further, samples of all HEG functionalised particles were coupled with a cheap, DMTr protected deoxycytidine phosphoramidite (**54**) so that the yields of multiple phosphoramidite couplings could be directly ascertained. Trityl measurements made by deprotecting particles coupled with the protected deoxycytidine showed very poor coupling efficiencies for all particles with final cytidine loading densities of less than 0.1 nmol cm^{-2} (a yield of less than 4% going by the loading density of the first phosphoramidite coupling being 2.25 nmol cm^{-2}). The poorest coupling was found to be between the cytidine phosphoramidite (**54**) and particles with two HEG spacers incorporated. From this can be concluded that the previously attempted stepwise couplings of acetyl-protected HEG and alkynyl phosphoramidite were also likely to be poor yielding, explaining the low fluorescences observed upon fluorophore conjugation. Something was affecting subsequent phosphoramidite couplings which had not inhibited the initial coupling or deprotection steps.

4.2.4 SU-8 porosity; swelling and the trapping of water

Phosphoramidites are sensitive to water and will react violently under aqueous conditions, for this reason all coupling steps during oligonucleotide synthesis are carried out under strictly anhydrous conditions. Following the coupling step are capping, oxidation and deprotection steps before the cycle is repeated with the addition of the next nucleotide. Oxidation takes place under aqueous conditions and the dehydration of the support after oxidation is therefore vital for high coupling efficiency during the following cycles. During oligonucleotide synthesis (Scheme 1) phosphoramidite coupling is usually high yielding as controlled pore glass (CPG), the support normally used does not swell and is easily dehydrated by washing in anhydrous solvent (acetonitrile).[279]

Water reacts stoichiometrically with phosphoramidites in a 1:1 ratio (Scheme 13) therefore small quantities of water would soon be removed by this mechanism. However the products of reaction with water can degrade further resulting in an acrylonitrile by-product (**65**). Acrylonitrile can react with phosphoramidite directly, the products of this degradation pathway being a cyanoethyl-phosphonoamidate (**67**) and another equivalent of the acrylonitrile (**65**), this therefore leads to the continuous

loss of phosphoramidite.[280] The slightest amount of water present can result in the eventual degradation of all phosphoramidite to the corresponding phosphonoamidate (**67**), the speed of this degradation being dependent upon the amount of water present.
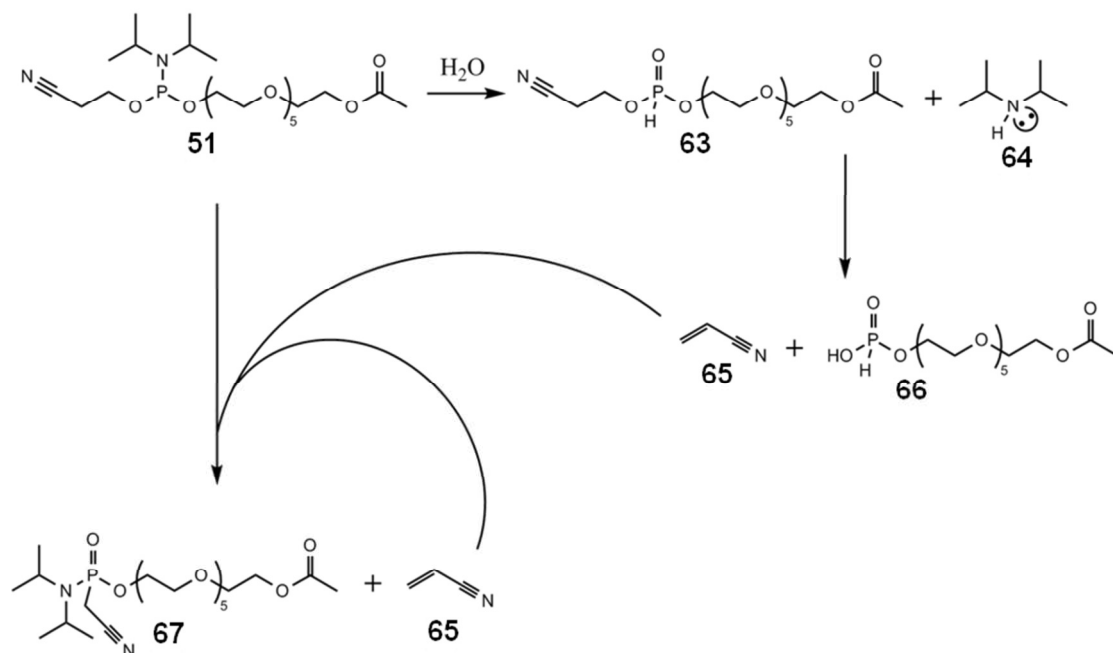
Scheme 13. Phosphoramidite degradation pathways. Phosphoramidite (51) is initially degraded in an acid catalysed hydrolysis to cyanoethyl-*H*-phosphonate (63) and diisopropylamine (64). The presence of diisopropylamine (base) leads to acrylonitrile (65) elimination and *H*-phosphonate (66). Acrylonitrile reacts with the original phosphoramidite to form the cyanoethyl-phosphonoamidate (67), acrylonitrile is also a product of this reaction and therefore degradation of the original phosphoramidite will be continuous, the rate being dependant on the concentration of acrylonitrile which itself is determined by the amount of water initially present

During the course of this work SU-8 particles were observed to swell under various solvent conditions, with an obvious volume increase when in acetonitrile followed by shrinking back to the original dimensions under aqueous conditions. Work published in recent years has studied this behaviour in more detail.[281,282] By exposing 200 μm thick SU-8 layers to various solvent conditions and measuring the mass change it was found that polar aprotic solvents caused the greatest mass gain (swelling) with DMF, DCM and acetonitrile leading to mass gains of 61, 26, and 15% respectively. Highly porous SU-8 structures have also been fabricated by altering the ratio of solvent to monomer during SU-8 cross-linking.[283] Rhodamine and glucose were both observed to diffuse through the manufactured polymer membrane, moving through pores in the SU-8 structure. Pores are formed during

monomer cross-linking by the presence of solvent which is removed by evaporation during later (baking) steps in the polymer fabrication. Electron microscopy of the SU-8 particles used in our studies revealed rough, pitted surfaces (Figure 74), which appeared similar in structure to the reported porous SU-8 membranes.

Figure 74. The surface of an SU-8 particle imaged by electron microscopy showing a pitted, porous surface. Scale bar represents 500 nm

The SU-8 particles having a porous structure could explain why the coupling of a second phosphoramidite is generally much more poorly yielding than the coupling of the first. Initially, reaction of the first phosphoramidite with hydroxyl SU-8 particles (**16**) takes place in anhydrous acetonitrile where particles would swell, opening up the pores in the cross-linked matrix. After coupling is complete the particles are suspended in oxidiser (Iodine/THF/pyridine/water) where the pores are kept open (THF being polar aprotic) and water is permitted to enter the bulk structure. Particles are then washed in anhydrous methanol (which leads to particle shrinking and a closing of pores) followed by extensive drying in a heated vacuum centrifuge, water however, may remained trapped within the now closed SU-8 structure. During the coupling of any subsequent phosphoramidites, the particles are again suspended in acetonitrile, at which point swelling will occur releasing trapped water into the presence of the fresh phosphoramidite reagent and degrading it. If a sufficient quantity of water remains trapped by the SU-8 upon drying it could result in the failure of all but the initial phosphoramidite coupling.

Direct evidence for the trapping of small molecules within the polymerised SU-8 matrix has been observed during the oxidation step; SU-8 particles have on occasion become stained brown due to the entrapment of iodine. The extent of staining was found to be reduced by soaking for extended periods (2 days) in an acetonitrile/water solution (80:20 v/v) however washing in distilled water (where pores are closed) was found to have no effect on the extent of staining.

Previously we have demonstrated a variation in the surface epoxide loading density between batches, thought to be due to different levels of cross-linking during particle fabrication. A similar variation was also observed between particle batches as to the extent of iodine staining, with some batches not showing any visible staining. Batches with increased cross-linking would be expected to have smaller pores and therefore swell to a lesser extent than batches with increased cross-linking.[251] This particle batch to batch variation in swelling properties also explained the variation seen in the successes of phosphoramidite couplings, occasionally the coupling of a second phosphoramidite had been found to proceed with high efficiency.

4.3 Alkyne loading control by the single addition of a well designed phosphoramidite

With both the unpredictable (batch-dependant) swelling of SU-8 particles and the subsequent trapping of water being a hindrance to sequential phosphoramidite coupling it was logical to design a reagent which could achieve a controlled surface density of reactive groups and incorporate a spacer group in a single step.

4.3.1 An alkyne-functionalised phosphoramidite incorporating a hexaethylene glycol spacer

Requirements of the new reagent molecule were for;

- The resulting SU-8 functionalisation to require no acid deprotection steps and to be able to covalently couple probe DNA in a highly chemoselective manner, therefore alkyne was retained as the functional group of choice for the click coupling of azide-modified probes.

- The inclusion of a spacer group no less than 29 atoms in length which would be inert and not lead to an increase in the non-specific binding of biomolecules and so a hexaethylene glycol spacer was incorporated in the final reagent.

- A similar coupling rate compared to the (blocking) CPR phosphoramidite reagent allowing the resulting loading density to be controlled by the proportional addition of blocking and functionalising compounds. As results had shown the acetyl-protected HEG phosphoramidite (**51**) synthesised previously to react at a similar rate to CPR phosphoramidite (**24**), the new reagent was also a phosphoramidite.

The phosphoramidite synthesised was a combination of elements of the HEG and alkynyl phosphoramidites previously used, resulting in the HEG-linked propargyl phosphoramidite (**53**). This compound was synthesised in two reaction steps and was found to contain no significant impurities.

Coupling of this new phosphoramidite and the control of its surface loading was assessed in the reaction between diol-functionalised SU-8 particles (**16**) and varying proportions of the propargyl-HEG-phosphoramidite (**53**) and the trityl-protected CPR phosphoramidite (**24**). This resulted in SU-8 particles having a mixed surface of phosphate and alkynyl moieties (**68**) (Figure 75). Further assessment of loading density and the viability for the alkynyl group's use as a handle for the immobilisation of oligonucleotide probes was tested by the click coupling of the azide-functionalised Cy-5 standard (Figure 76). Finally the azide-modified probe sequence, **PL**, was click coupled to these particles and the effects of loading density on the hybridisation of complementary, **TI**, and mismatching, **TG**, Cy-5 labelled target sequences investigated (Figure 77).
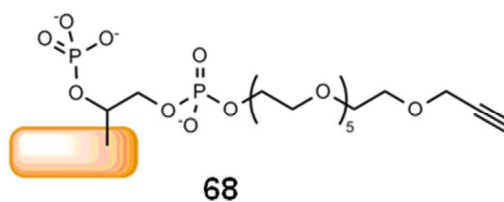
Figure 75. SU-8 particle functionalised with a mixture of both propargyl-HEG (53) and CPR (24) phosphoramidites. This surface modification incorporated all the elements which were expected to give particles suited to the click immobilisation of azide-functionalised oligonucleotide probes and their use in multiplexed DNA assays. This was a simplification of previous designs, aiming for particle functionalisation using a single phosphoramidite coupling step

Overall, total loading was found to be quite low compared with previous batches of SU-8 particles; trityl deprotection and quantification indicated that particles coupled with 100% CPR phosphoramidite (**24**) had a loading density of 0.1 nmol cm^{-2} (previous particle batches had been found to have loadings an order of magnitude more dense). This low loading density, whilst disappointing, was likely an effect of the variation in monomer cross-linking as a result of the batch-wise fabrication of the SU-8 particles, it did not imply any inherent problems to the phosphoramidite coupling step. Significantly, the particles showed trityl loading to be inversely proportional to the amount of propargyl-HEG-phosphoramidite and the resulting fluorescence upon the click coupling of azidoCy-5 was found to be directly proportional. These results demonstrated for the first time control of alkyne loading density, distanced from any blocking phosphate groups whilst retaining reactivity towards azides.
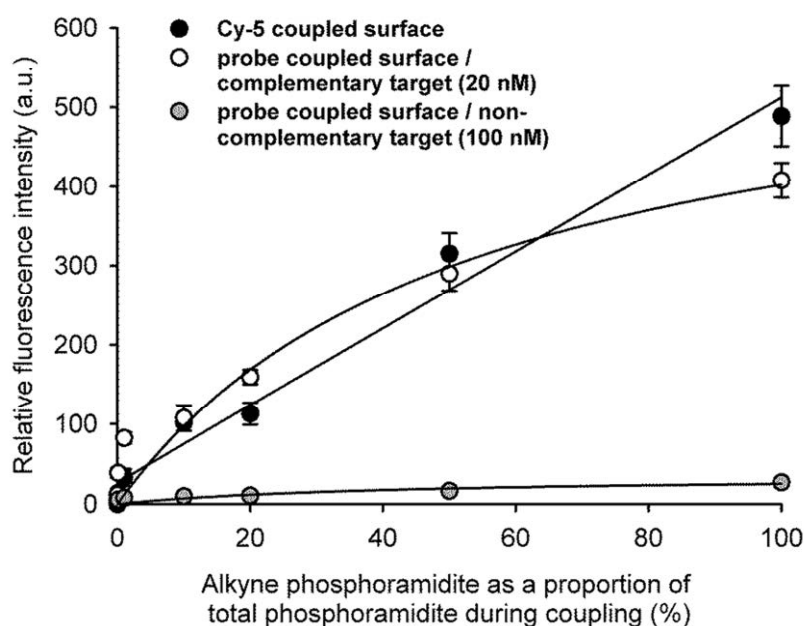
Figure 76. SU-8 particles were functionalised with various proportions of trityl-protected CPR (24) and propargyl-HEG (53) phosphoramidites. Alkyne loading was assessed by quantifying particle fluorescence resulting from the click coupling of azidoCy-5. Oligonucleotide probes were also click-coupled to alkyne particles and the hybridisations of Cy-5 labelled complementary (20 nM) and mismatching (100 nM) targets was also assessed using fluorescence quantification.
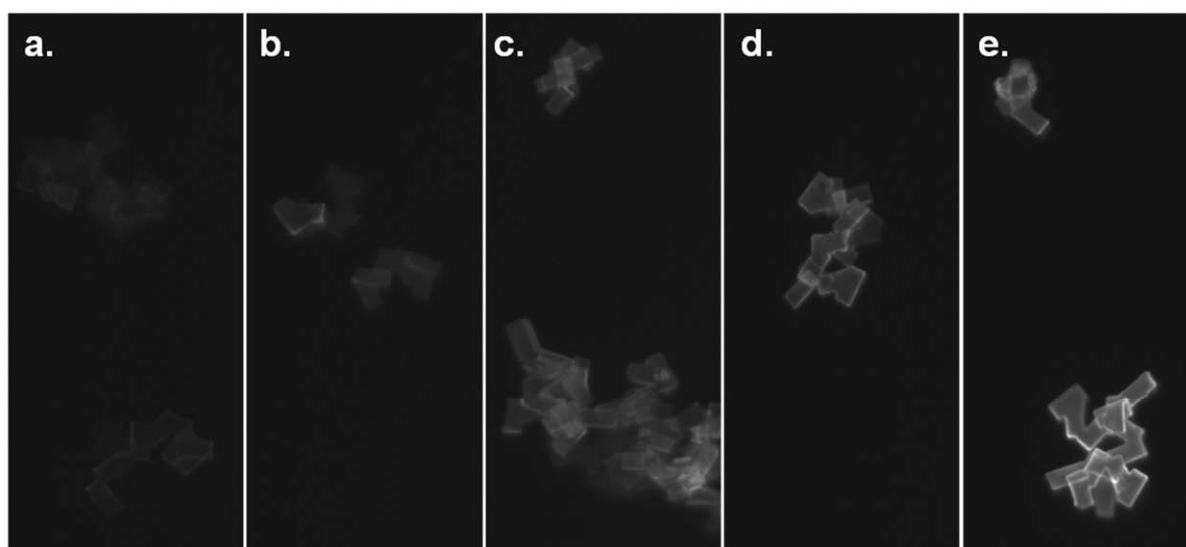
Figure 77. Cy-5 labelled complementary target (20 nM) hybridisation to probe-functionalised phosphate-blocked particles. The ratio of alkyne to phosphate surface functionality increases across the series from a) fully blocked, 0% alkyne to b) 0.1%, c) 1%, d) 10%, and e) 100%

The room temperature hybridisation of mismatching target oligonucleotide, **TG** (100 nM), was found to be inversely proportional to the density of phosphate blocking.

Although fluorescence was highest for particles with no phosphate blocking, the actual intensity was still found to be low, about one twentieth of the signal from azidoCy-5 coupled particles. This result would indicate a good coverage of oligonucleotide probes (a high yielding click reaction) as the non-specific binding to a DNA-functionalised surface had previously been found to be low (Figure 76).

Most encouraging was the hybridisation of complementary target oligonucleotide, **TI** (20 nM), to probe-functionalised particles at room temperature, the fluorescence of which was also shown to be proportional to the original surface loading of alkyne (Figure 77). The fluorescence intensity closely matched particles coupled with the azidoCy-5 standard, a result which indicated close to 100% hybridisation efficiency (saturation of immobilised probes) (Figure 76).

It was perhaps surprising to achieve such high efficiency of hybridisation on the particles with the highest alkyne loading densities as literature reports and our own theoretical calculations indicated that hybridisation efficiency would be maximised at a probe density of 0.55×10^{13} probes cm^{-2} (9.13×10^{-12} mol cm^{-2}). Above this loading complete hybridisation of all probes was expected to be hindered by steric factors.[262,263] As the surface loading density of our particles had been measured to be 1×10^{-10} mol cm^{-2}, particles with a probe to phosphate-blocker ratio of 1:9 might be expected to have resulted in the greatest capture of labelled target. This was clearly not the case with fluorescence increasing yet further with hybridisation to 20, 50 and 100% probe-functionalised particles.

A number of explanations for the apparent enhancement of hybridisation efficiency have been considered. Calculations of the reactive area of a particle are based upon the assumption that all surfaces are perfectly flat and we know this to not always be the case (Figure 74), the calculated surface area will therefore be an underestimate and likewise reported loading densities will thus be over estimated. It was thought unlikely that this simplification could account for (the entirety of) a ten-fold over estimate of loading densities, but it may make a significant contribution.

Perhaps more significant is the swelling of SU-8 whilst suspended in acetonitrile during phosphoramidite coupling. Following coupling are oxidation and washing steps during which particles shrink, however it is not known if particles fully revert to their pre-swelled dimensions. If pores in the extended SU-8 cross-linking remain

partially open, then a much greater surface area may be available for the immobilisation of probe sequences and for the hybridisation of targets. This would also result in the measured probe loading density of 0.1 nmol cm^{-2} being an over estimate. A ten-fold increase in surface area could well result from SU-8 having a porous structure.

Swelling could also result in an over calculation of amount of alkyne actually available during the click reaction. If propargyl-HEG phosphoramidites and trityl-protected CPR phosphoramidites could react within the open pores of SU-8, but the copper complex intermediate (**42**) (Figure 67) were too bulky to form there, not all of the alkyne would be available for probe coupling. The amount of available alkyne, as inferred from the measured total amount of phosphate would now be an over estimate, and therefore once again the loading density of probes would be an over estimate.

A fourth factor to be considered is the presence of the flexible hexaethylene glycol spacer. Between the 5' terminus of the oligonucleotide probe and the surface of the particle is a 33-atom (predominantly unsaturated) chain measuring approximately 50 Å. The flexibility of this tether may reduce the steric effects of probe overcrowding, allowing a closely packed surface with a lower associated energy cost than that achieved by using a more rigid tether, or no spacer at all. This reduction of steric hindrance may result in more duplex forming than originally expected.

It may be that the greater than predicted hybridisation efficiency experienced for these particles was due to a combination of a number of the above proposed explanations, further investigation was beyond the scope of this work.

4.3.2 Multiplexed hybridisation assays using the optimised encoded microparticle suspension array

To test the performance of the loading-controlled propargyl particles for use in DNA hybridisation arrays a number of multiplexing experiments were attempted. In a similar manor to that used for previous technology demonstrations (Chapters 2.8.3 & 2.8.4), differing oligonucleotide probes were coupled to samples of uniquely encoded particles forming probe-particle pairs. Covalently coupling the probes

allowed more freedom with regards to hybridisation conditions whereas previously, immobilising the probes by an affinity interaction (utilising labile avidin-biotin binding) forced the use of high concentrations of oligonucleotide target and stringent washing steps to force speedy hybridisation. The present assay design permitted longer hybridisation times, allowing equilibria to form and the use of lower concentrations of target. These multiplex assays were run at elevated temperatures, just below the calculated melting temperatures of the complementary probe-target duplex.[246] This was found to have afforded good discrimination between complementary and mismatching sequences without needing to resort to stringent urea washing steps, indeed particle mixtures were simply washed twice using room-temperature hybridisation buffer to remove unbound target.

All four different particle codes were used in these assays, after ring opening, a 50:50 mixture of the propargyl-HEG-phosphoramidite (**53**) and the blocking CPR phosphoramidite (**24**) were coupled to each code then deprotected. AzidoCy-5 was coupled to samples of all particle types as a positive control, fluorescence intensities ranged between 580,000 and 1,300,000 a.u. (Figure 78).
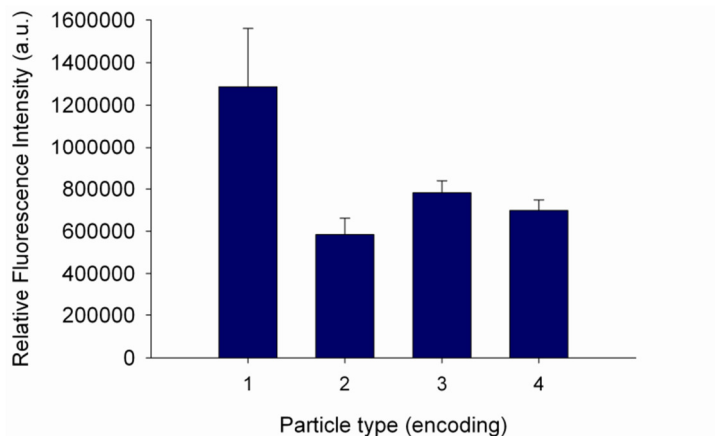
Figure 78. The fluorescence intensities of encoded SU-8 particles after the coupling of azidoCy-5 by click chemistry

Azide-modified oligonucleotide probes were click coupled to the alkyne-functionalised particles (Table 6) resulting in encoded microparticles with a 50:50 surface of probes and phosphate (**69**) (Figure 79).

Table 6. Sequences of oligonucleotide probes covalently coupled to encoded SU-8 particles

Name	Particle type (encoding)	Sequence (5' to 3')
PJ	1	AAA AAG TTG GAT CC
PK	2	CAA CCC CAG TTA ATA TTA TT
PL	3	CAA CCC CAG GTA ATA TTA TT
PM	4	GAG ATG CAC TCG AGT AAG TCA GTC G
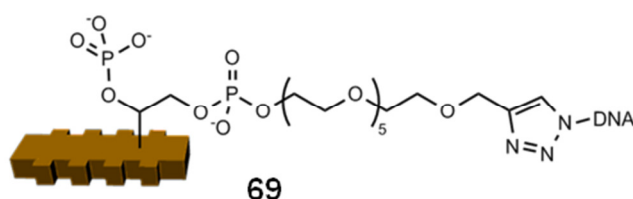
Figure 79. Oligonucleotide probes immobilised to encoded SU-8 microparticles, sequence running from the triazole ring reads 3' to 5'

Samples of each probe-particle pairing were mixed and used for the multiplex detection and discrimination of labelled target sequences. For each 4-plex, 20 nM target was added and the mixtures of particles suspended for two hours, initially temperature was elevated to 70°C for 3 minutes to denature all duplex DNA, this was then dropped slightly below the T_m of the corresponding complementary duplex (between 45 and 54 °C depending on target) for the remainder of the assay. After washing twice, the individual encoding and fluorescence intensity of each particle in an assay were analysed and the mean fluorescence signal for each probe-particle pair calculated (Figure 80).
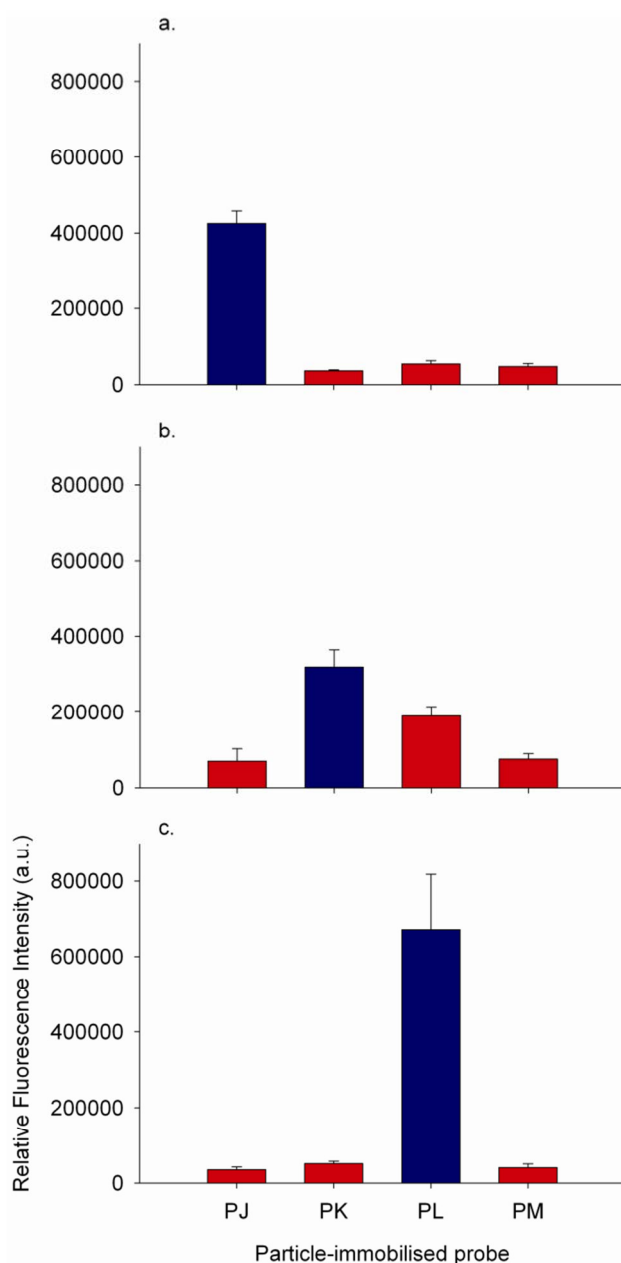
Figure 80. Multiplexed identification of labelled oligonucleotide target sequences (20 nM) using encoded microparticles functionalised with equal amounts of oligonucleotide probe and phosphate blocking moieties. Hybridisation assays were able to distinguish between sequences differing by a single base, and were performed at elevated temperatures to minimise mismatch binding. Mixtures of four different encoded microparticle-oligonucleotide probe pairs were exposed to 20 nM target a) (TG) 45°C, b) (TH) 54 °C and c) (TI) 54°C. The data from particles functionalised with the probe complementary to the added target are coloured blue

Three multiplex assays were performed. In each case discrimination was achieved between complementary and mismatching sequences, even when the probe and target sequences contained only a single non-complementary base pairing (Figure 80, b. and c.). Hybridisation to particles with type 2 encoding resulted in the lowest complementary signal (Figure 80, b.) which corresponded with the measurement of

probe loading; where the coupling of azidoCy-5 standard to these particles had also given the lowest signal (Figure 78). This lower probe loading to type 2 encoded particles resulted in the poorest discrimination in a single multiplex with the complementary signal being only 1.7 times the intensity of that representing a single base-pair mismatch and 4.1 times the signal of complete mismatches.

Figure 81. White light and fluorescence images of two encoded particle types (with all four types present in the assay). Three type 3 encoded particles functionalised with probe (PL) are visible on the left of the images along with a single type 2 encoded particle with probe (PK). Particles had been exposed to 20 nM labelled target (TI) at 54°C, the image shows the discrimination between complementary sequences and those mismatching by a single base-pair

Improved discrimination between sequences differing by a single base was achieved in the final multiplex (Figure 80, c.) where the fluorescent signal from particles functionalised with the complementary probe was greater than 13 times the intensity of particles functionalised with probe containing a single-base mismatch with respect to the target sequence (Figure 81). This complementary signal was also almost 20 times greater than that of particles functionalised with completely mismatching probe. An estimate of hybridisation efficiency could be gained by comparing the

fluorescent signals of complementary target hybridisation and azidoCy-5 click coupling, looking at type 3 encoded particles (Figure 80, c and Figure 78 respectively), hybridisation efficiency was calculated to be 86% (54°C), indicating that most of the immobilised probe sequences were in an orientation favourable for duplex formation. This was likely due to the controlled immobilisation via 5' azide and the low surface loading density of probe.

The degree of discrimination was an improvement on previous multiplex assays using affinity-immobilised probes (Chapters 2.8.3 & 2.8.4). Had the loading density of probe on particle been greater, complementary target hybridisation would likely have resulted in greater fluorescence intensities as well. In that scenario, nonspecific binding and mismatch hybridisation may also have been lower due to a higher loading density of phosphate. Neither had assay conditions, including hybridisation temperature, target concentration and the amount of particle washing been optimised. Therefore it was likely that the discrimination attained in these demonstrations of multiplexed DNA analysis could be further improved. These final results were hampered by a shortage of time (to put into assay development) and some poor batches of fabricated particles (which were overly cross-linked and thus had a low epoxide loading densities).

The new methodology of probe immobilisation was clearly an improvement on previous systems including affinity-capture. The orientation of probes to maximise hybridisation efficiency and the incorporation of phosphate groups to minimise nonspecific binding had been combined in an assay system which allowed control of parameters including assay time, temperature, salinity and probe loading density. In summary, the immobilisation scheme developed resulted in stable, oligonucleotide-functionalised encoded microparticles which could be used in the design and optimisation of multiplexed DNA suspension arrays.

4.4 Conclusions

The aqueous Huisgen 1,3-dipolar cycloaddition reaction was found to be ideal for the immobilisation of functionalised oligonucleotide probes to polymer microparticles. The chemistry involved was robust and chemoselective, only

occurring between azide-modified sequences and alkyne-modified surfaces in the presence of a synthesised tris-triazole ligand and Cu^I. The surface density of fluorophore resulting from the click coupling of azide-functionalised Cy-5 to alkyne-functionalised GMA beads was high enough to induce fluorescence quenching. The only requirement for an efficient coupling was the inclusion of a sufficiently long spacer group to distance the alkyne moiety from the surface of the support. For this purpose a 9-atom spacer was found to be of insufficient length, however spacers over 28 atoms long resulted in a high yielding reaction. It was speculated that the formation of the intermediate copper complex may be affected by steric factors due to its large size, incorporating the copper-bound ligand, azide-modified oligonucleotide and the alkyne-modified particle. Moving the reaction further from the surface on the end of a flexible spacer resulted in a more favourable reaction environment.

An azido-modifier was synthesised and subsequently used for the functionalisation of amino-terminated oligonucleotide probes. Functionalisation of the support surface to control both alkyne loading density and nonspecific DNA binding required significant development. Advancing on earlier work (Chapter 3) we continued to use phosphoramidite reagents for particle surface modification due to their compatibility with established oligonucleotide synthesis, the variety of reagents commercially available and the idea that the resulting phosphate bridges should reduce the nonspecific binding of DNA.

Control of loading density was achieved using varying ratios of different phosphoramidite reagents, forming surfaces with a mixture of both blocking and (trityl protected) reactive functionalities. However it was found that upon deprotection under acidic conditions hydroxyl loading control was lost and all surfaces would present a similar hydroxyl loading density regardless of the amount of blocking phosphoramidite initially coupled. Both literature and experimental evidence indicated that polymerised SU-8 was vulnerable to damage (etching) under acidic conditions and in the case of our particles, the mildly acidic trityl deprotection employed was likely etching the particle surface resulting in formation of new hydroxyl functionality. An acetyl-protected HEG phosphoramidite was synthesised so deprotection would occur under basic conditions and loading control was demonstrated using this reagent in conjunction with a blocking phosphoramidite.

The swelling properties of SU-8 in polar aprotic solvents was then found to be an issue, where the temporary entrapment of water molecules followed by their release in the presence of phosphoramidite reagent greatly reduced the yield of phosphoramidite coupling steps. This did not affect the coupling of initial phosphoramidites as before this step particles were not exposed to swelling solvents and had been kept under anhydrous conditions. Subsequent phosphoramidite coupling cycles after particles had swollen and been exposed to water, would show lower yields. Before the use of the acetyl-protected phosphoramidites these poor yields had been hidden by the regeneration of surface hydroxyl under acidic deprotection conditions. As the swelling of particles in acetonitrile and the use of aqueous steps could not be avoided, and the thorough drying of particles between coupling cycles was found to be insufficient to avoid retardation of the coupling, a new design of phosphoramidite was proposed. This reagent incorporated a flexible, hydrophilic spacer with alkyne functionality requiring no deprotection and allowed control of alkyne loading density in a single coupling cycle.

Following the click immobilisation of azide-modified oligonucleotide probes to particles with a controlled surface loading of alkyne, the hybridisation of DNA could be studied. Hybridisation to the SU-8 particles was found to be very efficient, as the fluorescence intensity of particles after the capture of a Cy-5 labelled complementary sequence was found to closely match that of particles with an azide-functionalised Cy-5 directly coupled. This was an improvement over the affinity probe capture system employed in preceding work (using immobilised avidin) where hybridisation efficiency had generally been found to be below 10%.

Improved hybridisation efficiency when covalently coupling probes using the click-based setup may have been due to a combination of factors resulting in the probe sequence adopting a conformation favourable to hybridisation. The use of a long, flexible spacer would allow the hybridised duplex further freedom of movement to form a stable conformation. In addition the targeted chemoselectivity of the click reaction guarantees the probe to be tethered through the terminal azide modification. Furthermore, the high density of negatively charged phosphate groups at the particle surface, which had been demonstrated to reduce DNA nonspecific binding, would, in a similar way, force the probe sequence to be held far from the surface therefore in an ideal position for interaction with target sequences. For the previously

investigated affinity captured probes, nonspecific binding of DNA to the protein-coated surface was found to be an issue, it is conceivable therefore that probe sequences may have also nonspecifically bound to this surface. If these probes were interacting directly with the surface it is likely they were in a less favourable orientation for hybridisation, explaining the poor hybridisation efficiencies observed.

The high efficiency, click coupled probe-particles were used for the multiplexed analysis of labelled target oligonucleotides. This demonstration suggested the array setup to be ideal for use in multiplexed DNA assays, with fluorescent ratios of 13:1 and 20:1 resulting between complementary : single base mismatching and complementary : completely mismatching sequences respectively. As the probe sequences were immobilised via covalent coupling, temperature could be increased to aid discrimination between similar target sequences. In summary, the encoded microparticle suspension array resulting from the Huisgen 1,3-dipolar cycloaddition coupling of azide-modified oligonucleotide probes to well-designed alkyne functionalised particles appeared to work as expected. Good discrimination between target sequences was achieved and the base sequence of these targets could be elucidated using the original microparticle encoding.

5.0 Conclusions and Future work

5.1 Conclusions

This project consisted of the design, development and implementation of multiplexed DNA hybridisation arrays, utilising encoded microparticles as oligonucleotide probe carriers. Assaying samples of short DNA sequences using this suspension array technology remains an emerging field with only a handful of kits commercially available, leaving scope for further development.

Prior to this work the polymeric material SU-8, used as a support for both encoding and probe immobilisation, had been extensively used for the microfabrication of small structures and moulds, reports of the chemical modification of SU-8 are rare. Functionalisation of the particle surface was achievable using residual surface epoxide groups which could be ring-opened with nucleophilic attack. This allowed for a number of different functionalities including alcohol, amine, acid, phosphate, ether and alkyne groups to be incorporated. From a chemist's view point SU-8 is hardly an ideal material as throughout the project epoxide loading levels were found to vary between particles fabricated in differing batches. A combination of factors was thought to affect the variation in monomer crosslinking which caused fluctuating epoxide loading. Between batches the energy of exposure (mW) during photolithography would change (usually by $\pm$ 10%), this could be minimised by the regular measurement of lamp (light) intensity (and the subsequent alteration of substrate exposure time) but could not be eliminated as the lamp had a natural variability. After exposure, SU-8 monomer crosslinks upon heating (PEB), as the baking times were controlled manually this added an element of human error into the fabrication process. Whilst perhaps the most significant variation was the amount of solvent in the pre-mixed monomer solution which would be reduced for batches fabricated from previously opened bottles of monomer compared with when using a new, fresh bottle. Changes to the amount of solvent have now been shown to affect the amount of monomer crosslinking and likely therefore the resultant surface epoxide loading levels.[283] Polymerised SU-8 was also found to swell in polar aprotic solvents like acetonitrile and the material was found to be incompatible with long term exposure to acidic conditions.

Despite these hindrances, protocols for the coupling of phosphoramidite moieties to the particles were developed which lead to orthogonal synthesis, reactive and blocking functionalities and various spacer lengths being incorporated. From this the loading density and distribution of chemistry could be controlled leading to different options regarding the modification of particles for use in DNA hybridisation assays.

Throughout the array development there were two main issues to tackle; the stable, simple and controlled immobilisation of oligonucleotide to the particles and the minimisation of nonspecific interactions between target DNA and the SU-8 polymer.

Utilising the specific affinity between the particle-immobilised protein avidin and its ligand biotin in the form of biotin-functionalised probes satisfied the requirements for a simple immobilisation method which resulted in the controlled orientation of probes, however the extensive modifications to both protein and ligand were found to weaken the normally very strong interaction. The half-life of the complex dropped from 200 days (wild-type) to less than 2 days (on-particle). This transient immobilisation was not detectable until assaying in multiplex when the ability of probe-particle pairs to discriminate between complementary and mismatching target sequences diminished with time as different probe sequences were migrating between particles. Amide coupling was also found to be unsuitable as coupling via nucleoside amines occurred in parallel with the intended coupling through terminal amine modification. The use of amine modified probes was also found to be incompatible with immobilised phosphate groups which were used as blocking moieties, as the two functionalities were found to couple.

As phosphate blocking and amide coupling could not be used in conjunction as they resulted in a loss of control of both probe loading density and probe orientation, more chemoselective reactive functionalities were required. The reaction between alkyne and azide groups to form functionalised triazole rings (Huisgen 1,3-dipolar cycloaddition, click coupling) did afford a stable covalent probe linkage. Due to the very specific nature of the reaction coupling only occurred through the intended chemical groups, so probe loading densities could now be controlled and the oligonucleotides tethered end-on (through a terminal azide modification) to maximise complementary target hybridisation.

Nonspecific DNA binding was found to be a problem which required attention so as not to interfere with detection of complementary sequences. Initially avidin DN was chosen as this form of the protein was reported to show reduced interaction with DNA, however biotinylated probes were found to bind both specifically and nonspecifically to protein-functionalised particles. Nonspecific binding could be blocked by using high concentrations of surfactants (significantly Tween-20®) but the move to covalent probe coupling increased the scope for surface optimisation to reduce this undesirable interaction. Surfaces could be functionalised with hydrophilic PEG spacers and negatively charged phosphate blocker groups, which greatly limited binding between generic oligonucleotides and the microparticles.

The final array design combined encoded microparticles with oligonucleotide probes orientated towards and accessible to target DNA. The use of phosphate groups minimised the nonspecific binding of completely mismatching target, whilst the stable click linkage allowed heating of assay suspensions in order to maximise discrimination between complementary sequences and those mismatching by a single base. This covalent probe immobilisation also allowed different probe-particle pairs to be stored in suspension together and for particles to be recycled by the heat denaturation of formed duplex.

The array was used for the successful multiplexed analysis of oligonucleotide solutions containing four labelled target sequences, hybridisation efficiency of immobilised probes was found to be greater than 85% and a complementary to mismatch signal to noise ratio of 20:1 was attained.

5.2 Future work

The array was optimised for the detection and identification of synthetic nucleotide sequences and it would be interesting to see how well the particles discriminate between sequences derived from biological samples. Any real samples would likely contain amplified target in a mixture with unamplified DNA and possibly PCR enzymes, dNTPs, labelling reagents and other contaminants depending upon the stringency of purification employed. It may be found that increased sample

complexity interferes with the accuracy of any assay developed, the conditions of which would require further optimisation.

Once optimised, it should be possible to use the array not simply for sequence detection but for quantification too. For this the microparticle fluorescence intensity after the capture of labelled target would be quantified and compared with a standard curve. The standard curve would have been already obtained from probe-particle titration with standard solutions of target.

Quantitative results could be obtained by kinetic measurements of the rate of fluorescence increase (rate of hybridisation). This rate would be proportional to the concentration of target. The system's association rate constant could be predetermined therefore there would be no need to wait for oligonucleotides to reach a binding equilibrium, only the initial rate of fluorescence increase would need to be measured sequencing and quantifying in minutes..

There is scope for expansion in the chemistry of polymerised SU-8. In this work surface modifications were focussed on minimising the nonspecific binding of DNA eventually settling on a negatively charged phosphate surface. This is not a universal blocking group, indeed interactions with positively charged molecules would likely be greatly enhanced compared with unmodified surfaces. In subsequent studies of the chemical functionalisation of SU-8 we have focussed on using PEG-based blocking and reactive spacers to minimise nonspecific protein binding. To date we have achieved control of functional group loading density by the radical polymerisation of PEG methacrylamide monomers to SU-8 surfaces pre-functionalised with radical initiators. Work is also ongoing to achieve initial epoxide/diol loading levels which are independent of fabrication/polymerisation protocols used to crosslink SU-8 monomer. Polymer etchants are being investigated which may negate the particle variation inherent with a batch fabrication process; these work by refreshing the SU-8 surface regardless of the initial level of crosslinking. In general SU-8 has been shown to be a useful, if sometimes temperamental, substrate for chemical modification and this may lead to the future functionalisation of interesting, well defined lithographic microstructures.

To date the split and mix synthesis of oligonucleotide or peptide probes has not been attempted using encoded microparticles. Synthesis on SU-8 has been accomplished

by our group and recently by others, but this has never been applied using either split and mix techniques or particle tracking by reading encoding.[191,284] This would help realise the potential of encoded microparticles for the formation of very large immobilised probe libraries and their subsequent use in highly multiplexed biological assays.

As may be expected from an interdisciplinary basic technology project, we only achieved the groundwork required to develop a working multiplexed DNA hybridisation array. It is hoped that in the not too distant future large scale encoded microparticle suspension arrays may be able to detect and quantify both proteins and oligonucleotide sequences in parallel, making fast and accurate point of care diagnostics a reality and ushering in a world of personalised medicine.

6.0 Experimental

6.1 Materials and apparatus used

6.1.1 Reagents and suppliers

Oligonucleotide sequences (both modified and unmodified) were obtained from either Sigma-Genosys (UK) or ATDBio (Southampton, UK) or were synthesised in-house using a MerMade 192 well DNA/RNA synthesiser, with reagents purchased from Link Technologies (UK) and Glen research (Virginia, USA).

Monomeric SU-8-5, EC solvent (polypropylene glycol methylether acetate, PGMEA) and Microposit MF-319 developer solution (tetramethylammonium hydroxide, 2.2% w/v solution in water) were purchased from Chestech Ltd, (Rugby, UK). Avidin DN was purchased from Vector laboratories (California, USA). BCA Assay Kit was obtained from Pierce Biotechnology (Illinois, USA). All other reagents and solvents were obtained from Sigma-Aldrich (UK), Fluka (UK), Acros (UK), Alfa Aesar (UK) and Fisher (UK).

6.1.2 Apparatus and equipment

Microparticle fabrication made use of an EVG 620 mask aligner with photomask (Compugraphic, UK). Accuspin^{TM} Micro centrifuges (Fisher Scientific, UK) (r = 8.5 cm) were used for particle sedimentation. Fluorescence intensity, fluorescence anisotropy and absorption measurements of solutions was measured using a SafireII microplate reader (Tecan, Switzerland). Particles were analysed under a fluorescence microscope (Carl Zeiss AG, Germany) or using a FACSaria flow cytometer (BD Biosciences, USA). Kinetic and thermodynamic constants were calculated by fitting data using commercially available software (SigmaPlot 11.0, Systat Inc, USA and Origin 8.1, OriginLab Corporation, USA).

6.2 General analytical methods

6.2.1 Amine quantification – Kaiser test

The Kaiser test was used to quantify on-particle amine loading density; ninhydrin reacts with particle-tethered primary amine to form the cleaved chromophore.[285] [286]

Kaiser solution A: phenol (4 g) was dissolved in ethanol (1 mL) and potassium cyanide (0.13 mg) was dissolved in water (200 μL). The aqueous potassium cyanide solution was diluted in pyridine (9.8 mL) and combined with the phenol/ethanol solution.

Kaiser solution B: ninhydrin (500 mg) was dissolved in ethanol (10 mL).

To a known quantity of SU-8 microparticles (~ 50 μg) were added Kaiser solutions A (60 μL) and B (60 μL), the particle suspension was then heated at 100 °C for five minutes with occasional agitation. Suspensions were allowed to cool and particles separated by centrifugation (1 min, 10,000 rpm, 9503 g). Supernatant (100 μL) was decanted and absorbance (570 nm) was measured using a microplate reader (Costar, transparent, flat-bottomed 96-well UV star plate). After subtraction of the absorbance from a blank sample, concentration of primary amine was calculated using the Beer-Lambert law, $\varepsilon = 15700$ M^{-1} cm^{-1}, $l = 0.28979$ cm (100 μL in well).

6.2.2 Protein quantification – Bicinchoninic acid (BCA) assay

The bicinchoninic acid (BCA) assay was used to quantify particle-immobilised protein.[208] Green Cu^{II} salts are reduced to Cu^{I} by peptide bonds, two molecules of bicinchoninic acid complex with the Cu^{I} ion and result in a purple colouration.[209]

A known quantity of protein-functionalised SU-8 microparticles (~ 20 μg) were suspended in BCA reagent (100 μL) (BCA, sodium bicarbonate, sodium carbonate, sodium tartrate, copper sulphate, water, pH 11.3). BCA reagent (100 μL) was also added to protein standards (0 – 4 μg avidin DN). All samples were heated at 60 °C for thirty minutes with occasional agitation. Samples were allowed to cool and particles separated by centrifugation (1 min, 10,000 rpm, 9503 g). The absorbance (562 nm) of supernatants (75 μL) and standard solutions (75 μL) were measured

using a microplate reader (Costar, transparent, flat-bottomed 96-well UV star plate). Absorbance measurements for protein standards were used to plot a standard curve to which supernatants from particle samples could be fitted.

6.3 Epoxy SU-8 microparticle fabrication (7)

7
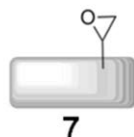
Particles were fabricated from photoactive epoxy SU-8-5 monomer. The commercial resist (a mixture of monomer and PGMEA) was spin coated as a 20 μm layer onto primed silicon wafers (525 ± 25 µm thick) onto which a thin layer of Al had been evaporated. The SU-8 layer was soft baked (65 °C, 4.5 min then 95 °C, 9 min), exposed to UV through a photomask and post exposure baked (65 °C, 2 min then 95 °C, 4 min). After allowing to relax for 24 hours, uncrosslinked monomer was removed by development in EC solvent (PGMEA) for 4 min with agitation. The wafers were thoroughly rinsed with isopropyl alcohol and blow dried. The Al sacrificial layer was removed by sonicating the wafers in Microposit MF-319 at room temperature for 20 min. Released microparticles were collected by centrifugation (1 min, 10,000 rpm, 9503 g), washed in water (4 × 1 mL) then methanol (4 × 1 mL) and dried under vacuum at room temperature for 4 h. Particles fabricated had dimensions 5 × 10 × 20 μm.

6.4 Preparation of amino functionalised SU-8 microparticles (Jeffamine® ED-900® spacer) (8)
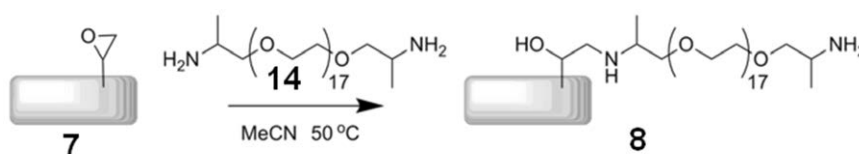
Dry epoxy SU-8 particles (5 mg) were suspended in MeCN and pelleted by centrifugation (1 min, 9503 g). A solution of *O,O'-Bis*(2-aminopropyl)

polypropylene glycol-*block*-polyethylene glycol-*block*-polypropylene glycol 800 (Jeffamine® ED-900®) (600 µl) in MeCN (600 µl) was added and the particles re-suspended. The reaction was agitated for 18 hours at 50 ºC. After centrifugation the supernatant was decanted and the SU-8 pellet washed in MeCN (6 × 1 mL) followed by MeOH (3 × 1 mL). The amino functionalised SU-8 was then dried by vacuum centrifugation (4 h).

Amino particles tested positive for a primary amine by Kaiser test, whereas unfunctionalised epoxy particles gave a negative result. Loading levels were typically in the range between 25 – 35 µmol g^{-1} (4.4 – 6.2 nmol cm^{-2}).

6.5 Preparation of carboxyl functionalised SU-8 microparticles (Jeffamine® ED-900® spacer) (9)
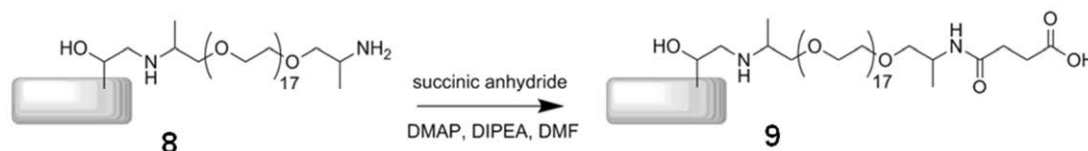
To a suspension of amino microparticles (5 mg, 125-175 nmol based on amino groups, suspended in dry DMF, 100 µL) was added a solution of succinic anhydride (10 mg, 100 µmol), DMAP (11 mg, 90 µmol) and DIPEA (5.5 mg, 7.5 µL, 42.7 µmol) in dry DMF (1.6 mL). The suspension was agitated at room temperature for 1 h. The suspension was centrifuged (1 min, 9503 g), the supernatant discarded and the reaction repeated with fresh reagents for a further 1 h. The microparticles were washed with DMF (4 × 1 mL) and MeOH (4 × 1 mL), and dried by vacuum centrifugation to afford carboxyl functionalised SU-8. The reaction was monitored by the ninhydrin test, which was negative on completion.

6.6 Preparation of biotin functionalised SU-8 microparticles (12)
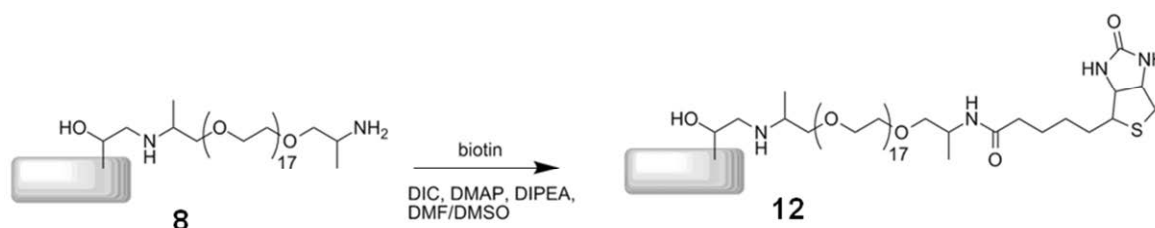
Biotin (24 mg, 98.1 μmol), DIC (12 mg, 95.1 μmol), DMAP (12 mg, 98.1 μmol) and DIPEA (8.9 mg, 12 μL, 63 μmol) were dissolved in a solution of 50% DMF in DMSO (1.6 mL). This solution was mixed for 10 minutes allowing reagents to dissolve. Amino functionalised SU-8 particles (5 mg, 125-175 nmol based on amino groups) were added to the biotin solution and the suspension agitated for 1 hour. The supernatant was decanted and fresh biotin coupling solution was added to the particles which were agitated in suspension for a further hour. Particles were washed in 50% DMF/DMSO (4 × 1 mL) and MeOH (4 × 1 mL), then dried by vacuum centrifugation to afford biotin-functionalised SU-8. The reaction was monitored using the Kaiser test, which was negative on completion.

6.7 Avidin DN functionalised SU-8 microparticles (coupling reagents *in-situ*) (avidin DN SU-8 Type I) (10)
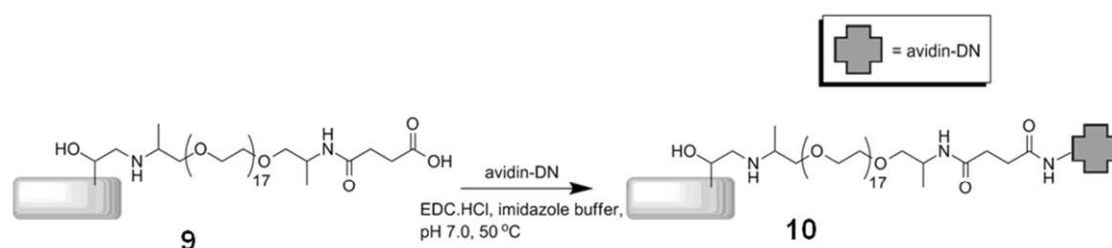
To carboxyl-functionalised SU-8 (5 mg, 125-175 nmol based on carboxyl groups) suspended in imidazole buffer (2 mL) were added; EDC.HCl (7.8 mg, 40.5 μmol) and avidin DN (200 μg, 2.94 nmol). The reaction mixture was agitated gently at 50 °C for 3 hours. The microparticles were washed with SSPE (5×) buffer (0.75 M NaCl, 50 mM sodium phosphate, 5 mM EDTA, 0.02% Tween-20®, adjusted to pH 7.0, 4 × 1 mL) and the supernatant separated by centrifugation (2 min, 2000 rpm, 380 g) to afford avidin DN-immobilised SU-8. Particles were washed again (2 × 1

mL) after overnight suspension and the amount of immobilised protein was determined by BCA assay to be reproducibly in the range 7.2 – 16.0 mol cm^{-2}. Particles were stored as a 1 mg mL^{-1} suspension in SSPE (5×) buffer with 0.02% Tween-20$^{®}$ and 0.01% sodium azide.

6.8 Avidin DN functionalised SU-8 microparticles (carboxyl pre-activation) (avidin DN SU-8 Type II) (11)
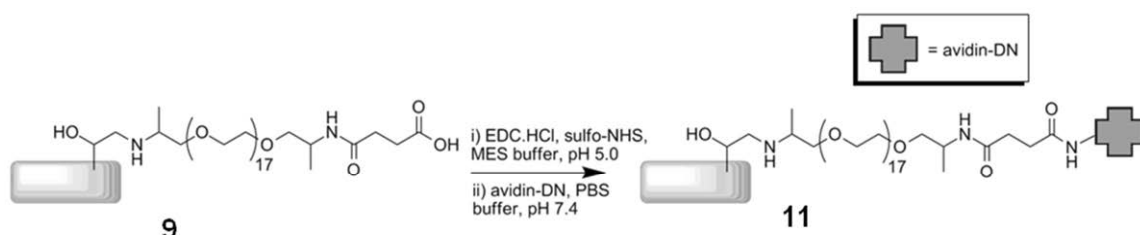
To carboxyl-functionalised SU-8 (5 mg, 125-175 nmol based on carboxyl groups) suspended in MES buffer (0.1 M MES, 0.5 M NaCl, 0.02% Tween-20, adjusted to pH 5.0, 2 mL) were added; EDC.HCl (7.8 mg, 40.5 μmol) and sulfo-NHS (2.9 mg, 25 μmol). Particles were agitated for 10 minutes after which the supernatant was decanted and the particles washed with deionised water (0.02 %Tween-20) (3 × 1 mL). Avidin DN (200 μg, 2.94 nmol) in PBS (0.14 M NaCl, 2.7 mM KCl, 10 mM Na$_2$HPO$_4$, 2 mM KH$_2$PO$_4$ adjusted to pH 7.4, 2 mL) was added to the particles and the suspension agitated gently for 2 hours. The microparticles were washed with SSPE (5×) buffer (0.02 % Tween-20$^{®}$, adjusted to pH 7.0, 4 × 1 mL) and the supernatant separated by centrifugation (2 min, 380 g) to afford avidin DN-immobilised SU-8. Particles were washed again (2 × 1 mL) after overnight suspension and the amount of immobilised protein was determined by BCA assay to be reproducibly in the range 5.7 – 7.7 mol cm^{-2}. Particles were stored as a 1 mg mL^{-1} suspension in SSPE (5×) buffer with 0.02% Tween-20$^{®}$ and 0.01% sodium azide.

6.9 Avidin DN functionalised SU-8 microparticles (affinity capture) (avidin DN SU-8 Type III) (13)
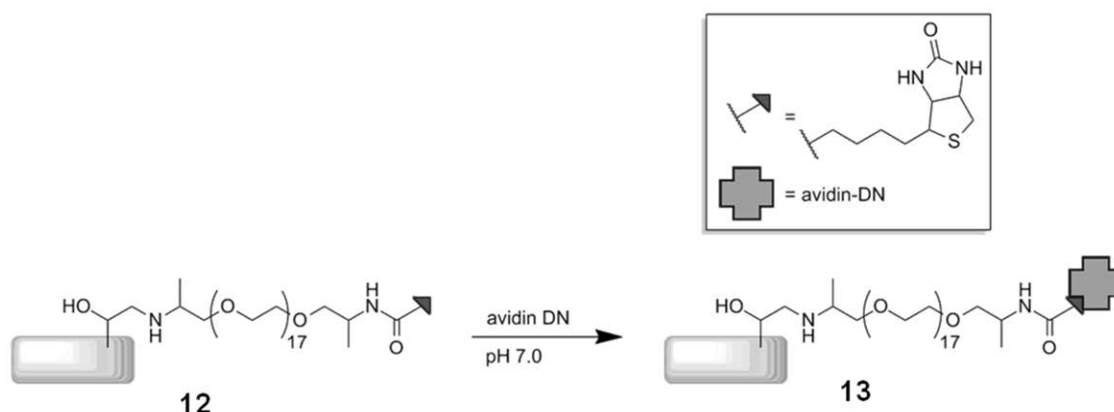
To biotin-functionalised SU-8 (5 mg, 125-175 nmol based on carboxyl groups) was added a solution of avidin DN (200 μg, 2.94 nmol) in SSPE (5×) buffer (0.02% Tween-20, adjusted to pH 7.0, 1.6 mL). Particles were agitated gently for 1 hour before the supernatant was decanted and the microparticles were washed with SSPE (5×) buffer (0.02% Tween-20, adjusted to pH 7.0, 4 × 1 mL) and the supernatant separated by centrifugation (2 min, 380 g) to afford avidin DN-immobilised SU-8. Particles were stored as a 1 mg mL^{-1} suspension in SSPE (5×) buffer with 0.02% Tween-20$^{®}$ and 0.01% sodium azide. Particles were washed again (2 × 1 mL) after overnight suspension and the amount of immobilised protein was determined by BCA assay to be reproducibly in the range 6.0 – 10.5 mol cm^{-2}. Particles were stored as a 1 mg mL^{-1} suspension in SSPE (5×) buffer with 0.02% Tween-20$^{®}$ and 0.01% sodium azide.

6.10 Covalent Cy-5 coupling to amino SU-8 under aqueous conditions (15)
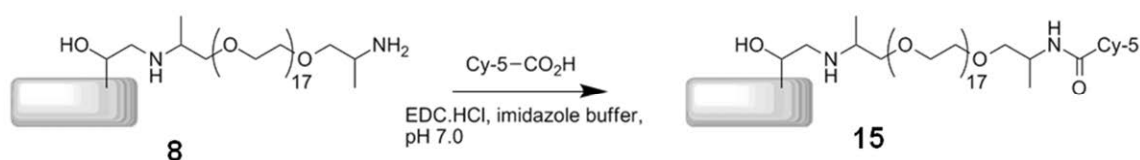
Cyanine-5 (Cy-5) dye (carboxyl functionality) (0.2 mg, 0.3 μmol) was dissolved in imidazole buffer (100 μL, pH 7.0) with EDC.HCl (0.5 mg, 2.6 μmol). Amino functionalised SU-8 particles (0.3 mg, 7.5-10.5 nmol based on amino groups) were

added to this solution and the suspension agitated for 40 minutes at room temperature. Particles were washed using SSPE (5×) buffer with 0.02% Tween-20® (5 × 1 mL). The particles were visibly blue.

6.11 Covalent Cy-5 coupling to amino SU-8 under organic conditions (55)
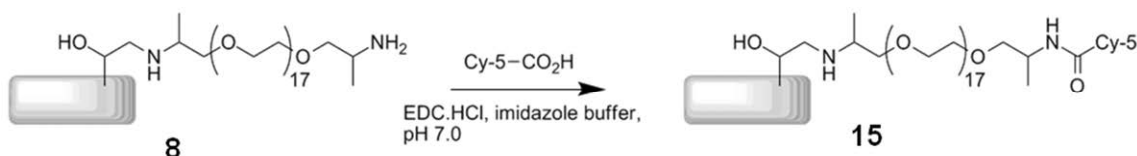
Cy-5 (0.2 mg, 0.3 μmol) was pre-activated using a solution of HOBt (0.1 mg, 0.74 μmol), TBTU (0.2 mg, 0.62 μmol), and DIPEA (0.13 μL, 0.1 mg, 0.77 μmol) in DMF (100 μL). After 30 minutes, amino functionalised SU-8 particles (0.3 mg, 7.5-10.5 nmol based on amino groups) were added to the Cy-5 activated-ester solution and agitated for 40 minutes at room temperature. Particles were washed using DMF (3 × 1 mL) followed by SSPE (5×) buffer with 0.02% Tween-20® (2 × 1 mL). The particles were visibly blue.

6.12 Preparation of *vic* diol functionalised SU-8 microparticles (16)
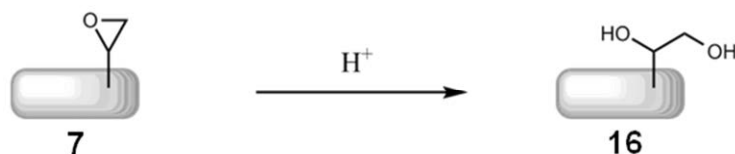
Un-functionalised (epoxide) SU-8 particles were suspended in hydrochloric acid solution (2 M) for 2 minutes then washed with NaOH$_{(aq)}$ (2 M) followed by water to afford *vic* diol functionalised SU-8 particles.

6.13 Preparation of carboxyl functionalised SU-8 microparticles (no spacer) (17)
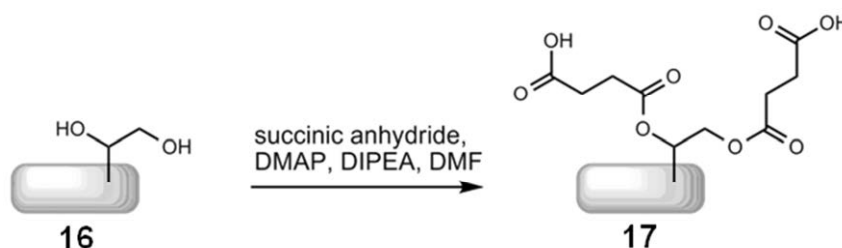
Vic diol functionalised SU-8 particles (1 mg) were suspended in DMF (200 μL) and a solution of succinic anhydride (2 mg, 20 μmol), DMAP (2.2 mg, 18 μmol) and DIPEA (1.1 mg, 1.5 μL, 8.54 μmol) in DMF (320 μL) was added. The suspension was agitated at room temperature for 1 hour. The suspension was centrifuged (1 min, 9503 g) and the supernatant discarded, the reaction was then repeated with fresh reagents for a further hour. Microparticles were washed with DMF (4 × 1 mL) and MeOH (4 × 1 mL), and dried by vacuum centrifugation to afford carboxyl functionalised SU-8.

6.14 Covalent DNA probe coupling to SU-8 microparticles (no spacer, amide coupling) (18)
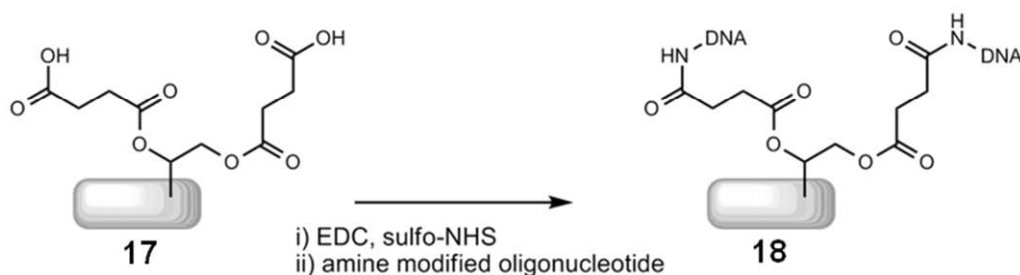
EDC.HCl (1.3 mg, 6.8 μmol) and sulfo-NHS (0.5 mg, 4.2 μmol) were added to a suspension of carboxyl functionalised SU-8 particles (20 μg) in MES buffer (0.1 M MES, 0.5 M NaCl, 0.02% Tween-20, adjusted to pH 5.0, 100 μL). Particles were agitated for 10 minutes after which the supernatant was decanted and the particles washed with deionised water (0.02% Tween-20) (3 × 200 μL). Amine modified oligonucleotide probe (10 nmol) in PBS (0.14 M NaCl, 2.7 mM KCl, 10 mM Na_2HPO_4, 2 mM KH_2PO_4 adjusted to pH 7.4, 100 μL) was added to the particles

and the suspension agitated gently for 2 hours. The DNA probe functionalised SU-8 particles were washed with SSPE (5×) buffer (0.02% Tween-20®, adjusted to pH 7.0, 4 × 200μL) and stored in the wash buffer with 0.01% sodium azide added.

6.15 Covalent DNA probe coupling to SU-8 microparticles (Jeffamine® ED-900® spacer, amide coupling) (20)

Amine modified DNA probes were coupled to carboxyl functionalised SU-8 particles which had a Jeffamine® spacer group. Coupling was achieved by the same technique used to couple to carboxyl functionalised particles lacking the spacer, as previously outlined (6.14).

6.16 General procedure for the coupling of phosphoramidites to hydroxyl SU-8
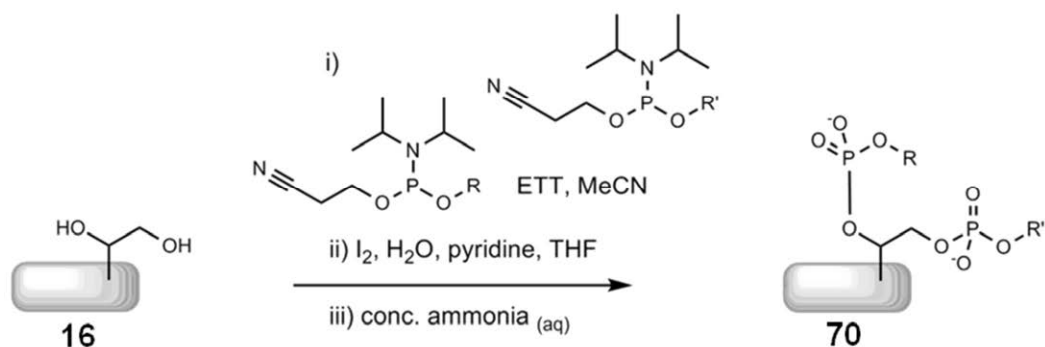
Hydroxyl functionalised SU-8 particles (400 μg) were dried thoroughly for 24 hours under vacuum at 50 °C. Phosphoramite(s) were dissolved in anhydrous MeCN (to a final concentration of 0.1 M). Phosphoramidite solution (200 μL) was mixed with a solution of 5-Ethylthio-1H-tetrazole (ETT) in MeCN (0.25 M, 320 μL) and this activated phosphoramidite solution added to the hydroxyl functionalised SU-8. This particle suspension was agitated under nitrogen for 30 minutes, after which the

supernatant was removed and discarded and the particles suspended in a second aliquot of activated phosphoramidite solution for a further 30 minutes.

These phosphite functionalised particles were next washed using anhydrous MeCN (3 × 500 µL) and oxidised using iodine (0.02 M) in THF/pyridine/water (7:2:1) (1 mL). Following this, the now phosphate functionalised particles were washed using MeOH (2 × 500 µL) and water (2 × 500 µL).

Cyanoethyl and sulphate (CPR phosphoramidite (**24**)) protecting groups were labile under basic conditions and were removed by the suspension of particles in concentrated aqueous ammonia (30% w/w, 17.6 M, 500 µL) at 60 °C for 1 hour, after which particles were washed with water (4 × 500 µL) and dried thoroughly.

DMTr protecting groups were labile under acidic conditions and were removed by the suspension of particles in perchloric acid.

6.17 Preparation of carboxyl functionalised SU-8 microparticles (HEG spacer) (72)
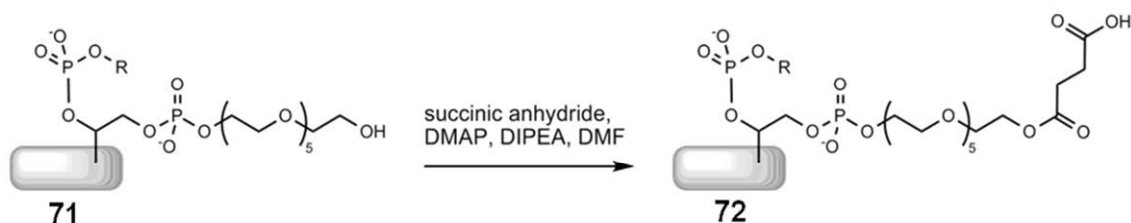
HEG phosphate functionalised SU-8 particles (1 mg) were suspended in DMF (200 µL) and a solution of succinic anhydride (2 mg, 20 µmol), DMAP (2.2 mg, 18 µmol) and DIPEA (1.1 mg, 1.5 µL, 8.54 µmol) in DMF (320 µL) was added. The suspension was agitated at room temperature for 1 hour after which particles were concentrated by centrifugation (1 min, 9503 g), the supernatant discarded and the reaction repeated with fresh reagents for a further hour. The microparticles were washed with DMF (4 × 1 mL) and MeOH (4 × 1 mL), and dried by vacuum centrifugation to afford carboxyl functionalised SU-8.

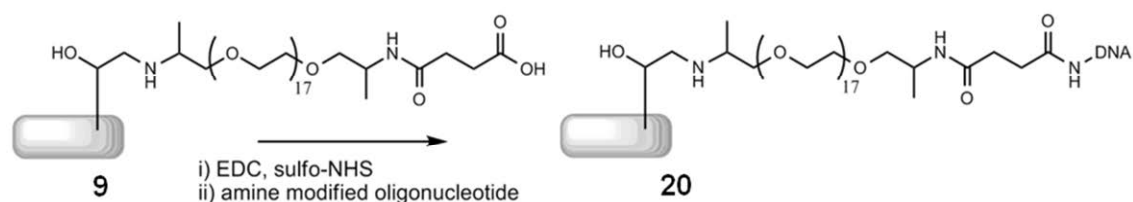## 6.18 Preparation of DNA probe functionalised SU-8 microparticles by amide coupling (HEG spacer) (73)
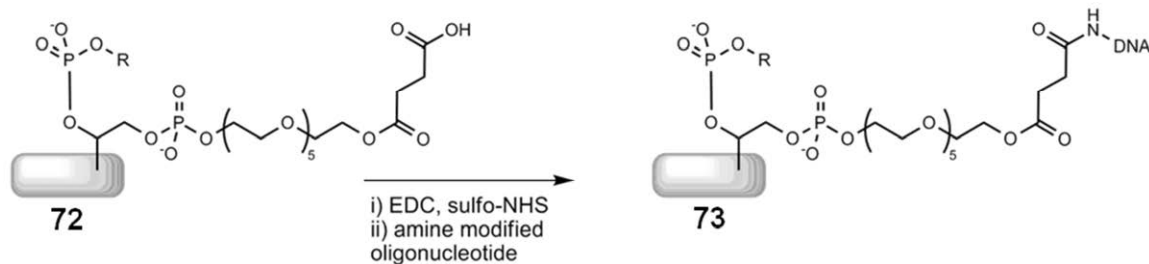
Amine modified DNA probes were coupled to carboxyl functionalised SU-8 particles which had a HEG phosphate spacer group. Coupling was achieved using the technique previously outlined (6.14).

6.19 Synthesis of 6-azidohexanoic acid ethyl ester (75)
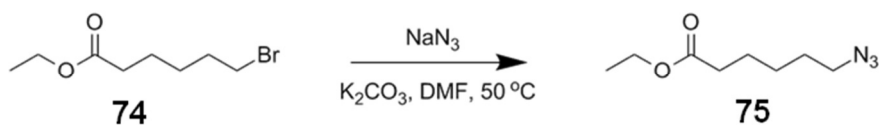
6-Bromohexanoic acid ethyl ester (2 mL, 2.516 g, 11 mmol) was mixed with DMF (25 mL). Sodium azide (1.466 g, 22.6 mmol) and potassium carbonate (2.338 g, 16.9 mmol) were added and the suspension stirred at 50°C, overnight under nitrogen. The reaction was monitored by TLC. The suspension was allowed to cool and was filtered (celite). The residue was washed with toluene (8 mL), supernatants were combined and solvent removed *in vacuo*. The crude product was purified by column chromatography (eluent; EtOAc/hexane 1/20) to yield 6-azidohexanoic acid ethyl ester (1.621 g, 8.8 mmol, 80%).

Physical state: colourless oil;

R_f = 0.30 (silica gel, 1:20 EtOAc:hexane);

MS (*m/z*): calcd for $C_8H_{15}N_3O_2$, 208.11 $[M+Na]^+$; found, 208;

¹H NMR (300 MHz, CDCl₃): δ 4.14 (q, 2H), 3.27 (t, 2H), 2.32 (t, 2H), 1.65 (m, 4H), 1.42 (dt, 2H), 1.25 (t, 3H).

¹³C NMR (75 MHz, CDCl₃): δ 173.4, 60.3, 51.2, 34.1, 28.6, 26.2, 24.5, 14.2.

Assignment ¹H NMR: δ 4.14 (CH₃**CH₂**OR), 3.27 (**CH₂**N₃), 2.32 (**CH₂**CO₂), 1.65 (**CH₂**), 1.42 (**CH₂**), 1.25 (**CH₃**).

Assignment ¹³C NMR: δ 173.4 (R**C**O₂R'), 60.3 (CH₃**C**H₂OR), 51.2 (**C**H₂N₃), 34.1 (**C**H₂CO₂), 28.6, 26.2 & 24.5 (**C**H₂), 14.2 (**C**H₃).

6.20 Synthesis of 6-azidohexanoic acid (76)
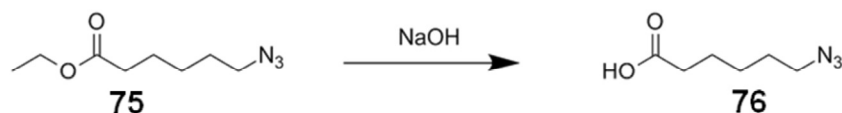
Sodium hydroxide (0.928 g, 23 mmol) was added to a solution of 6-azidohexanoic acid ethyl ether (1.074 g, 5.8 mmol) in water/dioxane (1:2, 11.6 mL). After 30 minutes the reaction mixture was passed down a dowex pyridinium column with water/MeOH (1:1) as eluent. Solvent was removed *in vacuo*. Product retained a NaOH impurity and was therefore partitioned between chloroform (10 mL) and water (10 mL). The aqueous phase was washed using chloroform (10 mL) and the organic fractions were combined, dried (anhydrous magnesium sulphate) and the solvent removed *in vacuo* to yield 6-azidohexanoic acid (0.609 g, 3.9 mmol, 67%).

Physical state: colourless oil;

MS (*m/z*): calcd for C₆H₁₁N₃O₂, 156.08 [M-H]⁻; found, 156;

¹H NMR (300 MHz, CDCl₃): δ 3.20 (t, 2H), 2.25 (t, 2H), 1.55 (m, 4H), 1.40 (m, 2H).

¹³C NMR (75 MHz, CDCl₃): δ 180.1, 51.6, 34.2, 28.9, 26.6, 24.6.

Assignment ¹H NMR: δ 3.20 (**CH₂**N₃), 2.25 (**CH₂**CO₂), 1.55 (**CH₂**), 1.40 (**CH₂**).

Assignment ¹³C NMR: δ 180.1 (R**C**O₂H), 51.6 (**C**H₂N₃), 34.2 (**C**H₂CO₂H), 28.9, 26.6 & 24.6 (**C**H₂).

6.21 Synthesis of 6-azidohexanoic acid NHS-ester (77)
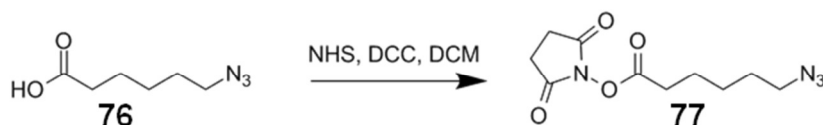
N,*N*′-Dicyclohexylcarbodiimide (DCC) (0.89 g, 4.3 mmol) was added to a suspension of 6-azidohexanoic acid (0.555 g, 3.5 mmol) and NHS (0.49 g, 4.3 mmol) in DCM (20 mL). The reaction was stirred for 4 hours with monitoring by TLC (eluent; DCM/MeOH 49:1). The mixture was partitioned between a saturated solution of potassium chloride (10 mL) and DCM (10 mL), the aqueous phase was washed using DCM (10 mL) and the organic fractions were combined, dried (anhydrous magnesium sulphate) and the solvent removed *in vacuo*. The product was purified by column chromatography (eluent; DCM/MeOH 99:1) to yield 6-azidohexanoic acid NHS-ester (0.482 g, 1.9 mmol, 54%).

Physical state: colourless oil;

MS (*m/z*): calcd for $C_{10}H_{14}N_4O_4$, 277.09 [M+Na]$^+$; found, 277; calcd 293.07 [M+K]$^+$; found, 294 (20%);

^{1}H NMR (300 MHz, CDCl$_3$): δ 3.32 (t, 2H), 2.82, (s, 4H) 2.62 (t, 2H), 1.79 (m, 2H), 1.65 (m, 2H), 1.53 (m, 2H).

^{13}C NMR (75 MHz, CDCl$_3$): δ 168.4, 51.1, 30.8, 28.4, 25.9, 25.6, 24.1.

Assignment ^{1}H NMR: δ 3.32 (**CH$_2$**N$_3$), 2.82 (**CH$_2$**C(O)N), 2.62 (**CH$_2$**CO$_2$), 1.79 (**CH$_2$**), 1.65 (**CH$_2$**), 1.53 (**CH$_2$**).

Assignment ^{13}C NMR: δ 168.4 (R**C**O$_2$R'), 51.1 (R**C**H$_2$N$_3$), 30.8 (R**C**H$_2$CO$_2$R'), 28.4 (R**C**H$_2$R'), 25.9 (R**C**H$_2$R'), 25.6 (R**C**H$_2$C(O)N), 24.1 (R**C**H$_2$R').

6.22 Synthesis of amino functionalised cyanine-5 fluorescent dye (78)
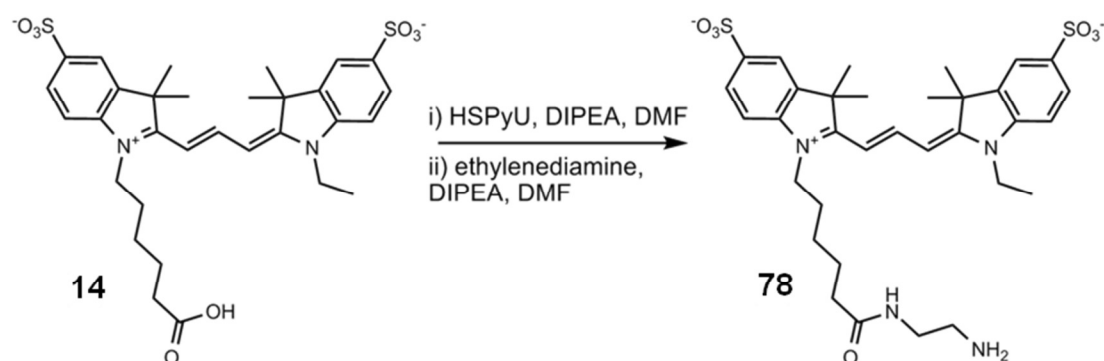
Cy-5 (4.2 mg, 6.4 μmol), *O*-(*N*-succinimidyl)-*N,N,N',N'*-bis-(tetramethylene)-uranium hexafluorophosphate (HSPyU) (11.3 mg, 27.4 μmol) and DIPEA (3.2 mg, 2.5 μL, 25 μmol) were dissolved in DMF (2.8 mL) and stirred. Reaction had gone to completion within forty minutes as monitored by TLC (eluent; $CHCl_3$/MeOH/H_2O 70/30/4, Cy-5 $R_f = 0.18$, NHS-activated Cy-5 $R_f = 0.36$).

The NHS-activated Cy-5 solution was added drop wise to a stirred solution of ethylenediamine (36.1 mg, 32 μL, 600 μmol) and DIPEA (38.8 mg, 30 μL, 300 μmol) in DMF (5 mL). The reaction was stirred for one hour and was found to have gone to completion by TLC.

Solvent was removed *in vacuo* and the crude product was purified by reverse phase column chromatography (pre-packed RP-18 gel column, 1.5 × 3.5 cm) (eluent; EtOH/n-propanol/H_2O/acetic acid 70/30/10/0.01). Removal of solvent *in vacuo* yielded product (4.4 mg, 6.3 μmol, 98%).

Physical state: blue solid;

R_f = 0.10 (silica gel, 70:30:4 $CHCl_3$:MeOH:acetic acid), 0.40 (NHS-activated Cy-5 intermediate);

MS (*m/z*): calcd for $C_{33}H_{45}N_4S_2O_7$, 348.635 [M-2H]$^{2-}$; found, 349 (57%); calcd, 698.28 [M-H]$^-$; found, 698 (61%);

¹H NMR (300 MHz, D₂O): δ 7.91 (m, 2H), 7.75 (s, 2H), 7.71 (d, 2H), 7.19 (d, 2H), 6.42 (m, 1H), 6.11 (m, 2H), 3.95 (m, 4H), 3.22 (t, 2H), 2.93 (t, 2H), 2.13 (m, 2H), 1.75 (m, 2H), 1.52 (s, 12H), 1.50 (m, 2H), 1.24 (t, 3H), 1.22 (m, 2H).

Assignment ¹H NMR: δ 7.91 (**CH**CHC), 7.75 (**CH**CSO₃H) 7.71 (CH**CH**CSO₃H), 7.19 (**CH**CHCSO₃H), 6.42 (CH**CH**CHC), 6.11 (CHCH**CH**C), 3.95 (**CH₂**N), 3.22 (**CH₂**CH₂NH₂), 2.93 (CH₂**CH₂**NH₂), 2.13 (**CH₂**C(O)N), 1.75 (**CH₂**), 1.52 (**CH₃**), 1.50 (**CH₂**), 1.24 (CH₂**CH₃**), 1.22 (**CH₂**).

6.23 Synthesis of azide functionalised cyanine-5 fluorescent dye (47)
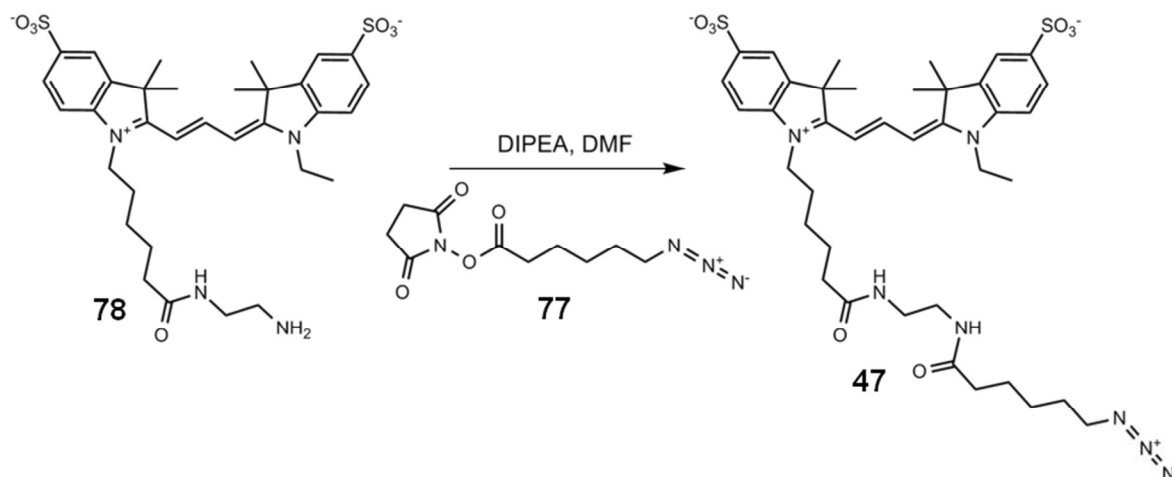
Amino functionalised Cy-5 (4.0 mg, 5.7 μmol) was dissolved in DMF (2.9 mL) with 6-azidohexanoic acid NHS-ester (7.2 mg, 28.5 μmol) and DIPEA (2.6 mg, 1.9 μL, 20 μmol). The reaction was stirred under nitrogen for one hour with monitoring by TLC and rpTLC (normal phase eluent; CHCl₃/MeOH/acetic acid 70/30/4, aminoCy-5 R_f = 0.05, NHS-azide R_f = 0.9, azidoCy-5 R_f = 0.1. reverse phase eluent H₂O/EtOH/n-propanol/acetic acid 70/21/9/0.07, aminoCy-5 R_f = 0.8, NHS-azide R_f = 0.15, azidoCy-5 R_f = 0.55).

Solvent was removed *in vacuo* and the crude product dissolved in water (1 mL) and purified by RP-HPLC (3 loadings of 333 μL, 150 × 10 mm column, increasing MeOH content from 0 to 50% in 0.1 M aqueous ammonium acetate over 15 minutes, product eluted after 28 minutes). AzidoCy-5 was concentrated by freeze drying (4.1 mg, 4.9 μmol, 86%).

Physical state: blue solid;

R_f = 0.1 (silica gel, 70:30:4 CHCl$_3$:MeOH:acetic acid), 0.55 (C$_{18}$-silica gel, 70:21:9:0.07 H$_2$O:EtOH:n-propanol:acetic acid);

MS (*m/z*): calcd for C$_{39}$H$_{54}$N$_7$S$_2$O$_8$, 418.175 [M-2H]$^{2-}$; found, 418 (42%); calcd, 837.36 [M-H]$^-$; found, 838 (6%).

6.24 Azide functionalisation of oligonucleotides (80)
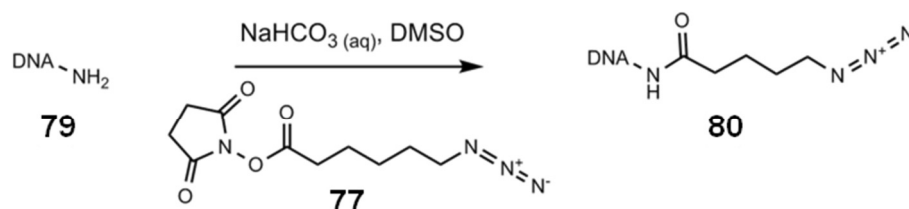
3' amino functionalised oligonucleotide (1 μmol) was dissolved in DMF (1 mL) with 6-azidohexanoic acid NHS-ester (1 mg, 4.0 μmol) and DIPEA (0.3 mg, 0.2 μL, 2.3 μmol) and the reaction was stirred under nitrogen for one hour.

Solvent was removed *in vacuo* and the crude product dissolved in water (200 μL) and purified by RP-HPLC.

6.25 Synthesis of 3-azidopropan-1-ol (82)
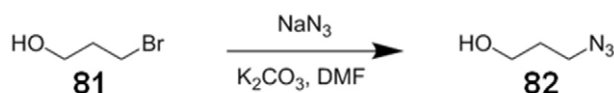
3-bromopropan-1-ol (1.02 mL, 1.64 g, 11.8 mmol) was added to DCM (50 mL). Sodium azide (1.63 g, 25 mmol) and potassium carbonate (2.59 g, 18.8 mmol) were added and the suspension stirred for 18 hours at 50 °C with monitoring by TLC (eluent; hexane/EtOAc 60:40). Solvent was removed *in vacuo* and the product purified by column chromatography (eluent; hexane/EtOAc 60:40) to yield 3-azidopropan-1-ol (0.60 g, 5.9 mmol, 50%).

Physical state: colourless oil;

MS (*m/z*): Unable to characterise (ESI +ve, ESI –ve & EI)

^{1}H NMR (300 MHz, CDCl$_3$): δ 3.78 (t, 2H), 3.48 (t, 2H), 1.82 (m, 2H).

^{13}C NMR (75 MHz, CDCl$_3$): δ 59.9, 48.5, 31.43.

Assignment ^{1}H NMR: δ 3.78 (**CH$_2$OH**), 3.48 (**CH$_2$N$_3$**), 1.82 (**CH$_2$**).

Assignment ^{13}C NMR: δ 59.9 (**CH$_2$OH**), 48.5 (**CH$_2$N$_3$**), 31.43 (**CH$_2$**).

6.26 Synthesis of Tris-triazole Cu(I) stabilising ligand (48)[269,270]
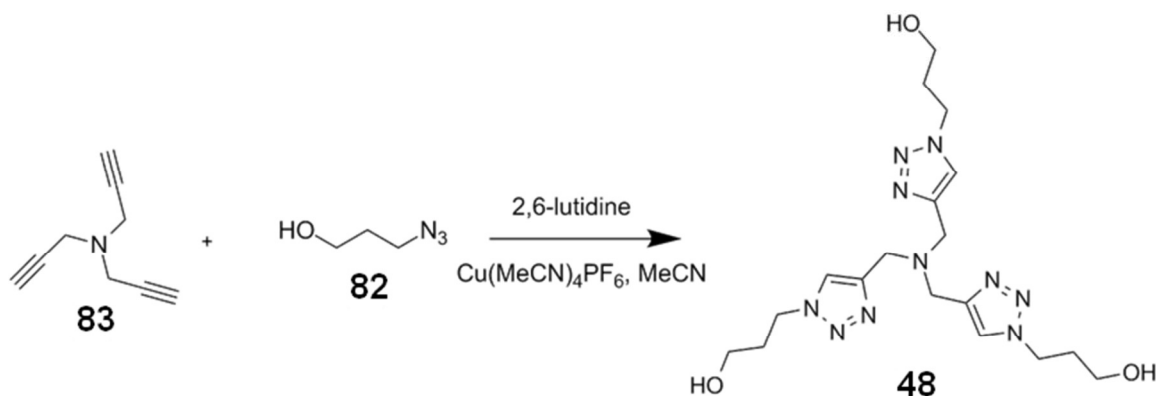
Tripropargyl amine (0.13 mL, 0.12 g, 0.92 mmol) was added to MeCN (2 mL) cooled over ice. Sequentially added were 3-azidopropan-1-ol (0.422 g, 4.2 mmol), 2,6-lutigine (0.11 mL, 0.1 g, 0.92 mmol) and Cu(MeCN)$_4$PF$_6$ (13.4 mg, 36 μmol). The reaction was cooled over ice for 20 minutes then allowed to reach room temperature, after stirring in the dark for 3 days the mixture turned a brown colour. The reaction was monitored by TLC (eluent; hexane/EtOAc 1:1).

The reaction mixture was cooled over ice to afford a white precipitate which was filtered and washed using cold MeCN (20 mL). The filtrate was concentrated by the partial removal of solvent *in vacuo* and left on ice to afford a second crop of product precipitate which was again filtered and washed. The tris-triazole Cu(I) stabilising ligand was found to be pure (0.18 g, 0.42 mmol, 46%).

Physical state: white fluffy solid;

MS (*m/z*): calcd for $C_{18}H_{30}N_{10}O_3$, 457.24 [M+Na]$^+$; found, 457 (100%); calcd, 435.26 [M+H]$^+$; found, 438 (18%);

^{1}H NMR (300 MHz, D$_2$O): δ 7.82 (s, 3H), 4.41 (t, 6H), 3.63 (s, 6H), 3.49 (t, 6H), 2.04 (m, 6H).

^{13}C NMR (75 MHz, D$_2$O): δ 143.3, 125.3, 58.2, 47.5, 47.2, 31.8.

Assignment ^{1}H NMR: δ 7.82 (C**H**N), 4.41 (C**H$_2$**OH), 3.63 (NC**H$_2$**C(N)CH), 3.49 (NC**H$_2$**CH$_2$), 2.04 (NCH$_2$C**H$_2$**).

Assignment ^{13}C NMR: δ 143.3 (CH$_2$**C**(N)CH), 125.3 (**C**HN), 58.2 (**C**H$_2$OH), 47.5 (N**C**H$_2$C(N)CH), 47.2 (N**C**H$_2$CH$_2$), 31.8 (NCH$_2$**C**H$_2$).

6.27 Preparation of alkyne functionalised SU-8 particles (Jeffamine ED-900$^®$ spacer) (56)
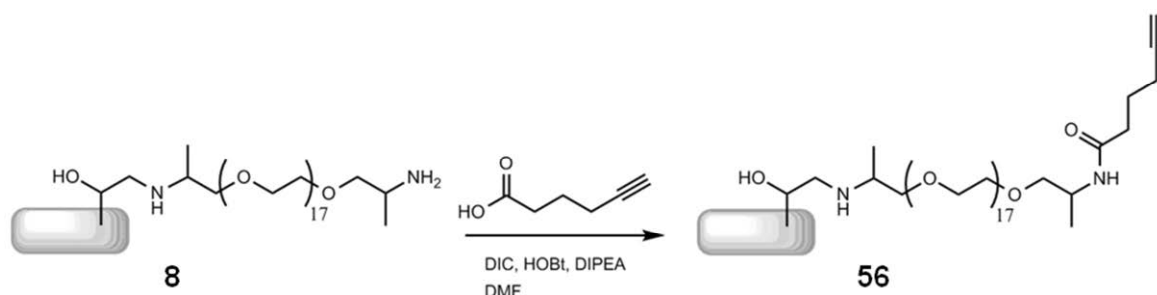
Pent-5-ynoic acid (6 mg, 61 μmol) was activated in a solution of DIC (5.2 μL, 4.2 mg, 33 μmol), HOBt (4.5 mg, 33μmol) and DIPEA (5.5 μL, 3.9 mg, 30 μmol) in DMF (1 mL) for five minutes. Amino functionalised SU-8 particles (Jeffamine$^®$ ED-900$^®$ spacer) were suspended in the activated acid solution and agitated for 90 minutes. Particles were washed thoroughly with DMF (2 mL) followed by water (3 mL). The reaction was monitored using the Kaiser test, which was negative on completion.

6.28 General procedure for the immobilisation of functionalised azides to alkyne functionalised SU-8 particles using Huisgen 1,3-dipolar cycloaddition reactions
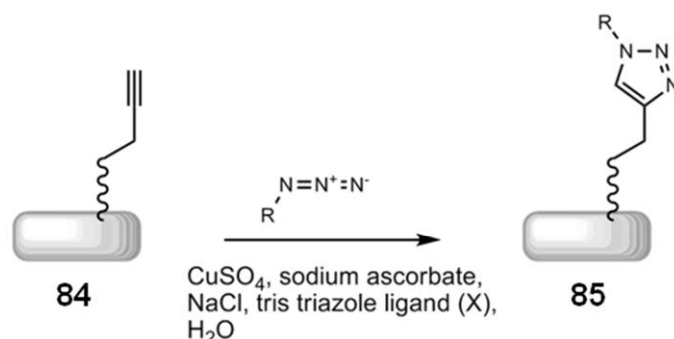
Huisgen 1,3-dipolar cycloadditions were used to immobilise azide-functionalised oligonucleotide probes and fluorophores to alkyne-functionalised SU-8 particles. Alkyne functionalised particles (40 μg) were suspended in a click reaction mixture consisting of NaCl (0.94 mg, 16 μmol), sodium ascorbate (32 μg, 160 nmol), Tris-triazole Cu(I) stabalising ligand (274 μg, 640 nmol), copper sulfate (20 μg, 80 nmol) and functionalised azide (4 nmol) in water (100 μL). Particles were agitated for four hours before washing in SSPE (5×) buffer with 0.02 % Tween-20® (3 mL) then in 0.5 M NaOH$_{(aq)}$ (1 mL).

6.29 Synthesis of monoacetyl hexaethylene glycol (87)[287]
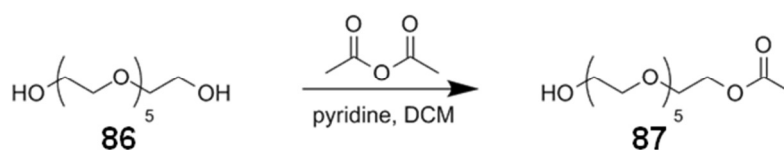
Hexaethyleneglycol (HEG) (2.35 g, 8.3 mmol) was diluted in DCM (5.5 mL) and pyridine (1.102 mL, 1.077 g, 13.6 mmol). The solution was cooled on ice and acetic anhydride (0.55 mL, 0.595 g, 5.83 mmol) added slowly with stirring. The reaction was allowed to warm to room temperature and left stirring for 18 hours. Solvent and base were removed *in vacuo* to yield a yellow oil. Products were purified by column chromatography (eluent; acetone:DCM 1:3, HEG R_f = 0.0, monoacetyl HEG R_f =

0.25, bisacetyl HEG R_f = 0.65, reagents and products stained with KMnO$_4$) to yield purified monoacetyl HEG (0.887 g, 2.74 mmol, 47%).

Physical state: colourless oil;

R_f = 0.25 (silica gel, 1:3 acetone:DCM);

MS (*m/z*): calcd for C$_{14}$H$_{28}$O$_8$, 347.17 [M+Na]$^+$; found, 347.2;

^{1}H NMR (300 MHz, CDCl$_3$): δ 4.22 (t, 2H), 3.75-3.6 (m, 22H), 2.65 (bs , 1H), 2.07 (s, 3H).

^{13}C NMR (75 MHz, CDCl$_3$): δ 171.1, 72.5, 70.6, 70.3, 69.1, 63.6, 61.7, 20.9.

Assignment ^{1}H NMR: δ 4.22 (**CH$_2$**OCOMe), 3.75-3.6 (**CH$_2$**), 2.65 (**OH**), 2.07 (**CH$_3$**).

Assignment ^{13}C NMR: δ 171.1 (**CO$_2$**Me), 72.5, 70.6, 70.3, 69.1, 63.6 & 61.7 (**CH$_2$**), 20.9 (**CH$_3$**).

6.30 Synthesis of acetyl hexaethylene glycol phosphoramidite (51)
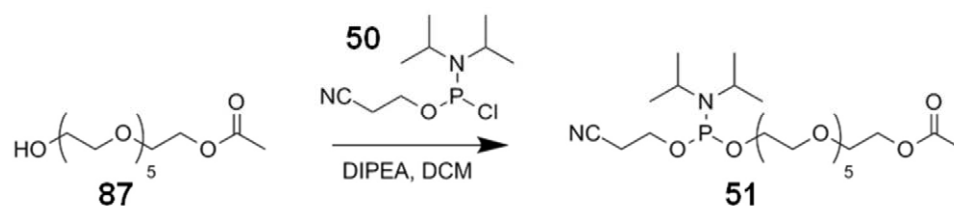
Monoacetyl HEG (392.9 mg, 1.21 mmol) was placed in a clean, dry R.B. flask (50 mL) with stirrer bar and dried *in vacuo* overnight. The flask was filled with nitrogen gas and DCM (6 mL) and DIPEA (319 mg, 499 µL, 3.03 mmol) (both distilled) were added via cannula. Chlorophosphitylating reagent (375 mg, 1.58 mmol) was added and the reaction stirred under nitrogen at room temperature with monitoring by TLC. TLC plates were pre-soaked in 10 % triethylamine (TEA), DCM before thorough drying, (eluent; acetone:TEA:DCM 25:1:74, chlorophosphitylating reagent R_f = 0.30, monoacetyl HEG R_f = 0.25, product R_f = 0.55, degradation product R_f = 0.05, 2D TLC confirmed that the degradation product was forming on the plate and not in the

reaction). After 2 hours the crude mixture was dried *in vacuo* then re-suspended in DCM (20 mL) and partitioned with saturated sodium bicarbonate$_{(aq)}$ (20 mL) under nitrogen. Phases were separated and the aqueous washed three times with DCM (45 mL), organic phases were combined and dried (magnesium sulfate). Solvent was removed *in vacuo* and the crude product purified by column chromatography (solid phase; silica, mobile phase; 1% TEA, DCM (dry), column dimensions; 1.5 × 5 cm). Fractions 3-6 (5 mL each) (TLC R_f = 0.55) were combined, solvent removed and dried under vacuum to yield purified product (387.4 mg, 0.74 mmol, 61%).

Physical state: colourless oil;

R_f = 0.55 (silica gel, 25:1:74 acetone:TEA:DCM);

MS (*m/z*): calcd for $C_{23}H_{45}N_2PO_9$, 464.17 [M$_{hydrolysed}$+Na]$^+$; found, 464.2; calcd, 547.28 [M+Na]$^+$; found, 547.3 (25%); calcd, 440.17 [M$_{hydrolysed}$-H]$^-$; found, 440.2;

^{1}H NMR (300 MHz, DMSO): δ 4.10 (t, 2H), 3.40-3.80 (m, 26H), 2.76 (t, 2H), 2.02 (s, 3H), 1.14 (d, 12H).

^{13}C NMR (75 MHz, DMSO): δ 170.3, 119.0, 70.5, 70.4, 69.8, 68.2, 63.1, 62.5, 62.2, 58.1, 42.4, 24.3, 19.7.

^{31}P NMR (120 MHz, DMSO): δ = 147.6

Assignment ^{1}H NMR: δ 4.10 (**CH$_2$**OCOMe), 3.40-3.80 (**CH$_2$**O, **CH**N), 2.76 (NC**CH$_2$**), 2.02 (CO$_2$**CH$_3$**), 1.14 (CH**CH$_3$**).

Assignment ^{13}C NMR: δ 170.3 (**C**O$_2$Me), 119.0 (**C**N), 70.5, 70.4, 69.8 (large), 68.2, 63.1, 62.5 & 62.2 (**C**H$_2$O), 58.1 (NCCH$_2$**C**H$_2$O), 42.4 (N**C**H(CH$_3$)$_2$), 24.3 (NCH(**C**H$_3$)$_2$), 19.7 (NC**C**H$_2$CH$_2$O).

6.31 Synthesis of monopropargyl hexaethylene glycol (88)
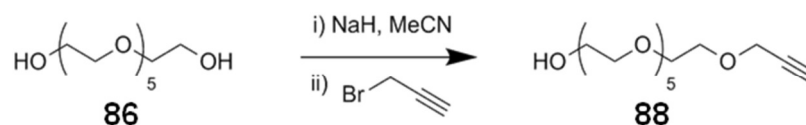
HEG (7.54 mL, 8.47 g, 30 mmol) was added to MeCN (70 mL) and stirred under nitrogen. Sodium hydride (0.29 g, 12 mmol) was added as a suspension in MeCN (10 mL) and the reaction stirred until all evolution of hydrogen gas had ceased. The solution was cooled over ice and propargyl bromide (0.95 g, 8 mmol) was added dropwise. The solution was allowed to warm to room temperature and the reaction was monitored by TLC (eluent; acetone:DCM 1:3, two product spots R_f = 0.2 & 0.45). After 1 hour, solvent was removed *in vacuo* and the product mixture dissolved in DCM (20 mL) then partitioned with a saturated solution of brine (20 mL). The aqueous phase was washed with DCM (3 × 15 mL) and the organic phases combined, dried (magnesium sulfate) and the solvent removed *in vacuo*. Products were purified by column chromatography (eluent; acetone:DCM, 1:3). The less polar product (TLC R_f = 0.45) was found to be the bis substituted product (by M.S.). monopropargyl hexaethylene glycol was isolated (1.41 g, 4.4 mmol, 55%).

Physical state: colourless oil;

R_f = 0.20 (silica gel, 1:3 acetone:DCM);

MS (*m/z*): calcd for $C_{15}H_{28}O_{12}$, 343.17 [M+Na]$^+$; found, 343.3;

^{1}H NMR (300 MHz, CDCl$_3$): δ 4.13 (d, 2H), 3.7 – 3.5 (m, 24H), 2.61 (t, <1H), 2.38 (t, 1H).

^{13}C NMR (75 MHz, CDCl$_3$): δ 79.7, 74.5, 72.5 – 58.4 (7 discernable peaks).

Assignment ^{1}H NMR: δ 4.13 (**CH$_2$**CCH), 3.7 – 3.5 (**CH$_2$**O), 2.61 (**OH**), 2.38 (CC**H**).

Assignment ^{13}C NMR: δ 79.7 (**C**CH), 74.5 (**C**CH), 72.5 – 58.4 (7 discernable peaks, **C**H$_2$O).

6.32 Synthesis of propargyl hexaethylene glycol phosphoramidite (53)
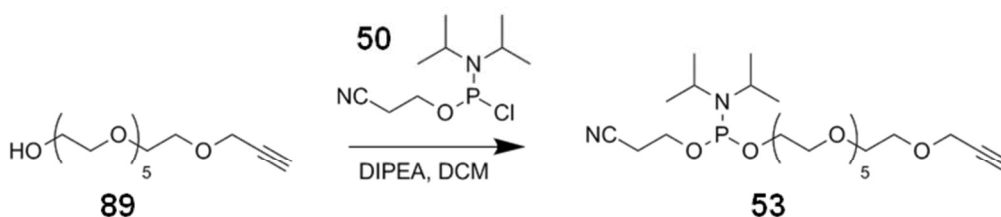
Monopropargyl HEG (480 mg, 1.5 mmol) was placed in a clean, dry 2-necked flask and dried *in vacuo* overnight. Distilled DCM (10 mL) and distilled DIPEA (0.65 mL, 0.48 g 3.7 mmol) were added via cannula and the solution stirred over ice and under nitrogen. Chlorophosphitylating reagent (0.44 g, 1.86 mmol) was added in one portion via cannula. The reaction was monitored by TLC (eluent; acetone:TEA:DCM, 25:1:75, silica plates were neutralised by dipping in TEA:DCM, 1:10 and drying prior to use, single product spot R_f = 0.6). After 40 minutes the solution was transferred to a nitrogen filled separating funnel and distilled DCM (10 mL) added. Degassed saturated KCl solution (20 mL) was added and the products partitioned, the organic phase was collected, dried (magnesium sulfate) and solvent was removed *in vacuo*. The product was quickly separated from unreacted reagent by column chromatography (eluent; TEA:DCM, 1:99), product containing fractions were combined and dried. Propargyl hexaethylene glycol phosphoramidite was isolated as a clear oil (0.54 g, 1.04 mmol, 69%).

Physical state: colourless oil;

R_f = 0.60 (silica gel, 25:1:75 acetone:TEA:DCM);

MS (*m/z*): calcd for $C_{24}H_{45}N_2PO_{13}$, 543.28 [M+Na]$^+$; found, 543.3;

^{1}H NMR (300 MHz, DMSO): δ 4.13 (d, H), 3.8 – 3.4 (m, 28H), 2.74 (t, 2H), 2.51 (t, 1H), 1.15 (d, 12H).

^{13}C NMR (75 MHz, DMSO): δ 119.0, 80.3, 77.0, 70.5 – 57.5 (14 peaks), 42.5, 24.3, 19.8.

Assignment ^{1}H NMR: δ 4.13, (OC**H**$_2$CCH), 3.8 – 3.4 (OC**H**$_2$, NC**H**(CH$_3$)$_2$), 2.74 (C**H**$_2$CN), 2.51 (OCH$_2$CC**H**), 1.15 (NCH(C**H**$_3$)$_2$).

Assignment ^{13}**C NMR**: δ 119.0 (**C**N), 80.3 (OCH$_2$**C**CH), 77.0 (OCH$_2$C**C**H), 70.5 – 57.5 (**C**H$_2$), 42.5 (N**C**H(CH$_3$)$_2$), 24.3 (NCH(**C**H$_3$)$_2$), 19.8 (**C**H$_2$CN).

6.33 Solution-phase avidin DN-FP1 association constant, k_{on}, determination

The protein-FP1 complex was quantified in solution by measuring the fluorescence polarisation (anisotropy) of the fluorescence signal from the Cy-5 label on **FP1**. For solution experiments, it was necessary to use an excess of unlabelled biotin in the reaction mixture, since solutions containing only **FP1** and avidin DN were found to undergo self-quenching upon binding, likely due to the proximity of four fluorophores to each other in the protein tetramer.[215]

The association of biotin and avidin was measured throughout a time course experiment and the resultant data analysed to determine the association rate constant, k_{on}. For the solution phase reaction this was achieved with real-time monitoring on a Tecan SafireII plate reader. At t$_0$ avidin DN (2.5 nM) was added to total biotin (biotin + **FP1**, 10 nM), mixed and anisotropy measurements swiftly initiated. Measurements were recorded until equilibrium had been obtained (< 30 min). Anisotropy was converted to concentration of protein-ligand complex on the assumption that there was no complex at t$_0$ and anisotropy at equilibrium represented complete complexation (10 nM).

6.34 Solution-phase avidin DN-FP1 dissociation constant, k_{off}, determination

Dissociation kinetics were obtained by monitoring the decrease in the fluorescence anisotropy of avidin DN-**FP1** complex (2 nM) in solution in the presence of a large excess of free biotin (200 nM) to perturb steady-state dynamics. Controls included avidin DN-**FP1** complex (2 nM) without free biotin (-ve control) and **FP1** (2 nM) (+ve control), data were recorded over a period of 19 days.

6.35 Conversion from particle fluorescence to concentration of particle-bound fluorophore

In order to determine thermodynamic and kinetic binding constants the measurements taken of particle fluorescence require conversion into measurements of the concentration of complexed **FP1**. As fluorescence is proportional to the concentration of complexed **FP1**, these values can be easily interconverted once the maximum binding (b_{max}) of the system is known, this value is the concentration of complex once all working active sites have been filled.

For on-particle measurements b_{max} can be obtained from the titration of **FP1** against avidin particles. Plotting particle fluorescence vs [**FP1**] gives a binding curve (Figure 82). Taking the tangent of the initial gradient (where [active sites] >> [**FP1**] and essentially all **FP1** can be assumed to be bound at equilibrium and fluorescent signal is linear with respect to increasing ligand) and projecting this up to the level of maximum fluorescence gives the b_{max} as read as the value at the intercept with the x-axis ([**FP1**]). Other examples of the use of this method for the determination of b_{max} have been published.[288,289]
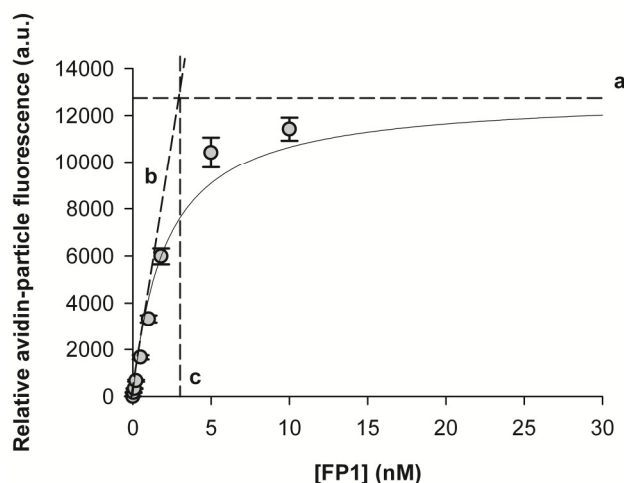
Figure 82. A diagram of titration results measuring the fluorescence of immobilized-avidin particles in increasing concentrations of FP1 ligand. b_{max} can be ascertained from this data by determining the intersect between the saturation fluorescence (a) and the tangent of the initial gradient (b), the concentration of FP1 at this point (c) is equal to b_{max}.

6.36 Particle-immobilised avidin DN-FP1 association constant, k_{on}, determination

The association of **FP1** and immobilised-avidin DN was measured throughout a time course experiment and the resultant data analysed to determine the association rate constant, k_{on}. Binding of FP1 (2 nM) to a suspension of protein-coated particles (1 mg mL^{-1}, 8.06 × 10^5 particles mL^{-1}, ~ 2 nM dependent on avidin immobilisation method used) was terminated at time-points (0-30 min) by the addition of an excess of biotin. Fluorescence microscopy was used to analyse particle samples, fluorescence values could then be converted to a measure of complexed ligand.

6.37 Particle-immobilised avidin DN-FP1 dissociation constant, k_{off}, determination

Dissociation kinetics were obtained by monitoring the decrease in fluorescence of particles with the complex immobilised when was exposed to an excess of biotin to impose effectively irreversible complex dissociation. Fluorescence could be converted into a measure of the proportion of filled binding sites where fluorescence at t_0 represented site saturation (100% complexation) whereas the fluorescence of particles not previously exposed to **FP1** represented complete dissociation (0%). Measurements were recorded over a period of 5 days.

6.38 Particle-immobilised avidin DN-FP1 equilibrium dissociation constant, K_d, determination

By titrating **FP1** (range = 0-100 nM) against particle-immobilised avidin DN (with working site concentrations of; Type I, 2.5 nM; Type II, 7.75 nM; Type III, 3.5 nM), total binding (at equilibrium) could be monitored as a function of particle fluorescence at equilibrium. Fluorescence values were converted to a concentration of protein-ligand complex and plotted against free ligand in order to determine equilibrium dissociation constants, K_d (Figures 19 & 34). These measured equilibrium dissociation constants were found to match the expected values as calculated from the experimentally determined rate constants (Equation 6).

6.39 Optimised multiplex hybridisation protocol

Assays involved suspension of oligonucleotide-functionalised microparticles in solutions of fluorescently labelled target DNA followed by quantification of individual particles' surface fluorescence intensities. Depending on the hybridisation conditions employed, wash steps were often found to be unnecessary.

A typical singleplexed assay as used to determine complementary hybridisation efficiency or the level of nonspecific DNA binding at varying surface densities of probe and blocking moieties would proceed as follows; probe particles (**69**) (2 µg) were suspended in SSPE (5×) buffer (200 µL) containing either complementary or noncomplementary Cy5-labelled target DNA (20 – 100 nM) and gently agitated for 2 hours at room temperature. Supernatant was removed and particles washed with buffer (2 × 200 µL). Particles were analysed by fluorescence microscopy and the fluorescence intensity of individual particles quantified using image processing software.

A typical multiplexed assay as used for the identification of target DNA proceeded as follows; a hybridisation array was formed by the mixing of different oligonucleotide probe-encoded microparticle conjugates (where particles of identical encoding had been functionalised with probes of the same base sequence, i.e. all type 1 (encoded) particles being functionalised with oligonucleotide **PJ**, those with Type 2 encoding functionalized with **PK**). This mixture of particles was suspended in SSPE (5×) buffer (200 µL) containing Cy5-labelled target DNA (20 nM) and gently agitated for 2 hours at elevated temperature. Supernatant was removed and particles resuspended in buffer, omitting any washing steps. Individual particles were analysed by fluorescence microscopy as previously and decoded using instrumentation and software developed in-house. Decoding allowed the identity of oligonucleotide probes immobilised on each particle to be determined.

7.0 Appendices

7.1 Appendix I: Graphical fitting and coefficient of determination for presented data, including that of kinetic and thermodynamic studies

Figure	Description of data set	Equation used	R^2
20a	Biphasic dissociation from Type I particles	Exponential decay, double	0.995
20a	Biphasic dissociation from Type II particles	Exponential decay, double	0.982
20a	Biphasic dissociation from Type III particles	Exponential decay, double	0.983
20b	Dissociation (Ln[complex] vs. time) fast (non-specific) Type I	Polynomial, linear	0.995
20b	Dissociation (Ln[complex] vs. time) slow (specific) Type I	Polynomial, linear	0.991
20c	Dissociation (Ln[complex] vs. time) fast (non-specific) Type II	Polynomial, linear	0.999
20c	Dissociation (Ln[complex] vs. time) slow (specific) Type II	Polynomial, linear	0.799
20d	Dissociation (Ln[complex] vs. time) fast (non-specific) Type III	Polynomial, linear	0.934
20d	Dissociation (Ln[complex] vs. time) slow (specific) Type III	Polynomial, linear	0.881
23	Non-specific FP1 binding vs. [Tween-20 surfactant]	Exponential decay, double	0.999
23	Specific FP1 binding vs. [Tween-20 surfactant]	Polynomial, linear	0.971
24	Stability of the specific immobilised complex (fluorescence) vs. time	Polynomial, linear	0.599
27 & 32	Association ([complex] vs. time) in solution	Exponential rise to maximum, single	0.925
27 & 32	Association ([uncomplexed]$^{-1}$ vs. time) in solution	Polynomial, linear	0.943
32	Association ([complex] vs. time) on Type I particles	Exponential rise to maximum, single	0.991
32	Association ([complex] vs. time) on Type II particles	Exponential rise to maximum, single	0.993
32	Association ([complex] vs. time) on Type III particles	Exponential rise to maximum, single	0.989
32	Association ([uncomplexed]$^{-1}$ vs. time) on Type I particles	Polynomial, linear	0.988
32	Association ([uncomplexed]$^{-1}$ vs. time) on Type II particles	Polynomial, linear	0.987
32	Association ([uncomplexed]$^{-1}$ vs. time) on Type III particles	Polynomial, linear	0.953
28 & 33	Dissociation (% complex vs. time) in solution	Exponential decay, single	0.955
33	Dissociation (% complex vs. time) on Type I particles	Exponential decay, single	0.972

Figure	Description of data set	Equation used	R^2
33	Dissociation (% complex vs. time) on Type II particles	Exponential decay, single	0.939
33	Dissociation (% complex vs. time) on Type III particles	Exponential decay, single	0.980
28 & 33	Dissociation (Ln[complex] vs. time) in solution	Polynomial, linear	0.951
33	Dissociation (Ln[complex] vs. time) on Type I particles	Polynomial, linear	0.956
33	Dissociation (Ln[complex] vs. time) on Type II particles	Polynomial, linear	0.920
33	Dissociation (Ln[complex] vs. time) on Type III particles	Polynomial, linear	0.979
34	Binding titration ([complexed] vs. [free]) on Type I particles	Ligand binding, one site saturation	0.985
34	Binding titration ([complexed] vs. [free]) on Type II particles	Ligand binding, one site saturation	0.987
34	Binding titration ([complexed] vs. [free]) on Type III particles	Ligand binding, one site saturation	0.993
42	Probe migration t = 0 min	Gaussian, multipeaks fit	0.961
42	Probe migration t = 143 min	Gaussian, multipeaks fit	0.992
42	Probe migration t = 1114 min	Gaussian, multipeaks fit	0.998

7.2 Appendix II: Oligonucleotide sequences

Name	5' modification	3' modification	Sequence (5' to 3')
FP1	Cy-5	biotin	CTA GTT ACT CTT GTT C
FP2	Cy-5	amine	GAG ATG CAC TCG AGT AAG TCA AGT CG
O1	–	–	CCA TCG ACT TGA CTT ACT CGA GTG CAT CTC
T1	Alexa	–	GCA ACT AAA TTC A
P2	amine	–	GAG ATG CAC TCG AGT AAG TCA AGT CG
T2	Cy-5	–	CCA TCG ACT TGA CTT ACT CGA GTG CAT CTC
T3	Cy-5	–	TTT CTT GAT CAC TCC ACT GTT C
PA	biotin	–	TTG TTA TAG TTC TCT C
TA	Cy-5	–	GAG AGA ACT ATA ACA A
PB	biotin	–	CTA GTT ACT CTT GTT C
TB	Cy-5	–	GAA CAA GAG TAA CTA G
O2	–	–	TTT CTT GAT CAC TCC ACT GTT C
PC	biotin	–	AAA AAC TTG GAT CC
TC	Cy-5	–	GGG ATC CAA GTT TTT T
PD	biotin	–	AAA AAG TTG GAT CC
TD	Cy-3	–	GGG ATC CAA CTT TTT T
PE	biotin	–	CAA CCC CAG CTA ATA TTA TT
TE	Cy-5	–	AAT AAT ATT AGC TGG GGT TG
PF	amine	–	AAA AAC TTG GAT CC
PG	amine	–	AAA AAG TTG GAT CC
TG	Cy-5	–	GGG ATC CAA CTT TTT T
PH	amine	–	CAA CCC CAG TTA ATA TTA TT
TH	Cy-5	–	AAT AAT ATT AAC TGG GGT TG
PI	amine	–	CAA CCC CAG GTA ATA TTA TT
TI	Cy-5	–	AAT AAT ATT ACC TGG GGT TG
PJ	azide	–	AAA AAG TTG GAT CC
PK	azide	–	CAA CCC CAG TTA ATA TTA TT
PL	azide	–	CAA CCC CAG GTA ATA TTA TT
PM	azide	–	GAG ATG CAC TCG AGT AAG TCA AGT CG

7.3 Appendix III: Buffer solutions

Buffer	Constituents
imidazole	Imidazole (0.1 M)
SSPE (20×)	NaCl (3.0 M), NaH$_2$PO$_4$ (200 mM), EDTA (20 mM)
SSPE (5×)	NaCl (0.75 M), NaH$_2$PO$_4$ (50 mM), EDTA (5 mM)
MES	MES (0.1 M), NaCl (0.5 M)
PBS	NaCl (0.14 M), KCl (2.7 mM), Na$_2$HPO$_4$ (10 mM), KH$_2$PO$_4$ (2 mM)

8.0 References

Note: *et al* is used for the purposes of conciseness when referring to a manuscript authored by greater than 7 individuals.

[1] Lander, E.S., *et al. Nature.* **2001**, *409*, 860.

[2] Service, R. F. *Science* **2006**, *311*, 1544.

[3] http://www.cng.fr/READNA

[4] http://www.genomics.xprize.org

[5] Fiers, W. *et al. Nature*. **1976**, *260*, 500.

[6] Fleischmann, R. D. *et al. Science.* **1995**, *269*, 496.

[7] http://www.genomenewsnetwork.org

[8] International Human Genome Sequencing Consortium. *Nature*, **2004**, *431*, 931.

[9] Gregory, S. G., *et al. Nature.* **2006**, *441*, 315.

[10] Kidd, J. M., *et al. Nature.* **2008**, *453*, 56.

[11] James, P. *Q. Rev. Biophys.* **1997**, *30*, 279.

[12] Dhingraa, V., Gupta, M., Andacht, T., Fu, Z. F. *Int. J. Pharm.* **2005**, *299*, 1.

[13] Wolfsberg, T., McEntyre, J., Schuler, G. *Nature.* **2001**, *409*, 824.

[14] Xavier, R. J., Rioux, J. D. *Nat. Rev. Immunol.* **2008**, *8*, 631.

[15] Altshuler, D., Daly, M. J., Lander, E. S. *Science.* **2008**, *322*, 881.

[16] Pillai, S. G., *et al. Plos. Genet.* **2009**, *5*, e1000421.

[17] Coronary Artery Disease Consortium. *Arterioscler. Thromb. Vasc. Biol.* **2009**, *29*, 774.

[18] Kouduka, M. *et al. Int. J. Plant Genomics*. **2007**, *2007*, 27894.

[19] Gozua, H. I., Lublinghoff, J., Bircan, R., Paschke, R. *Mol. Cell. Endocrinol.* **2010**, *322*, 125.

[20] Walker, F. O. *Lancet* **2007**, *369*, 218.

[21] Bobadilla, J. L., Macek, M., Fine, J. P., Farrell, P. M. *Hum. Mutat.* **2002**, *19*, 575.

[22] http://www.ncbi.nlm.nih.gov/mapview

[23] Deloukas, P., *et al. Science*. **1998**, *282*, 744.

[24] GeneTests: Medical Genetics Information Resource (database online). Copyright, University of Washington, Seattle. **1993-2010**. Available at http://www.genetests.org

[25] Dong, L. M., Potter, J. D., White, E., Ulrich, C. M., Cardon, L. R., Peters, U. *JAMA-J. Am. Med. Assoc.* **2008**, *299*, 2423.

[26] Kuliev, A., Verlinsky, Y. *Am. J. Med. Genet.* **2005**, *134A*, 105.

[27] Poulton, J., Chiaratti, M. R., Meirelles, F. V., Kennedy, S., Wells, D., Holt, I. J. *Plos. Genet.* **2010**, *6*, e1001066.

[28] Van't Veer, L. J., Bernards, R. *Nature.* **2008**, *452*, 564.

[29] Mansour, J. C., Schwarz, R. E. *J. Am. Coll. Surg.* **2008**, *207*, 250.

[30] Lee, P.S., Lee, K.H. *Curr. Opin. Biotechnol.* **2000**, *11*, 171.

[31] Hubank, M., *Brit. J. Haematol.* **2004**, *124*, 577.

[32] Bhattacharya, S., Mariani, T. J. *Biochem. Soc. Trans.* **2009**, *37*, 855.

[33] Chen, X., Jorgenson, E., Cheung, S. T. *Drug Discov. Today*. **2019**, *14*, 754.

[34] Kramer, R., Cohen, D. *Nat. Rev. Drug. Discov*. **2004**, *3*, 965.

[35] Ferrer-Alcón, M., Arteta, D., Guerrero, M. J., Fernandez-Orth, D., Simón, L., Martinez, A. *Toxicol. Lett. 2009*, *186*, 45.

[36] Allison, D. W., Aboytes, K. A., Fong, D. K., Leugers, S. L., Johnson, T. K., Loke, H. N., Donahue, L. M. *Bioprocess Int.* **2005**, *3*, 38.

[37] Eszlinger, M., Krohn, K., Kukulska, A., Jarzab, B., Paschke, R. *Endocr. Rev.* **2007**, *28*, 322.

[38] Marchionni, L., Wilson, R. F., Wolff, A. C., Marinopoulos, S., Parmigiani, G., Bass, E. B., Goodman, S. N. *Ann. Intern. Med.* **2008**, *148*, 358.

[39] Gupta, P., Lee, K. H. *Trends. Biotechnol.* **2007**, *25*, 324.

[40] Onyango, P. *Curr. Can. Drug Targ.* **2004**, *4*, 111.

[41] Letunic, I., Bork, P. *Bioinformatics.* **2006**, *23*, 127.

[42] Gibson, G. *Mol. Ecol.* **2002**, *11*, 17.

[43] Woese, C. R. *et al. Nature*. **1975**, *254*, 83.

[44] Fox, G. W., Woese, C. R. Nature. **1975**, *256*, 505.

[45] Woese, C. R., Fox, G. E. *PNAS.* **1977**, *74*, 5088.

[46] Hinchliffe, S. J. *et al*. *Genome Res*. **2003**, *13*, 2018.

[47] Litrup, E., Torpdahl, M., Malorny, B., Huehn, S., Helms, M., Christensen, H., Nielsen, E. M. *BMC. Microbiol.* **2010**, *10*, 96.

[48] Harris, S. R., *et al. Science.* **2010**, *327*, 469.

[49] Weber, J. L., Wong, C. *Hum. Mol. Genet.* **1993**, *2*, 1123.

[50] Hammond, H. A., Jin, L., Zhong, Y., Caskey, C. T., Chakraborty, R. *Am. J. Hum. Genet.* **1994**, *55*, 175.

[51] Budowle, B., Moretti, T. R. *Forensic Sci. Commun. 1999*, *1*, 2.

[52] Lynch, M. *Endevour*. **2003**, *27*, 93.

[53] http://www.ornl.gov/sci/techresources/Human_Genome/research/elsi

[54] Wadman, M. *Nature*. **2008**, *453*, 9.

[55] Golden, J. M. *Emory Law Journal.* **2001**, *50*, 101.

[56] Editorial. *Nature*. **2010**, *464*, 957.

[57] Hardiman, G. *Pharmacogenomics*. **2008**, *9*, 5.

[58] Dharia, N. V., *et al. PNAS.* **2010**, *16*, 20045.

[59] Molecular Cloning a Laboratory Manual. Sambrook, J., Russell, D. W. *Cold Spring Harbor Laboratory Press*. **2001**.

[60] PCR Protocols: A Guide to Methods and Applications. Innis, M. A., Gelfand, D. H., Sninsky, J. J., White, T. J. eds. *Acedemic Press, Inc*. **1990**.

[61] Staden, R. *Nucleic Acids Res.***1979**, *6*, 2601.

[62] Anderson, S. *Nucleic Acids Res.* **1981**, *9*, 3015.

[63] Delcher, A. L., Kasif, S., Fleischmann, R. D., Peterson, J., White, O., Salzberg, S. L. *Nucleic Acids Res.* **1999**, *27*, 2369.

[64] Couronne, O. *et al. Genome Res.* **2003**, *13*, 73.

[65] Fortina, P., Surrey, S., Kricka, L. J. *TRENDS Mol. Med*. **2002**, *8*, 264.

[66] Yager, P., Domingo, G. J., Gerdes, J. *Annu. Rev. Biomed. Eng*. **2008**, *10*, 107.

[67] Sanger, F., Nicklen, S., Coulson, A. R. *PNAS.* **1977**, *74*, 5463.

[68] Smith, L. M. *et al*. *Nature.* **1986**, *321*, 674.

[69] Ju, J., Kheterpal, I., Scherer, J. R., Ruan, C., Fuller, C. W., Glazer, A. N., Mathies, R.A. *Anal. Biochem*. **1995**, *231*, 131.

[70] Lauer, H. H., McManigill, D. *Anal. Chem*. **1986**, *58*, 166.

[71] Cohen, A. S.,Najarian, D. R., Paulus, A., Guttman, A., Smith, J. A., Karger, B. L. *PNAS.* **1988**, *85*, 9660.

[72] Shibata, K., Itoh, M., Aizawa, K. *Genome Res.* **2000**, *10*, 1757.

[73] Dovichi, N. J. *Chem*. *Eng. News: Lett.* **2000**, *78*, 10.

[74] Bentley, D. R. *Curr. Opin. Genet. Dev*. **2006**, *16*, 545.

[75] Ronaghi, M., Karamohamed, S., Pettersson, B., Uhlen, M., Nyren, P. *Anal. Biochem.* **1996**, *242*, 84.

[76] Ronaghi, M., Uhlen, M., Nyren, P. *Science.* **1998**, *281*, 363.

[77] Ronaghi, M. *Genome Res*. **2001**, *11*, 3.

[78] Ronaghi, M. *Anal*. *Biochem*. **2000**, *286*, 282.

[79] Patrick, K, L. *Yale J. Biol. Med*. **2007**, *80*, 191.

[80] Rothberg, J. M., Leamon, J. H. *Nat. Biotechnol*. **2008**, *26*, 1117.

[81] Mardis, E. R. *Annu. Rev. Genom. Human Genet*. **2008**, *9*, 387.

[82] Venter, J. C., Adams, M. D., Sutton, G. G., Kerlavage, A. R., Smith, H. O., Hunkapiller, M. *Science.* **1998**, *280*, 1540.

[83] Kaiser, R. J., MacKellar, S. L., Vinayak, R. S., Sanders, J. Z., Saavedra, R. A., Hood, L. E. *Nucleic Acids Res*. **1989**, *17*, 6087.

[84] Kulesh, D. A., Clive, D. R., Zarlenga, D. S., Greene, J. J. *PNAS*. **1987**, *84*, 8453.

[85] Schena, M., Shalon, D., Davis, R. W., Brown, P. O. *Science*. **1995**, *270*, 467.

[86] Lashkari, D. A. *et al. PNAS*. **1997**, *94*, 13057.

[87] Whiteford, N. *et al*. *Nucleic Acids Res.* **2005,** *33*, e171.

[88] Relogio, A., Schwager, C., Richter, A., Ansorge, W., Valcarcel, J. *Nucleic Acids Res*. **2002**, *30*, e51.

[89] Miyazaki, K. *et al*. *Blood*. **2009**, *113*, 1071.

[90] Wong, N. *et al*. *Int. J. Cancer*, **2009**, *124*, 644.

[91] Palka-Santini, M., Cleven, B., Eichinger, L., Kronke, M., Krut, O. *BMC. Microbiol*. **2009**, *9*, 1.

[92] Shen, Y., Wu, B. *Clin. Chem*. **2009**, *55*, 659.

[93] Situma, C., Hashimoto, M., Soper, S. A. *Biomol. Eng*. **2006**, *23*, 213.

[94] Angenendt, P. *Drug Discov. Today.* **2005**, *10*, 503.

[95] Marti, G. E., Gaigalas, A., Vogt, R. F. *Cytometry*. **2000**, *42*, 263.

[96] Battaglia, C., Salani, G., Consolandi, C., Bernardi, L. R., DeBellis, G. *Biotechniques*. **2000**, *29*, 78.

[97] Drummond, T. G., Hill, M. G., Barton, J. K. *Nat. Biotech*. **2003**, *21*, 1192.

[98] Ramachandran, N., Larson, D. N., Stark, P. R. H., Hainsworth, E., LaBaer, J., *FEBS J*. **2005**, *272*, 5412.

[99] Koehne, J. E., Chen, H., Cassell, A. M., Ye, Q., Han, J., Meyyappan, M., Li, J. *Clin. Chem*. **2004**, *50*, 1886.

[100] Gao, Z. *et al. Anal. Chem*. **2007**, *79*, 3291.

[101] Zhang, G., Chua, J. H., Chee, R., Agarwal, A., Wong, S. M. *Biosens. Bioelectron.* **2009**, *24*, 2504.

[102] Wu, C., Ko, F., Yang, Y., Hsia, D., Lee, B., Su, T. *Biosens. Bioelectron.* **2009**, *25*, 820.

[103] Pang, S., Smith, J., Onley, D., Reeve, J., Walker, M., Foy, C. *J. Immunol. Methods*. **2005**, *302*, 253.

[104] Epstein, J.R., Biran, I., Walt, D. R. *Anal. Chim. Acta*. **2002**, *469*, 3.

[105] Nolan, J. P., Sklar, L. A. *Trends. Biotechnol*. **2002**, *20*, 9.

[106] Nolan, J. P., Mandy, F. *Cytom. A.* **2006**, *69*, 318.

[107] Wallace, J., Woda, B. A., Pihan, G. *J. Mol. Diagn*. **2005**, *7*, 72.

[108] Pappaert, K., Desmet, G. *J. Biotechnol*. 2006, 123, 381.

[109] Burden, C. J., Binder, H. *Phys. Biol*. **2010**, *7*, 016004.

[110] Kim, J. H., Marafie, A., Jia, X., Zoval, J. V., Madou, M. J. *Sens. Actuators, B*. **2006**, *113*, 281.

[111] Birtwell, S. W., Morgan, H. *Integr. Biol*. **2009**, *1*, 345.

[112] Cederquist, K. B., Dean, S. L., Keating, C. D. *Nanomed. Nanobiotechnol.* **2010**, 2*, 578.*

[113] Pregibon, D. C., Toner, M., Doyle, P. S. *Science.* **2007**, *315.* 1393.

[114] http://www.luminexcorp.com

[115] Mahony, J. B., Chong, S., Luinstra, K., Petrich, A., Smieja, A. *J. Clin. Virol*. **2010**, *49*, 277.

[116] Stevens, P. W., Wang, C. H. J., Kelso, D. M. *Anal. Chem*. **2003**, *75*, 1141.

[117] Kleppe, K., Ohtsuka, E., Kleppe, R., Molineux, I., Khorana, H. G. *J. Mol. Biol*. **1971**, *56*, 341.

[118] Saiki, R., Scharf, S., Faloona, F., Mullis, K., Horn, G., Erlich, H. *Science* **1985**, *230*, 1350.

[119] Mullis, K., Faloona, F. *Methods Enzymol*. **1987**, *155*, 335.

[120] Saiki, R. *et al. Science.* **1988**, *239*, 487.

[121] Innis, M. A., Myambo, K. B., Gelfand, D. H., Brow, M. A. *PNAS.* **1988**, *85*, 9436.

[122] Seo, T. S., Li, Z., Ruparel, H., Ju. J. *J. Org. Chem.* **2003**, *68* , 609.

[123] Celeda, D., Bettag, U., Cremer, C. *Biotechniques*. **1992**, *12*, 98.

[124] Ried, T., Baldin, A., Rand, T. C., Ward, D. C. *PNAS*. **1992**, *89*, 1388.

[125] Gierlich, J., Burley, G. A., Gramlich, P. M. E., Hammond, D. M., Carell, T. *Org. Lett.*, **2006**, *8*, 3639.

[126] Klenow, H., Henningsen, I. *PNAS.* **1970**, *65*, 168.

[127] Iwahana, H., Adzuma, K., Takahashi, Y., Katashima, R., Yoshimo, K., Itakura, M. *PCR Methods Applic.* **1995**, *4*, 275.

[128] Inazuka, M., Tahira, T., Hayashi, K. *Genome Res*. **1996**, *6*, 551.

[129] Pastinen, T., Raitio, M., Lindroos, K. *Genome Res.* **2000**, *10*, 1031.

[130] Gheit, T. *et al. J. Clin. Microbio*. **2006**, *44*, 2025.

[131] O'Meara, D., Ahmadian, A., Odeberg, J., Lundeberg, J. *Nucleic Acids Res.* **2002**, *30*, e75.

[132] Wang, X., Krull, U. J. *Anal. Chim. Acta*. **2002**, *470*, 57.

[133] Kohler, O., Jarikote, D. V., Seitz, O. *Chembiochem*. **2005**, *6*, 69.

[134] Tyagi, S., Kramer, F. R. *Nat. Biotechnol*. **1996**, *14*, 303.

[135] Tan, W. H., Wang, K. M., Drake, T. J. *Curr. Opin. Chem. Biol*. **2004**, *8*, 547.

[136] McBride, L. J., Caruthers, M. H. *Tetrahedron Lett.* **1983**, *24*, 245.

[137] Beaucage, S. L., Iyer, R. P. *Tetrahedron*. **1992**, *48*, 2223.

[138] Reese, C. B. *Org. Biomol. Chem.* **2005**, *3*, 3851.

[139] Temsamani, J., Kubert, M., Agrawal, S. *Nucleic Acids Res*. **1995**, *23*, 1841.

[140] Hecker, K.H., Rill, R. L. *Biotechniques*, **1998**, *24*, 256.

[141] Iyer, R. P., Egan, W., Regan, J. B., Beaucage, S. L. *J. Am. Chem. Soc.* **1990,** *112*, 1254.

[142] Nielsen, P. E., Egholm, M., Berg, R. H., Buchardt, O. *Science*, **1991**, *254*, 1497.

[143] Pellestor, F., Paulasova, P. *Chromosoma.* **2004**, *112*, 375.

[144] Nielsen, P. E., Egholm, M. *Curr. Issues Mol. Biol*. **1999**, *1*, 89.

[145] Lam, K. S., Salmon, S. E., Hersh, E. M., Hruby, V. J., Kazmierski, W. M., Knapp, R. J. *Nature*. **1991**, *354*, 82.

[146] Furka, A., Sebestyen, F., Asgedom, M., Dibo, G. *Int. J. Pept. Protein Res*. **1991**, *37*, 487.

[147] Battersby, B. J., Lawrie, G. A., Johnston, A. P. R., Trau, M. *Chem. Commun.*, **2002**, *14*, 1435.

[148] Meldal, M., Christensen, S. F. *Angew. Chem*. **2010**, *122*, 3551.

[149] Peluso, P. *et al*. *Anal. Biochem*. **2003**, *312*, 113.

[150] Singh, M., Briones, M., Ott, G., O'Hagan, D. *PNAS.* **2000**, *97*, 811.

[151] Yamaguchi, S., Shimomura, T. *Anal. Chem.* **1993**, *65,* 1925.

[152] Ezaki, T., Hashimoto, Y., Yabuuchi, E. *Int. J. Syst. Bacteriol.* **1989**, *39*, 224.

[153] Melzak, K. A., Sherwood, C. S., Turner, R. F. B., Haynes, C. A. *J. Colloid Interf. Sci*. **1996**, *181*, 635.

[154] Zammatteo, N., Jeanmart, L., Hamels, S., Courtois, S., Louette, P., Hevesi, L., Remacle, J. *Anal. Biochem*. **2000**, *280*, 143.

[155] Chan, V., Graves, D. J., Fortina, P., McKenzie, S. E. *Langmuir.* **1997**, *13,* 320.

[156] Okahata, Y., Kobayashi, T., Tanaka, K. *Langmuir.* **1996**, *12,* 1326.

[157] Voller, A., Bartlett, A., Bidwell, D. E. *J. Clin. Pathol*. **1978**, *31*, 507.

[158] Elia, G., Silacci, M., Scheurer, S., Scheuermann, J., Neri, D. *Trends Biotechnol.* **2002**, *20*, S19.

[159] Verkaik, N., Brouwer, E., Hooijkaas, H., Van Belkum, A., Van Wamel, W. *J. Immunol. Methods.* **2008**, *335*, 121.

[160] Lauer, S. A., Nolan, J. P. *Cytometry.* **2002**, *48*, 136.

[161] Forsgren, A., Sjöquist, J. *J. Immunol.* **1966**, *97*, 822.

[162] Green, N. M. *Methods Enzymol.* **1990**, *184*, 51.

[163] Wilchek, M., Bayer, E. A. *Anal. Biochem.* **1988**, *171*, 1.

[164] Green, N. M. *Biochem. J.* **1963**, *89*, 585.

[165] Green, N. M. *Avd. Protein Chem*. **1975**, *29*, 85.

[166] Gonzalez, M., Argarana, C. E., Fidelio, G. D. *Biomol. Eng.* **1999**, *16*, 67.

[167] Shao, W., Zhang, X., Liu, H., Zhang, Z. *Bioconjugate Chem.* **2000**, *11*, 822.

[168] Lesaicherre, M., Uttamchandani, M., Chen, G. Y. J., Yao, S. Q. *Bioorg. Med. Chem. Lett*. **2002**, *12*, 2079.

[169] Caruso, F., Rodda, E., Furlong, D. N. *Anal. Chem.* **1997,** *69*, 2043.

[170] Vermette, P., Gengenbach, T., Divisekera, U., Kambouris, P. A., Griesser, H. J., Meagher, L. *J. Colloid Interf. Sci.* **2003**, *259*, 13.

[171] Boncheva, M., Scheibler, L., Lincoln, P., Vogel, H., Akerman, B. *Langmuir.* **1999,** *15,* 4317.

[172] Steinberg, G., Stromsborg, K., Thomas, L., Barker, D., Zhao, C. *Biopolymer.* **2004**, *73*, 597.

[173] Rusmini, F., Zhong, Z., Feijen, J. *Biomacromolecules.* **2007**, *8*, 1775.

[174] Wong, L. S., Khan, F., Micklefield, J. *Chem. Rev.* **2009**, *109*, 4025.

[175] Liu, J., Cao, Z., Lu, Y. *Chem. Rev.* **2009**, *109*, 1948.

[176] Li, P., Medon, P. P., Skingle, D. C., Lanser, J. A., Symons, R. H. *Nucleic Acids Res.* **1987**, *15*, 5275.

[177] Ghosh, S. S., Kao, P. M., McCue, A. W., Chappelle, H. L. *Bioconjugate Chem.* **1990**, *1*, 71.

[178] Kim, Y., Ho, S. O., Gassman, N. R., Korlann, Y., Landorf, E. V., Collart, F. R., Weiss, S. *Bioconjugate Chem*. **2008**, *19*, 786.

[179] Lin, D., Saleh, S., Liebler, D. C., *Chem. Res. Toxicol.* **2008**, *21*, 2361.

[180] Borges, C. R., Watson, J. T. *Protein Sci.* **2003**, *12*, 1567.

[181] Johnson, S. L. Advances in physical organic chemistry, Vol 5. *Academic Press, Inc*. **1967**, 237-325.

[182] Banks, P. R., Paquette, D. M*. Bioconjugate Chem.* **1995**, *6*, 447.

[183] Lefevre, C., Kang, H. C., Haugland, R. P., Malekzadeh, N., Arttamangkul, S., Haugland, R. P. *Bioconjugate Chem.* **1996**, *7*, 482.

[184] Seiler, N. *Methods Biochem. Anal.* **1970**, *18*, 259.

[185] Huisgen, R. *Angew. Chem. int. Ed*. **1963**, *2*, 565.

[186] Rostovtsev, V. V., Green, L. G., Fokin, V. V., Sharpless, K. B. *Angew. Chem. Int. Ed.* **2002**, *41*, 2596.

[187] Zhu, X. Y. *et al*. *Langmuir.* **2001**, *17*, 7798.

[188] Jeon, S. I., Lee, J. H., Andrade, J. D., Degennes, P. G. *J. Colloid Interface Sci.* **1991**, *142*, 149.

[189] Dolan, P. L., Wu, Y., Ista, L. K., Metzenberg, R. L., Nelson, M. A., Lopez, G. P. *Nucleic Acids Res.* **2001**, *29*, e107.

[190] Benters, R., Niemeyer1, C. M., Drutschmann, D., Blohm, D., Wöhrle, D. *Nucleic Acids Res.* **2002**, *30*, e10.

[191] Cavalli, G. *et al*. *J. Comb. Chem.* **2007**, *9*, 462.

[192] Weber, G., Haslam, N., Whiteford, N., Prugel-Bennett, A., Essex, J. W., Neylon, C. *Nat. phys*. **2006**, *2*, 55.

[193] Weber, G., Haslam, N., Essex, J. W., Neylon, C. *J. Phys. Condens. Matter.* **2009**, *21*, 1.

[194] Rudd, K. E. *Nucleic Acids Res*. **2000**, *28*, 60.

[195] Lorenz, H., Despont, M., Fahrni, M., LaBianca, N., Vettiger, P., Renaud, P. *J. Micromech. Microeng.* **1997**, *7*, 121.

[196] Banu, S., Birtwell, S. W., Galitonov, G., Chen, Y., Zheludev, N., Morgan, H. *J. Micromech. Microeng*. **2007**, *17*, S116.

[197] Galitonov, G. S., Birtwell, S. W., Zheludev, N. I., Morgan, H. *Opt. Express.* **2006**, *14*, 1382.

[198] Birtwell, S. W., Galitonov, G. S., Morgan, H., Zheludev, N. I. *Opt. Commun.* **2008**, *281*, 1789.

[199] Birtwell, S. W., Banu, S., Zheludev, N. I., Morgan, H. *J. Phys. D: Appl. Phys.* **2009**, 42, 055507.

[200] Elshal, M. F., McCoy, J. P. *Methods*. **2006**, *38*, 317.

[201] Broder, G. R. *et al. Anal. Chem*. **2008,** *80*, 1902.

[202] Herzenberg, L. A., Herzenberg, L. A. Handbook of Experimental Immunology, 3rd Ed. *Blackwell Scientific Publications, Ltd*. **1978**, 22.1-22.21.

[203] Baumgarth, N., Roederer, M. *J. Immunol. Methods*. **2000**, *243*, 77.

[204] Yuste, R. *Nat. Methods*. **2005**, *2*, 902.

[205] Davis, C. B., Shamansky, L. M., Rosenwald, S., Stuart, J. K., Kuhr, W. G., Brazill, S. A. *Biosens. Bioelectron*. **2003**, *18*, 1299.

[206] Djelloulia, N., Rochelet-Dequaire, M., Limogesb, B., Druetb, M., Brossier, P. *Biosens. Bioelectron*. **2007**, *22*, 2906.

[207] http://vectorlabs.com

[208] Smith, P.K. *et al. Anal. Biochem., 1985, 150, 76.*

[209] Wiechelman, K., Braun, R., Fitzpatrick, J. *Anal. Biochem.* **1988***, 175, 231.*

[210] Pugliese, L., Coda, A., Malcovati, M., Bolognesi, M. *J. Mol. Biol*. **1993**, *231*, 698.

[211] Aboul-ela, F., Koh, D., Tinoco, I. *Nucleic Acids Res*. **1985**, *13*, 4811.

[212] Werntges, H., Steger, G., Riesner, D., Fritz, H. *Nucleic Acids Res.* **1986**, *14*, 3773.

[213] Gaffney, B. L., Jones, R. A. *Biochemistry.* **1989**, *28*, 5881.

[214] Ke, S., Wartell, R. M. *Nucleic Acids Res.* **1993**, *21*, 5137.

[215] West, W., Pearce, S. *J. Phys. Chem.* **1965**, *69*, 1984.

[216] http://www.vectorlabs.com

[217] Squires, T. M., Messinger, R. J., Manalis, S. R. *Nat. Biotechnol*. **2008**, *26*, 417.

[218] Chignell, C. F., Starkweather, D. K., Sinha, B. K. *J. Biol. Chem.* **1975**, *250*, 5622.

[219] Garlick, R. K., Giese, R. W. *J. Biol. Chem.* **1988**, *263*, 210.

[220] Schwarz, A., Rossier, J. S., Roulet, E., Mermod, N., Roberts, M. A., Girault, H. H. *Langmuir.* **1998,** *14,* 5526.

[221] Smoluchowski, M. V. *Z. Phys. Chem.* **1917**, *92*, 129.

[222] Meiser, F. *Angew. Chem. Int. Ed*. **2004**, *43*, 5954.

[223] Wu, Y. C. *J. Phys. Chem.* **1968**, *72*, 2663.

[224] Zhang, C. Y. *Analyst.* **2006**, *131*, 484.

[225] Astumian, R. D. *J. Am. Chem. Soc.* **1984**, *106*, 304.

[226] Northrup, S. H., Erickson, H. *PNAS.* **1992**, *89*, 3338.

[227] Green, N. M. *Biochem. J.* **1963**, *89*, 599.

[228] Livnah, O., Bayer, E. A., Wilchek, M., Sussman, J. L. *PNAS*. **1993**, *90,* 5076.

[229] Atkins, P. *The Elements of Physical Chemistry 3rd Ed.* **2001**, Oxford University Press.

[230] Mujumdar, R. B., Ernst, L. A., Mujumdar, S. R., Lewis, C. J., Waggoner, A. S. *Bioconjugate Chem*. **1993**, *4*, 105.

[231] Fureder-Kitzmuller, E., Hesse, J., Ebner, A., Gruber, H. J., Schutz, G. J., *Chem. Phys. Lett.* **2005**, *404*, 13.

[232] Foote, C. S. *Science.* **1968**, *162*, 963.

[233] Byers, G. W., Gross, S., Henrichs, P. M. *Photochem. Photobiol.* **1976**, *23*, 37.

[234] Wong, A. L. *J. Phys. Chem.* **1991**, *95*, 4489.

[235] Wayment, J. R., Harris, J. M. *Anal. Chem.* **2009,** *81,* 336.

[236] Zhao, S., Reichert, W. M. *Langmuir.* **1992**, *8*, 2785.

[237] Polzius, R., Dießel, E., Bier, F. F., Bilitewski., U. *Anal. Biochem.* **1997**, *248*, 269.

[238] Green, N. M., Toms, E. J. *Biochem. J.* **1973**, *133*, 687.

[239] Marek, M., Kaiser, K., Gruber, H. J. *Bioconjugate Chem*. **1997**, *8*, 560.

[240] Ateya, D. A., Erickson, J. S., Howell, P. B., Hilliard, L .R., Golden, J. P., Ligler, F. S. *Anal. Bioanal. Chem*. **2008**, *391*, 1485.

[241] Chang, C. C., Huang, Z. X., Yang, R. J. *J. Micromech. Microeng.* **2007**, *17*, 1479.

[242] Scott, R., Sethu, P., Harnett, C. K. *Rev. Sci. Instrum*. **2008**, *79*, 046104.

[243] Lin, C. H., Lee, G. B., Fu, L. M., Hwey, B. H. *J. Microelectromech. Syst*. **2004**, *13*, 923.

[244] Van Ness, J., Chen.L. *Nucleic Acids Res*. **1991**, *19*, 5143.

[245] Maskos, U., Southern, E. M. *Nucleic Acids Res*. **1991**, *20*, 1675.

[246] Kibbe, W. A. *Nucleic Acids Res*. **2007**, *35*, W43.

[247] Vainrub, A., Pettitt, B. M. *J. Am. Chem. Soc*. **2003**, *125*, 7798.

[248] Peterson, A. W., Heaton, R. J., Georgiadis, R. M. *Nucleic Acids Res*. **2001**, *29*, 5163.

[249] Wong, D., Tan, T. L., Lee, P., Rawat, R. S., Patran, A. *Microelectron. Eng*. **2006**, *83*, 1912.

[250] Images taken with the aid of Bashevoy, M. Optoelectronics Research Centre, University of Southampton, UK.

[251] Chang, C. J., Tseng, F. G., Yang, C. S., *NSTI Nanotech*. **2005**, *1*, 296.

[252] Walther, F., Davydovskaya, P., Zurcher, S., Kaiser, M., Herberg, H., Gigler, A. M., Stark, R. W. *J. Micromech. Microeng*. **2007**, *17*, 524.

[253] Sassolas, A., Leca-Bouvier, B. D., Blum, L.J. *Chem. Rev*. **2008**, *108*, 109.

[254] Teles, F. R. R., Fonseca, L. P. *Talanta*, **2008**, *77*, 606.

[255] Strother, T., Hamers, R. J., Smith, L. M. *Nucleic Acids Res*. **2000**, *28*, 3535.

[256] Wang, S. G., Wang, R. L., Sellin, P. J., Zhang, Q. *Biochem. Biophys. Res. Commun*. **2004**, *325*, 1433.

[257] Teh, H. F., Gong, H. Q., Dong, X. D., Zeng, X. T., Tan, A. L. K., Yang, X. H., Tan, S. N. *Anal. Chim. Acta.* **2005**, *551*, 23.

[258] Ito, K., Hashimoto, K., Ishimori, Y. *Anal. Chim. Acta*. **1996**, *327*, 29.

[259] Stigter, D. *Biopolymers*. **1977**, *16*, 1435.

[260] Rybenkov, V. V., Cozzarelli, N. R., Vologodskii, A. V. *P.N.A.S.* **1993**, *90*, 5307.

[261] Hales, T. C. *Ann. Math*. **2005**, *162*, 1065.

[262] Cattaruzza, F. *et al*. *Nucleic Acids Res*. **2006**, *34*, e32.

[263] Steel, A. B., Herne, T. M., Tarlov, M. J. *Anal. Chem*. **1998**, *70*, 4670.

[264] Mortati, L., Miletto, I., Alberto, G., Caputo, G., Sassi, M. P. *J. Fluoresc*. **2010**, online edition.

[265] Work done in part by Ranasinghe, R. T. Department of Chemistry, University of Southampton, UK.

[266] Saprigin, A. V., Thomas, C. W., Dulcey, C. S., Patterson, C. H., Jr; Spector, M. S. *Surf. Interface Anal.* **2004**, *36*, 24.

[267] Kolb, H. C., Finn, M. G., Sharpless, K. B. *Angew. Chem. Int. Ed*. **2001**, *40*, 2004.

[268] Tornøe, C. W., Christensen, C., Meldal, M. *J. Org. Chem*. **2002**, *67*, 3057.

[269] Kanan, M. W., Rozenman, M. M., Sakurai, K., Snyder, T. M., Liu, D. R. *Nature*. **2004**, *431*, 545.

[270] Chan, T. R., Hilgraf, R., Sharpless, K. B., Fokin, V. V. *Org. Lett*. **2004**, *6*, 2853.

[271] Kumar, R., El-Sagheer, A., Tumpane, J., Lincoln, P., Wilhelmsson, L. M., Brown, T. *J. Am. Chem. Soc.* **2007**, *129*, 6859.

[272] Work done in part by Ranasinghe, R. T. Department of Chemistry, University of Southampton, UK.

[273] Gruber, H. J. *et al*. *Bioconjugate Chem.* **2000**, *11*, 696.

[274] Himo, F., Lovell, T., Hilgraf, R., Rostovtsev, V. V., Noodleman, L., Sharpless, K. B., Fokin, V. V. *J. Am. Chem. Soc.* **2005**, *127*, 210.

[275] Donnelly, P. S., Zanatta, S. D., Zammit, S. C., White, J. M., Williams, S. J. *Chem. Commun*. **2008**, *21*, 2459.

[276] Armenante, P. M., Kirwan, D. J. *Chem. Eng. Sci*. **1989**, *44*, 2781.

[277] Vyver, O. V., Nelissen, G., Weyns, G., Deconinck, J., Degrez, M., Godet, S. *Electrochim. Acta.* **2008**, *53*, 6452.

[278] Zhang, J., Chan-Park, M. B., Li, C. M. *Sens. Actuators, B*. **2008**, *131*, 609.

[279] Köster, H., Biernat, J., McManus, J., Wolter, A., Stumpe, A., Narang, CH. K., Sinha, N. D. *Tetrahedron*. **1984**, *40*, 103.

[280] Krotz, A. H., Rentel, C., Gorman, D., Olsen, P., Gaus, H. J., McArdle, J. V., Scozzari, A. N. *Nucleosides Nucleotides Nucleic acids*. **2004**, *23*, 764.

[281] Sikanen, T., Tuomikoski, S., Ketola, R. A., Kostiainen, R., Franssila, S., Kotiaho, T. *J. Mass Spectrom*. **2008**, *43*, 726.

[282] Wouters, K., Puers, R. *J. Micromech. Microeng.* **2010**, *20*, 095013.

[283] Chang, C. J., Yang, C. S., Chuang, Y. J., Khoo, H. S., Tseng, F. G. *Nanotechnology*. **2008**, *19*, 365301.

[284] Qvortrup, K., Taveras, K. M., Thastrup, O., Nielsen, T. E. *Chem. Commun.* **2011**, *47*, 1309.

[285] Kaiser, E., Colescott, R. L., Bossinger, C. D., Cook, P. I. *Anal. Biochem.* **1970**, *34*, 595.

[286] Sarin, V. K., Kent, S. B. H., Tam, J. P., Merrifield, R. B. *Anal. Biochem.* **1981**, *117*, 147.

[287] Hashimoto, M., Liu, Y., Fang, K., Li, H., Campiani, G., Nakanishi, K. *Bioorg. Med. Chem*. **1999**, *7*, 1181.

[288] Kelly, R. C., Jensen, D. E., Von Hippel, P. H. *J. Biol. Chem.* **1976**, *251*, 7240.

[289] Freeman, J. L., Abo, A., Lambeth, J. D. *J. Biol. Chem.* **1996**, *271*, 19794.